NASA/CR—1999-209008

Thermal Control Surfaces Experiment

D.R. Wilkes
AZ Technology, Inc., Huntsville, Alabama

Prepared for Marshall Space Flight Center
under Contract NAS8-38939

National Aeronautics and
Space Administration

Marshall Space Flight Center • MSFC, Alabama 35812

January 1999

Available from:

NASA Center for AeroSpace Information
800 Elkridge Landing Road
Linthicum Heights, MD 21090–2934
(301) 621–0390

National Technical Information Service
5285 Port Royal Road
Springfield, VA 22161
(703) 487–4650

TABLE OF CONTENTS

TABLE OF CONTENTS (Continued)

TABLE OF CONTENTS (Continued)

LIST OF FIGURES

LIST OF FIGURES (Continued)

LIST OF FIGURES (Continued)

LIST OF FIGURES (Continued)

LIST OF TABLES

LIST OF ACRONYMS

A-D .....Analog to Digital
AO.....Atomic Oxygen
ATR.....Attenuated Total Reflectance

BDRF .....Bi-Directional Reflectance Function

CCD .....Charge Coupled Device
CPU.....Central Processor Unit
CRT.....Cathode Ray Tube

DACS.....Data Acquisition and Control System
DC .....Direct Current
DOD.....Department of Defense
DSC.....Differential Scanning Calorimetry

EDAX .....Electron Dispersive X-ray Analysis
EMI .....Electromagnetic Interference

GRU .....Ground Reproduce Unit
GSE.....Ground Support Equipment
GSFC .....Goddard Space Flight Center

HST.....Hubble Space Telescope

IITRI .....Illinois Institute of Technology Research Institute
IN-STEP.....In-Space Technical Experiments Program
IR.....Infrared
IRS .....Internal Reflection Spectroscopy
ISEM.....Integrated Spacecraft Environments Model

JSC .....Johnson Space Center

KSC.....Kennedy Space Center

LaRC.....Langley Research Center
LDEF.....Long Duration Exposure Facility
LEC.....Lockheed Electronics Company
LEO.....Low Earth Orbit
LIF.....Laser-Induced Fluorescence

M&D.....Micrometeoroid and Debris
M&P.....Materials and Processes

LIST OF ACRONYMS (Continued)

MSFC.....George C. Marshall Space Flight Center
MTA.....Multiple Time Averaging

NASA.....National Aeronautics and Space Administration

OPM.....Optical Properties Monitor

PI.....Principal Investigator
PRT.....Platinum Resistance Thermometer
PSD.....Phase Sensitive Detector

SEM.....Scanning Electron Microscopy
SIG.....Special Investigative Group
SRB.....Solid Rocket Booster

TCSE.....Thermal Control Surfaces Experiment
THERM.....Thermal Measurement System

UAH.....University of Alabama in Huntsville
UV.....Ultraviolet

VCM.....Vacuum Condensable Material
VDC.....Volts Direct Current

XPS.....X-ray Photoelectron Spectroscopy

1.0 INTRODUCTION

The natural and induced long term effects of the space environment on spacecraft surfaces are critically important to many of NASA's future spacecraft including the International Space Station. The damaging constituents of this environment, as illustrated in Figure 1, include thermal vacuum, solar ultraviolet (UV) radiation, atomic oxygen (AO), ionizing particulate radiation, and the spacecraft induced (contamination) environment. The inability to exactly simulate this complex combination of constituents results in a major difference in the stability of materials between laboratory testing and flight testing. To study these environmental effects on surfaces, particularly on thermal control surfaces, the Thermal Control Surfaces Experiment (TCSE) was proposed for the National Aeronautics and Space Administration (NASA) Long Duration Exposure Facility (LDEF) mission. The TCSE was selected as one of the first six experiments for the LDEF.

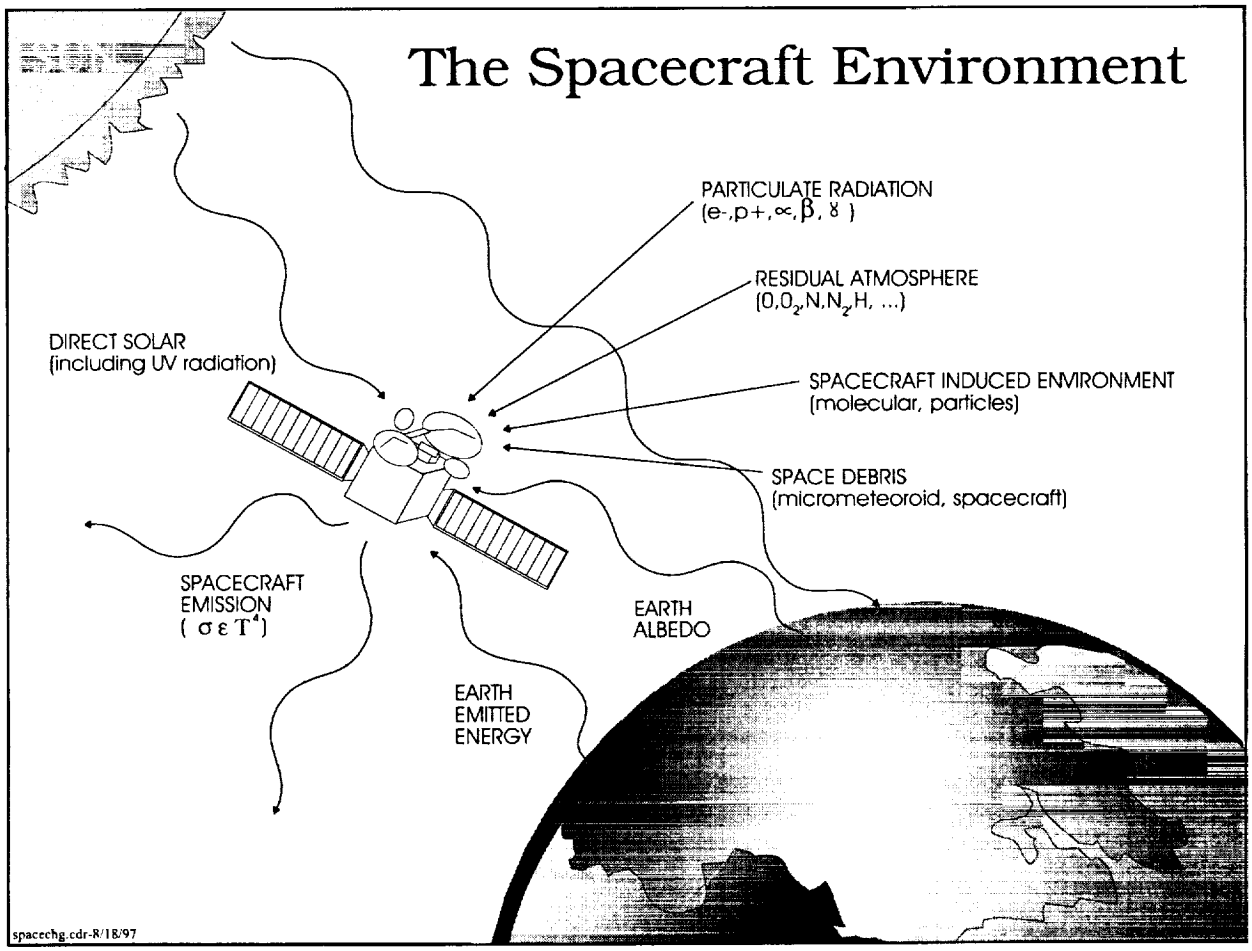

Figure 1. The Spacecraft Environment.

On April 7, 1984, the LDEF, with the TCSE as one of its complement of 57 experiments, was deployed in low earth orbit (LEO) by the Space Shuttle. The LDEF was to have been retrieved after 9 to 12 months in orbit. However, due to the solid rocket motor redesign effort

resulting from the Challenger accident and launch schedule priorities, the LDEF retrieval was delayed approximately 60 months (until January 12, 1990). After retrieval by the Shuttle, the TCSE was deintegrated from the LDEF at the Kennedy Space Center (KSC) and returned to the George C. Marshall Space Flight Center (MSFC) for analysis on March 7, 1990.

The TCSE was a comprehensive experiment that combined in-space measurements with extensive post-flight analyses of thermal control surfaces to determine the effects of exposure to the LEO space environment. The TCSE was the first space experiment to measure the optical properties of thermal control surfaces the way they are routinely measured in the laboratory. While the TCSE marks a milestone in understanding the performance of materials in space, other experiments similar to the TCSE will be required to fully understand the diverse effects of the space environment. These experiments will provide additional optical and environmental monitoring.

This report is the final experiment report for the TCSE and summarizes many years of hardware development and analyses. This final report serves as the contract final report for NASA contract NAS8-38939, but encompasses work also performed under other contracts including NASA contract NAS8-36289,[1] and Boeing contracts HJ-3234,[2] and HK-7879.[3] Also included are analyses presented in a number of TCSE papers that were prepared and given at scientific conferences including the three LDEF Post-Retrieval Symposiums. The bibliography of the TCSE papers, presentations, and reports are listed in Appendix A and are widely cited in this report.

Section 2 describes the TCSE objectives, experimental method, and the flight hardware. Section 3 summarizes the LDEF and TCSE mission. Section 4 presents the performance and anomalies of the TCSE hardware system. Section 5 discusses the results of the materials experiment. Section 6 is a summary of this effort.

1.1 TCSE Program Participants

The success of the TCSE is due to the work of many NASA and contractor personnel. The TCSE was originally proposed in 1975 by the Principal Investigator (PI), Mr. Donald R. Wilkes, and Co-Investigator, Mr. Harry M. King. At that time, both investigators were with NASA/MSFC. In 1977, a competitive procurement was issued for the development of the TCSE flight hardware. Aerojet ElectroSystems of Azusa, California was selected as the prime contractor. They designed, fabricated, and assembled the TCSE protoflight unit and performed the initial functional testing. Due to a two year delay in the LDEF program and associated funding problems, the TCSE development contract with Aerojet was terminated and the partially operating TCSE instrument delivered to MSFC. The TCSE protoflight unit was then completed and tested in-house at MSFC with the assistance of Radiometrics, Inc. in Huntsville, Alabama.

The TCSE post-flight analysis was performed as a joint effort by the MSFC Materials and Processes (M&P) Laboratory and the PI and his staff now at AZ Technology, Inc. in Huntsville, Alabama.

There are far too many participants in the TCSE program to list in this publication. Table 1 is a list of the participants who had formal responsibility for the success of the TCSE. Significant credit for the TCSE success should also go to the LDEF Chief Scientist, Dr. William Kinard, and the entire LDEF staff along with the Shuttle astronauts who deployed and retrieved the LDEF.

Table 1. TCSE Program Participants.

PRE-FLIGHT	
NASA/MSFC:	
Principal Investigator	D.R. Wilkes, Space Sciences Laboratory
Co-Investigator	H.M. King, M&P Laboratory
Chief Engineers	L.W. Russell, Space Sciences Laboratory
	G.M. Arnett, Science & Engineering
Program Manager	B.J. Schrick, Special Projects Office
NASA/LaRC:	
Guest Investigator	W. Slemp
Aerojet ElectroSystems:	
Project Manager	M.J. Brown
Chief Engineer	R. Emerling
Radiometrics:	
Lead Engineer	R. Schansman
POST-FLIGHT	
NASA/MSFC:	
Co-Investigator	J.M. Zwiener, M&P Laboratory
AZ Technology, Inc.:	
Principal Investigator	D.R. Wilkes
Lead Engineer	L.L. Hummer

2.0 EXPERIMENT DESCRIPTION

The TCSE was designed to be a comprehensive experiment to study the effects of the space environment on thermal control surfaces. This section describes the basic objectives of the TCSE, the experimental method, the materials tested, and the TCSE flight hardware.

2.1 TCSE Objectives and Experimental Method

The basic objective of the TCSE on the LDEF was to determine the effects of the near-Earth orbital environment and the LDEF induced environment on spacecraft thermal control surfaces. In summary, the specific mission objectives of TCSE were to:

- determine the effects of the natural and induced space environment on thermal control surfaces,

- provide in-space performance data on thermal control surfaces,
- provide in-space comparison to ground-based environmental testing of materials, and
- develop and prove instrumentation to perform in-space optical testing of materials.

To accomplish these objectives, the TCSE exposed selected material samples to the space environment and used in-flight and post-flight measurements of their thermo-optical properties to determine the effects of this exposure.

The TCSE hardware was designed to expose 25 "active" and 24 "passive" test samples to the LDEF orbital environment. The active and passive test samples differed in that the space effects on the passive test samples were determined only by pre- and post-flight evaluation. The optical properties of the 25 "active" samples were measured in-space as well as in pre- and post-flight analysis.

The "passive" samples were duplicates of critical "active" samples as well as specially prepared samples for surface analysis techniques, such as Internal Reflection Spectroscopy (IRS). The post-flight analysis of these passive samples, as well as the active samples, is used to determine the effects of the LDEF mission in more detail than is feasible with "in-situ" measurements. Of special importance are the detailed surface effects of the AO fluence and the identification of any molecular contaminant film on the sample surfaces.

2.2 In-Space Measurements

The primary TCSE in-space measurement was hemispherical reflectance as a function of wavelength (100 wavelength steps from 250 to 2500 nm) using a scanning integrating sphere reflectometer. The measurements were repeated at preprogrammed intervals over the mission duration.

The secondary measurement used calorimetric methods to calculate solar absorptance and thermal emittance from temperature-versus-time measurements. The "active" sample surfaces were applied to thermally isolated (calorimeter) sample holders. To aid in the calorimetric calculations, three radiometers were used to measure the radiant energy (direct solar, Earth albedo, and Earth infrared (IR) emitted) incident upon the samples. The radiometers were to also determine the total exposure of the samples to direct solar irradiance. The TCSE measurements are more fully described in section 2.4.

2.3 Flight Samples

The materials chosen for the TCSE mission comprised the thermal control surfaces of the greatest current interest (in 1983) to NASA, MSFC and the thermo-physical community. The samples flown on the TCSE mission were:

- A276 White Paint
- A276/OI650 Clear Overcoat
- Silver/FEP Teflon (5 mil)
- Silver/FEP Teflon (5 mil Diffuse)

- A276/RTV670 Clear Overcoat
- S13G/LO White Paint
- Z93 White Paint
- YB71 White Paint
- YB71 over Z93
- Chromic Acid Anodize
- Silver/FEP Teflon (2 mil)
- White Tedlar
- D111 Black Paint
- Z302 Black Paint
- Z302/OI650 Clear Overcoat
- Z302/RTV670 Clear Overcoat
- KRS-5 IR Crystal
- Silver

Many of these materials were selected because they are good reflectors of solar energy while also being good emitters of thermal energy to the cold sink of space, i.e. they have a low solar absorptance (α_S) and a high room temperature emittance (ε_T). The range of low α_S/ε_T thermal control surfaces include materials that were expected to be very stable for the planned 9-12 month LDEF mission while others were chosen because they were expected to degrade significantly.

A second class of materials flown on the TCSE was black paints. These are important as solar energy absorbers and light absorbers for science instruments.

Some of the materials were expected to react with the residual AO at the LDEF orbital altitude. Transparent coatings were applied over a few of these samples to protect the sample from AO.

The remainder of this section discusses each of the materials flown on the TCSE.

2.3.1 A276 White Paint

Chemglaze A276 white paint is a Titanium Dioxide (TiO_2) pigment in a polyurethane binder. It has been used on many space vehicles including Spacelab.

In early Shuttle experiments[4] and ground testing, A276 had been shown to be susceptible to erosion by AO. It had been suggested that clear overcoatings would protect AO susceptible coatings. The effectiveness of two protective coatings over the A276 were evaluated on the TCSE. These overcoatings were Owens Illinois OI650 glass resin and RTV670.

A276 is manufactured by the Lord Corporation Chemical Division. The samples for the TCSE were prepared by personnel in the M&P Laboratory, NASA/MSFC.

2.3.2 S13G/LO White Paint

S13G/LO white paint has been the most widely used white thermal control coating for space vehicle thermal control. S13G/LO consists of zinc oxide (ZnO) pigment in a General Electric RTV602 methyl silicone binder. The pigment particles were treated with potassium silicate before processing into paint to inhibit the photodesorption of oxygen from the ZnO pigment when subjected to solar UV exposure.[5]

The S13G/LO formulation used for the TCSE samples is no longer available because the RTV602 binder is not currently manufactured. A new methyl silicone binder is used in S13G/LO-1 white paint which is a replacement for S13G/LO. S13G/LO and S13G/LO-1 are manufactured by the Illinois Institute of Technology Research Institute (IITRI). IITRI prepared the S13G/LO samples for the TCSE. Table 2 summarizes the TCSE samples prepared by IITRI.

Table 2. IITRI Prepared TCSE Flight Samples.

Coating Material	Sample Number	Coating Thickness (mils)	Batch Number
S13G/LO	C92	12.0	I-097
	P7	9.5	I-097
Z93	C95	4.5	I-100
	P5	5.0	I-100
	P6	6.5	I-100
YB71	C96	6.5	I-061
	C97	9.5-10.5	I-061
	P1	9.5	I-099
	P2	9.0	I-099
YB71 over Z93	C93	9.0-9.5	I-061 (YB71)
	C94	8.5-9.5	I-100 (Z93)
	P3	11.0-12.0	
	P4	10.0	
D111	C99	2.5	I-101
	P10	4.0	I-101

2.3.3 Z93 White Paint

Z93 is another widely used white thermal control coating that is manufactured by IITRI. Z93 is the same zinc oxide pigment as S13G/LO, but in a potassium silicate binder. IITRI also prepared the Z93 samples for the TCSE.

2.3.4 YB71 White Paint

YB71 white paint is a zinc orthotitanate (Zn_2TiO_4) pigment in a potassium silicate binder. When the TCSE samples were prepared, YB71 was just completing development. YB71 offered the potential for solar absorptance values less than 0.10 while maintaining an emittance of 0.90. This coating also offered improved stability in the space environment, especially for ionizing particulate radiation exposure.

Because the manufacturing and application process was not finalized when the TCSE samples were prepared, the α_s values for the YB71 were somewhat higher than desired $\alpha_s = 0.11$ to .15). Somewhat lower α_s values for the TCSE samples were achieved by applying a primer coat of Z93 white paint before the YB71 was applied. Current versions of the YB71 have

resolved this problem and α_s values around 0.08 are being achieved. YB71 is manufactured by IITRI, who also prepared the TCSE samples.

2.3.5 Chromic Acid Anodize

Two chromic acid anodized aluminum samples were tested on the TCSE. These samples were provided by Mr. Wayne Slemp of Langley Research Center (LaRC) who is a TCSE guest investigator. Anodized coatings have long offered the potential for stable coatings for large surfaces and are being considered for use on the International Space Station.

2.3.6 Silver Teflon Surfaces

Silverized FEP Teflon* is another widely used thermal control surface. Two different thicknesses of silver Teflon were flown on the TCSE: 2 mil and 5 mil. The 2 mil material was used on the TCSE front cover as part of the passive thermal control system. A sample of the 2 mil silver Teflon was also flown on the active sample array. The 2 mil material was attached to the substrate with 3M Y-966 acrylic pressure sensitive adhesive tape. A Teflon squeegee was used to remove air bubbles followed by a wipedown with isopropyl alcohol.

Two configurations of the 5 mil silver Teflon material were flown on the TCSE sample array: the normal specular type and an embossed or diffuse type. The normal silver Teflon material has a mirror-like finish which is undesirable for some applications. The diffuse material has a dimpled pattern embossed into its surface to minimize specular surface reflections. The 5 mil material was attached to the sample substrates with P223 adhesive.

The silver Teflon used on the TCSE was manufactured by Sheldahl. The 2 mil calorimeter sample was prepared by Aerojet ElectroSystems. The TCSE cover material was applied by personnel in the M&P Laboratory, MSFC. The 5 mil samples were provided by Wayne Slemp of LaRC.

2.3.7 White Tedlar Film

White Tedlar® is a pigmented plastic film manufactured by Dupont. White Tedlar was a candidate for the external covering of insulating blankets used on spacecraft. This material was flown on the TCSE because its solar absorptance was expected to degrade a measurable amount in the planned 9-12 month LDEF mission. The TCSE Tedlar samples were prepared by the M&P Laboratory at MSFC.

2.3.8 D111 Black Paint

The performance of many spacecraft and instruments depends on light absorbing coatings. D111 black paint was developed by IITRI as a stable diffuse coating for this

---

* Teflon is a registered trademark of Dupont.

® Tedlar is a registered trademark of Dupont.

application. The D111 formulation is a bone black carbonaceous pigment in an inorganic potassium silicate binder. D111 coatings provide high absorptance over the solar region (250-2500 nm) with a near zero Vacuum Condensable Material (VCM). The TCSE D111 samples were prepared by IITRI.

2.3.9 Z302 Black Paint

Chemglaze Z302 is a gloss black paint from Lord Chemical. Z302 is an aromatic polyurethane coating with a carbon black pigment. It was used on the aperture door of the Hubble Space Telescope (HST) as a light absorber coating. The specularity of Z302 was required to reflect any light, not absorbed, away from the telescope aperture and prevent scattering into the field-of-view.

Laboratory and flight testing of Z302 determined that this material was very susceptible to AO erosion.[4] Clear overcoatings might be used to protect the Z302 from AO. The effectiveness of two transparent protective coatings were evaluated on the TCSE: Owens Illinois OI650 glass resin and RTV670. The Z302 samples for the TCSE were prepared by the M&P Laboratory, MSFC.

2.3.10 Other Samples

Two other types of samples were flown on the TCSE passive sample array: two KRS-5 crystals and three silver samples. The KRS-5 crystals were flown to evaluate any molecular contamination deposited on the TCSE sample surfaces. KRS-5 crystals are typically measured in an internal reflection IR spectrometer. This measurement can provide IR absorption spectra from very small amounts of material deposited on the surface of the crystal. This spectra can aid in determining the species of any deposited contaminant.

The silver samples were flown on the TCSE to evaluate the fluence and behavior of AO. These samples consisted of three stacked silver coated disks. The top two disks had a pinhole in the center of each disk to act as a pinhole camera and evaluate the directionality and accommodation of the incident AO molecular beam. The silver samples were designed and built by Dr. Palmer Peters of the MSFC Space Science Laboratory and Dr. John Gregory of the University of Alabama in Huntsville (UAH).

These special samples were so degraded by the extended space exposure that analysis could not be done.

2.4 TCSE Flight Hardware

The TCSE is a completely self-contained experiment package providing its own power, data system, and pre-programmed controller for automatically exposing, monitoring, and measuring the sample materials. The TCSE was developed as a protoflight instrument where one instrument was built, made to work within required specifications, tested, and flown.

Environmental qualification testing was performed at MSFC that included vibration, thermal vacuum, and electromagnetic interference (EMI) tests.

The TCSE was built in a 305mm (12 in.) deep LDEF tray (see Figure 2). The active and passive samples were mounted in a semicircular pattern on a circular carousel with three radiometers. The carousel is tilted at 11° from the outer tray surface to allow a 115mm (4.5 inch) diameter integrating sphere to fit between the deep end of the carousel and the outer shroud. This design satisfied the LDEF requirements to remain within the outer edges of the tray and also provided a field-of-view of space greater than 150° for the samples. This design maintained mechanical simplicity and inherent reliability.

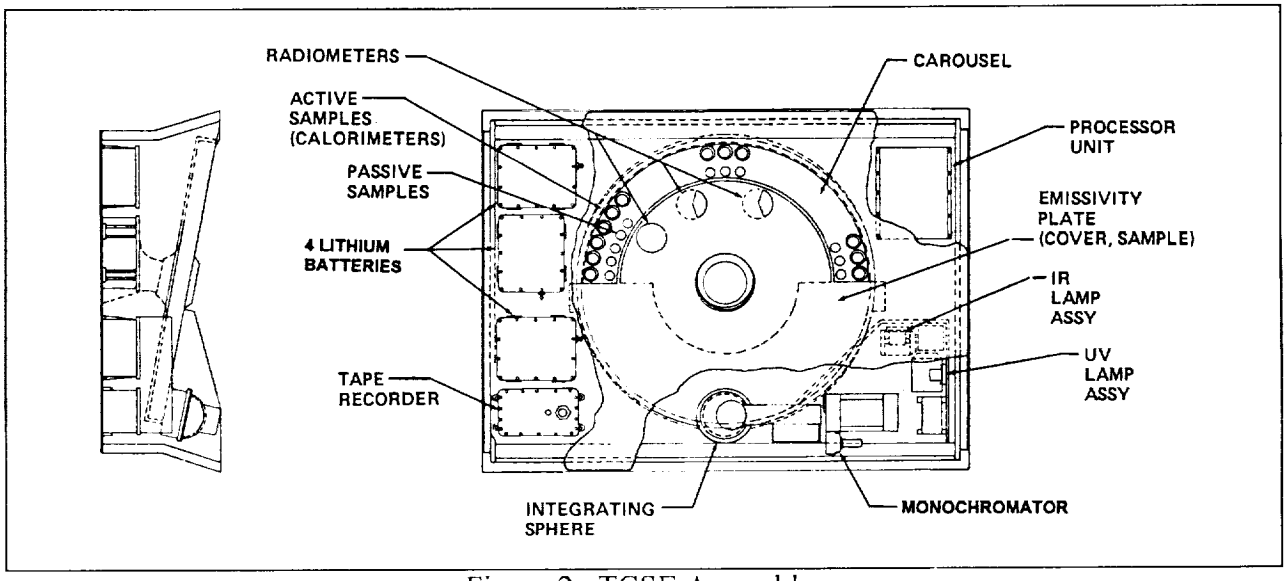

Figure 2. TCSE Assembly.

The TCSE flight system is the most complex mechanism (other than the LDEF) ever retrieved from space after nearly six years of exposure. It represents a microcosm of the large electro-optical payloads in development by NASA, Department of Defense (DOD), and industry. The performance of the TCSE provides a better understanding of the performance of complex systems, subsystems, and components in the space environment. Table 3 shows the basic specifications for the TCSE flight hardware.

2.4.1 Sample Carousel

The TCSE sample carousel design enabled the test samples to be either protected from or exposed to the space environment as well as to be positioned for optical measurement. Figure 3 illustrates the sample positions on the carousel during various exposure or measurement times during the LDEF mission. The radiometers are also shown, referenced to the flight sample positions. In the exposed condition, the samples experienced space exposure for approximately 23.5 hours each earth day. During the protected period of time (approximately 1/2 hour), calorimetric measurements of emittance were made. The protected environment also prevented exposure of the experiment test samples to ground processing and launch contamination.

Table 3. TCSE Flight Hardware Specifications.

Size	1.24m x .84m x .30m (48.75 in x 33 in x 12 in)
Weight	80.5kg (177 pounds)
System Controller	1802 Microprocessor
Battery Capacity	72 Amp Hours at 28 VDC
Data Recorder • Capacity	Lockheed 4200 54 x 10^6 Bits
Reflectometer • Wavelength Range • Wavelength Resolution ($\Delta\lambda/\lambda$) • Reflectance Accuracy • Reflectance Repeatability	 250 to 2500 nm $\leq$ 5% 2% 1%
Calorimetric Measurements • Solar Absorptance • Total Emittance	 Accuracy - 5% Accuracy - 5%

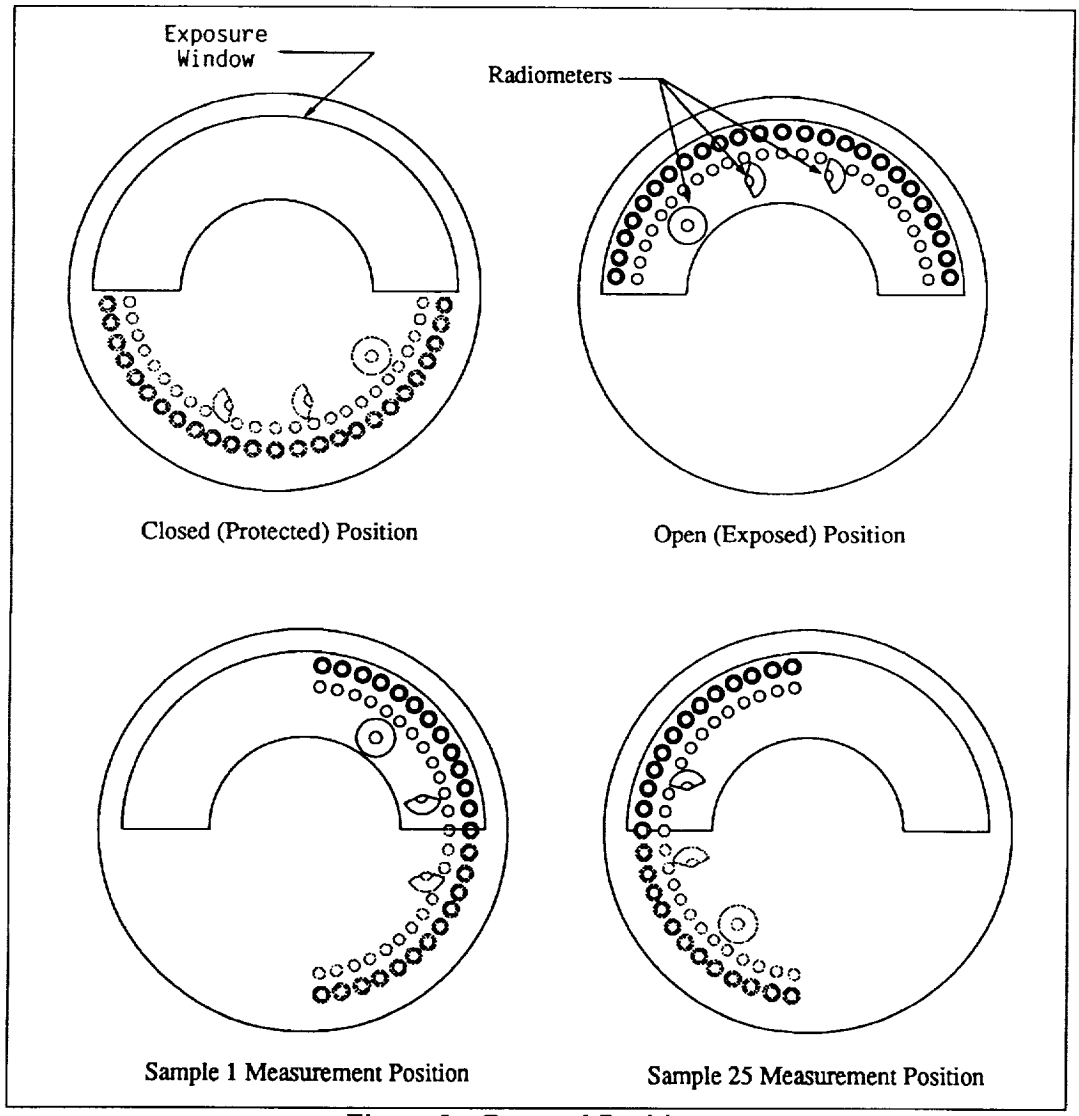

Figure 3. Carousel Positions.

The carousel subsystem was comprised of the carousel assembly, a stepper motor controlled by the Data Acquisition and Control System (DACS) to effect movement of the carousel assembly, a geneva drive assembly consisting of the drive gear and cam, and an emissivity plate. The geneva drive enabled precise repeatable angular rotation such that the same spot on the flight sample was measured. A magnetic sensor on the geneva drive gear sensed a home position to provide the positive indication of a complete movement of one sample position and the locked position of the cam. Pre-flight testing proved the inherent reliability of the geneva drive assembly and the positioning accuracy of each sample. The emissivity plate, combined with calorimeters, was used for the emittance measurements.

2.4.1.1 Radiometers

Three radiometers were used to monitor the irradiance from the sun (direct solar), earth albedo (reflected solar), and earth IR (emitted) incident on the TCSE. Radiometer data enables calculation of solar absorptance and total emittance when combined with calorimeter temperature data. The radiometers were mounted on the carousel and were rotated with the flight samples. The three radiometers used thermopile detectors painted flat black and domed collection optics to measure the energy flux on the TCSE. The direct solar radiometer was installed with a field-of-view equal to the flight samples. A quartz lens was used for the spectral region of 200-3000 nm. This region contains over 98% of the sun's electromagnetic energy. Like the direct solar radiometer, the earth albedo radiometer used a quartz lens. However, the earth IR radiometer used a germanium lens for the IR spectrum from 2000-20,000 nm. Making use of the stable attitude of the LDEF, the earth albedo and earth IR radiometers were installed with covers such that they had a clear view of only the earth. Data from the radiometers were recorded at one minute intervals over a two hour period each day of the active mission during the daily measurement sequence.

2.4.1.2 Calorimeters

Calorimeter sample holders provided a simple method to determine the solar absorptance (α_S) and total emittance (ε_T) of the active flight samples. This calorimetric technique measured the inputs to the heat balance equation and calculated solar absorptance and total emittance for the flight samples. The in-space measurements required for this calculation were the temperature of the test sample and the external heat inputs as measured by the irradiance monitors. The calorimeters were designed to isolate the flight sample material thermally from the TCSE to minimize errors caused by radiative and conductive losses. The TCSE calorimeter design was developed originally by the Goddard Space Flight Center (GSFC) and flown on the ATS-1, ATS-2, and OAO-C satellites.[6]

The calorimetric measurement procedure used on the TCSE is an improvement over past experiments for determining total emittance. Previous experiments determined total emittance when the calorimeter viewed deep space only (i.e., no view of the sun or earth). This orientation was difficult to ensure and the time spent in this orientation was, at times, too short to provide accurate measurements. The TCSE procedure, however, rotated the samples inside the

instrument where they viewed only a heavy black "emissivity" plate. This geometry greatly simplifies the heat balance equation and removes any sun or earth effects.

The calorimeter consisted of three major parts: the sample disk, the inner cup, and the outer cup. Figure 4 illustrates the construction of the calorimeter.

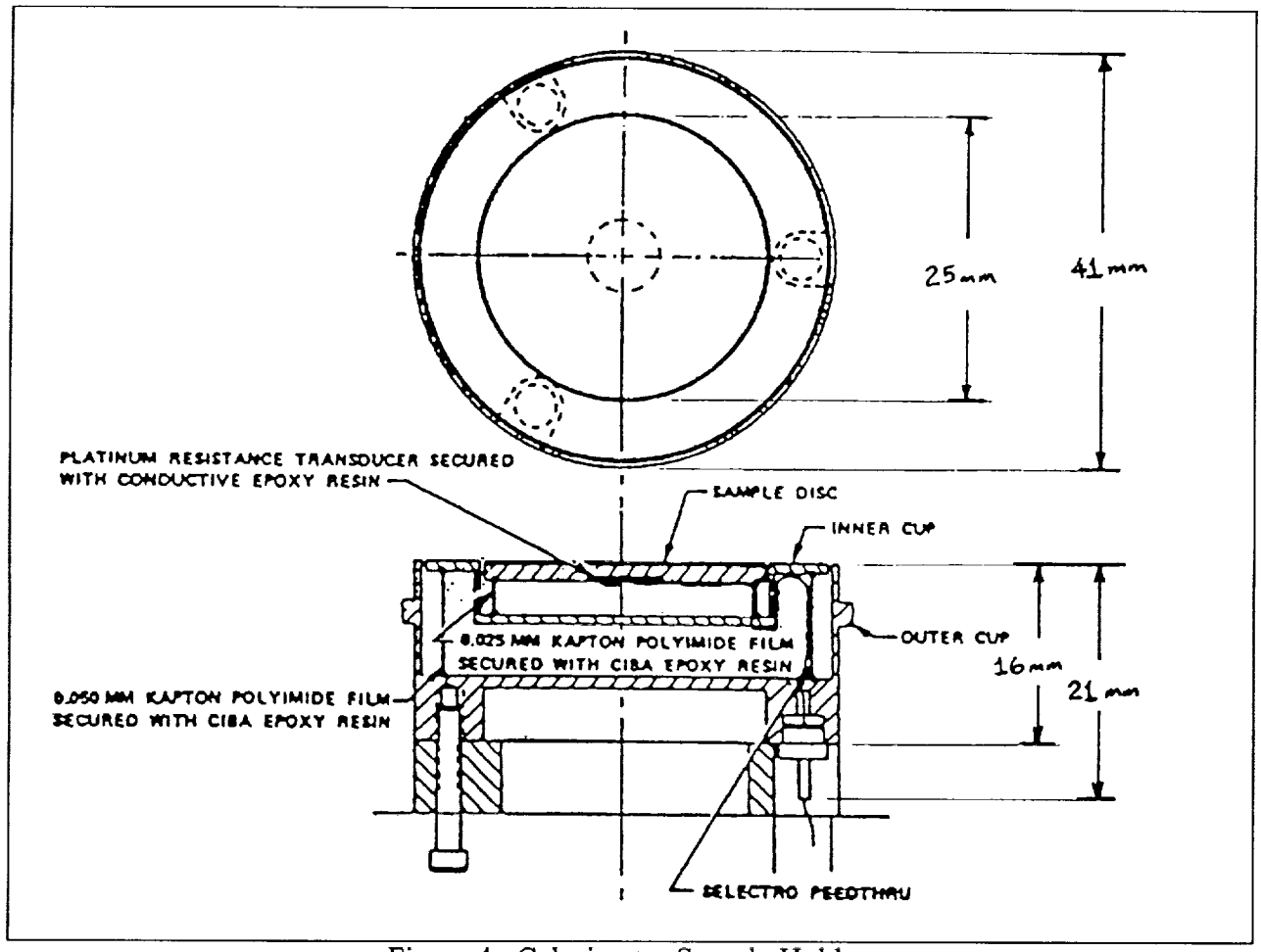

Figure 4. Calorimeter Sample Holder.

The concept for the three-part calorimeter was for the inner cup to act as a thermal guard for the sample disk. This design featured virtually zero conduction back through the sample holder, low measurable radiative heat transfer to the carousel, and no radiative heat transfer to the sides. The inner cup, or "guard," had the same area and coating as the sample disk to maintain the inner cup temperature close to the temperature of the sample. The thermal capacitance of the inner cup was also as close as possible to that of the sample disk to ensure the guard is effective even during transient sample temperatures. Kapton film, formed into cylinders, was used to fasten the sample disk to the inner cup and to fasten the inner cup to the outer cup (as illustrated in Figure 4). Crimped double-faced aluminized Mylar sheets were placed inside each cylinder to reduce the radiative heat losses. Vent holes were put in the cylinders and bases of the inner and outer cups, enabling the interior of these cups to vent to the vacuum environment. A solar

absorber material was applied to the inner sides of both the inner cup and the outer cup to minimize errors caused by light leaks through the gaps between the sample, inner cup, and outer cup. A Platinum Resistance Thermometer (PRT) was attached to the underside of each sample disk with thermally conducting silver epoxy to assure good thermal contact with the sample substrate. The DACS monitored the PRT to measure the temperature of the sample disk.

The calorimeter was clamped onto the carousel by the carousel mounting cover. The top of the calorimeter was flush with the top of the carousel.

2.4.2 Reflectometer Subsystem

Techniques to evaluate the optical properties of thermal control surfaces have been standardized for the past 25 years and consist of spectral reflectance measurements from 250-2500 nm to determine solar absorptance (α_S) and total hemispherical emittance (ε_T). Solar absorptance is calculated from the spectral reflectance data. The α_S and ε_T values determine how the thermal energy is exchanged between a spacecraft and its environment and the resultant temperature values for the spacecraft. The spectral reflectance provides details of the physics of the material and is the best method to calculate solar absorptance.

The TCSE reflectometer optical design, illustrated in Figure 5, is one that is used routinely in the laboratory to measure spectral reflectance. Two light sources, tungsten and deuterium lamps, are used with a scanning prism monochromator with selectable slit widths to provide the monochromatic energy for the spectral measurement. A 115mm (4.5 inch) diameter integrating sphere collects both the specularly- and diffusely-reflected light from a wall mounted sample to provide the hemispherically integrated measurement capability. Figure 6 illustrates the integrating sphere geometry. Kodak Barium Sulfate ($BaSO_4$) was selected for the sphere coating because it was easy to apply, durable enough to withstand the launch environment, and had good optical properties. A UV enhanced silicon photodiode detector and a lead sulfide detector were used with the integrating sphere for the required 250-2500 nm spectral range.

2.4.3 Data Acquisition and Control System (DACS)

The TCSE DACS is shown in Figure 7 and controls all aspects of the TCSE operation. The heart of the DACS is an RCA 1802 CMOS microprocessor with associated memory and input/control ports. A 12-bit A-D converter and analog multiplexer are used to read to measurement data.

A low-power, 25-bit real-time clock was used to keep mission elapsed time. The real-time clock was the only TCSE subsystem that ran continuously from the LDEF "start" signal through battery depletion. The clock subsystem turned on the DACS once each 24 hour day of the active TCSE mission. The DACS, in turn, looked at its internal schedule to determine what functions were to be done that day. At the completion of the day's measurements, the DACS turned itself off leaving only the real-time clock operating.

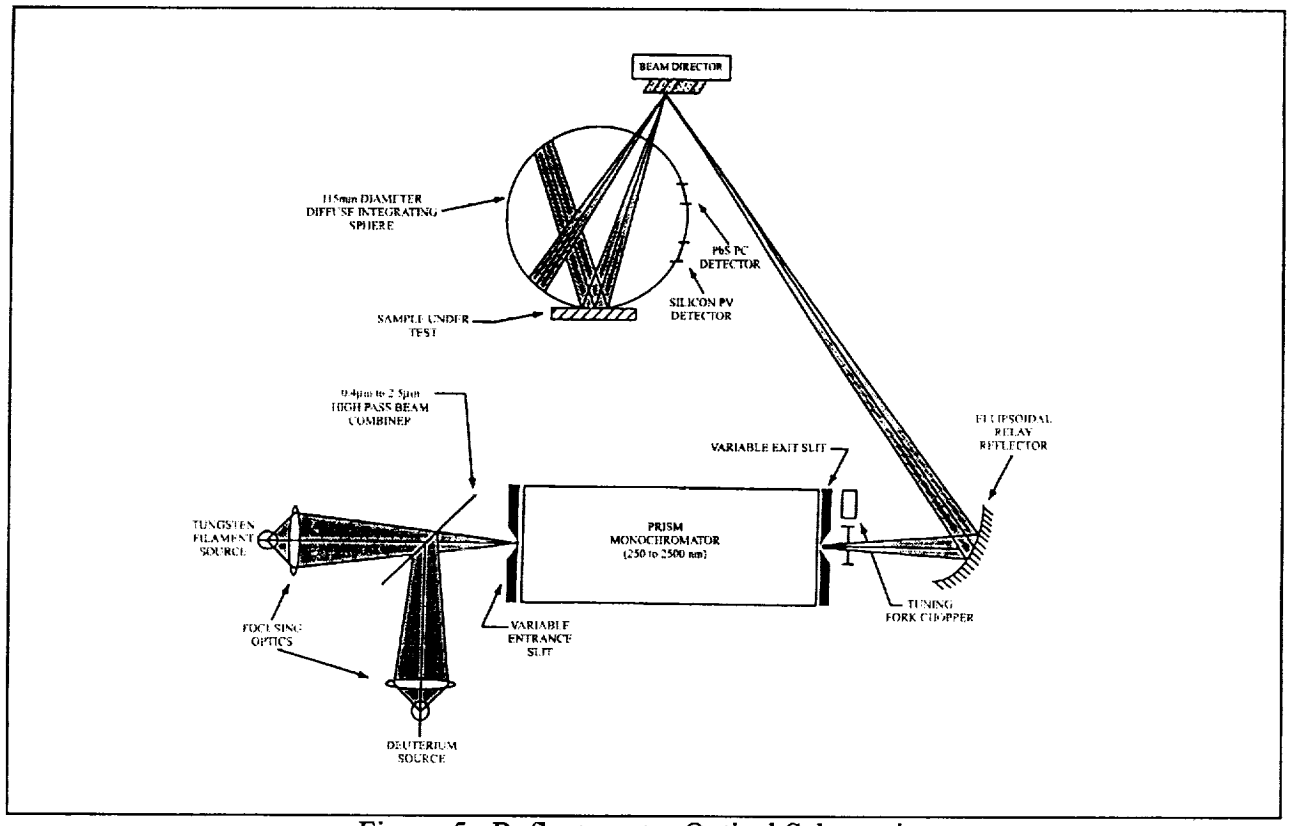

Figure 5. Reflectometer Optical Schematic.

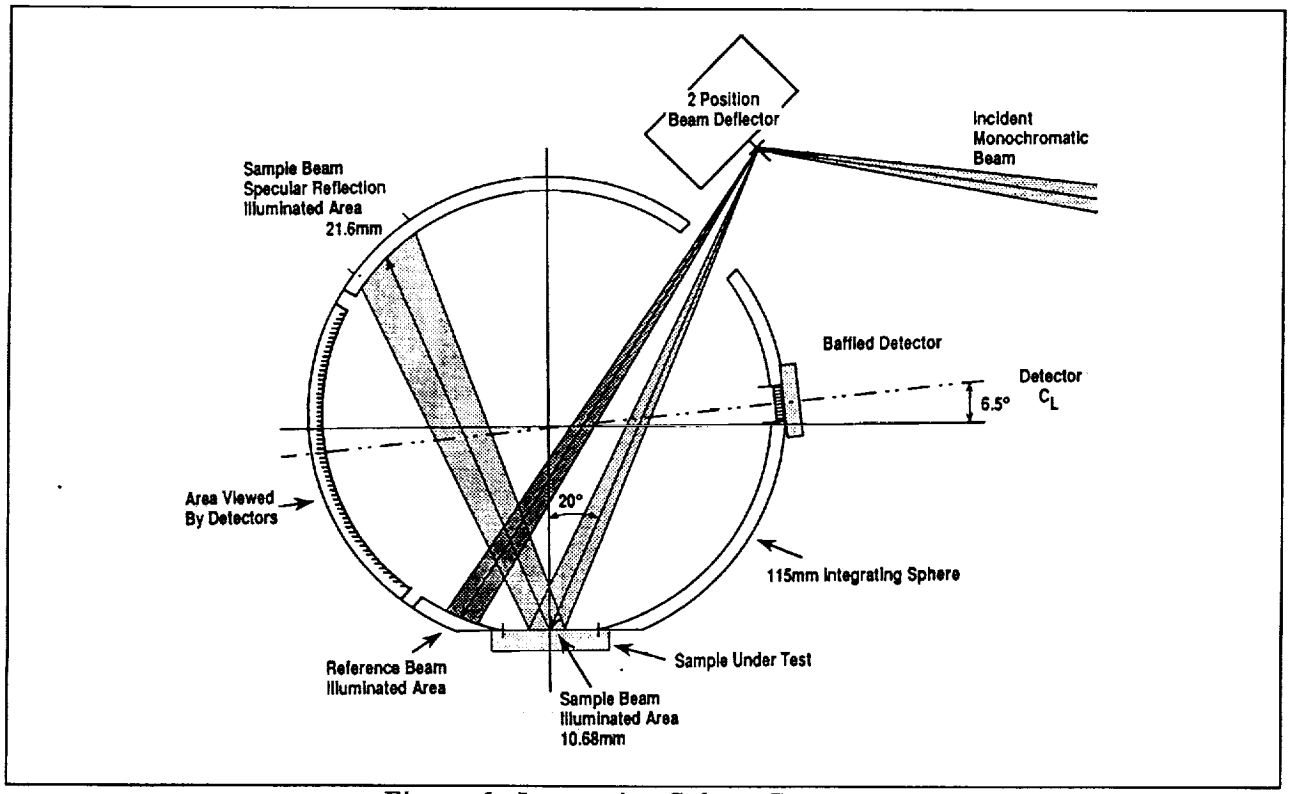

Figure 6. Integrating Sphere Geometry.

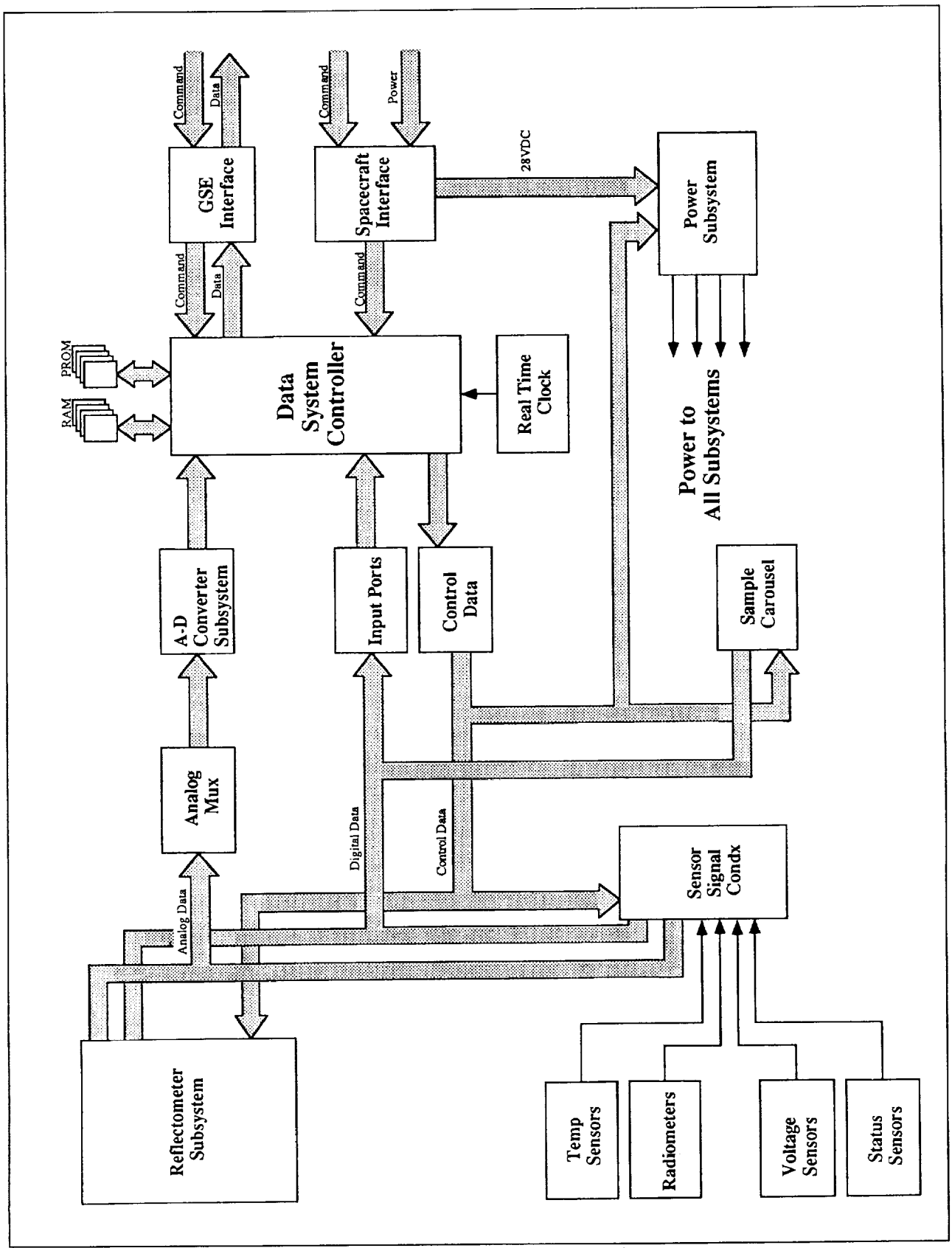

Figure 7. Data Acquisition and Control System.

There were two measurement cycles that the data system controlled: the "daily" measurements and the "reflectance" measurements. The daily measurements were performed once each day after the initial turn-on delay period (refer to Section 3.0). The reflectance measurements were done at intervals varying from once a week at the beginning of the mission to once a month after three months as defined by the stored program in the data system. The test samples were mounted on a carousel which rotated to the protective position for launch and re-entry, to the exposed position where it resided for most of the mission, and positioned each active sample in turn to the reflectance measuring position (see Figure 3, Section 2.4.1).

In the daily measurement sequence (with the carousel in the exposed position), each of 64 analog channels were sampled once each 64 seconds for 90 minutes. The carousel was then rotated to the protected position and the measurements continued for another 30 minutes. At the end of this cycle, the carousel rotated the samples to the exposed position. The analog channels monitored by the DACS are summarized in Table 4.

Table 4. Analog Channels Monitored.

Component	Quantity of Sensors
Radiometers	3
Battery Voltage	3
PRTs (Calorimeters)	25
PRTs (Other)	2
References	4
Thermistors	27
Total	64

In the reflectance measurement sequence, each sample was positioned in-turn under the integrating sphere twice for reflectance measurements. Each sample, beginning with sample one and continuing through sample 25, was positioned under the integrating sphere and the UV portion of the measurements taken. This sequence was then repeated, only in reverse order (sample 25 through sample 1) for the visible and IR measurements. At the completion of this sequence, the carousel rotated the samples to the exposed position.

The reflectometer subsystem is shown in Figure 8. The DACS controls the monochromator wavelength and slit width, selects the appropriate detector and lamp, and measures the reflectance values.

The analog signal processing for the reflectometer is shown in Figure 9. The output from the detector is an AC signal modulated by the 160 Hz chopper and 16 Hz beam director. Figure 10 illustrates the chopped analog signal input to the system multiplexer. This signal is amplified and the 160 Hz modulation is removed using a Phase Sensitive Detector (PSD). The sample and reference portions of the signal selected by the 16 Hz beam director are then separated into two separate channels. Each channel is further processed through active analog integrators providing Multiple Time Averaging (MTA). The output of the integrators is digitized by the system A-D converter and stored in the DACS where further digital MTA can be used as

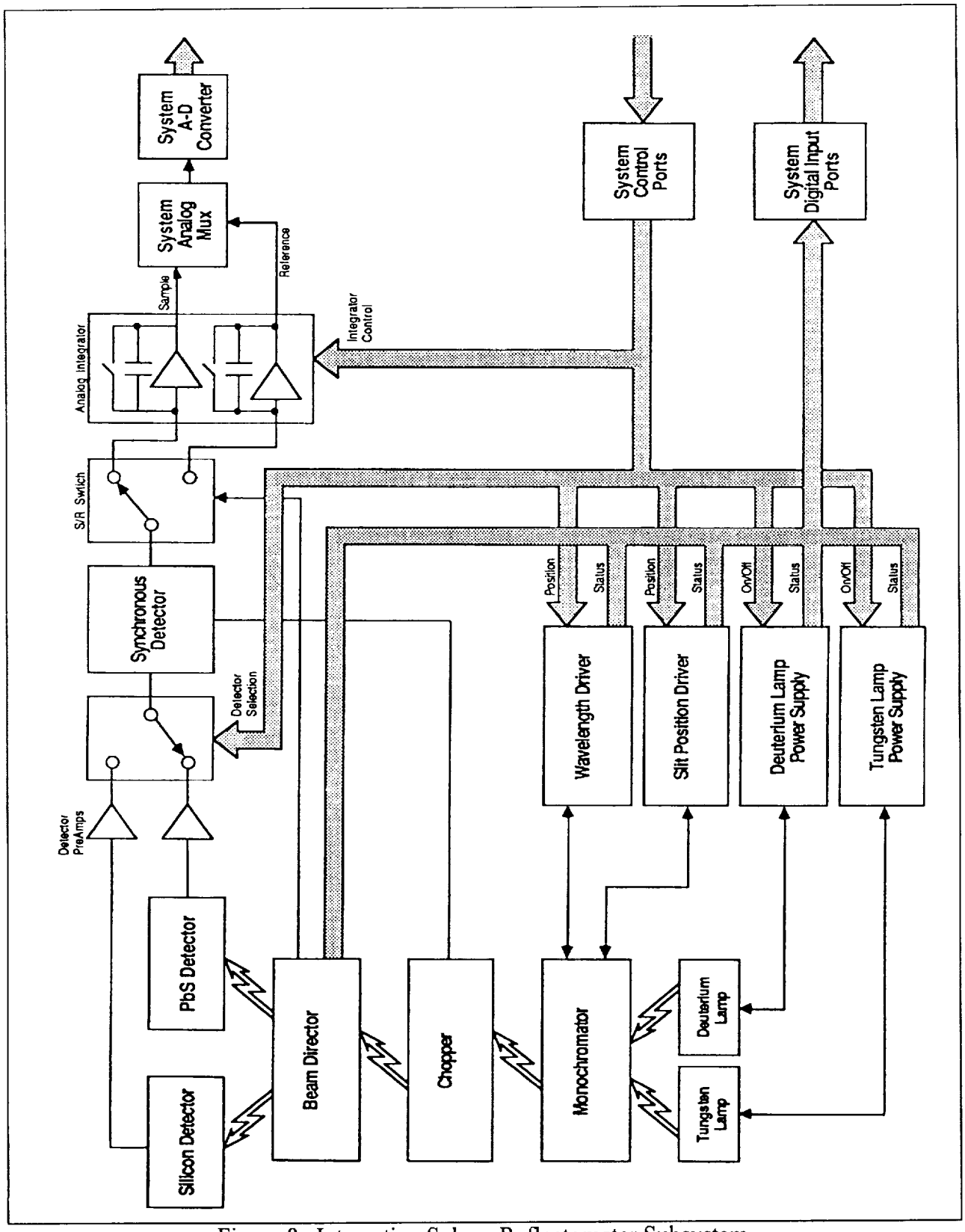

Figure 8. Integrating Sphere Reflectometer Subsystem.

needed to obtain the desired precision. The amplifier gain and the analog integrators are controlled by the DACS. The use of phase sensitive detection techniques, combined with analog and digital MTA, provides an efficient method to minimize the effects of stray light, drift, offset, 1/f noise and white noise.[7]

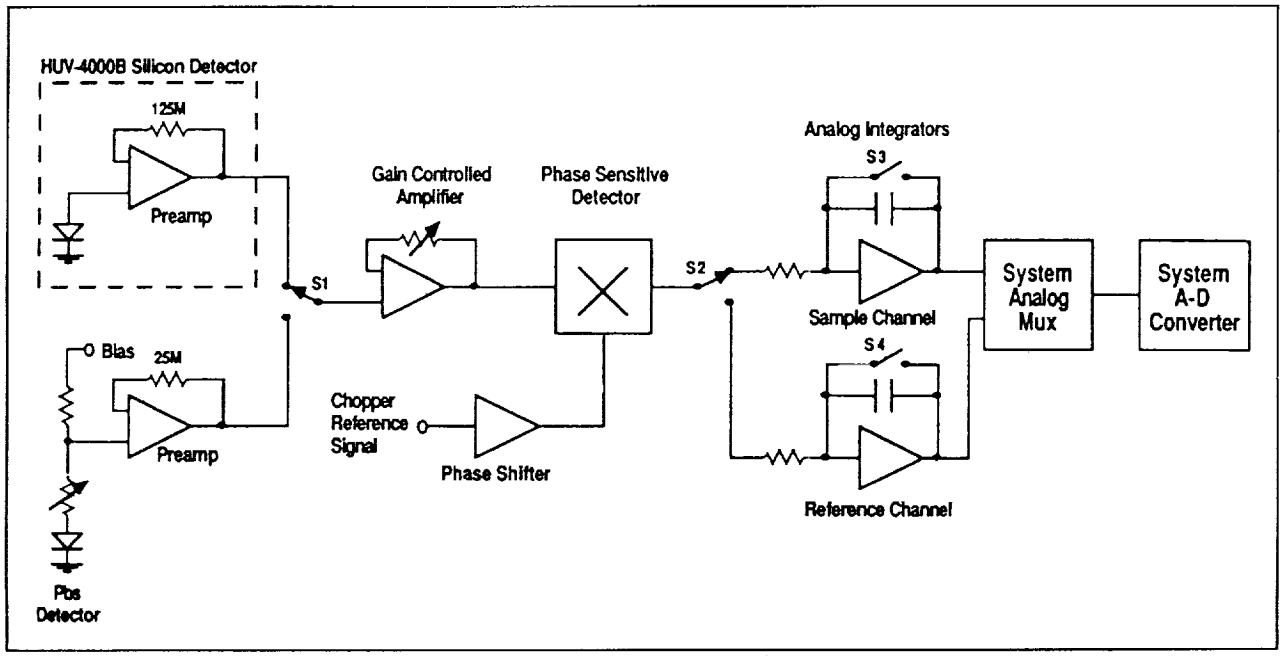

Figure 9. Reflectometer Analog Signal Processor.

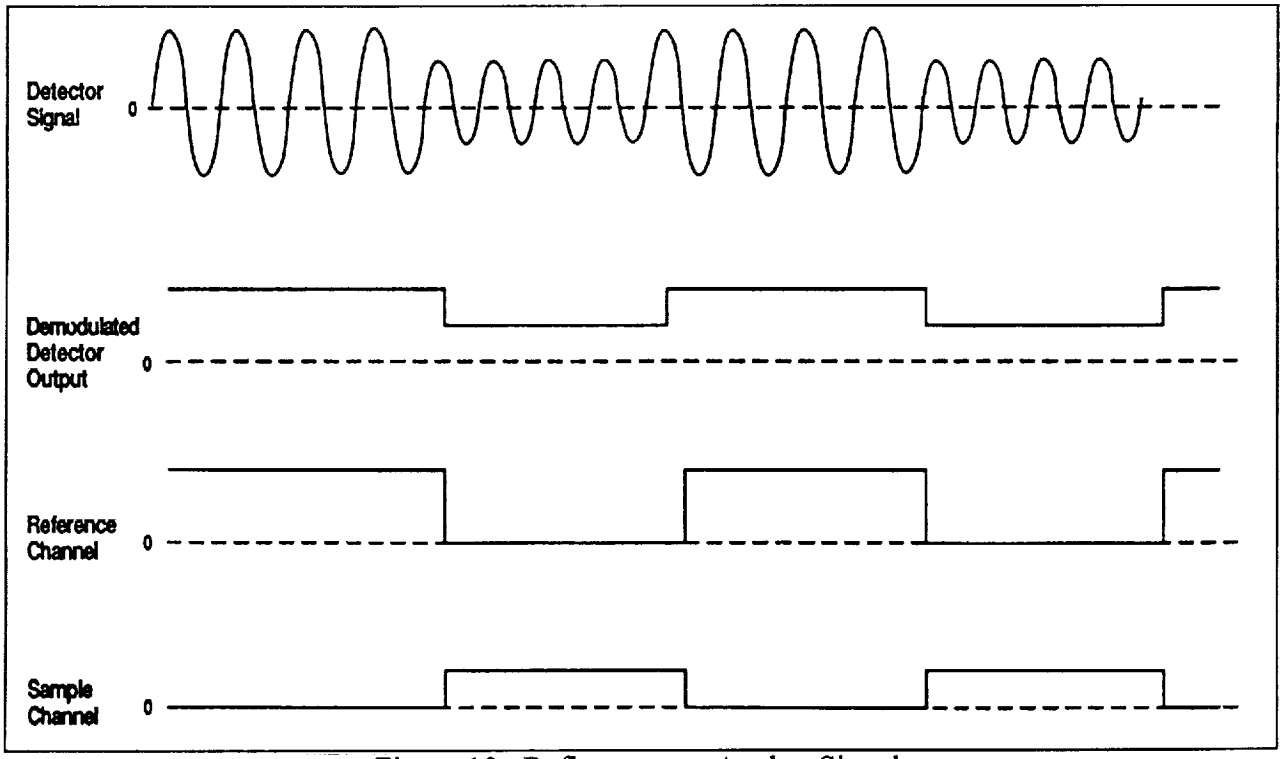

Figure 10. Reflectometer Analog Signal.

2.4.4 Ground Support Equipment (GSE)

For checkout and test, a set of Ground Support Equipment (GSE) was developed to operate the TCSE, read data from the TCSE and/or recorder, decode the data, and present the data for analysis. The GSE, as shown in Figure 11, consists of a GSE control box, an RCA 1802 MicroMonitor, a tape recorder ground reproduce unit (GRU), and a GSE computer including Cathode Ray Tube (CRT) terminal, disk drive, printer, and plotter. The GSE control box simulates the LDEF interface, provides power and power monitoring for ground testing, and provides provisions to input an external clock to speed up ground testing.

Figure 11. TCSE Ground Support Equipment.

The MicroMonitor is an interface to the 1802 Central Processing Unit (CPU) in the flight data system and provides control of the CPU, sets break-points in software, changes and examines memory data, and runs external test software. The GRU provides ground test control of the flight tape recorder for tape motion, tape erasing, and data playback.

The GSE computer system acts as a smart terminal to the MicroMonitor and as a test data storage, decoding, and analysis system. As a smart terminal, the GSE computer can control the MicroMonitor functions and load TCSE test software into the MicroMonitor. The GSE computer can control and test the TCSE tape recorder through the GRU and store TCSE test data

on the GSE disks for analysis. In addition, the GSE computer can test the flight recorder by storing data on tape, replaying it and comparing the data. The GSE computer can also directly record TCSE data by "eavesdropping" on data being sent to the flight recorder by TCSE. The GSE computer can decode the packed TCSE data format, analyze the data, print the daily data, and print (or plot) the reflectometer data.

3.0 TCSE MISSION SUMMARY

The LDEF was placed in LEO by the Shuttle Challenger on April 7, 1984 (see Figure 12). LDEF was retrieved by the Shuttle on January 12, 1990 after 5 years 10 months in space (see Figure 13). The orbit had a 28.5° inclination and an initial altitude of 463 km (250 N mi). The orbit degraded over the 5 year 10 month mission to an altitude of 330 km (178 N mi).

The LDEF was gravity-gradient stabilized and mass loaded so that one end of LDEF always pointed at the earth and one side pointed into the velocity vector or RAM direction (see Figure 14). The LDEF was deployed with the TCSE located on the leading edge (row 9) of LDEF and at the earth end of this row (position A9). In this configuration, the TCSE was facing the RAM direction. The actual LDEF orientation was slightly offset from this planned orientation. The LDEF was rotated about the long axis where row 9 was offset from the RAM direction by about 8°[8] (see Figure 15). This LDEF/TCSE orientation and mission duration provided the following exposure environment for the TCSE:

Total space exposure	5 years 10 months
Atomic oxygen fluence	8.0×10^{21} atoms/cm^2 [9]
Solar UV exposure	1.0×10^4 ESH[10]
Thermal cycles	3.3×10^4 cycles
Radiation (at surface)	3.0×10^5 rads[11]

When the LDEF was placed in orbit by the Shuttle, a "start" signal was sent to the TCSE to engage a relay and turn on the TCSE power. The TCSE was preprogrammed to wait for ten days before exposing the samples to allow the initial outgassing load to diminish.

The TCSE was launched aboard the LDEF with the carousel rotated to the "closed" position to protect the samples from ground processing and the launch environment (see Figure 3).

On mission day 10, the initial daily and reflectance measurements were performed. The carousel was rotated to the open position to expose all test samples. The daily measurements were repeated every day until the TCSE batteries were depleted which occurred on mission day 582 (19.5 months). The reflectance measurements on the test samples were repeated once a week for four weeks, then once every two weeks for eight weeks, and then once a month until battery power was depleted. The TCSE batteries were sized to provide a 50% margin of additional energy for the nominal 9-12 month LDEF mission. The TCSE mission timeline is summarized in Table 5.

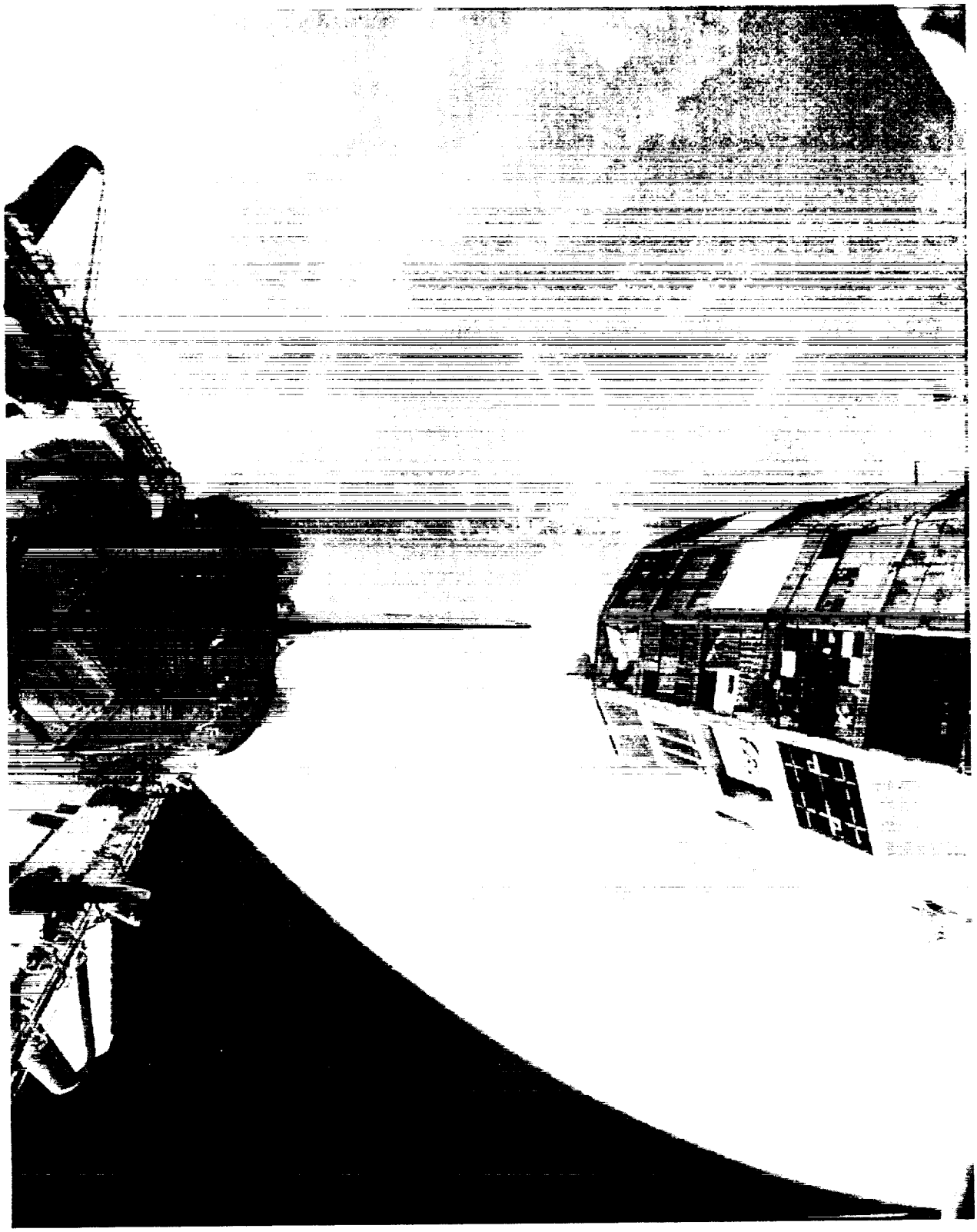

Figure 12. LDEF Deployment.

Figure 13. LDEF Retrieval.

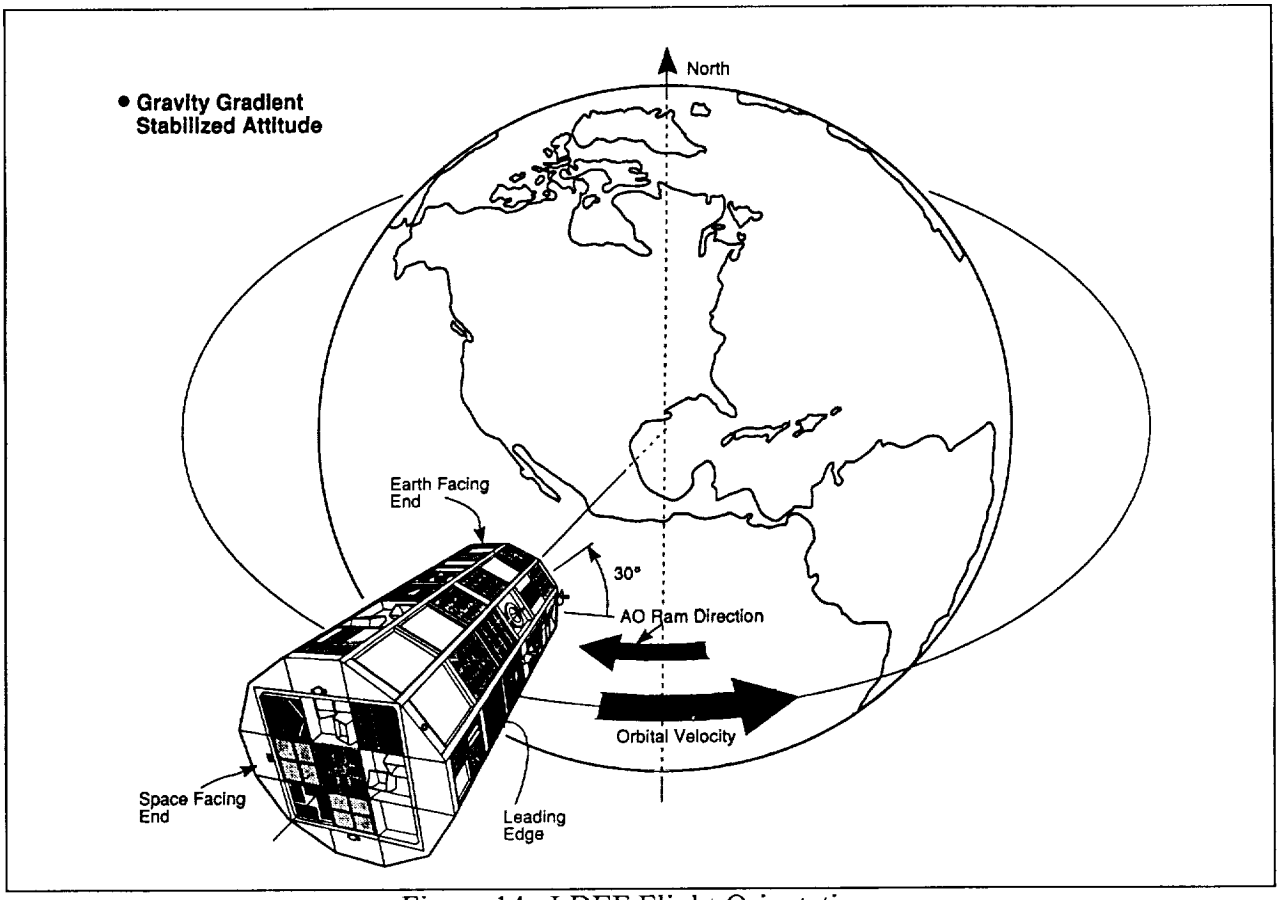

Figure 14. LDEF Flight Orientation.

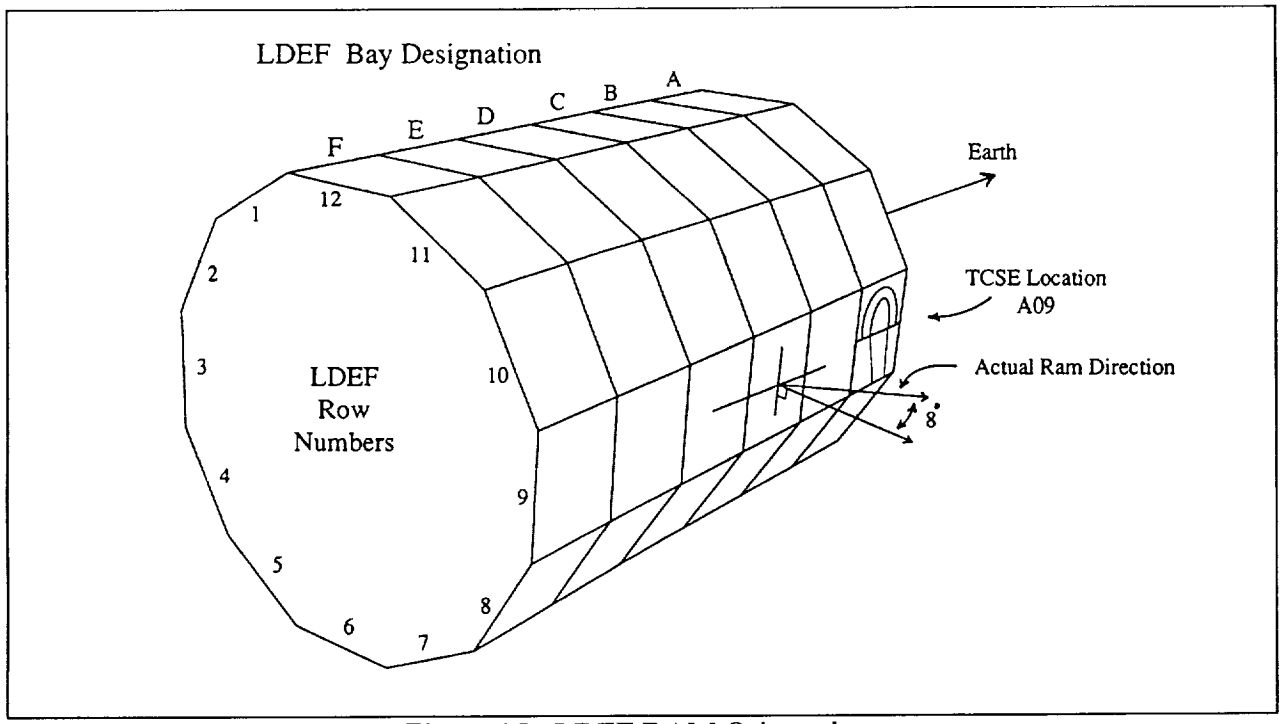

Figure 15. LDEF RAM Orientation.

Table 5. TCSE Mission Timeline Summary.

Mission Time (Days)	
0	LDEF deployment, TCSE start signal
10	Perform initial in-space reflectance and calorimetric measurements
11 (and each day of mission)	Repeat calorimetric and housekeeping measurements
17*	Repeat reflectance measurements *Reflectance measurements were made once every week for the first four weeks, once every two weeks for the next eight weeks, and once a month thereafter.
582	Batteries were depleted and the TCSE systems shut down

As discussed previously, the TCSE operated for 582 days before battery depletion. The battery power was finally expended while the sample carousel was being rotated. This left the carousel in a partially closed position. Figure 16 is a photograph taken during the LDEF retrieval operations showing where the carousel rotation stopped. This carousel position caused 35 of the samples to be exposed for the complete LDEF mission (69.2 months) and 14 exposed for only 582 days (19.5 months) and therefore protected from the space environment for the subsequent four years.

3.1 LDEF/TCSE Deintegration Activities

On February 1, 1990, the LDEF was removed from the Shuttle Columbia at KSC and transferred to a payload processing room for the initial close-up inspection. Special Investigative Groups (SIGs), established by NASA to ensure all LDEF relevant data were collectively archived for future analyses, began their investigations.

The Micrometeoroid and (orbital) Debris Special Investigation Group (M&D SIG) conducted an initial inspection of the entire LDEF structure on February 20-23, 1990 while all 57 experiments were mounted to the structure. From February 23 through April 19, 1990, detailed examination and photo documentation of all experiments was conducted by the M&D SIG team as each experiment was removed from the LDEF structure. The TCSE deintegration occurred in early March. This team documented all craters greater than 0.5mm in diameter and all penetration holes greater than 0.3mm in diameter. The size, type, location and feature characteristics of all documented impacts were recorded.[12] Stereo-microscope imaging systems were fitted with color Charge Coupled Device (CCD) cameras, 35mm cameras, and fiber optic cold-light illuminators for viewing. Data were recorded on optical-disk cartridges and archived in the Johnson Space Center (JSC) Curatorial Facility Data Vault. A summary of these results is presented in Table 6.

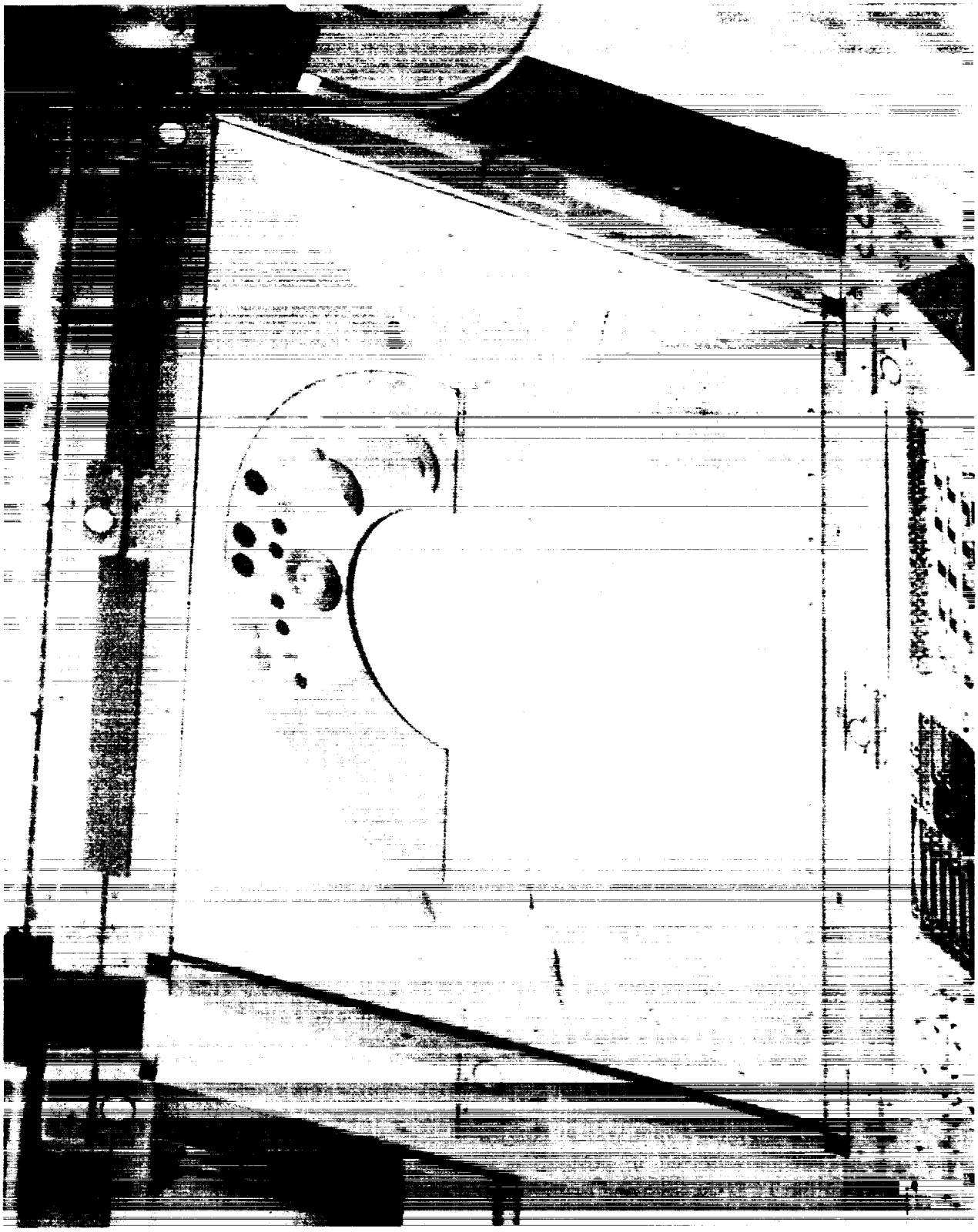

Figure 16. TCSE Condition at LDEF Retrieval.

Table 6. M&D SIG TCSE Feature Summary.

Impact Dimensions	Mounting Shims	Clamps, Bolts Flanges	Tray Surfaces	Experiment Surfaces
<0.5mm*	6	0	0	543
>0.5mm	5	3	3	39
Totals	**11**	**3**	**3**	**582**

*Impacts less than 0.5mm were counted, not photo documented. Impacts less than 0.1mm were not counted.

One penetration occurred on the TCSE front cover. The M&D published report states, "The largest documented feature was a 2.5mm diameter impact in the silver Teflon cover. This impact delaminated a considerable amount of the Teflon blanket and exposed the silver backing to oxygen erosion." Figure 17A provides a close-up view of the impact showing the crater and silver Teflon layer "blown" back from the crater rim. At location "1" of Figure 17A, the Teflon layer has radial cracks emanating from the crater impact center. Some of the silver/inconel layer is still attached to the Teflon. For the silver Teflon closest to the impact area, the silver/inconel and adhesive layers are missing. The exit of the impact event is shown in Figure 17B, with the small region indicated at area "1".

Following the M&D SIG investigation, the TCSE was shipped back to MSFC for data analysis. At MSFC, the TCSE covers were removed and the interior of the instrument visually and photographically inspected.

Data from the LDEF, and the TCSE, soon became the focus of other space programs. In March 1990, during the early phase of data analysis, the HST program office requested information from the MSFC and TCSE investigators regarding the space environmental effects on silver Teflon. This material is installed on the HST 2.7 m (9 feet) aft shroud external surfaces and questions had arisen about its durability for extended space missions, especially with the visual appearance of the LDEF silver Teflon surfaces. To support this inquiry and respond in a timely fashion for the planned April 1990 launch of the HST, portable instruments were used to measure the optical properties of the silver Teflon surfaces on TCSE and other MSFC experiments. The TCSE and other MSFC experiments were deintegrated earlier than planned in the LDEF post-mission processing so additional analyses could be performed.

The results of these studies determined that the HST thermal system had sufficient margins to function with the degradation observed on the LDEF mission. This cooperative effort exemplifies the significance of the TCSE and LDEF data for future long duration space missions.

4.0 TCSE SYSTEM PERFORMANCE

The TCSE flight hardware system performed very well during the LDEF mission. A few anomalies have been detected in post-flight data analysis, inspection, and functional tests. Performance of the TCSE system and operational anomalies are described in this section.

Front View

Rear View

Figure 17. Impact Penetration of Front Panel.
(Panel: 6061AL; 0.063 MIL Thickness)

4.1 Recorder

The TCSE data system utilized a Lockheed Electronics Company (LEC) model MTM four-track tape recorder to store the flight data. The flight recorder was removed and hand-carried to the LEC for transcription of the flight data and an analysis of the condition of the recorder.[13]

Upon opening the recorder it was determined that a relay in the track switching circuit had failed with the wiper on one set of contacts stuck in an in-between state. This condition prevented the relay from receiving additional track switching commands and resulted in the overwriting of one of the three tracks of data collected by the TCSE. The LEC engineers manually energized the relay coil and the relay contact latched properly. This relay and the complete recorder system performed within specification for the check-out tests and flight data playback.

The MTM tape recorder is a four-track unit that records tracks 1 and 3 in the forward direction and tracks 2 and 4 in the reverse direction. At the completion of the TCSE mission, the recorder stopped with the tape positioned near the end of track 1. However, it was determined that track 3 data was written over track 1 data. Because the MTM recorder uses a saturation recording method, track 3 data was recovered. Track 2 data was recovered with no problems. Some track 1 data was apparent in gaps between track 3 data blocks. The LEC and NASA/LaRC personnel provided a very valuable service in this analysis and in the recovery of the TCSE flight data.

The recovered TCSE flight data was decoded and separated into data sets. By analyzing the clock data in each data set, it was determined that the TCSE operated for 582 days (19.5 months) after LDEF deployment. Data were recovered for the last 421 days of this operational period. The overwriting of track 1 data by the recorder resulted in the loss of data for the first 161 days of the TCSE mission. The recovered data included eleven reflectometry data sets and 421 daily data sets.

4.2 Reflectometer

Data reduced from the flight recorder indicate the reflectometer performed very well. In Figure 18, the measurement repeatability over several months is observed to be generally within 1-2%. This excellent performance indicates that measured changes by the TCSE reflectometer were accurate and did occur.

The post-flight analyses of the TCSE reflectometer consisted of visual inspections and functional tests. Visual and black light inspections of the reflectometer components revealed no unusual surface features (i.e., discoloration, deformation, aging, etc.). The integrating sphere coating was intact. There was no evidence of mechanical misalignment after the extended mission. Functional tests were conducted on the reflectometer subsystem components, including the tungsten and deuterium lamps and the monochromator wavelength and slit stepper motors, to determine their status after the prolonged space exposure. A functional test was also conducted

on the complete reflectometer subsystem. Functional tests on components were performed first to verify function and check for start-up power transients. System level tests followed to verify system performance.[2]

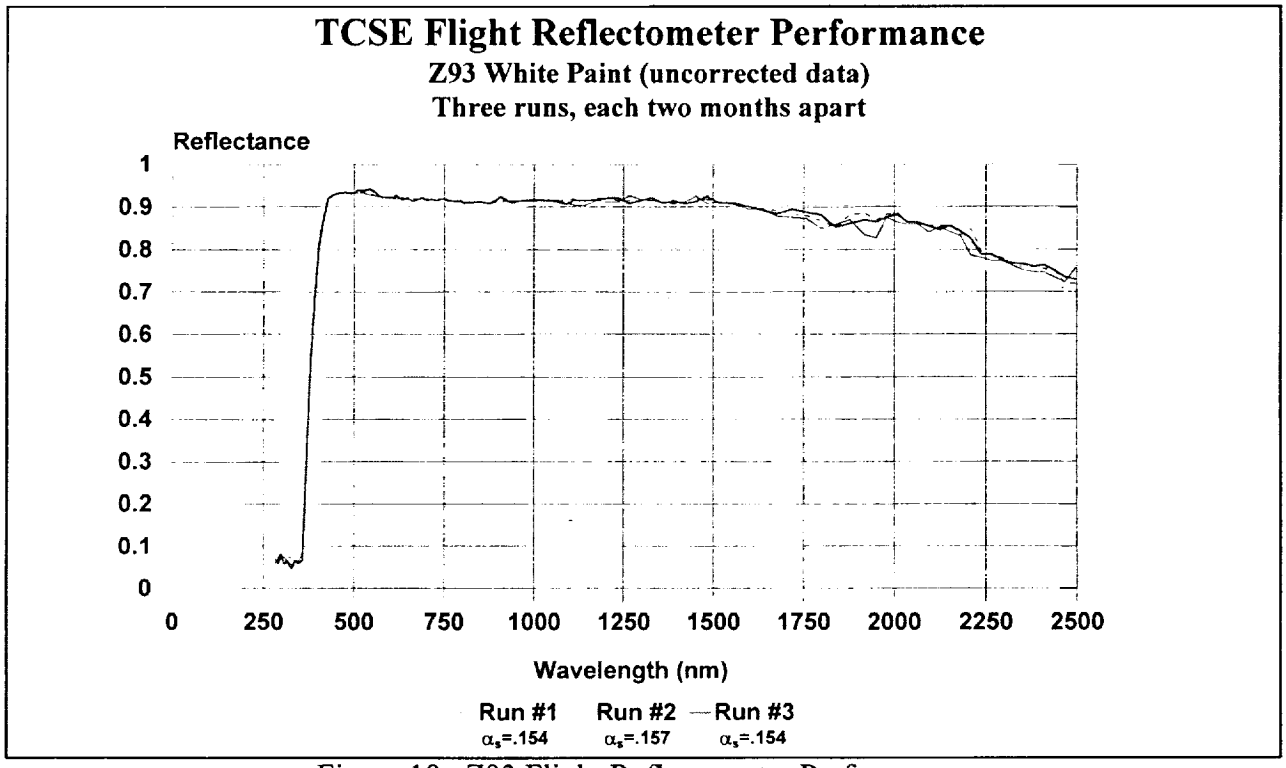

Figure 18. Z93 Flight Reflectometer Performance.

The component functional test results of the two lamps and power supplies were nominal. The lamps and power supplies responded to computer control as designed. There were no measured atypical power transients. The tungsten lamp irradiated normally at power on, and a visual check in the integrating sphere verified the visible spectrum between 500 and 700 nm. The deuterium lamp irradiance appeared slightly unstable due to flickering of the lamp arc. No visual inspection was possible of the UV energy from the monochromator.

Functional tests of the two stepper motors on the monochromator were nominal. No adverse power transients were recorded at power on and the stepper motors responded to computer control.

A functional test of the reflectometer subsystem followed the component level functional tests to determine overall system health. The functional test measured reflectance of ground control samples. The reflectometer subsystem operated normally.

The reflectance data from this functional test was decoded and analyzed to determine the condition of the reflectometer subsystem. The near IR data from 2500 nm to about 600 nm looks reasonable with signal levels on the same order as pre-flight values (even a little higher above 1500 nm); however, a little more noise is evident in the data. From 600 nm to 400 nm, signal levels are significantly lower and noisier but some data is usable. Below 380 nm, where the deuterium lamp is used, the data is suspect. Signal levels appear to be high enough to provide good measurements but the data do not agree with ground measurements. For example, the white paint test samples should have low reflectances (<10%) below 380 nm, but very few points are in that range. The data in the lower visible and UV suggest a wavelength shift in the measurements. Figures 19-21 are examples of the post-flight measurements made with the TCSE reflectometer. Several data points in the UV were well over 100% and were omitted from these curves.

4.3 Batteries

Four standard lithium range safety batteries were used to power the TCSE. These batteries were developed for the Shuttle Solid Rocket Booster (SRB) range safety system. The batteries were selected based on their high energy density and ready availability at MSFC. These batteries had a predicted life of greater than 15 months from calculated power requirements which was more than adequate for the planned 9-12 month LDEF mission. Each battery was rated at 28 Volts Direct Current (VDC) and self-contained in a two-part Nylafil case. An ethylene propylene o-ring was used to seal the case. Due to the characteristics of the lithium electrolyte, each cell was designed to vent into the cavity when overpressurization occurred. During an overpressurization condition, a small diaphragm on each cell balloons out and is pricked by a metal pin to relieve pressure. The escaping gas is then contained within the Nylafil case by the ethylene propylene o-ring.

During the initial post-flight analysis, a noticeable odor was evident during TCSE deintegration at the MSFC. The source of odor from inside the TCSE was identified as the electrolyte from the lithium batteries. The batteries were removed from the TCSE and bagged. Each of the four batteries in the TCSE had this odor. One battery was cut open to check the cell diaphragms and the battery o-ring. All cells had vented, noted by punctured diaphragms. In addition, the battery o-ring was checked for compression sets and was measured to be 100% (see Figure 22). Since the compression set on the o-ring was 100%, electrolyte gas was able to escape from the batteries. The o-ring did not operate as designed.

Post-flight data reduction revealed the battery temperature ranged from 13 to 27°C (refer to Section 4.6). This temperature range permitted most of the battery energy to be utilized and enabled a long-life mission. Battery voltage ranged from a nominal 36 VDC near mission initiation down to 25 VDC at battery depletion. Figures 23 and 24 illustrate measured battery voltages during the TCSE mission. The battery voltage was measured at very low current draw which represented a nearly open circuit condition.

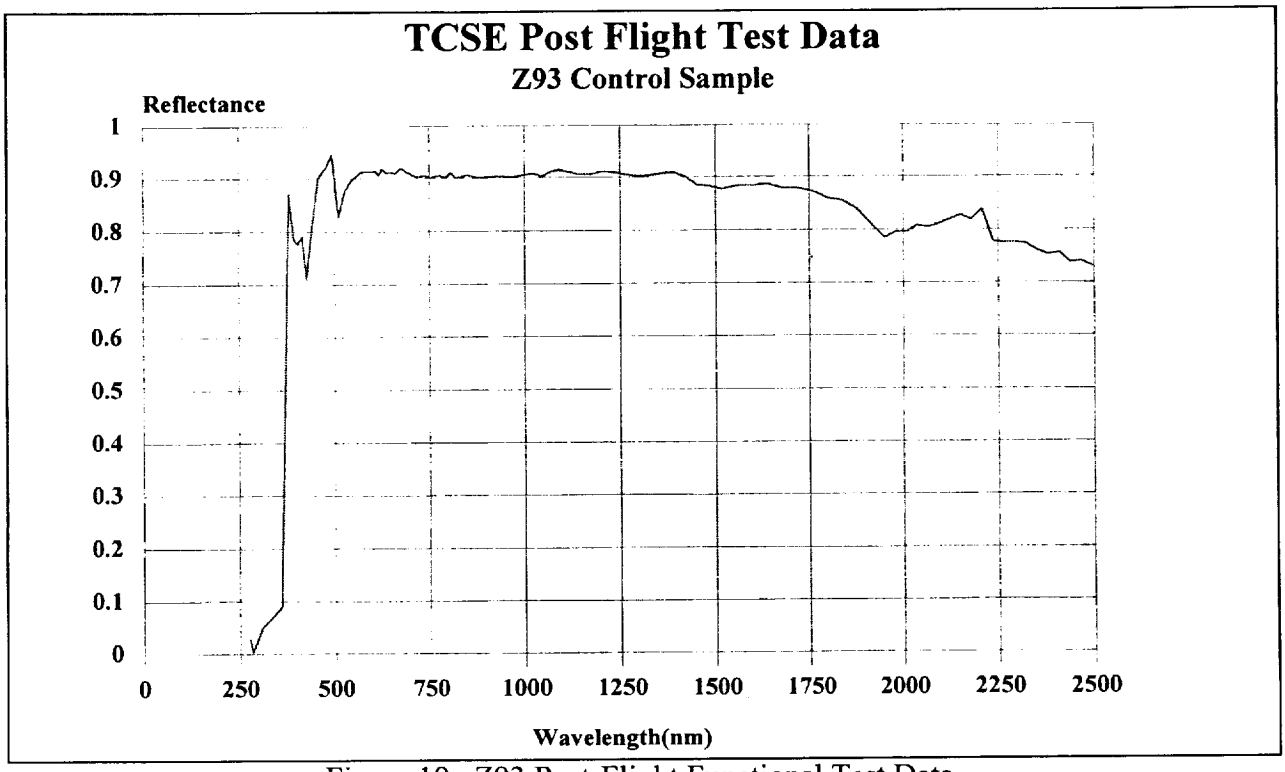

Figure 19. Z93 Post-Flight Functional Test Data.

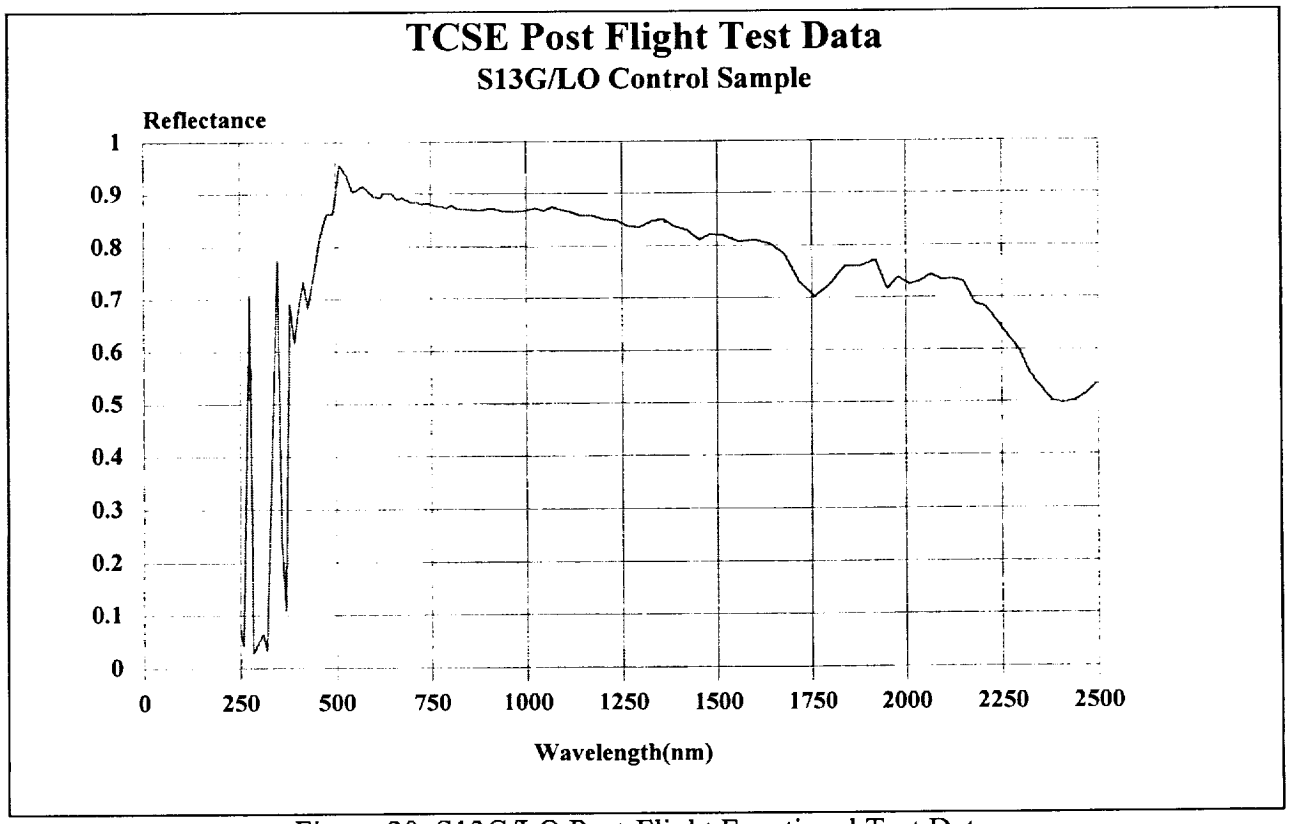

Figure 20 S13G/LO Post-Flight Functional Test Data.

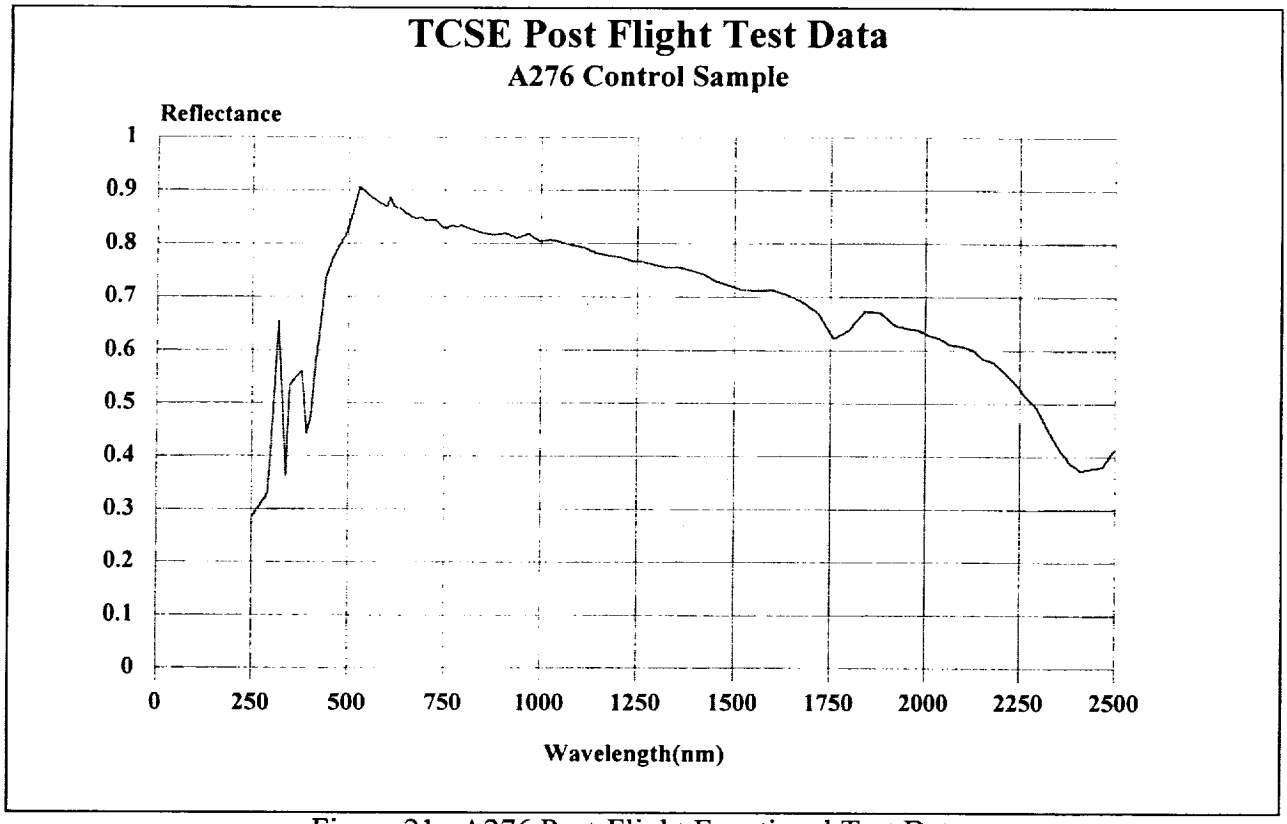

Figure 21. A276 Post-Flight Functional Test Data.

Battery life extended through 582 mission days (19.5 months), well beyond the intended mission time of 12 months, and beyond the anticipated battery lifetime of 15-18 months.

4.4 Sample Carousel

The carousel subsystem provided protection for the samples during launch and positioned the active flight samples under the reflectometer integrating sphere for measurement.

Post-flight analyses of the recorded TCSE data showed that the carousel subsystem operated as designed most of the time, but indicated an intermittent rotational problem. From the recorded flight data, the carousel drive mechanism experienced some difficulty in rotating reliably from sample position 25 to sample 24 during the reflectance measurement. This difficulty appeared to be more prominent towards the end of the useful battery life. This problem was investigated during the post-flight functional check-out test.[2] Attempts were made to simulate the problem by adjusting the battery supply voltage (and energy levels) from 28 to 21 volts as well as energizing the lamps and other components of the reflectometer subsystem to simulate increased energy requirements on the power system. Unfortunately, the carousel rotation anomaly could not be reproduced in these ground tests. Other conditions of the space environment (i.e., thermal, vacuum, etc.) were not simulated which may have synergistic effects on the carousel drive motor operation. All other post-flight carousel functional tests were normal.

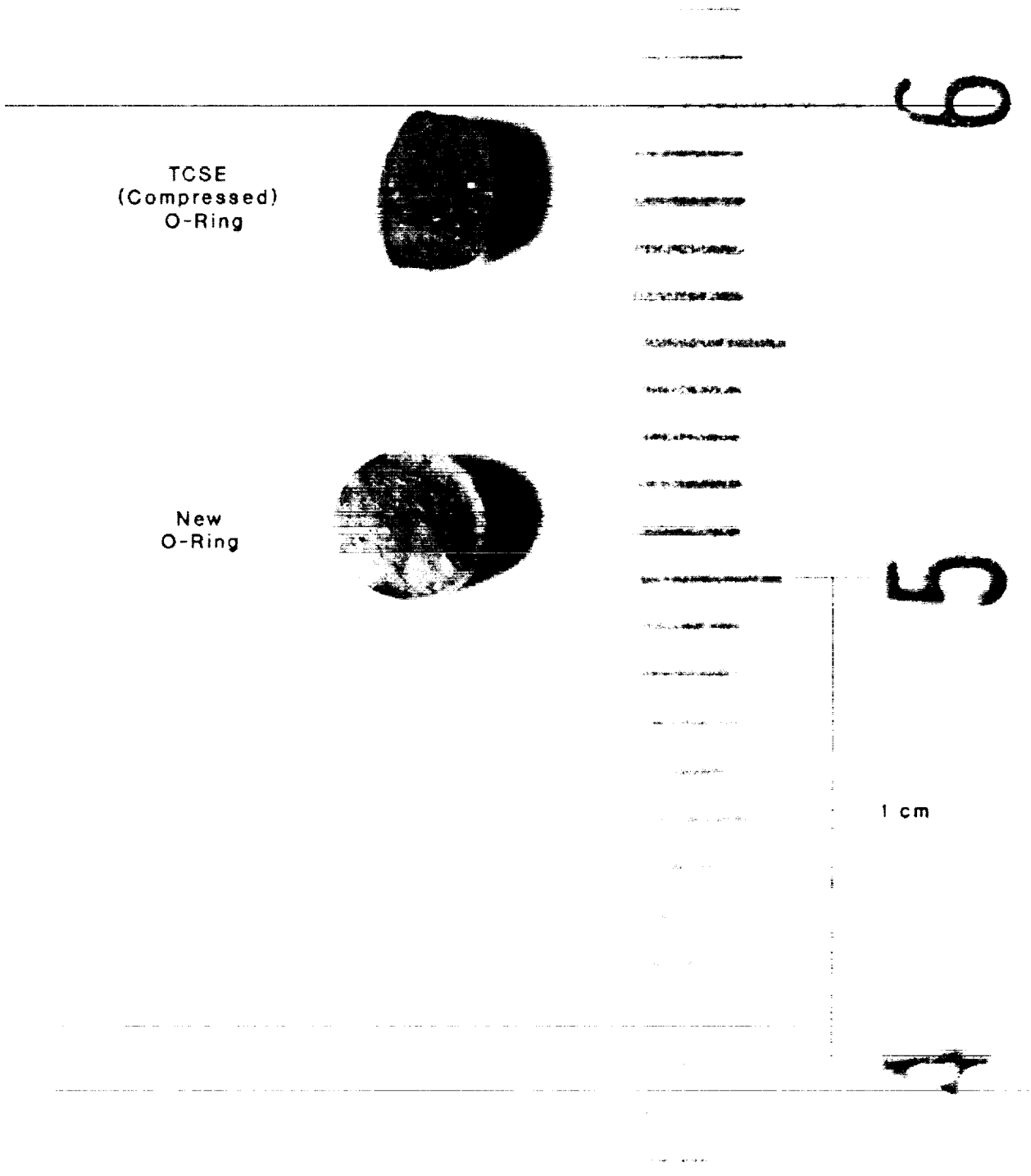

Figure 22. Battery O-Ring Deformation.

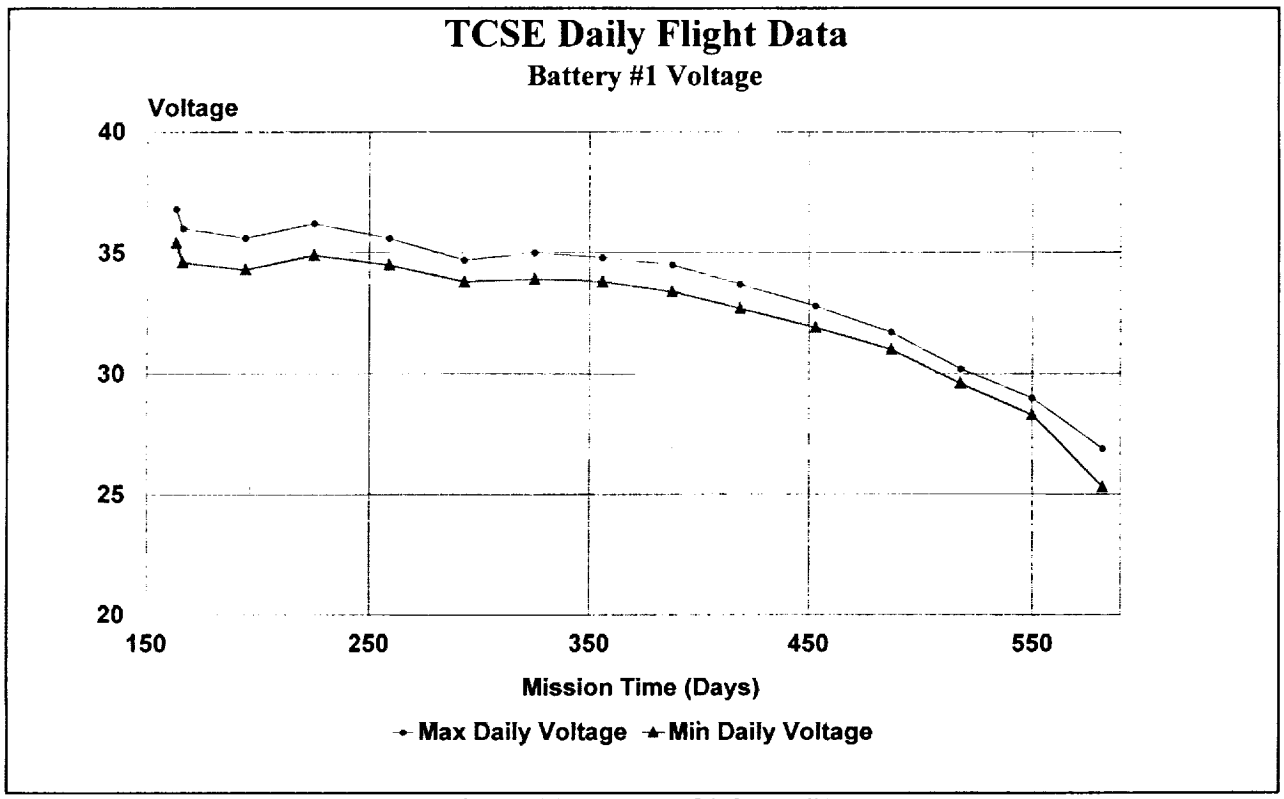

Figure 23. Battery Voltage #1.

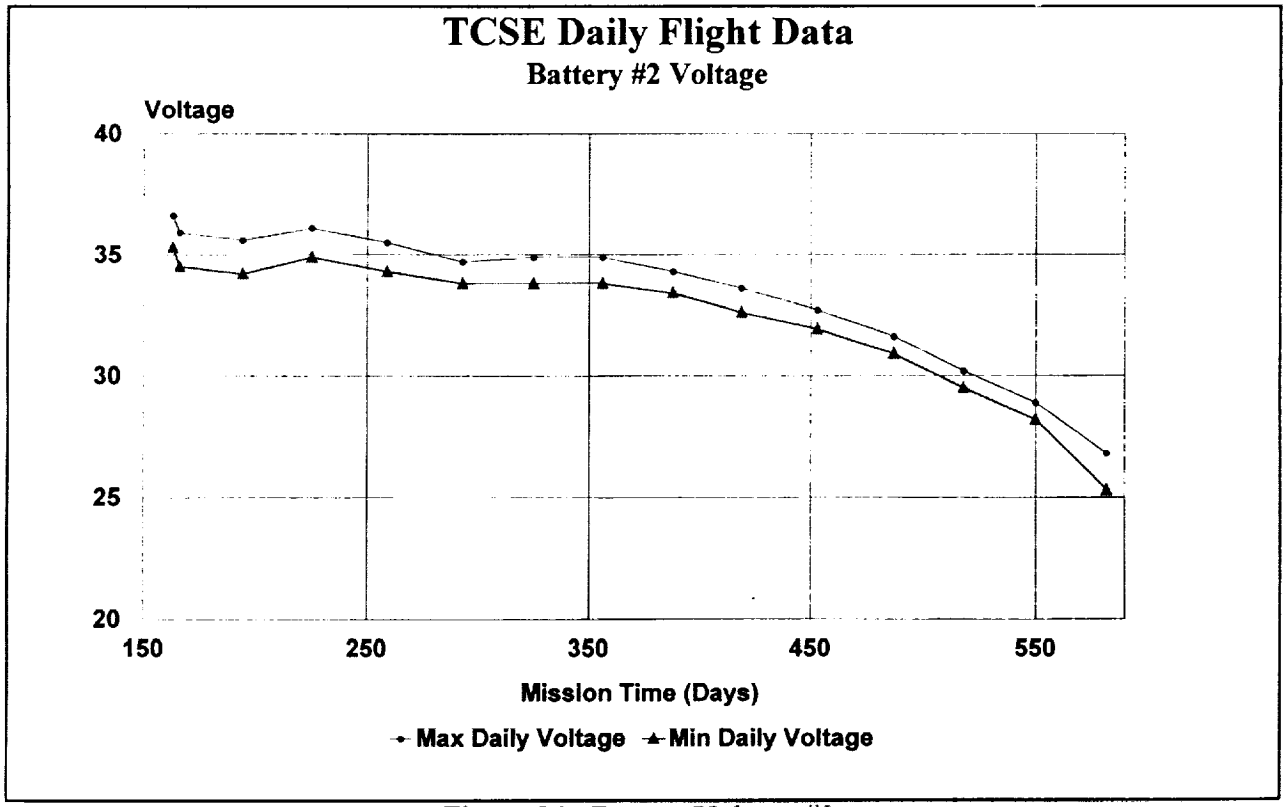

Figure 24. Battery Voltage #2.

4.5 Data Acquisition and Control System (DACS)

The analysis of the TCSE flight data shows that the DACS performed very well during the active TCSE mission. Post-flight functional tests show that the DACS remains functional after the extended dormant period in space.[11]

The clock data on each recorded data buffer showed that the DACS started a measurement sequence precisely on 24 hour increments as measured by the TCSE clock. The daily sequence was repeated for 582 days until the batteries were depleted. Because of the recorder malfunction, only the last 421 days of data were recovered.

The data from the post-flight functional tests were analyzed to check the condition of the analog measurement system. There were five reference channels among the 64 analog channels. These provided a calibration for thermistors and platinum thermometers on the calorimeters. The values of these readings depend on the current sources in the measurement circuits, the precision reference resistors, the scaling amplifiers, and the A-D converter. For four of these reference channels, the range of values measured over the two hour test exactly matched the in-flight values. The fifth measurement was off one count in 900 or just over 0.1%. This test verified that the analog measurement system remains within design specifications.

Only one anomaly has been observed in the DACS operation. The 25th clock bit appeared to be set to a logical "1" too early and remained in that condition throughout the mission. This bit was also set to "1" during the post-flight testing, indicating a failure. This condition was not a problem in the data analysis because the sequential nature of the data allowed recovery of the full clock data.

4.6 Thermal

The thermal design requirements for the TCSE mission, defined at the TCSE Critical Design Review, are given in Table 7. Scenarios for zero solar input (cold case or minimum temperatures) and predicted solar input (hot case or maximum temperatures) were used as specified in the LDEF Users Handbook[14] to determine the thermal environment that the TCSE could expect during its mission. Some yaw (x-axis) instability was expected for this gravity-gradient stabilized satellite and was considered in the thermal analysis. However, little yaw occurred, and the satellite proved to be very stable, resulting in very moderate temperatures.

Table 7. Allowable and Predicted Thermal Data.

Component	Allowable Temp. Limit		Predicted Temp. Limit	
	Min (°C)	Max (°C)	Min (°C)	Max (°C)
Integrating Sphere	-50	60	-25	41
Batteries	-30	60	-23	43
Electronics (DACS)	-40	70	-27	41
Emissivity Plate			-25	40

The TCSE used 2 mil silver Teflon as the outside (exposed) surface coating and black painted aluminum for inside and back surfaces. The top cover (shroud) was thermally isolated from the TCSE structure. The TCSE was thermally coupled to the massive LDEF structure for passive thermal control, and was dependent upon this environment for thermal stability.

Thermistors were used to sense temperature extremes throughout the TCSE. Fifty three temperature sensors (thermistors) and PRTs were installed on the TCSE. The components measured and quantity of sensors used are given in Table 8. Only the thermistor data is presented in this report. Figure 25 illustrates the general placement of the thermistors. The DACS recorded the temperature data at predetermined intervals during the TCSE mission until the power source (4 batteries) was expended. Data recovered from the flight recorder were reduced and calibrations applied to determine temperature data on selected TCSE components. Table 9 compares predicted data to measured data for some components, and presents other data for reference. The measured data temperature ranges represent the lowest and highest temperatures recorded by any of the applicable sensors. Figures 26-32 represent typical daily thermal excursions experienced by selected TCSE components.

Table 8. Thermal Monitored Components.

Component/Quantity	**Type of Sensor**		**Quantity of Sensors**
	Thermistor	**PRT**	
Integrating Sphere/1	X		1
Batteries/4	X		3
Electronics (DACS)/1	X		2
Emissivity Plate/1	X		4
Radiometers/3	X		3
Passive Sample Holders/5	X		5
Shroud (Top Cover)/1	X		5
Calorimeters/25		X	25
Reference Sensors/4	X	X	4
Flight Recorder/1	X		1
			53

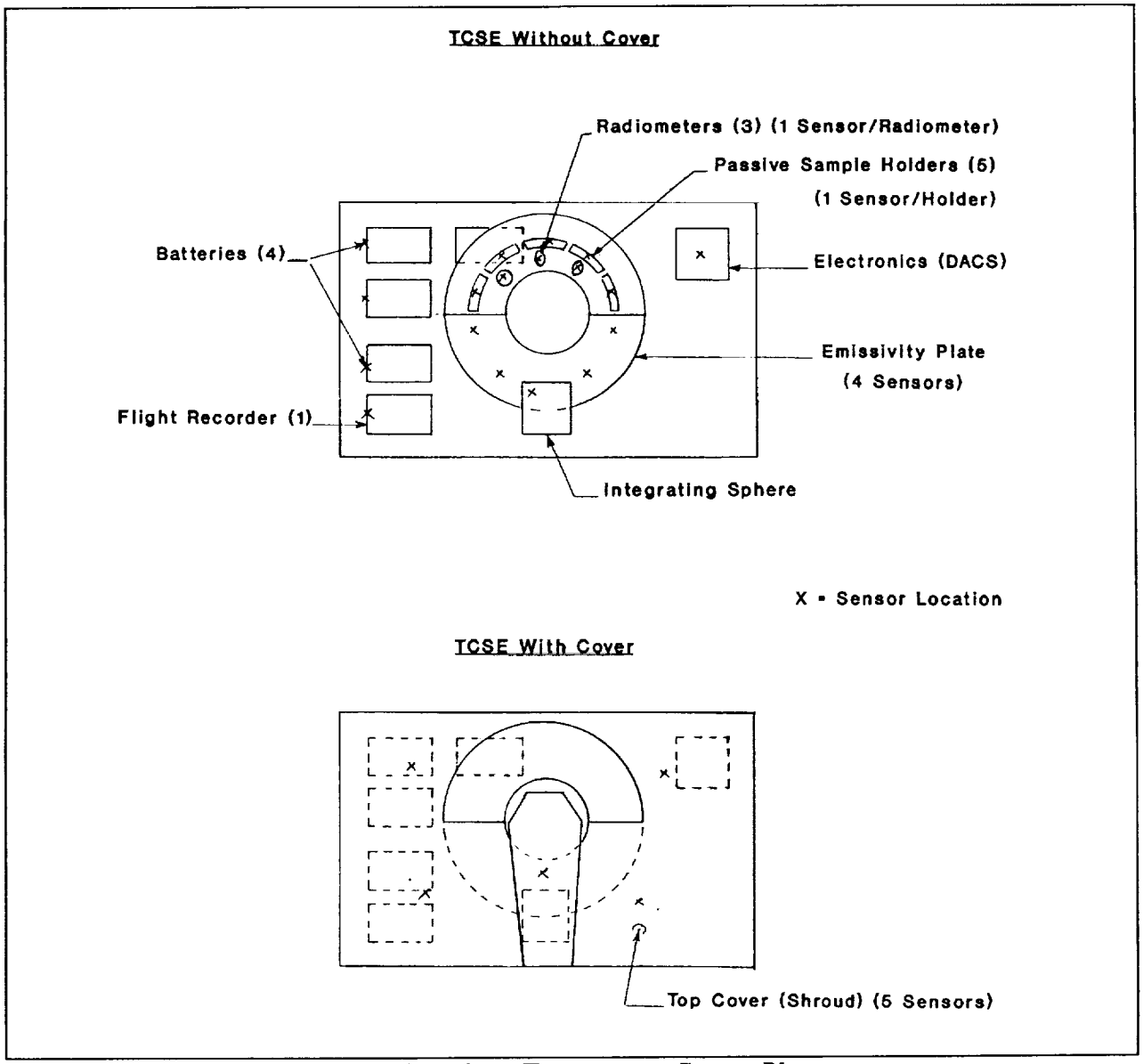

Figure 25. Thermistor Temperature Sensor Placement.

Table 9. Predicted vs. Measured Thermal Data.

Component	Predicted Temp. Limit		Measured Temp. Limit*	
	Min (°C)	Max (°C)	Min (°C)	Max (°C)
Integrating Sphere	-25	41	6	19
Batteries	-23	43	13	27
Electronics (DACS)	-27	41	17	29
Emissivity Plate	-25	40	-2	17
Radiometers			14	39
Passive Sample Holders			15	43
Shroud (Front Cover)			-43	5

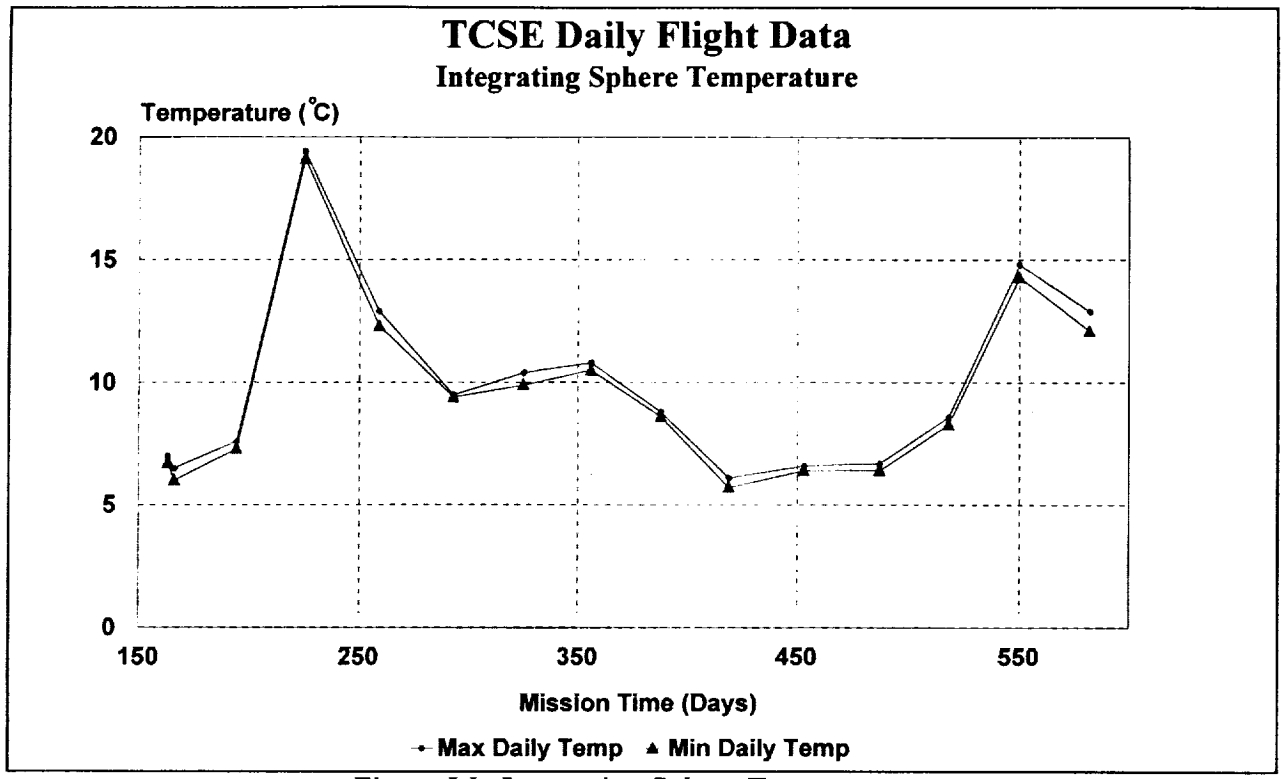

Figure 26. Integrating Sphere Temperatures.

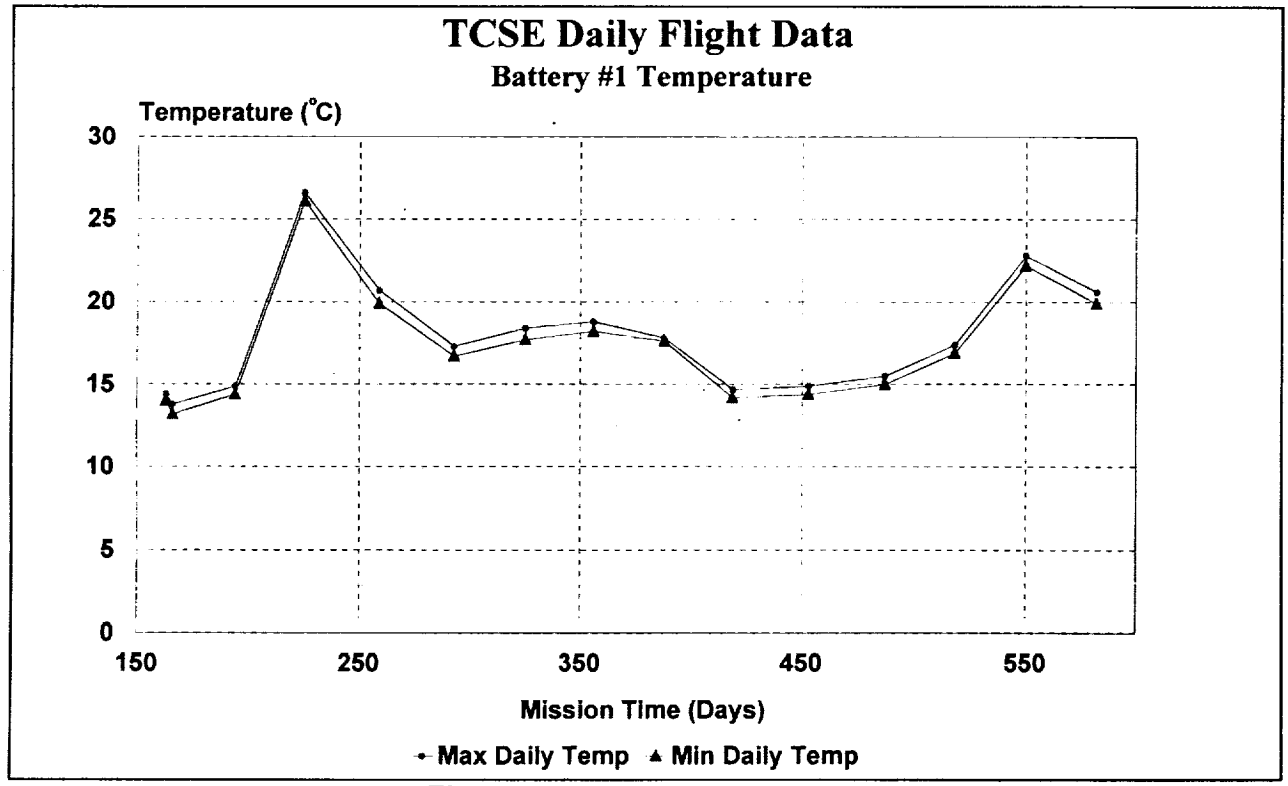

Figure 27. Battery Temperatures.

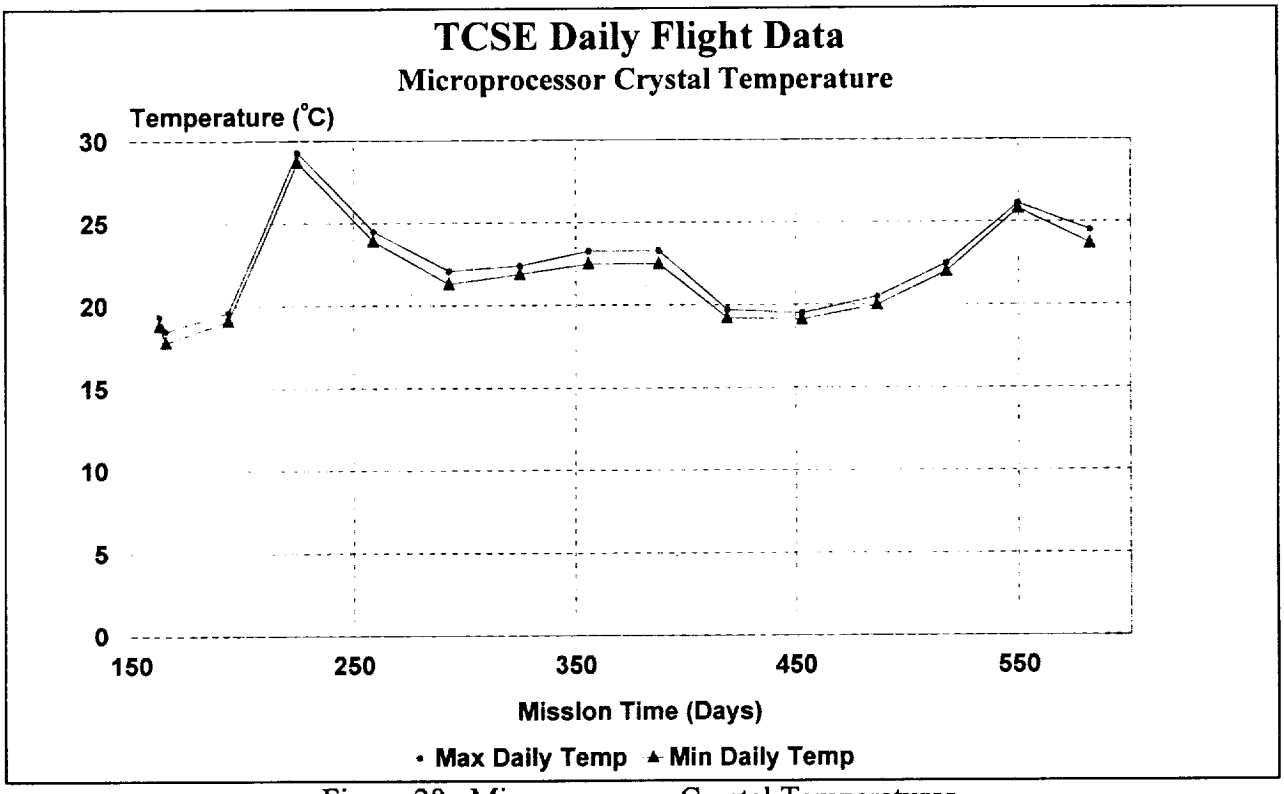

Figure 28. Microprocessor Crystal Temperatures.

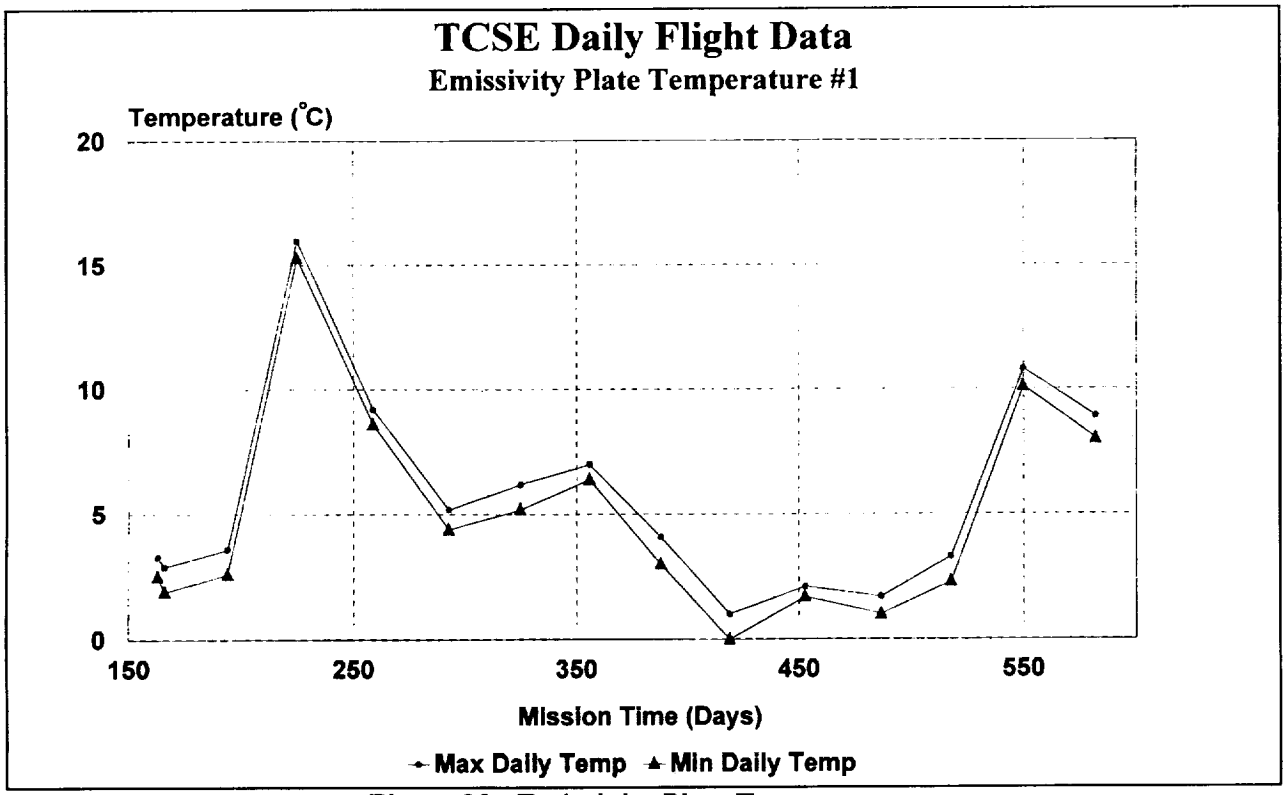

Figure 29. Emissivity Plate Temperatures.

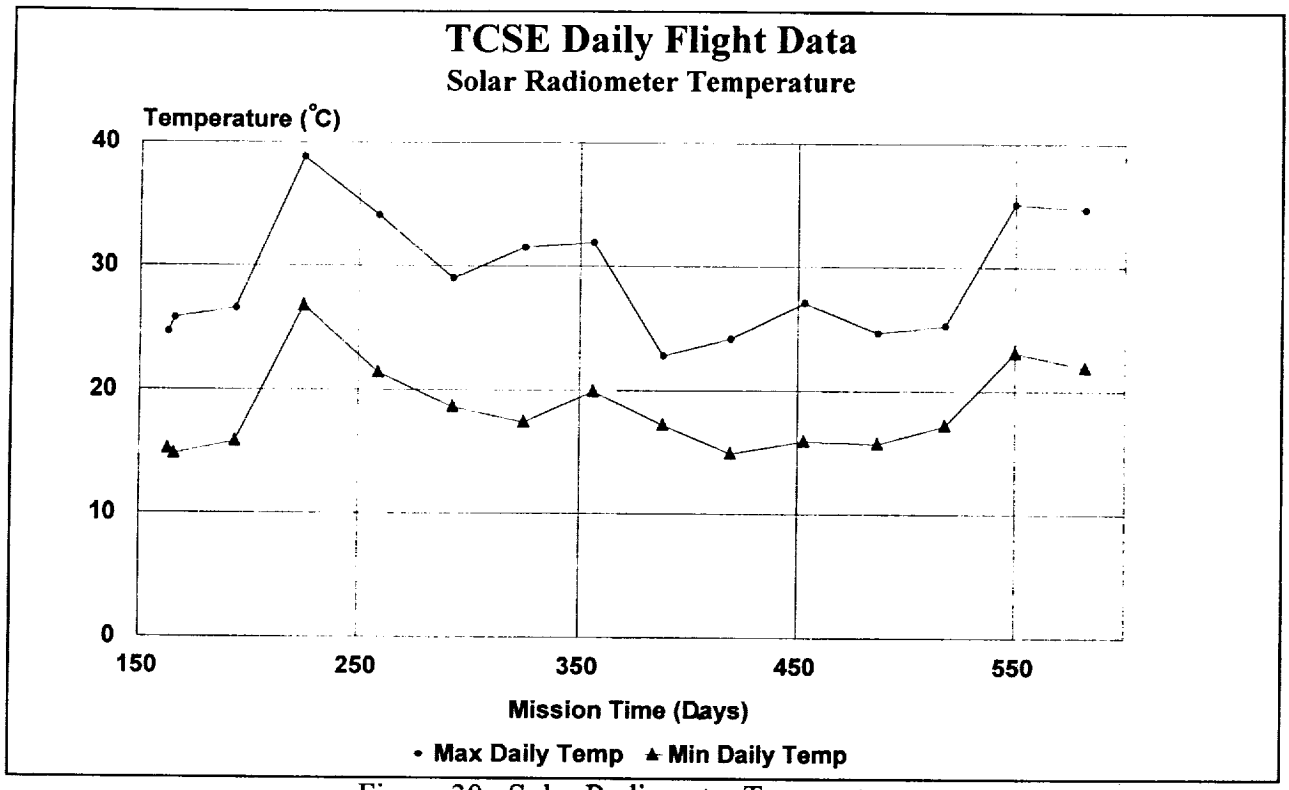

Figure 30. Solar Radiometer Temperatures.

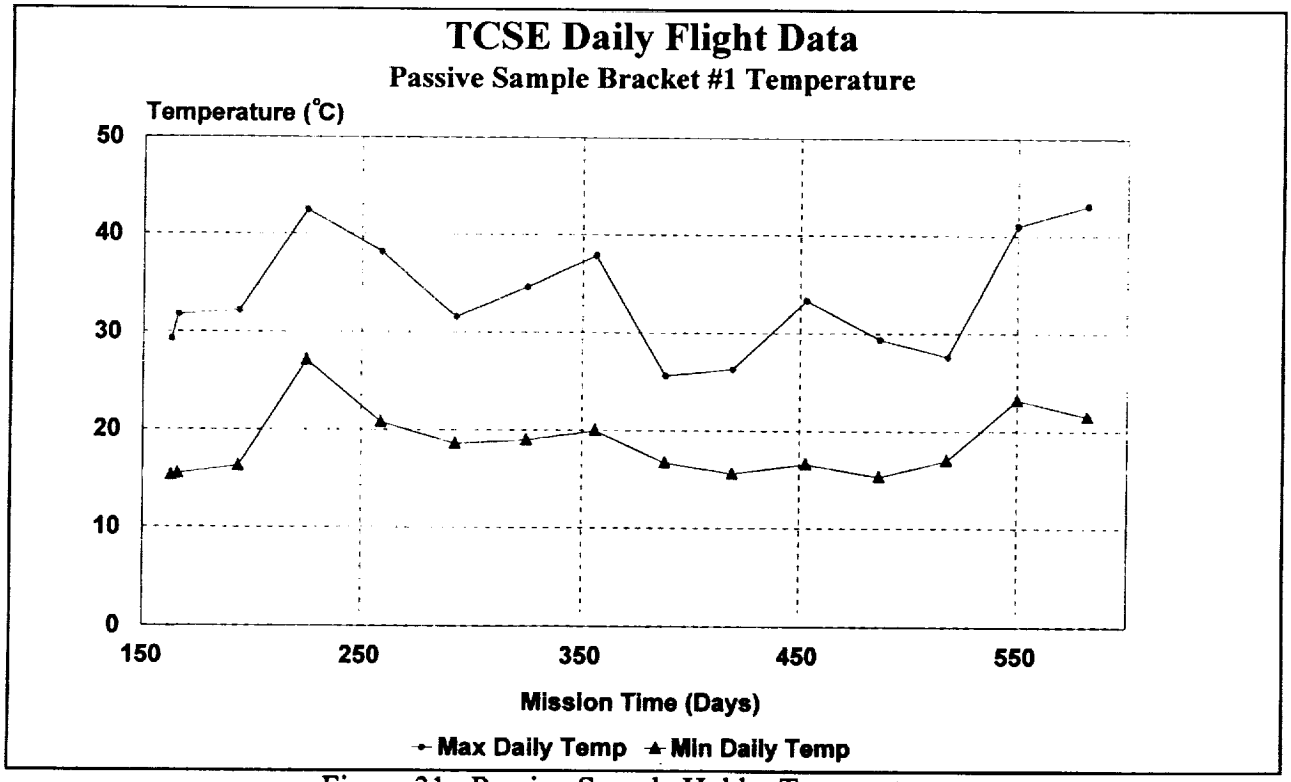

Figure 31. Passive Sample Holder Temperatures.

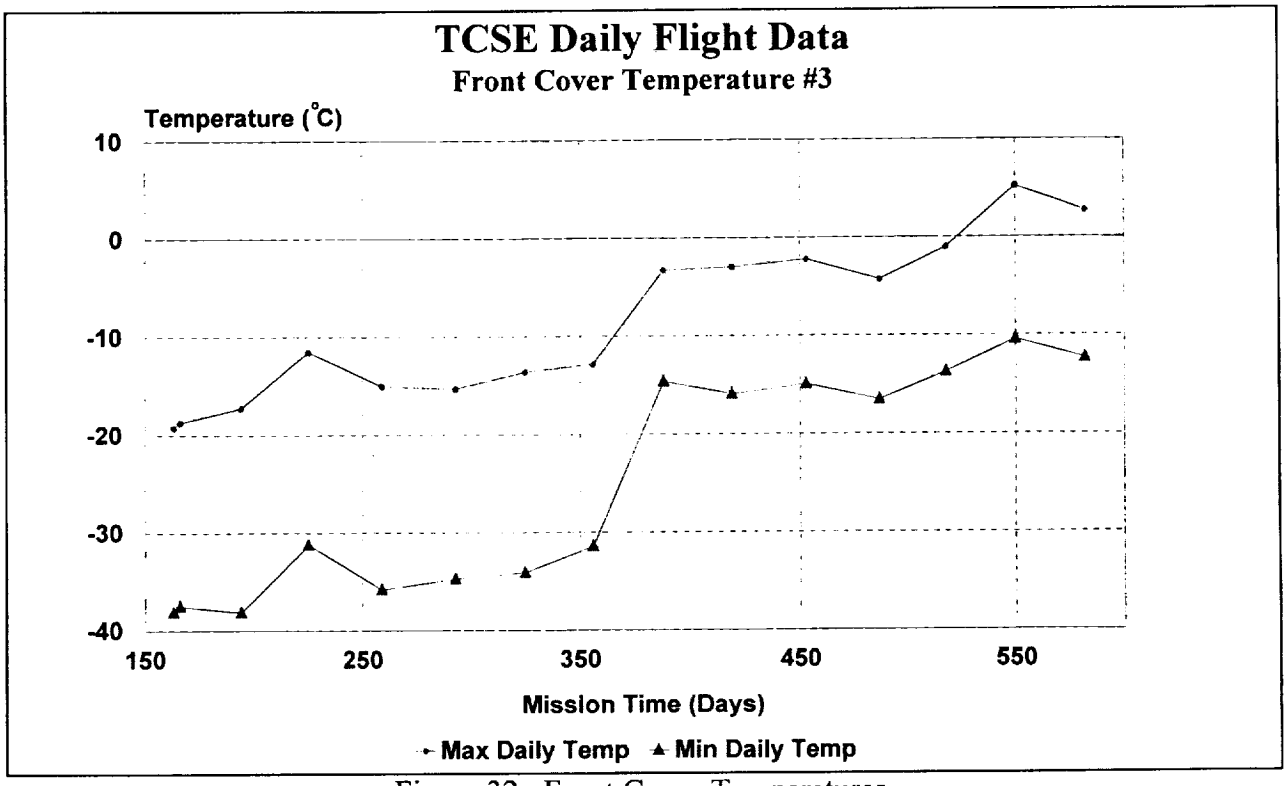

Figure 32. Front Cover Temperatures.

5.0 MATERIALS ANALYSIS

The primary objective of the TCSE mission was to determine the effects of the space environment on thermal control surfaces. The effects and the mechanisms of these changes are very complex because of the synergism of the constituents of the space environment. This section describes the results of the analyses performed on the flight samples and other materials on the TCSE.

Many different changes were observed in the TCSE samples due to their prolonged space exposure. These changes ranged from the obvious cracking and peeling of the overcoated samples to the subtle inducement of UV fluorescence in some samples. Some samples changed more than expected while others changed less than expected. The measured effects of the atmospheric AO are probably the most significant because of the large total AO fluence (8×10^{21} atoms/cm^2)[9] on the TCSE surfaces due to the LDEF orbital attitude. Figures 33 and 34 are pre-flight and post-flight photographs of the TCSE samples showing changes to many of the samples. Figure 35 shows the position and material of each of the 49 TCSE flight samples.

Many analysis tools were used to determine the effects of the LDEF LEO exposure environment on the TCSE flight materials. Section 5.1 discusses the primary optical properties measurements and the condition of the flight sample materials. Section 5.2 discusses the trend analysis of the data to develop a long term degradation model for selected materials. A number of other analyses were used to further define the material changes due to the LDEF LEO

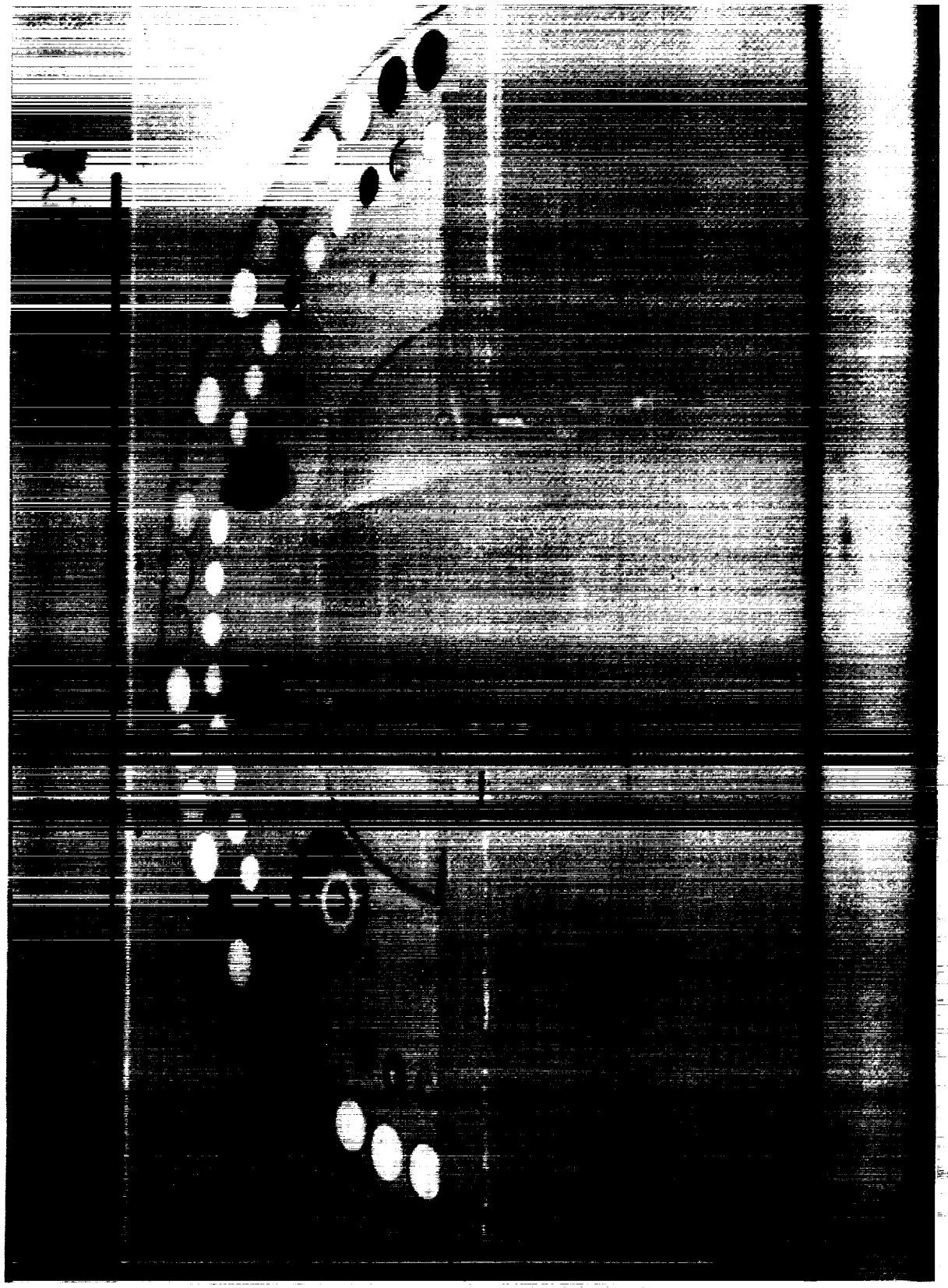

Figure 33. Pre-flight Photograph of the TCSE Flight Samples.

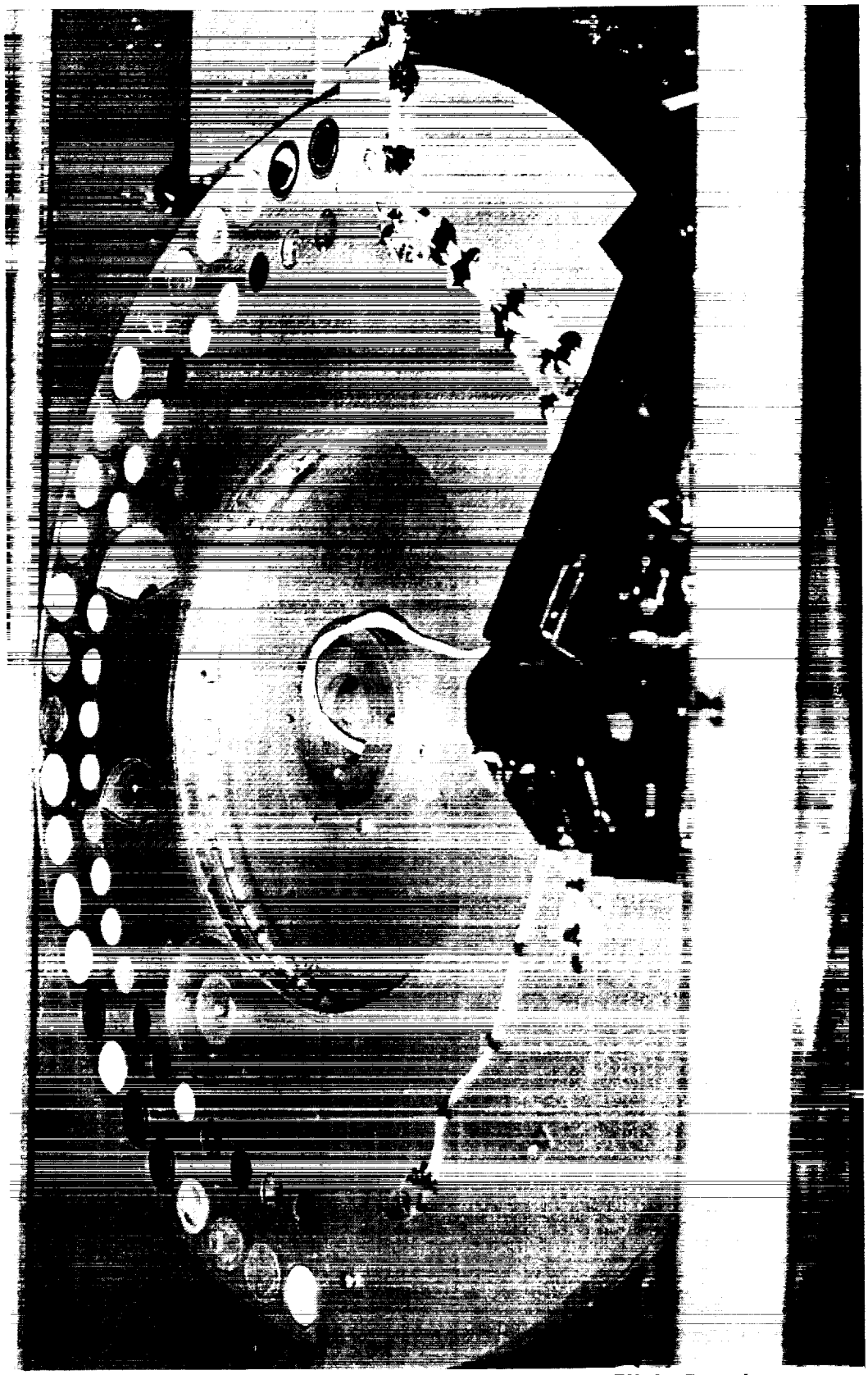

Figure 34. Post-flight Photograph of the TCSE Flight Samples.

TCSE Active Samples		
Sample #	Material	C ID #
13	Ag/Teflon	C 90
14	YB 71/Z 93	C 93
15	S13G/LO	C 92
16	YB 71	C 96
17	Z 93	C 95
18	D-111	C 99
19	Tedlar	C110
20	Z 302/RTV 670	C105
21	Z 302/OI 650	C104
22	Z 302	C101
23	A 276/RTV 670	C 88
24	A 276/OI 650	C 87
25	A 276	C 82

TCSE Passive Samples		
Sample #	Material	P ID #
13	YB 71	P 2
14	Tedlar	P23
15	A 276/OI 650	P13
16	A 276	P11
17	Tedlar	P24
18	A 276/RTV 670	P16
19	Z 302/RTV 670	P21
20	Z 302/OI 650	P20
21	Z 302	P17
22	Silver	...
23	Z 302/OI 650	P22
24	KRS-5	...
25	Silver	...

TCSE Passive Samples		
Sample #	Material	P ID #
1	Silver	...
2	KRS-5	...
3	Z 302	P18
4	Z 93	P 5
5	YB 71/Z 93	P 4
6	D-111	P10
7	YB 71/Z 93	P 1
8	A 276	P12
9	Z 93	P 6
10	• No Sample •	...
11	YB 71/Z 93	P 3
12	S13G/LO	P7

TCSE Active Samples		
Sample #	Material	C ID #
1	Z 302	C102
2	Z 302/RTV 670	C108
3	A 276/RTV 670	C100
4	A 276	C 83
5	Anodize	C 63
6	Diffuse Ag/Teflon	C 73
7	YB 71 White Paint	C 97
8	Ag/Teflon	C 75
9	YB 71/Z 93	C 94
10	Anodize	C 61
11	Diffuse Ag/Teflon	C 74
12	Ag/Teflon	C 76

Figure 35. TCSE Sample Identification.

environment. These other investigations are discussed in Sections 5.3 through 5.5. Section 5.3 discusses several investigations including Scanning Electron Microscope (SEM), IR spectroscopy, Bi-Directional Reflectance Function (BDRF), X-ray Photoelectron Spectroscopy (XPS), and Differential Scanning Calorimetry (DSC) analyses. Post-flight inspections of the TCSE using black light showed significant fluorescence changes in the test samples. The investigation of these changes are discussed in Section 5.4. Section 5.5 discusses a strange material deposit observed during routine SEM investigations of the TCSE front cover. This strange deposit draws much interest as to the origin of this material.

5.1 Optical Properties Analysis

The primary measurements used for this analysis were total hemispherical reflectance from 250-2500 nm. Both in-space and laboratory reflectance measurements were performed on the test samples. Section 2.4.2 described the flight reflectometer which is very similar to the laboratory instrument used for this effort.

Laboratory measurements of spectral reflectance were obtained using a computer controlled Beckman model DK-2A Spectrophotometer equipped with a Gier-Dunkle 203mm (8 inch) integrating sphere. The integrating sphere was coated internally with magnesium oxide (MgO smoke, electrostatically deposited) to provide a near-perfect standard of reflectance. Reflectance data were integrated with respect to the solar spectrum to calculate solar absorptance.[15]

The spectral measurements made with the TCSE reflectometer show differences from the laboratory DK-2A instrument. This is caused by a combination of differing sphere geometries, detector types, and sphere coatings. To enhance the comparison analysis of flight and ground data, a method was developed to correlate the flight data to the laboratory data. The pre-flight DK-2A measurements were compared to the pre-flight measurements made on the TCSE reflectometer and a correlation curve developed for each sample.[3] This correlation curve was applied to each flight measurement to complete the correction. This data correction process is shown in Figure 36.

The correlation curve for each sample was developed by a point-by-point division of the DK-2A pre-flight data curve by the pre-flight reflectance measurements made on the TCSE flight instrument. Figure 36, Step 2, is a typical correlation curve for a high reflectance surface (i.e., white paint). The larger correction values around 350 nm may be due to small wavelength errors in the TCSE monochromator. A small shift at these wavelengths would cause a larger correction because of the fundamental absorption edge of the white paint samples. Once these corrections are applied, the flight measurements compare well to the laboratory measurements.

Post-flight spectral IR reflectance measurements were made on selected control and flight samples. A new instrument was developed to perform these measurements. The AZ Technology SpectraFire measures the spectral total hemispherical reflectance of test samples over the wavelength range of 2.5 μm to 34 μm. SpectraFire is a Nicolet Model 550 Fourier Transform

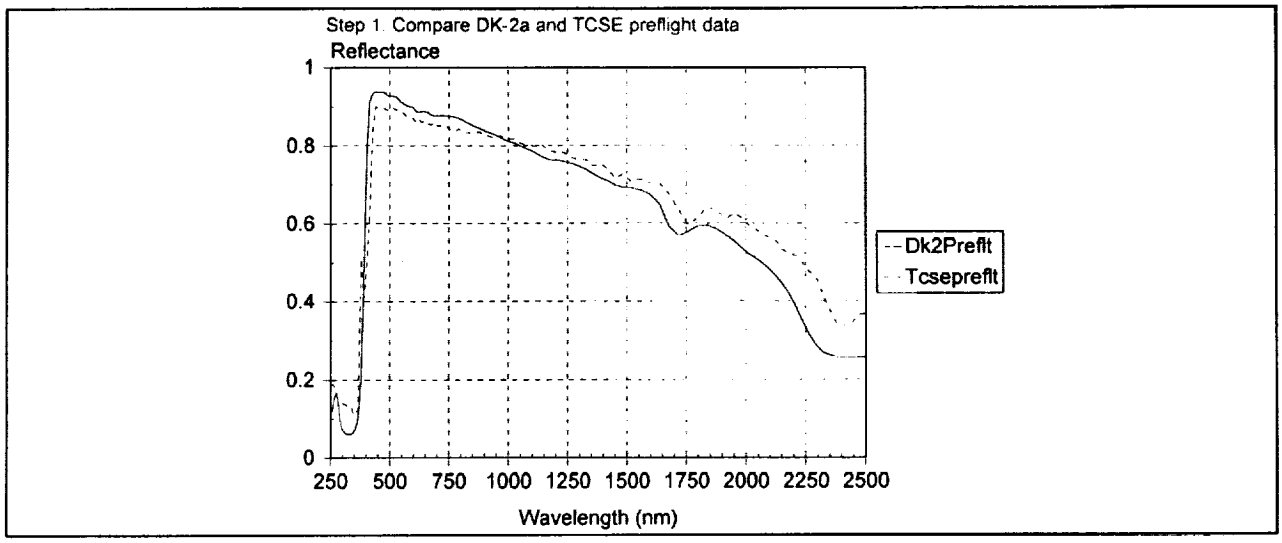

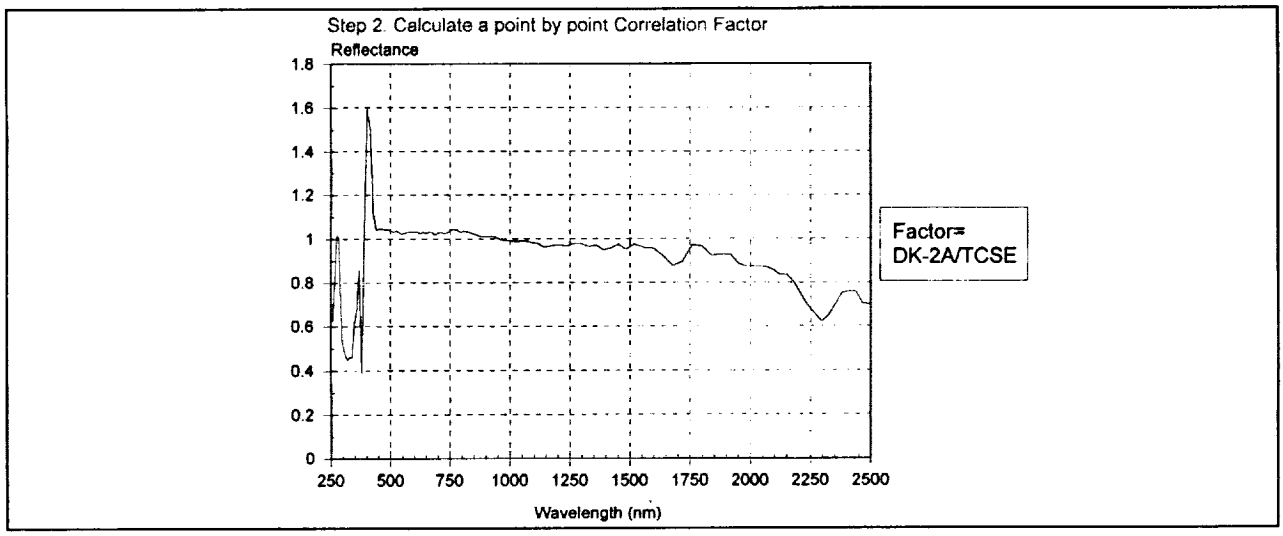

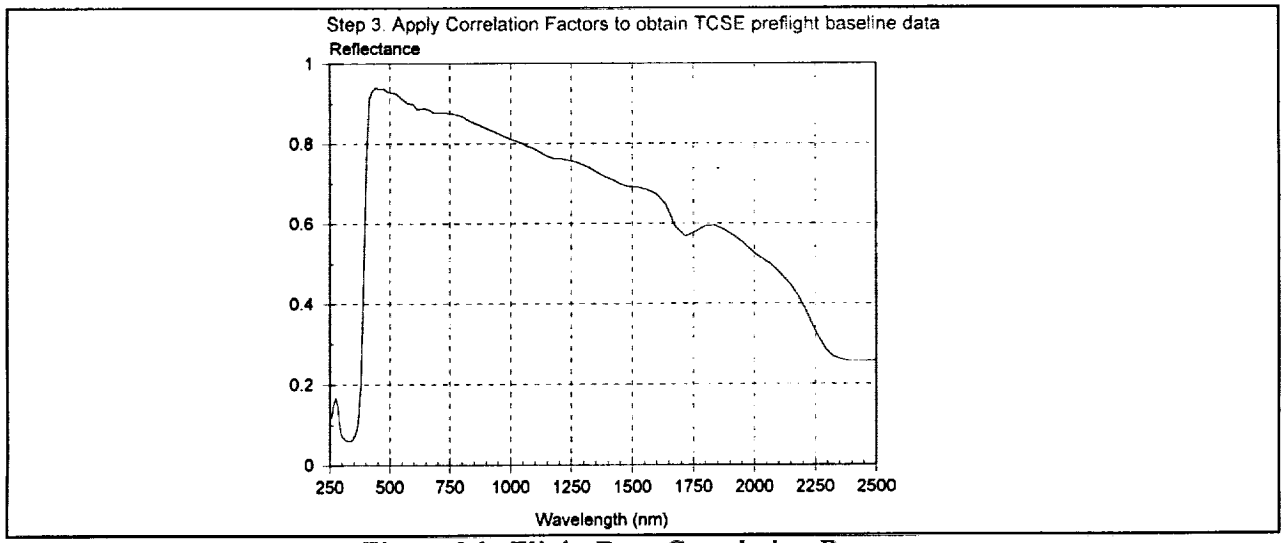

Figure 36. Flight Data Correlation Process.

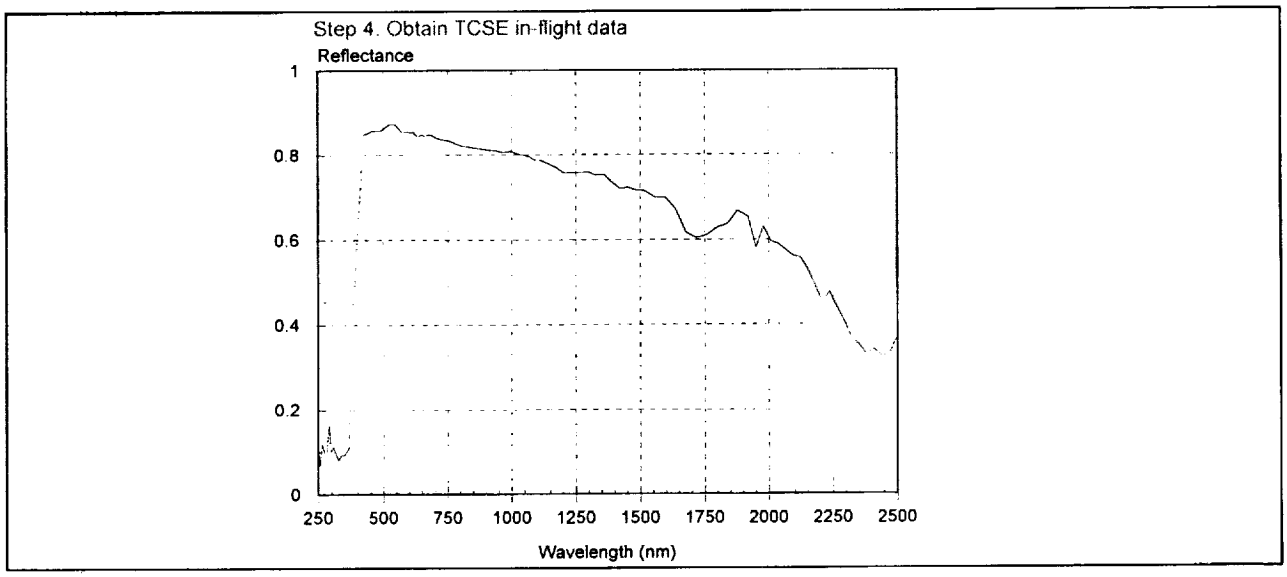

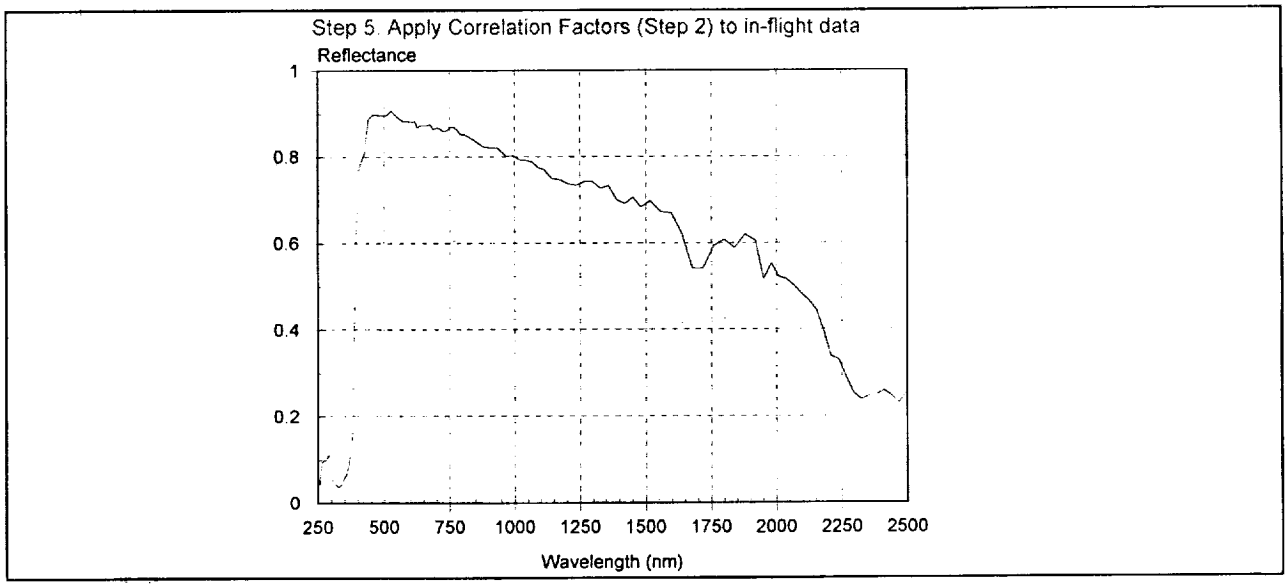

Step 6. Now, the TCSE corrected data can be directly compared to the DK-2A post-flight measurement data to determine the magnitude of change in the material properties.

Figure 36. Flight Data Correlation Process. (Continued)

Infrared (FTIR) spectrometer combined with a special total hemispherical reflectance attachment. This attachment uses the patented AZ Technology ellipsoidal collector system to perform the desired hemispherical measurements.

In addition to the reflectance measurements, the total emittance of the TCSE samples was also measured by a Gier-Dunkle model DB100 IR reflectometer. Tables 10-13 summarize the optical measurements of α_S and ε_T on the TCSE flight samples.

The following sections first discuss the different sample materials followed by a discussion of the measurement results.

5.1.1 A276 White Paint

Chemglaze A276 polyurethane white paint has been used on many short term space missions including Spacelab. It was known to degrade moderately under long term UV exposure and to be susceptible to AO erosion.[4,16] To evaluate the effectiveness of AO protective coatings, A276 samples were flown with and without overcoatings. Two materials were used as protective coatings over A276: RTV670 and Owens Illinois OI650.

The post-flight condition of the A276 samples were somewhat surprising in that the unprotected TCSE A276 samples are very white. Previous flight and laboratory tests indicate that almost six years of solar UV exposure should have rendered the A276 a medium brown color. The overcoated TCSE samples, however, do exhibit the characteristic UV darkening as anticipated. Visual inspection at KSC of unprotected A276 samples on the trailing edge of LDEF (almost no AO exposure) showed that they also degraded as expected.

Apparently as the unprotected A276 samples on the RAM side of LDEF degraded, their surfaces were eroded away leaving a fresh, undamaged surface. Pippin[17] reported that the A276 binder eroded away leaving the white pigment exposed. Some degradation of this TiO_2 pigment should have also been observed due to UV exposure (in the absence of AO). It is possible that there was sufficient oxygen on leading edge surfaces to inhibit oxygen based pigment damage.[18]

Figure 37 shows pre-flight, in-space, and post-flight measurement of solar absorptance (α_S) for the unprotected A276 and overcoated A276 samples. Figures 38-40 are the detailed reflectance curves for selected A276 samples. These data show that both protective coatings protected the A276 from AO erosion but allowed the A276 coating to degrade from solar UV exposure. Some degradation may be due to darkening of the thin overcoating.

The data for the unprotected A276 shows only a small amount of degradation early in the almost 6 year exposure. While most of the AO fluence occurred late in the LDEF mission, the TCSE in-space measurements show there was sufficient AO present early in the mission to erode the damaged A276 or otherwise inhibit UV degradation.

Table 10. Active Sample α_S Summary.

CORRECTED SOLAR ABSORPTANCE VS. EXPOSURE

Exposure (Months)		0	6.5	7.5	8.6	9.8	11.9	12.9	14.0	15.0	16.2	69.2	
MATERIAL	SAMPLE #	PRE-FLT										POST FLIGHT	$\Delta\alpha_S$
Z93	C95	.140	.124	.120	.125	.122	.119	.120	.124	.129	.125	.150	.010
YB71	C93	.101	.080	.075	.080	.079	.078	.080	.078	.087	x	.118	.017
YB71/Z93	C94	.101	.100	.098	.104	.102	.106	.105	.106	.114	x	.112	011
YB71	C96	.138	.115	.115	.116	.119	.115	x	.116	.126	x	.153	.025
YB71	C97	.110	.092	.097	x	.095	.096	.096	.102	x	x	.131*	.021
A276	C82	.253	.276	.264	.287	.279	.281	.300	.304	.305	.330	.236	-.017
A276	C83	.255	.261	.271	x	x	x	x	x	x	x	.272*	.017
A276/0I650	C87	.247	.436	.455	.476	.506	.525	.542	.544	.541	.554	.592	.345
A276/RTV670	C88	.266	.464	.470	.486	.500	.510	.522	.525	.533	.529	.623	.357
A276/RTV670	C100	.258	x	.270	Coating gone by 8.6 months exposure								-----
S13G/LO	C92	.168	.176	.176	.193	.195	.203	x	.216	.221	x	.368	.200
Tedlar	C110	.248	.263	.262	.260	.264	.261	.259	.260	.258	.260	.224	-.024
Anodize	C61	.409	.461	.466	.465	.487	.495	.502	.506	.504	x	.466	.057
Anodize	C63	.402	.456	.462	x	.485	.494	.497	.503	x	x	.540*	.138
Ag-Tef-5 mil	C75	.063	x	x	x	x	x	x	x	x	x	.076	.013
Ag-Tef-5 mil	C76	.058	.053	.049	.049	.073	.058	.054	.056	.059	x	.075	.017
Ag-Tef-2 mil	C90	.075	.064	.062	.063	.082	.075	.075	.076	.081	x	.161	.086
Ag-Tef-diff	C73	.077	x	x	x	x	x	x	x	x	x	.100*	.023
Ag-Tef-diff	C74	.075	.067	.065	.071	.074	.073	.073	.077	.077	x	.103	.028
D111	C99	.980	.985	.985	.986	.985	.986	.986	.986	.986	x	.996	.016
Z302	C101	.975	.981	.982	.981	.981	.980	.983	.980	.979	.981.	.603	**
Z302	C102	.976	x	.983	x	x	x	x	x	x	x	.982*	.006
Z302/0I650	C104	.983	.986	.986	.986	.986	.986	.986	.986	.986	.986	.990	.007
Z302/RTV670	C105	.985	.987	.987	.988	.987	.988	.988	.987	.988	.986	.988	.003
Z302/RTV670	C108	.984	x	.984	x	x	x	x	x	x	x	.983*	-.001

x - Data unavailable
* - 19.5 months exposure
** - Coating eroded away leaving primer

Table 11. Passive Sample α_S Summary.

MATERIAL	SAMPLE #	SPACE EXPOSURE (MONTHS)	SOLAR ABSORPTANCE (α_S) PRE-FLIGHT	SOLAR ABSORPTANCE (α_S) POST-FLIGHT	$\Delta\alpha_S$
D111	P10	19.5	.992	.992	0
Z302	P17	69.2	.970	.570	*
Z302	P18	19.5	.969	.994	.025
Z302/0I650	P20	69.2	.983	.985	.002
Z302/OI650	P22	69.2	.982	.978	-.004
Z302/RTV670	P21	69.2	.980	.979	-.001
Z93	P5	19.5	.142	.151	.009
Z93	P6	69.2	.133	.134	.001
YB71	P1	19.5	.143	.150	.007
YB71/Z93	P3	69.2	.084	.089	.005
YB71/Z93	P4	19.5	.089	.085	-.005
YB71	P2	69.2	.152	.181	.029
A276	P11	69.2	.262	.268	.006
A276	P12	69.2	.257	.230	-.027
A276/OI650	P13	69.2	.256	.583	.327
A276/RTV670	P16	69.2	.282	.524	.242
S13G/LO	P7	69.2	.200	.418	.218
Tedlar	P23	69.2	.253	.214	-.039
Tedlar	P24	69.2	.241	.213	-.028

*Coating eroded away leaving primer.

Table 12. Active Sample ε_T Summary.

SAMPLE #	MATERIAL	SAMPLE ID#	EMITTANCE MEASUREMENTS CONTROL	EMITTANCE MEASUREMENTS POST-FLIGHT	$\Delta\varepsilon_T$
1	Z302 Black Paint	C102	.912	.920	-.008
2	Z302/RTV670	C108	.907	*	*
3	A276/RTV670	C100	.907	*	*
4	A276 White Paint	C83	.987	*	*
5	Anodize	C63	.840	.839	.001
6	Diffuse Silver Teflon	C73	.821	.817	.004
7	YB71 White Paint	C97	.901	.880	.021
8	Silver Teflon	C75	.812	.802	.010
9	YB71 over Z93	C94	.849	.878	-.029
10	Anodize	C61	.840	.834	.006
11	Diffuse Silver Teflon (5 mil)	C74	.917	.788	.129
12	Silver Teflon (5 mil)	C76	.812	.782	.030
13	Silver Teflon (2 mil)	C90	.812	.458	.354
14	YB71 over Z93	C93	.849	.880	-.031
15	S13G/LO White Paint	C92	.900	.883	.017
16	YB71 White Paint	C96	.901	.880	.021
17	Z93 White Paint	C95	.915	.918	-.003
18	IITRI D111 Black Paint	C99	.929	.903	.026
19	Tedlar White Film	C110	.899	.936	-.037
20	Z302/RTV670	C105	.907	.899	.008
21	Z302/OI650	C104	.905	.896	.009
22	Z302 Black Paint	C101	.912	*	*
23	A276/RTV670	C88	.907	*	*
24	A276/OI650	C87	.896	*	*
25	A276 White Paint	C82	.897	.931	-.034

*Unable to measure due to sample condition.

Table 13. Passive Sample ε_T Summary.

SAMPLE #	MATERIAL	SAMPLE ID#	EMITTANCE MEASUREMENTS		$\Delta\varepsilon_T$
			CONTROL	POST-FLIGHT	
1	Auger Silver Sample	----	----	.461	
2	KRS-5 IR Crystal	----	----	----	
3	Z302 Black Paint	P18	.912	.928	-.016
4	Z93 White Paint	P5	.915	.930	-0.15
5	YB71 over Z93	P4	.849	.857	-.008
6	IITRI D111 Black Paint	P10	.929	.921	.008
7	YB71	P1	.849	.901	-.052
8	A276 White Paint	P12	.897	.931	-.034
9	Z93 White Paint	P6	.915	.921	-.006
10	No Sample	----	----	----	----
11	YB71 over Z93	P3	.849	.863	-.014
12	S13G/LO White Paint	P7	.900	.887	.013
13	YB71 White Paint	P2	.901	.905	-.004
14	Tedlar White Film	P23	.899	.939	-.040
15	A276/OI650	P13	.896	.893	.003
16	A276White Paint	P11	.897	.920	-.023
17	Tedlar White Film	P24	----	.925	----
18	A276/RTV670	P16	.907	.877	.030
19	Z302/RTV670	P21	.907	.889	.008
20	Z302/OI650	P20	.905	.894	.009
21	Z302 Black Paint	P17	.912	.901	.011
22	Auger Silver Sample	----	----	.307	----
23	Z302/OI650	P22	.905	.892	.013
24	KRS-5 IR Crystal	----	----	----	----
25	Auger Silver Sample	----	----	.532	----

---- Not Applicable

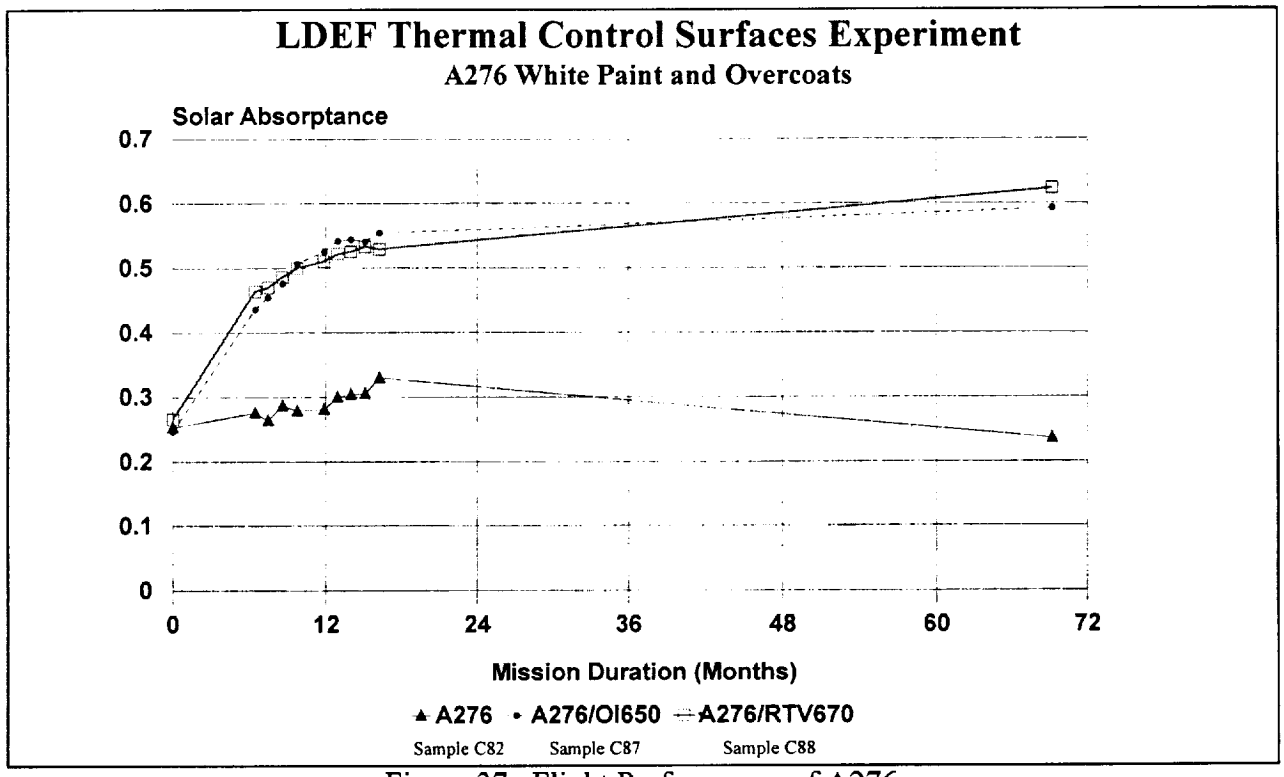

Figure 37. Flight Performance of A276.

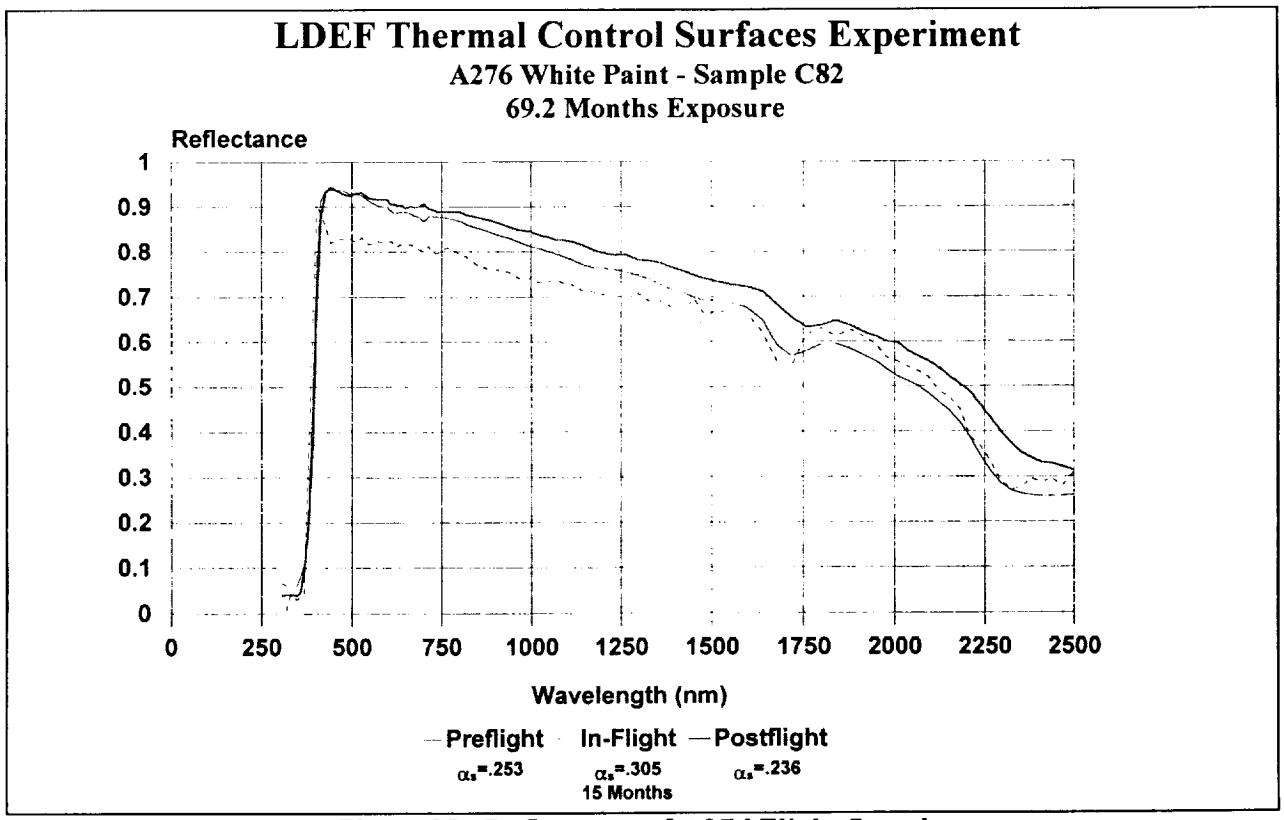

Figure 38. Reflectance of A276 Flight Sample.

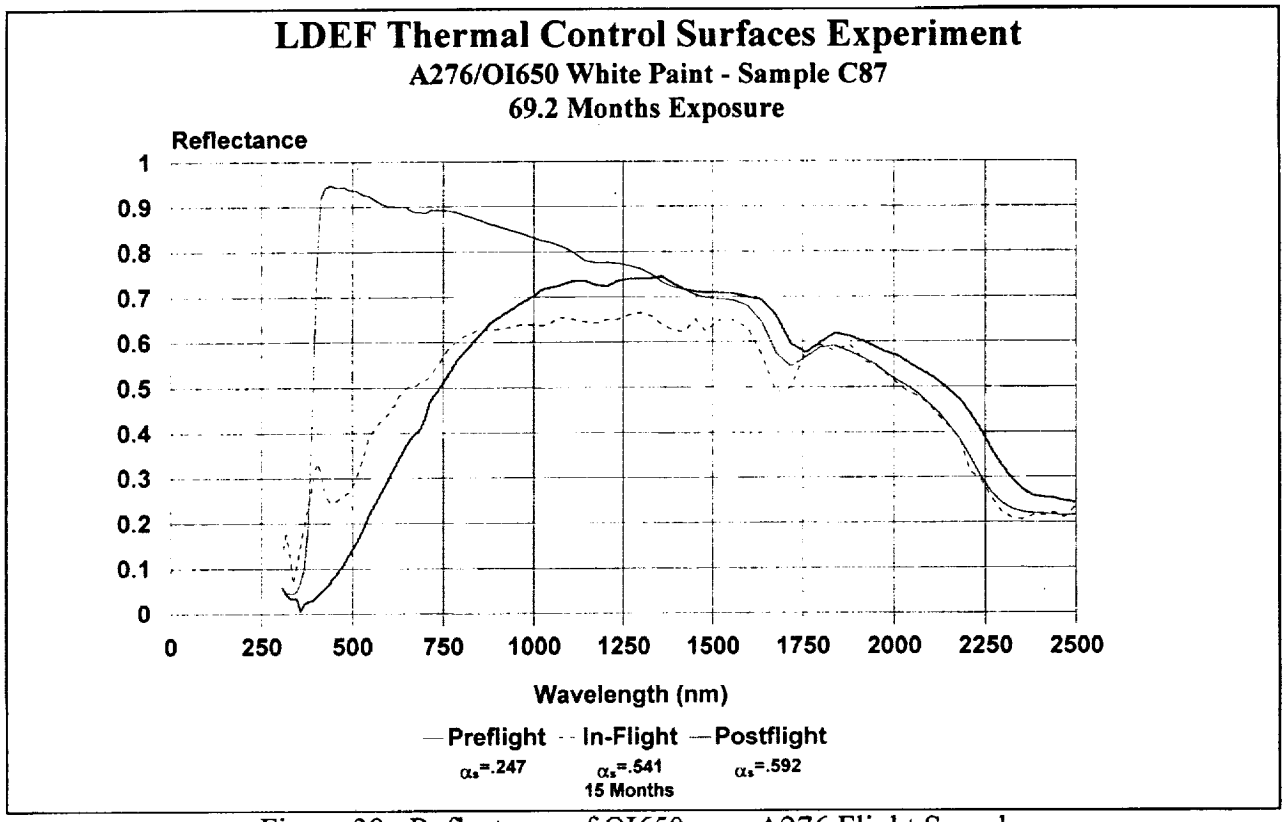

Figure 39. Reflectance of OI650 over A276 Flight Sample.

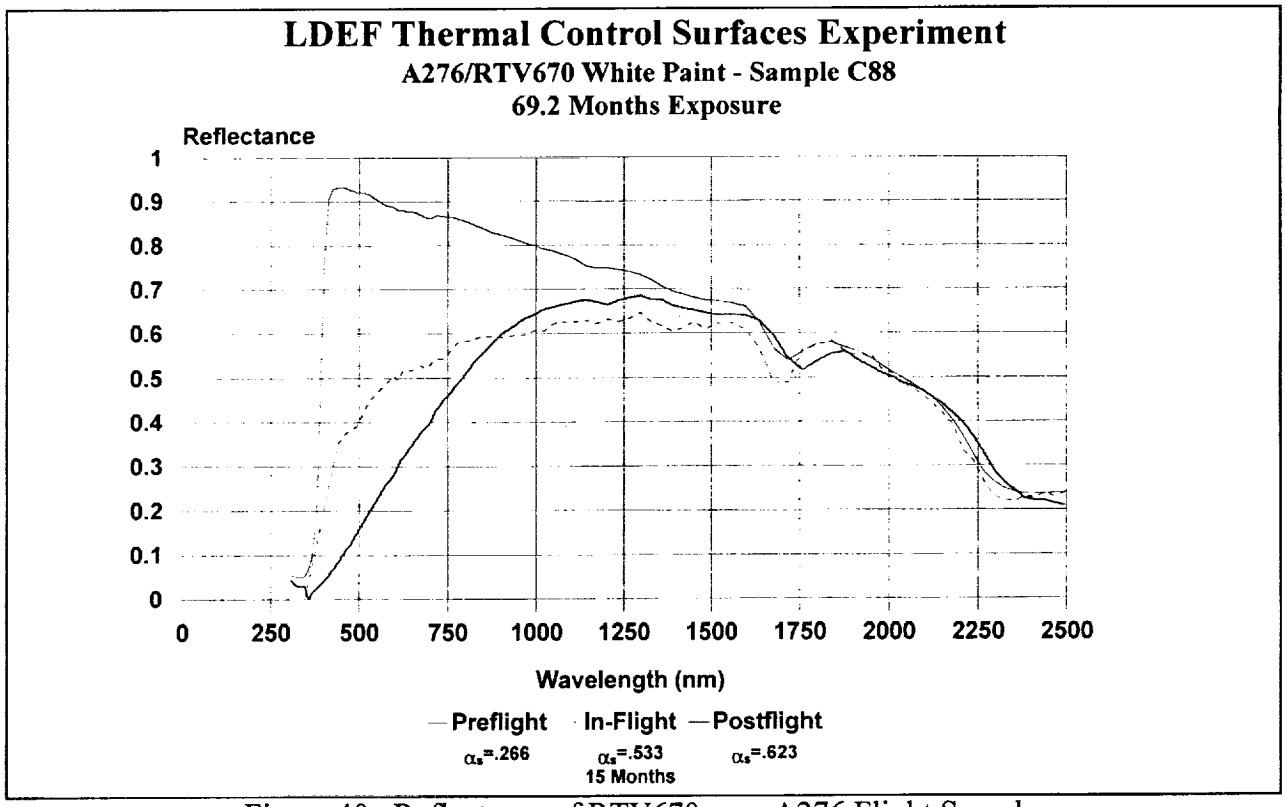

Figure 40. Reflectance of RTV670 over A276 Flight Sample.

Figures 41 and 42 show the extensive physical damage on the overcoated A276 calorimeter samples. The unprotected A276 samples (see Figure 43) did not crack or peel. The passive samples with these same protective coatings also crazed and cracked, but did not peel. The calorimeter samples were thermally isolated from the TCSE structure and therefore saw wider temperature excursions, possibly causing the peeling of the overcoated samples.

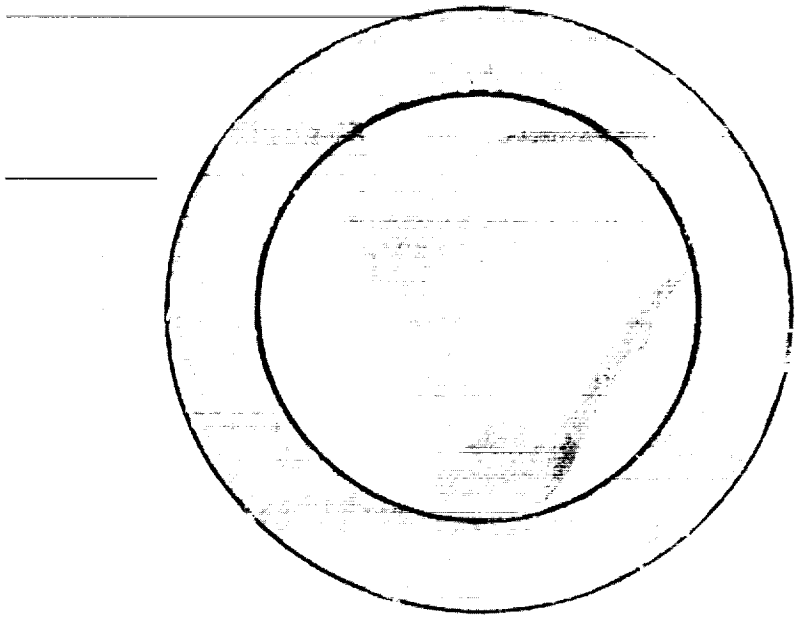

Figure 41. Post-flight Photograph of RTV670 over A276 Flight Sample C88.

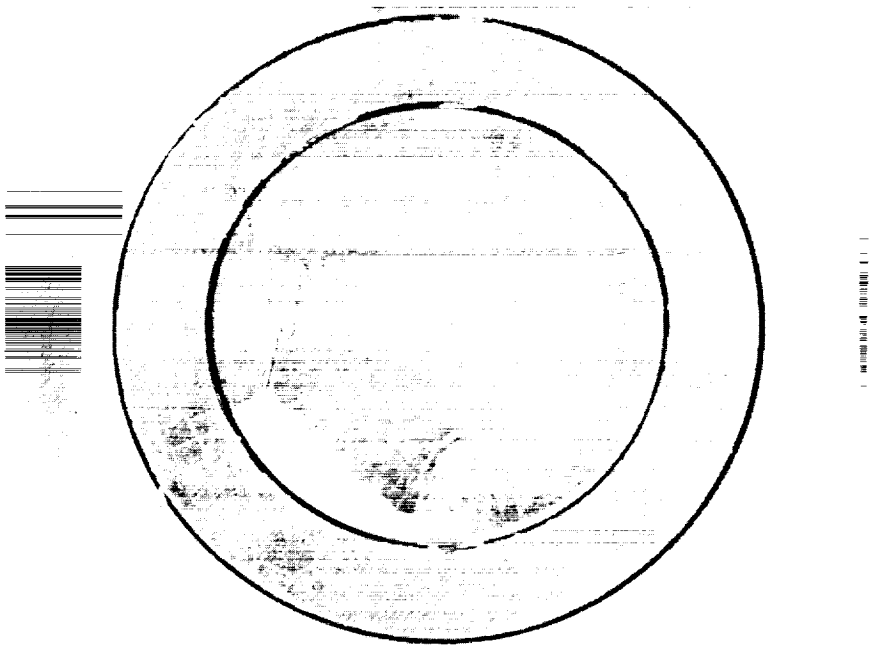

Figure 42. Post-flight Photograph of OI650 over Z276 Flight Sample C87.

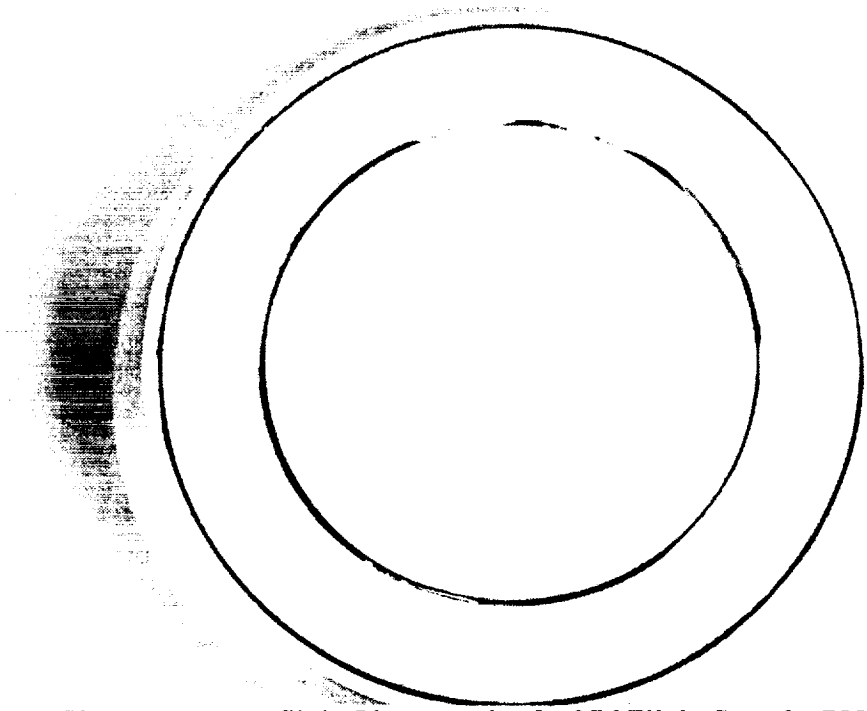

Figure 43. Post-flight Photograph of A276 Flight Sample C82.

Figures 44-46 show the IR reflectance changes of the exposed samples versus controls for A276 and the two overcoated A276 samples. No dramatic changes were seen in the IR reflectance, but some chemical changes are evident in the overcoated samples with the relative changes in the spectral peaks. The minimum reflectance changes correspond well with the minimal changes in the measured ε_T (Tables 12 and 13.)

The extended space exposure also changed the UV fluorescence of both the A276 and overcoated A276 coatings. This fluorescence is easily seen using a short wavelength inspection black light. The RTV670 and OI650 coatings glow a bright yellow under this UV illumination. Preliminary measurements show both a change in the peak wavelength and an increase in the magnitude of the fluorescence. See Section 5.4 for results of fluorescence studies.

5.1.2 Z93 White Paint

The Z93 white thermal control coatings on the TCSE samples were almost impervious to the 69 month LDEF mission (see Figures 47 and 48). The Z93 samples showed an initial improvement in the solar absorptance-which is typical of silicate coatings[19] in a thermal vacuum environment. The initial improvement is due to an increased reflectance above 1300 nm. This is offset by a very slow degradation below 1000 nm and results in only a 0.01 overall degradation in solar absorptance for the extended space exposure.

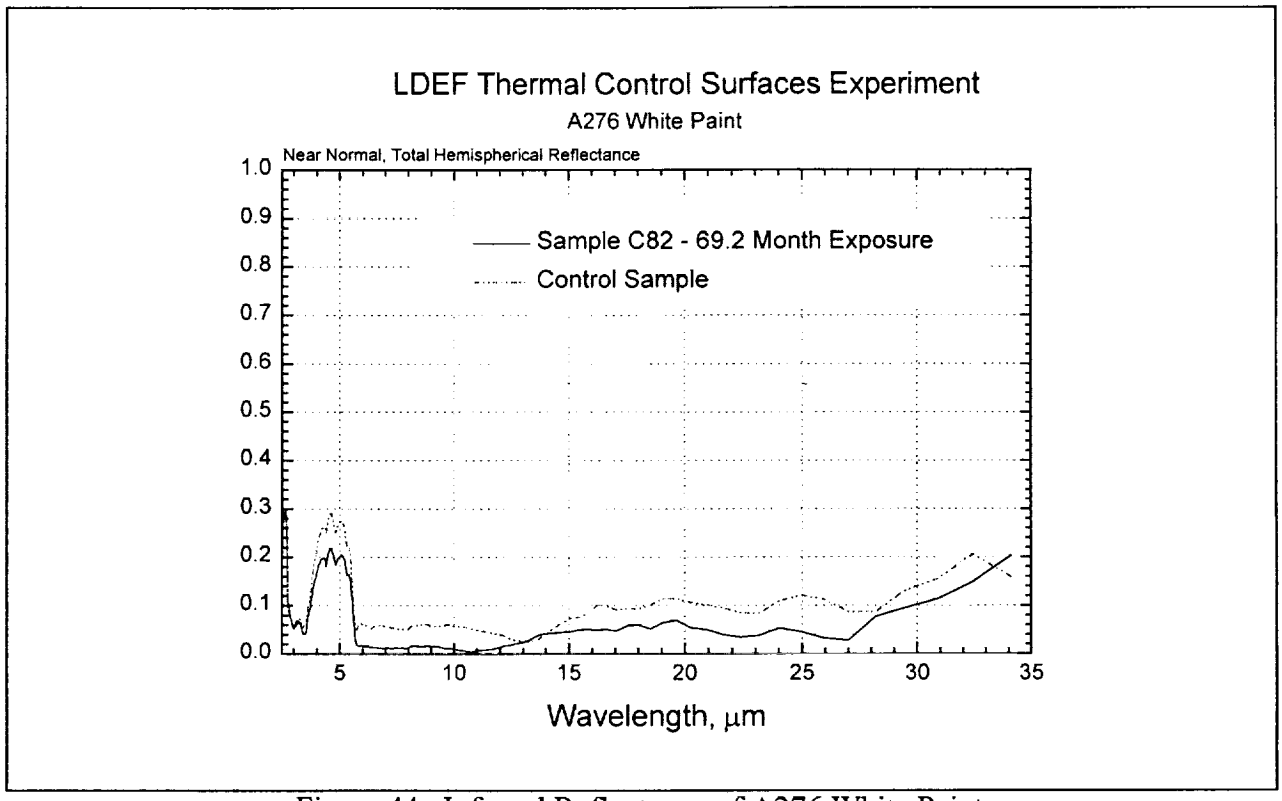

Figure 44. Infrared Reflectance of A276 White Paint.

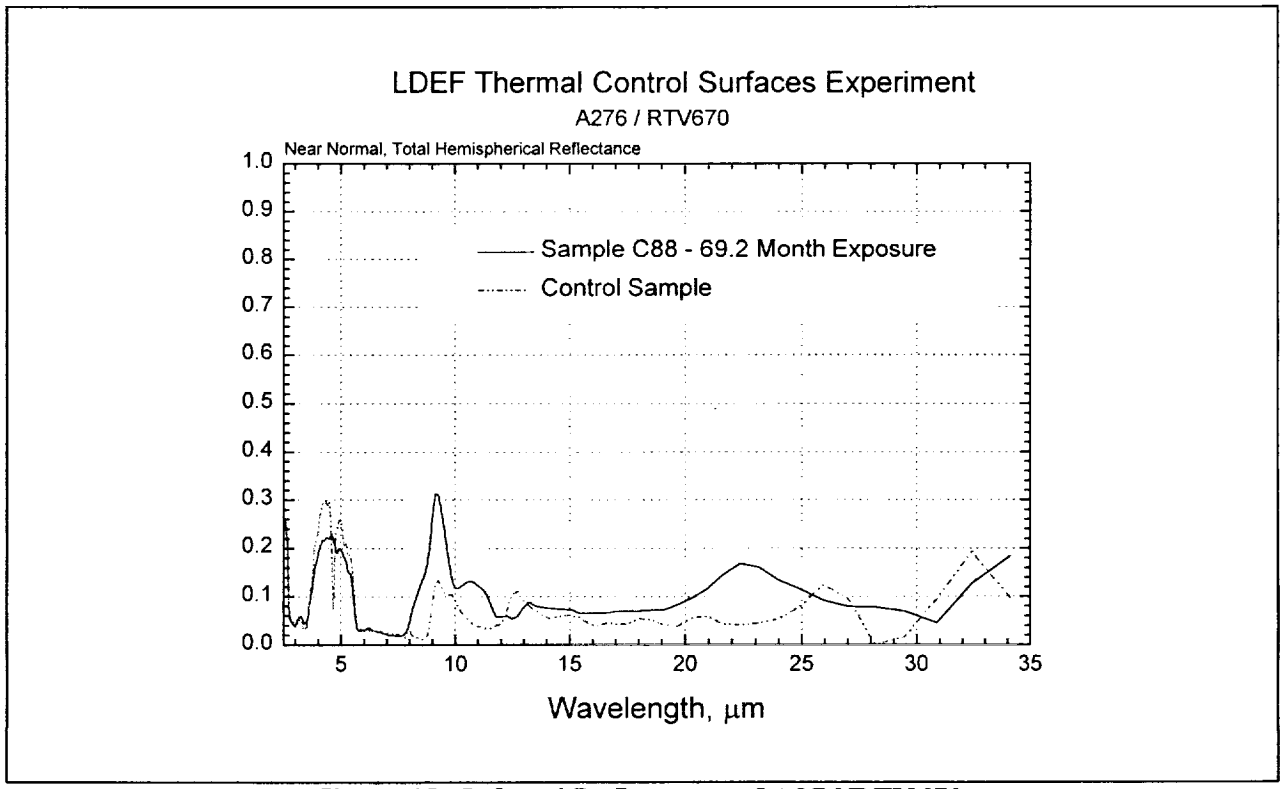

Figure 45. Infrared Reflectance of A276/RTV670.

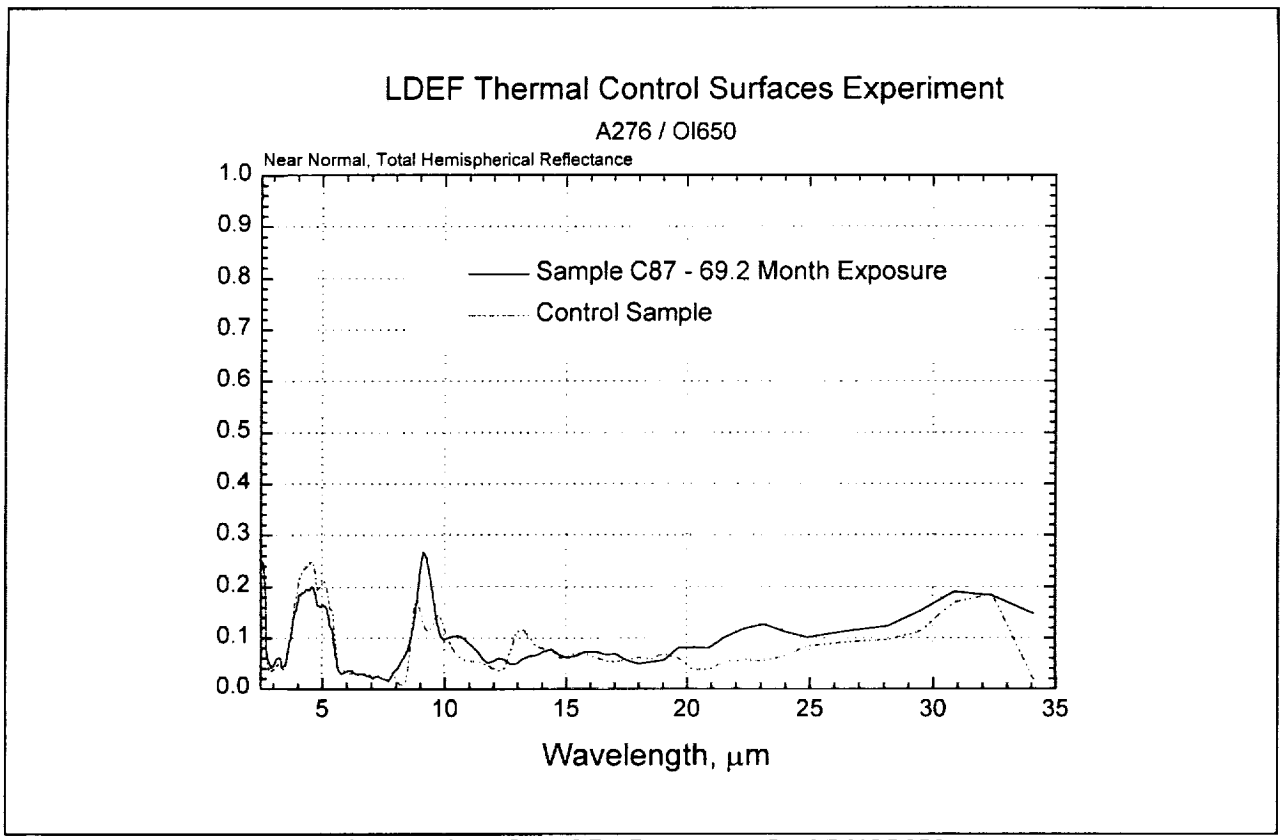

Figure 46. Infrared Reflectance of A276/OI650.

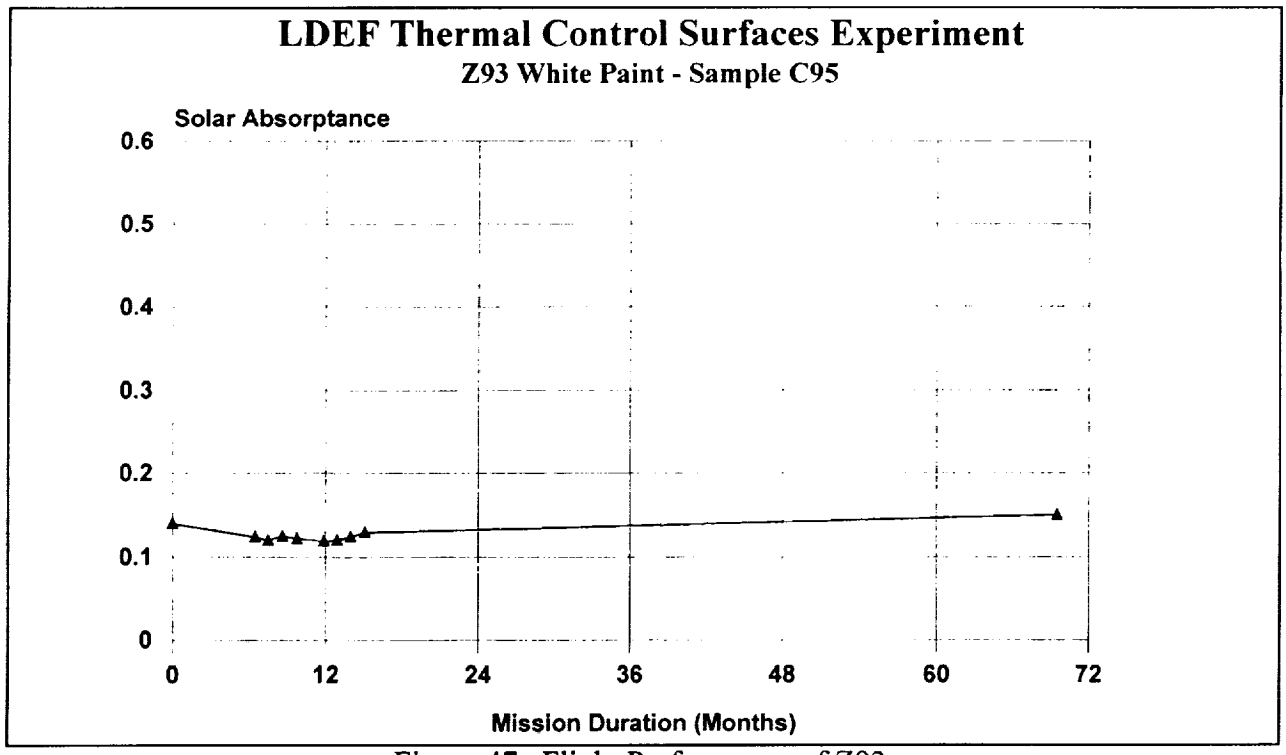

Figure 47. Flight Performance of Z93.

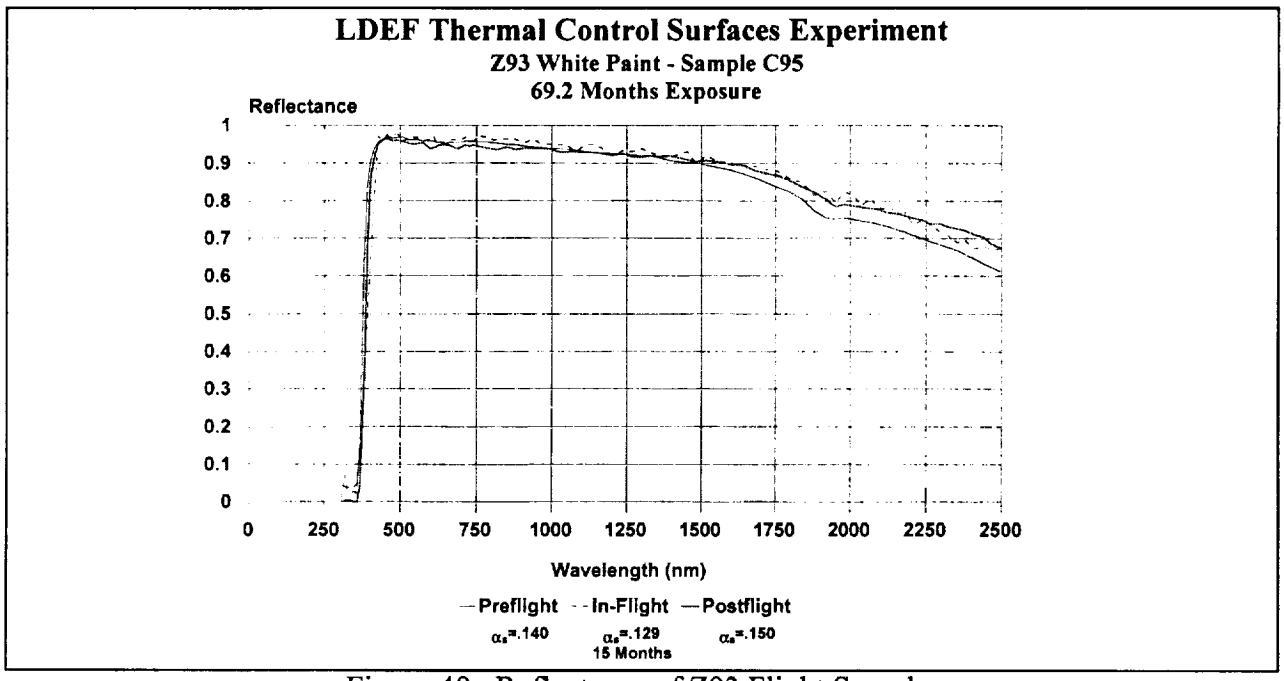

Figure 48. Reflectance of Z93 Flight Sample.

The environmental stability of Z93 is also confirmed in the IR reflectance data as shown in Figure 49. Because of the excellent performance of the Z93 on TCSE and other LDEF experiments, it is being widely used on the International Space Station.

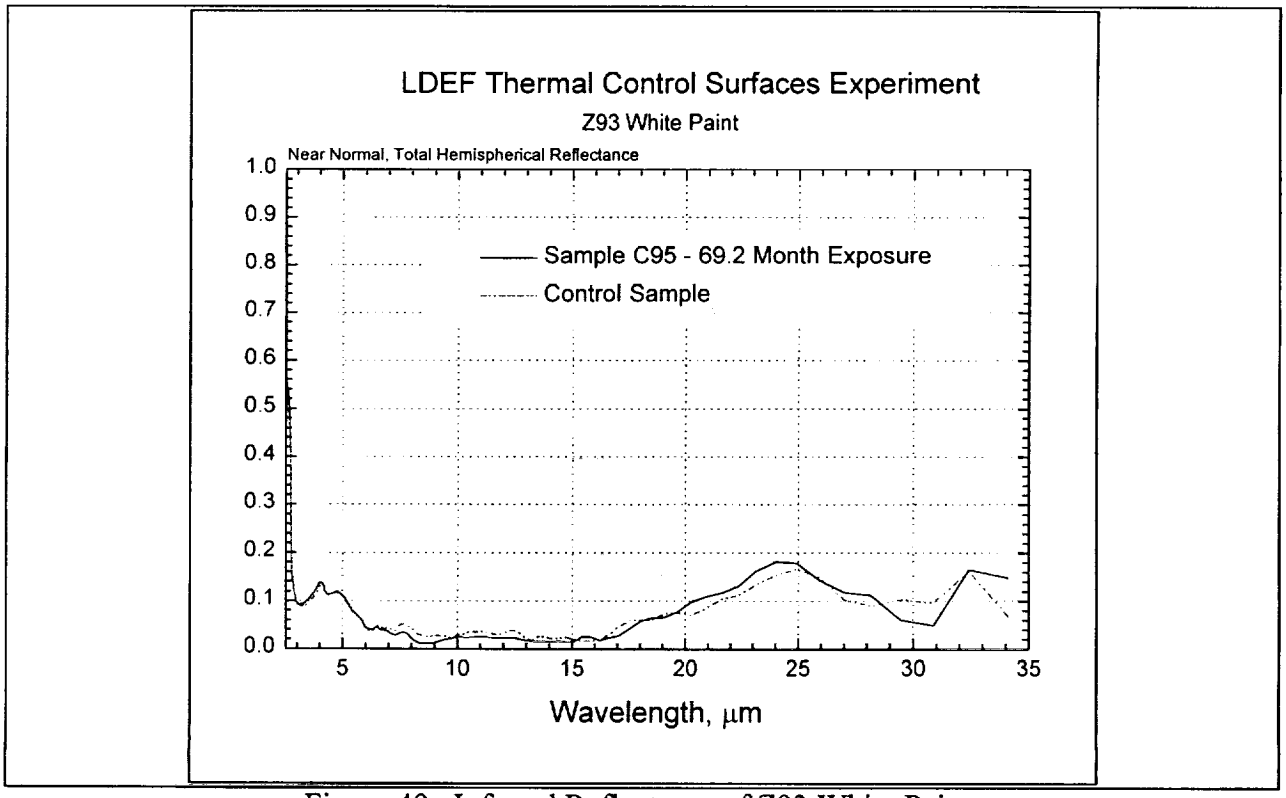

Figure 49. Infrared Reflectance of Z93 White Paint.

One concern for Z93 and the other silicate coatings is the effects of Micrometeoroid & Debris (M&D) impacts. Figure 50 shows the result of an impact on a Z93 sample. This small impact is about 0.4mm in diameter and occurred near the edge of the guard ring of the calorimeter. The impact caused a larger area of the coating to break away. The affected area did not propagate throughout the coating and was limited to the immediate area around the impact.

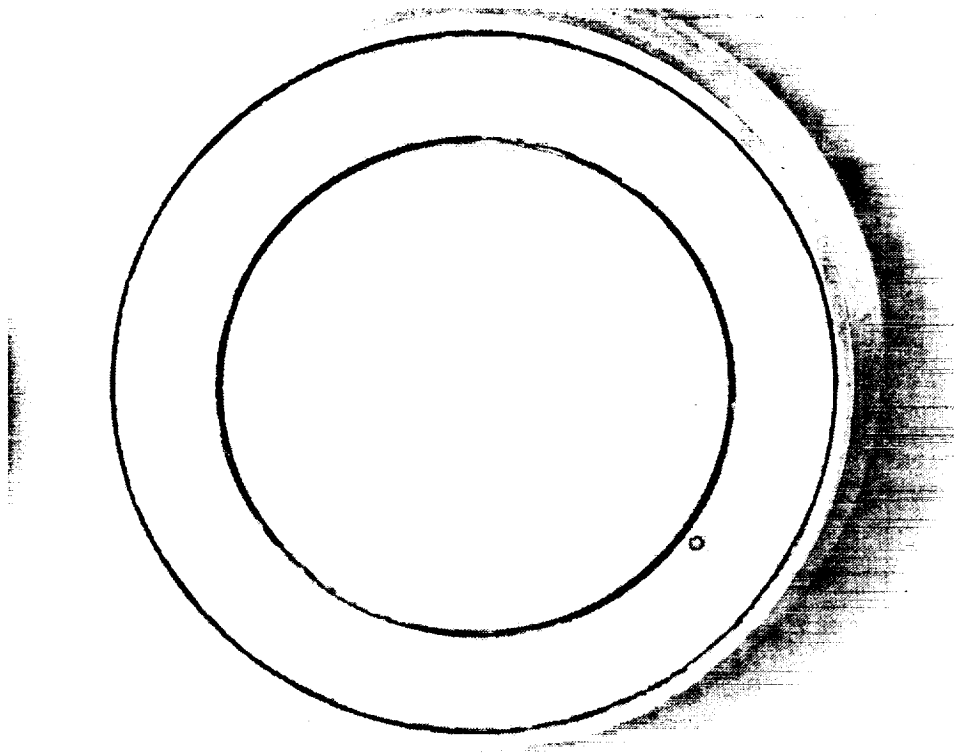

Figure 50. Post-flight Photograph of Z93.

As with the A276 samples, the LDEF space exposure also changed the UV fluorescence in the Z93 samples. The unexposed Z93 coatings fluoresce naturally, but much of this fluorescence was quenched by the LDEF exposure. Fluorescence of the ZnO pigment in Z93 and its decrease under UV exposure has been previously reported.[20] This quenched fluorescence in Z93 samples is not confined to the leading edge samples, but is found on LDEF trailing edge samples as well. Figures 51 through 54 are white light and black light photographs of samples from the LDEF experiment AO114. AO114 had Z93 samples on both the leading edge (location C9) and on the trailing edge (location C3). The samples were mounted with a cover that had a semicircular exposure window. Under white light, it is difficult to determine what area of the sample was exposed. However, the exposed area becomes very obvious under the black light. These photographs are used by permission of Dr. J. Gregory (UAH). See Section 5.4 for results of fluorescence studies.

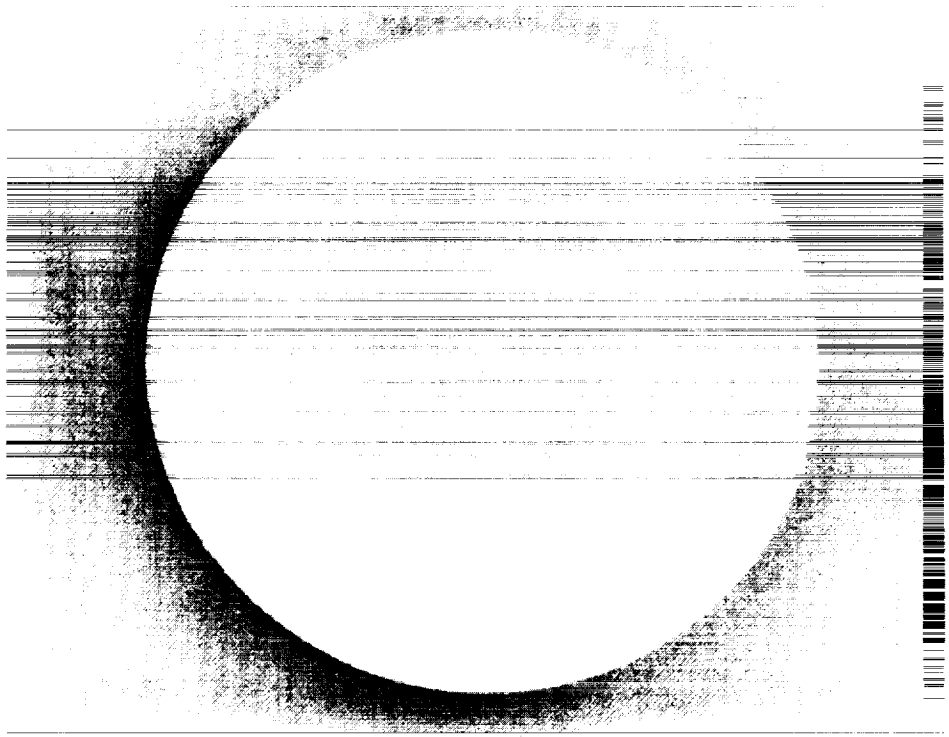

Figure 51. White Light Post-flight Photograph of Z93 Flight Sample - Leading Edge.

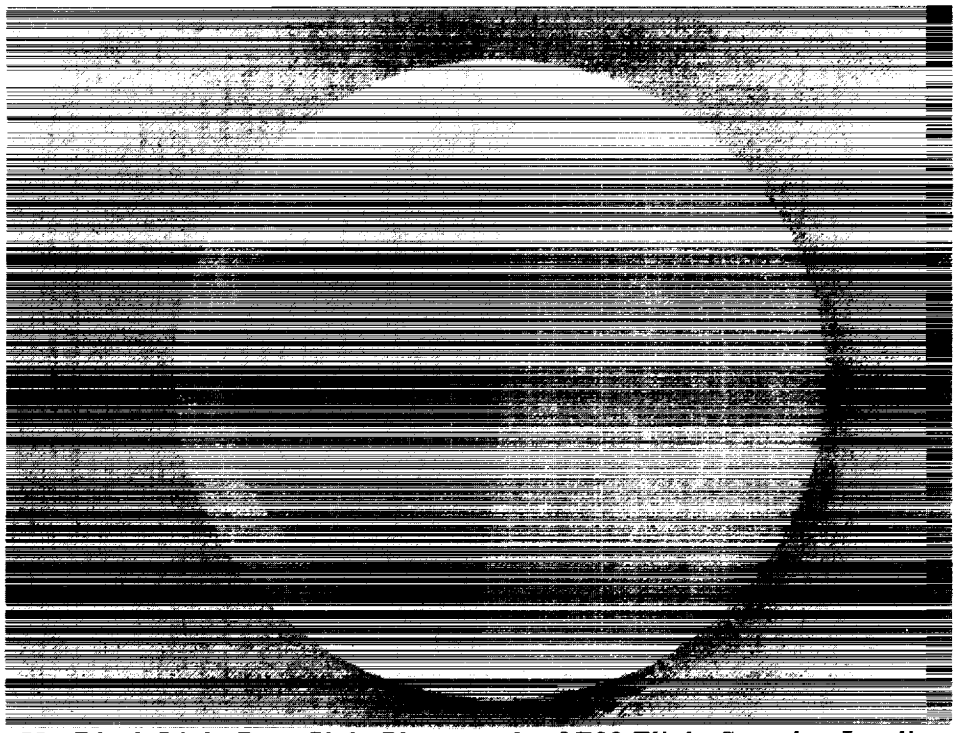

Figure 52. Black Light Post-flight Photograph of Z93 Flight Sample - Leading Edge.

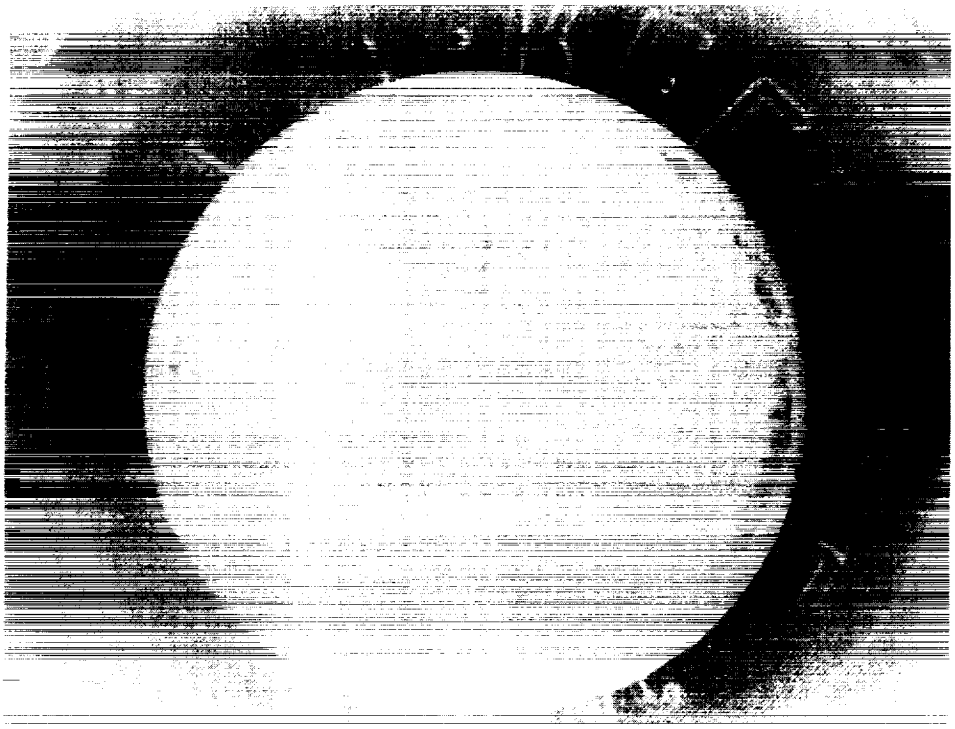

Figure 53. White Light Post-flight Photograph of Z93 Flight Sample - Trailing Edge.

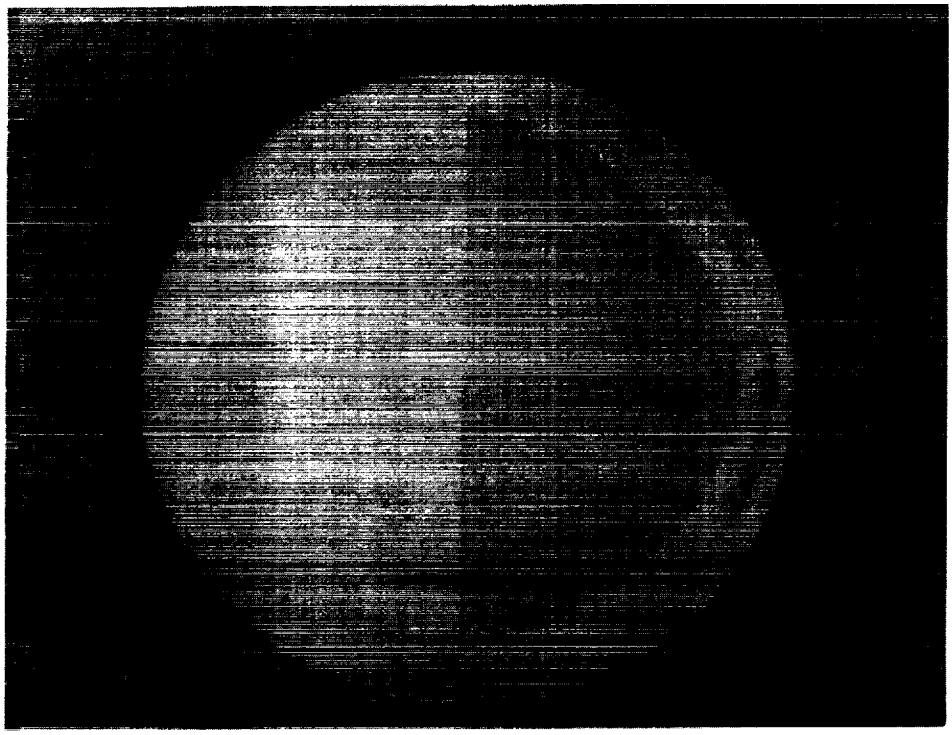

Figure 54. Black Light Post-flight Photograph of Z93 Flight Sample - Trailing Edge.

5.1.3 YB71 White Paint

The YB71 coatings on the TCSE behaved similarly to the Z93 samples. A small increase in the IR reflectance early in the mission caused a decrease in solar absorptance (see Figures 55 and 56). This was offset by a slow long term degradation resulting in a small overall increase in solar absorptance. The TCSE YB71 samples were made before the preparation and application parameters for this new coating were finalized. This resulted in a wide spread in the initial solar absorptance for the different samples. The samples with YB71 applied over a primer coat of Z93 had a somewhat lower α_s than the other YB71 samples.

While minimal changes are also observed in the overall IR reflectance (Figures 57 and 58), some changes are seen for the YB71 (without Z93 undercoat) in the 3 to 8 μm spectral range.

5.1.4 S13G/LO White Paint

The S13G/LO samples on the TCSE degraded significantly in the solar spectral range on the LDEF mission. Figure 59 shows the change in solar absorptance for the LDEF mission of the TCSE S13G/LO calorimeter sample. Figure 60 shows the solar spectral reflectance measurements of the S13G/LO sample. Contrary to the changes observed in the solar spectral region, the IR reflectance (Figure 61) shows very little change. The IR data is consistent with the measured changes in ε_T.

Figure 62 is a post-flight photograph of an S13G/LO coated calorimeter sample holder. Notice the color grading of the degraded (darker) surface with lighter colors near the edges. As with Z93, the UV fluorescence of the S13G/LO coatings decreased markedly in the flight samples. See Section 5.4 for results of the fluorescence studies.

Degradation of the S13G/LO samples for the almost 6 year space exposure was expected. However, the magnitude of this degradation is significantly greater than ground testing predictions. Figure 63 compares the performance of the S13G/LO and Z93 on the LDEF/TCSE mission to a ground simulated space exposure test previously performed at MSFC.

These data show the flight degradation of S13G/LO to be significantly more than predicted while it is just the opposite for Z93. This is difficult to explain since the two coatings are similar in formulation. Both use ZnO pigment but the S13G/LO has a methyl silicone binder while Z93 has a potassium silicate binder. The S13G/LO pigment particles are encapsulated in potassium silicate.

The S13G/LO flown on the TCSE is not the currently available formulation. A new silicone binder is used in the current S13G/LO-1 coating.

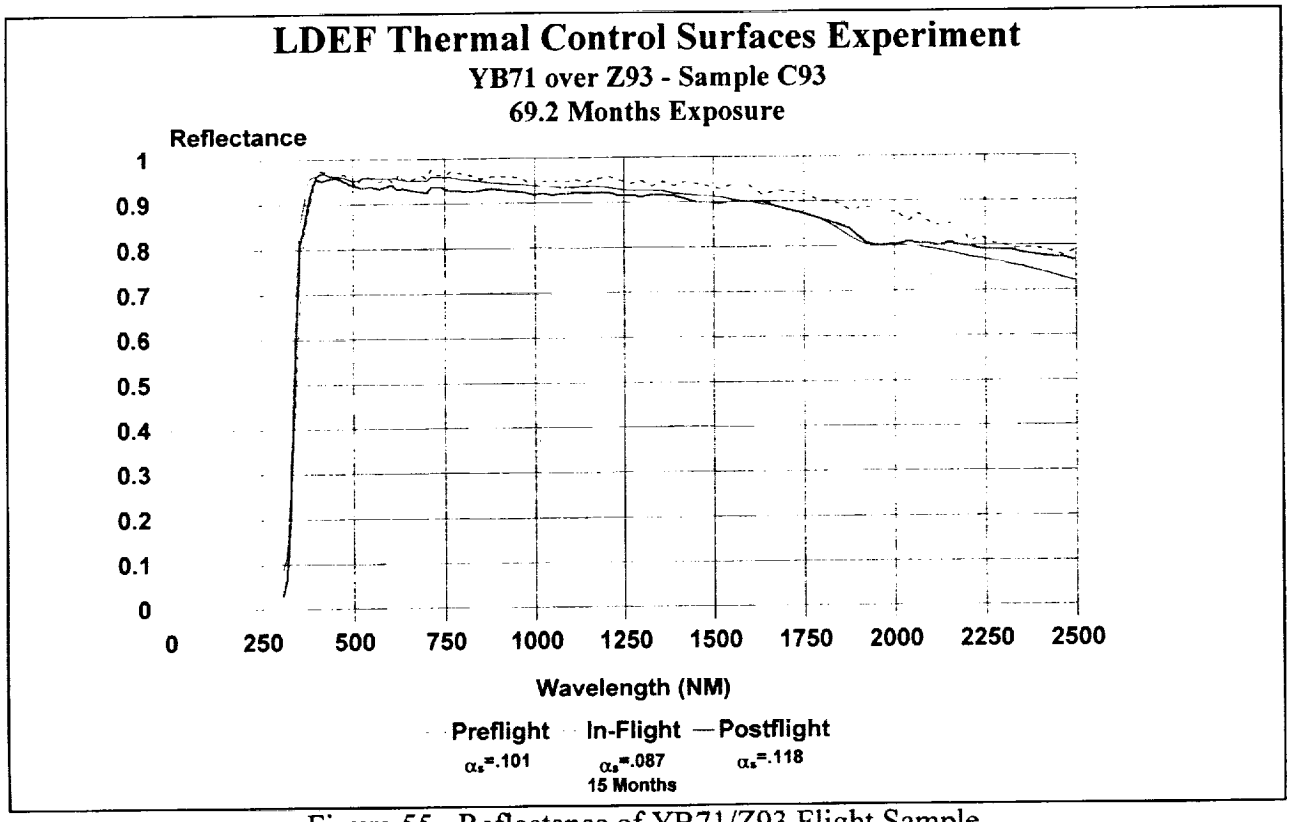

Figure 55. Reflectance of YB71/Z93 Flight Sample.

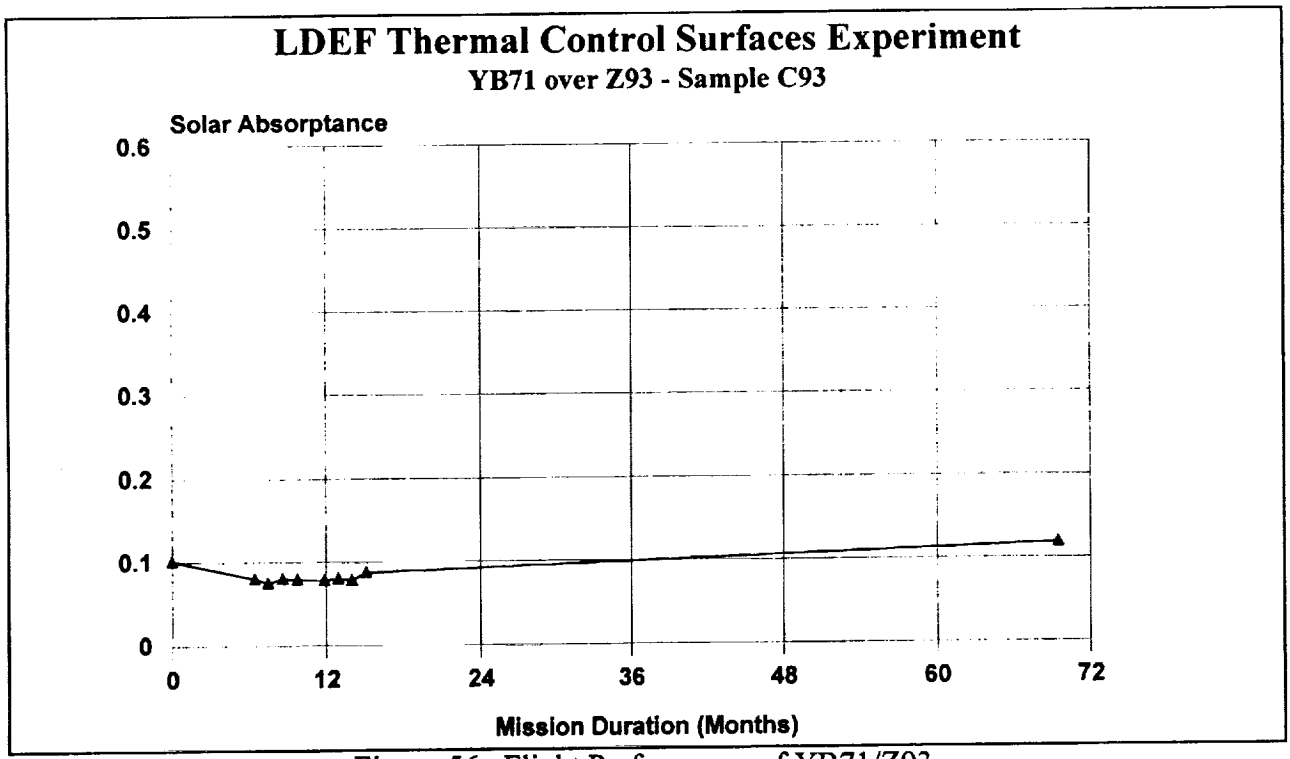

Figure 56. Flight Performance of YB71/Z93.

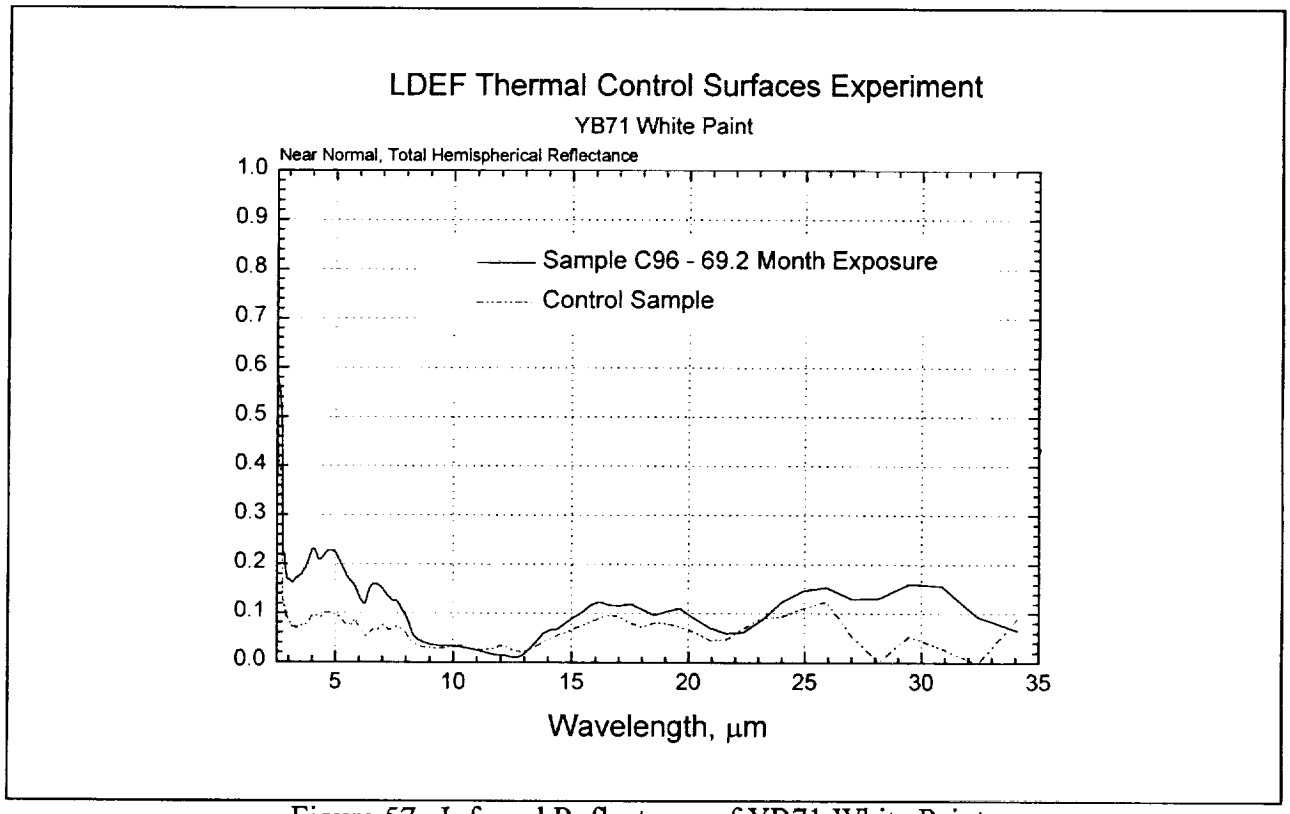

Figure 57. Infrared Reflectance of YB71 White Paint.

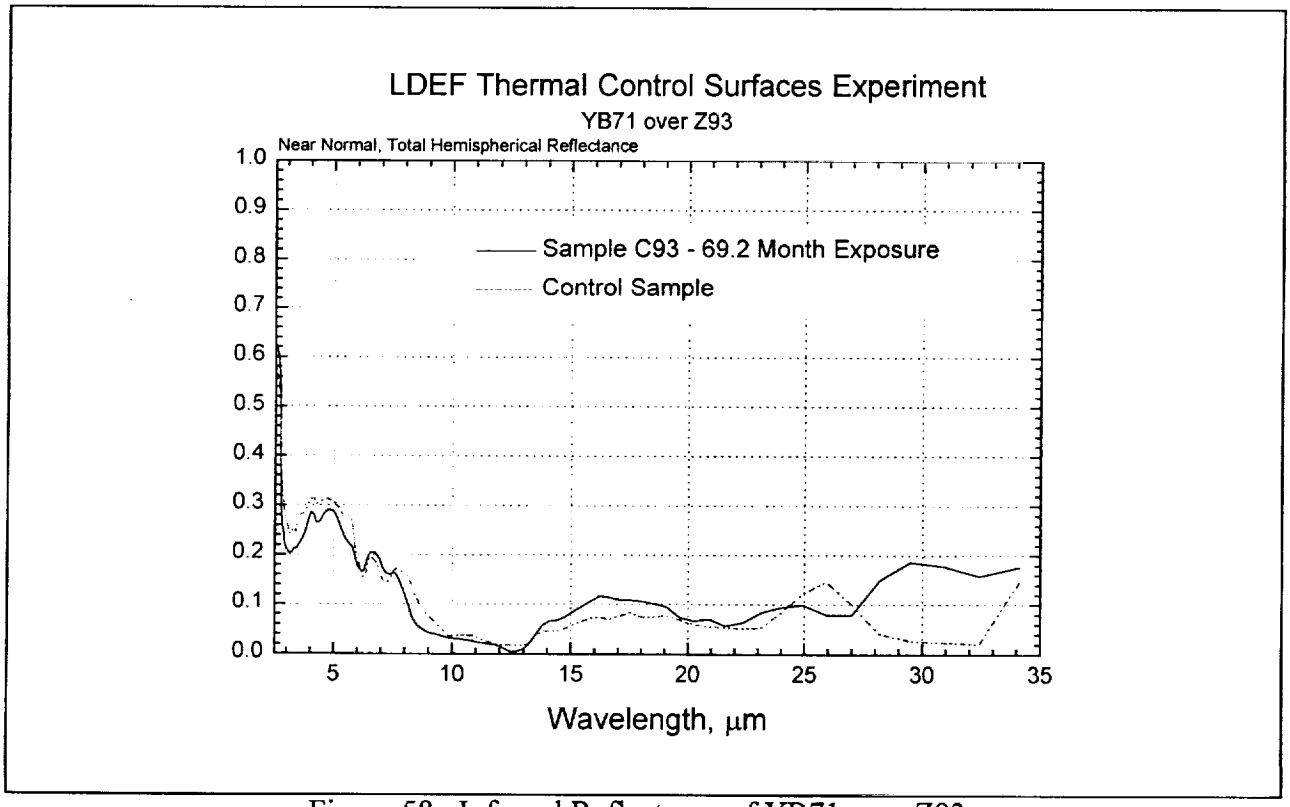

Figure 58. Infrared Reflectance of YB71 over Z93.

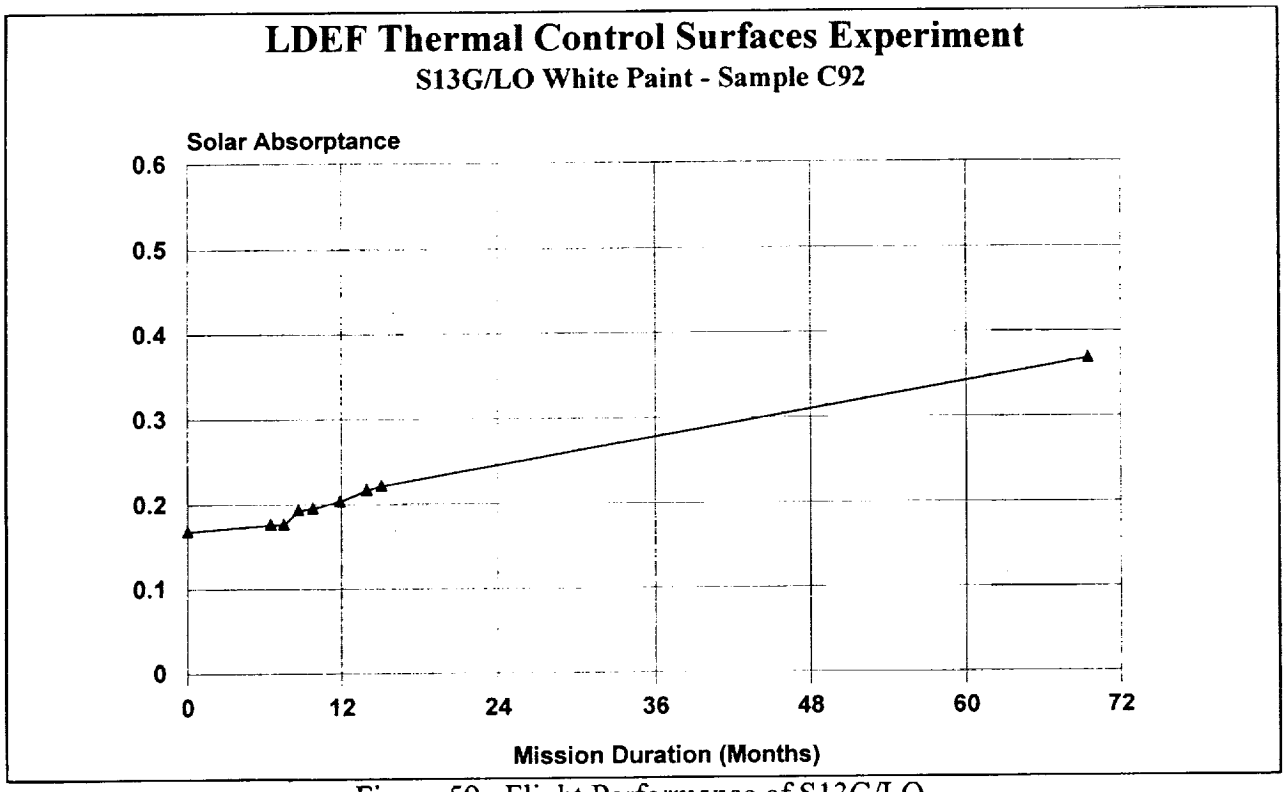

Figure 59. Flight Performance of S13G/LO.

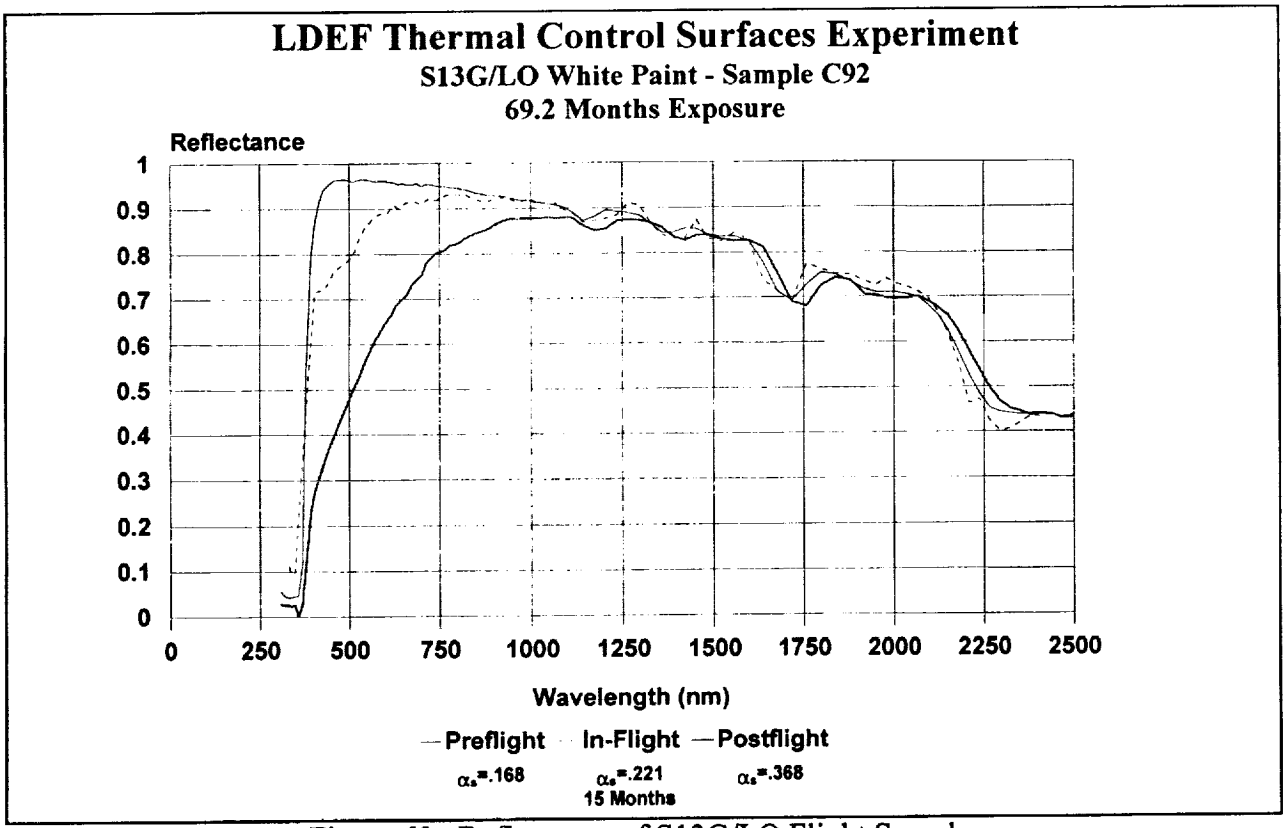

Figure 60. Reflectance of S13G/LO Flight Sample.

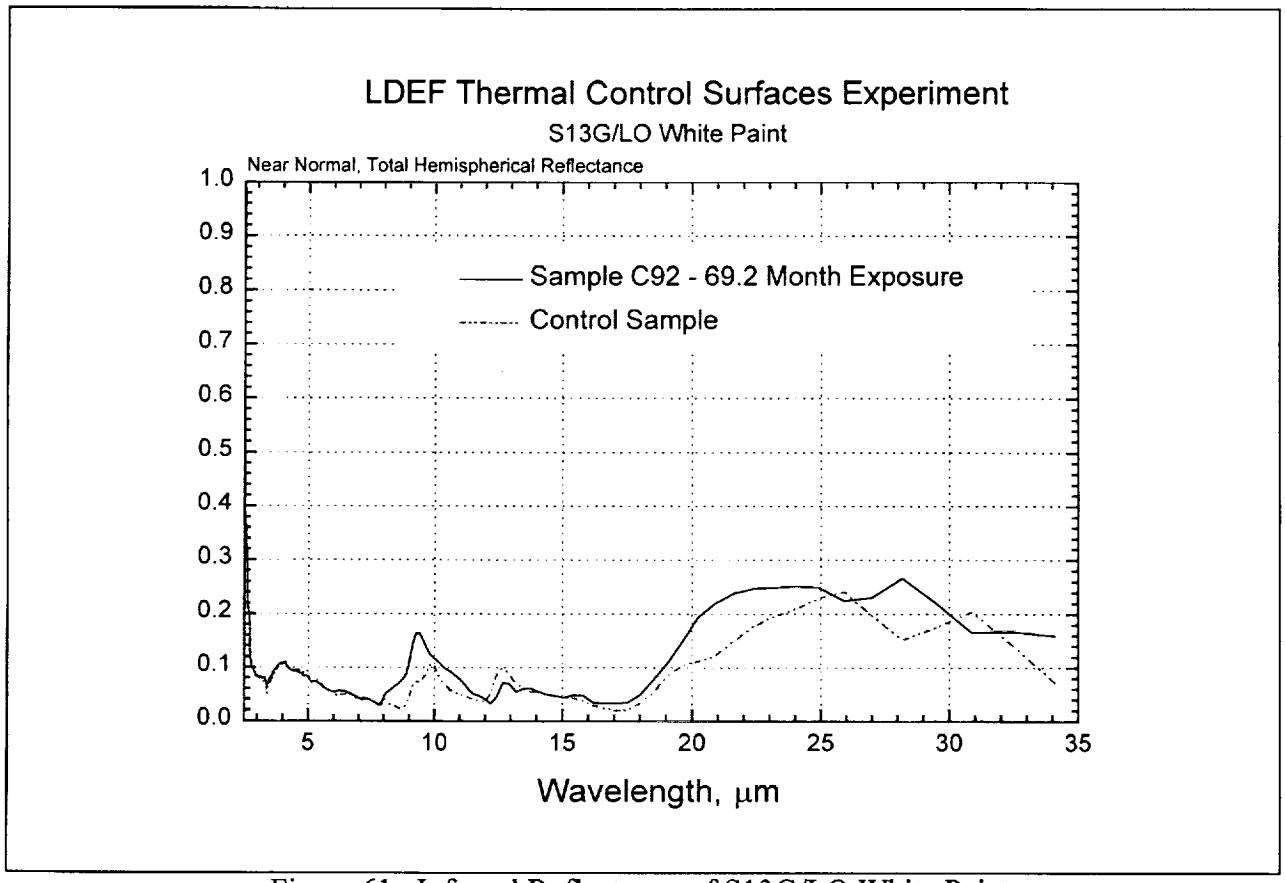

Figure 61. Infrared Reflectance of S13G/LO White Paint.

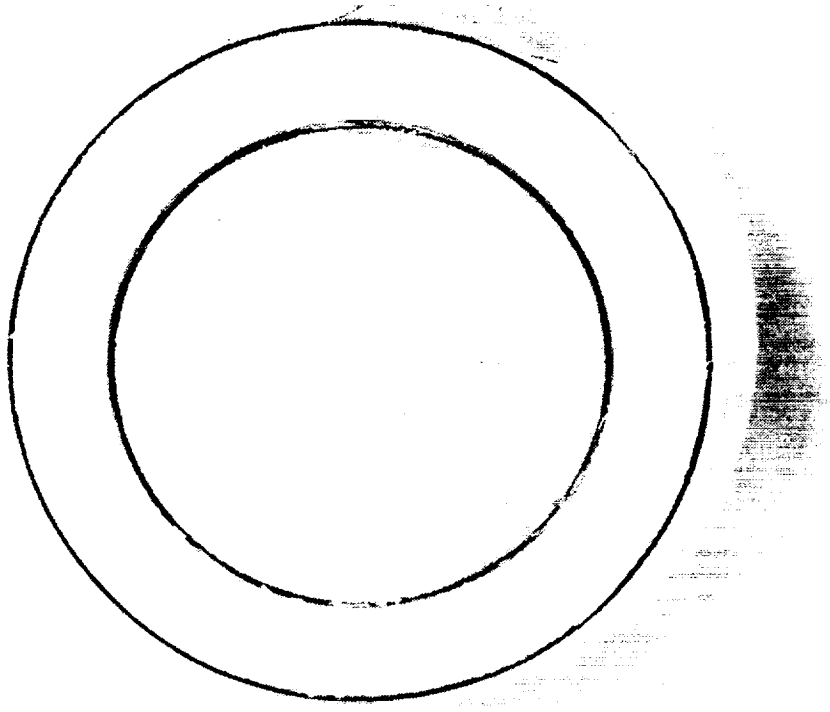

Figure 62. Post-flight Photograph of S13G/LO Sample.

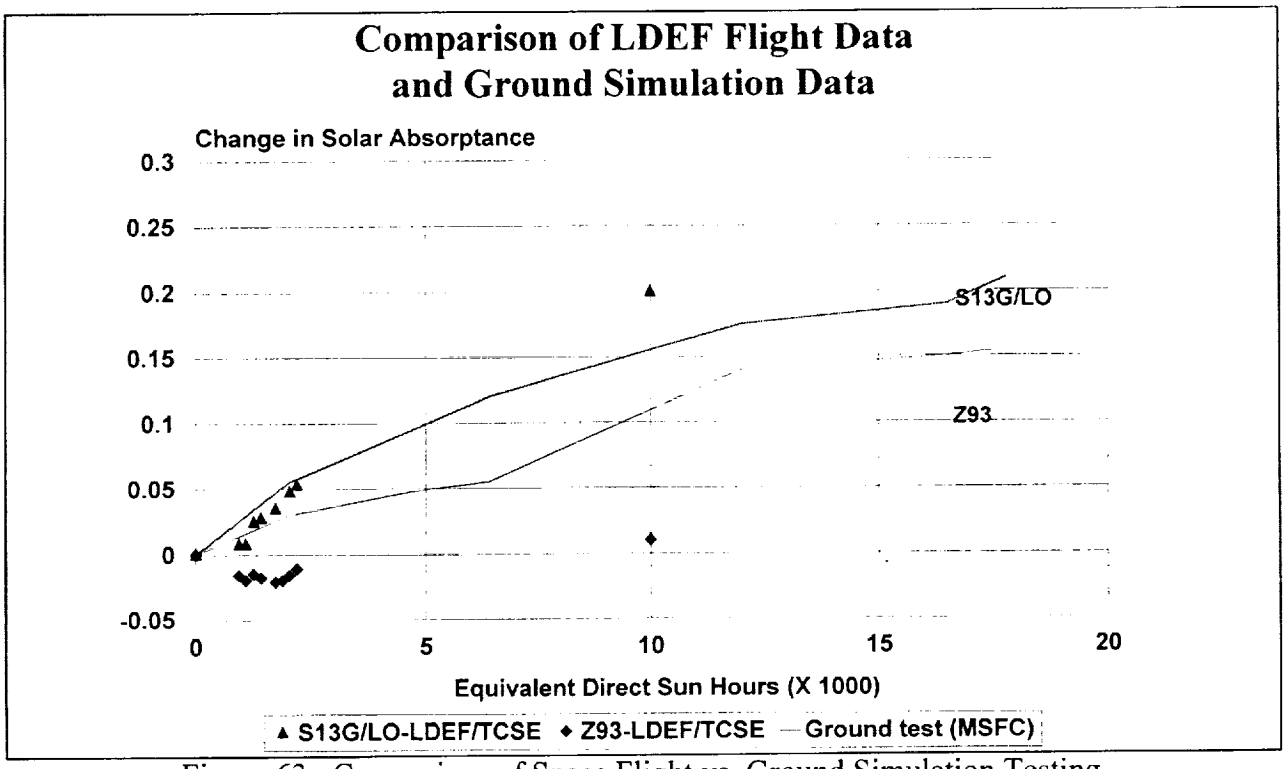

Figure 63. Comparison of Space Flight vs. Ground Simulation Testing.

5.1.5 Chromic Acid Anodize

There were two chromic anodize samples on the TCSE sample carousel provided by Wayne Slemp (LaRC). These two samples degraded significantly during the first 18 months of the LDEF/TCSE mission as shown by the TCSE in-space measurements (see Figure 64). When the TCSE batteries were depleted (19.5 months mission time) the carousel stopped where one of the two anodize samples was exposed for the remainder of the LDEF mission while the other was protected. Photographs of the two samples (Figures 65 and 66) show significantly different appearance. The sample with 19.5 months exposure has an evenly colored appearance except for several small impact craters. The sample that was exposed for the entire 69.2 month mission has a mottled, washed out appearance. Figures 67 and 68 are the detailed pre- and post-flight reflectance curves for the two anodize samples.

5.1.6 Silver Teflon Solar Reflector

There were three different silver Teflon materials on the TCSE. The front cover of the TCSE and one calorimeter sample had 0.05 mm (two mil) thick silver FEP Teflon bonded to the substrate with Y966 acrylic adhesive. The other samples had 0.125 mm (five mil) thick silver FEP Teflon (specular and diffuse) that were bonded to the substrate with P223 adhesive.

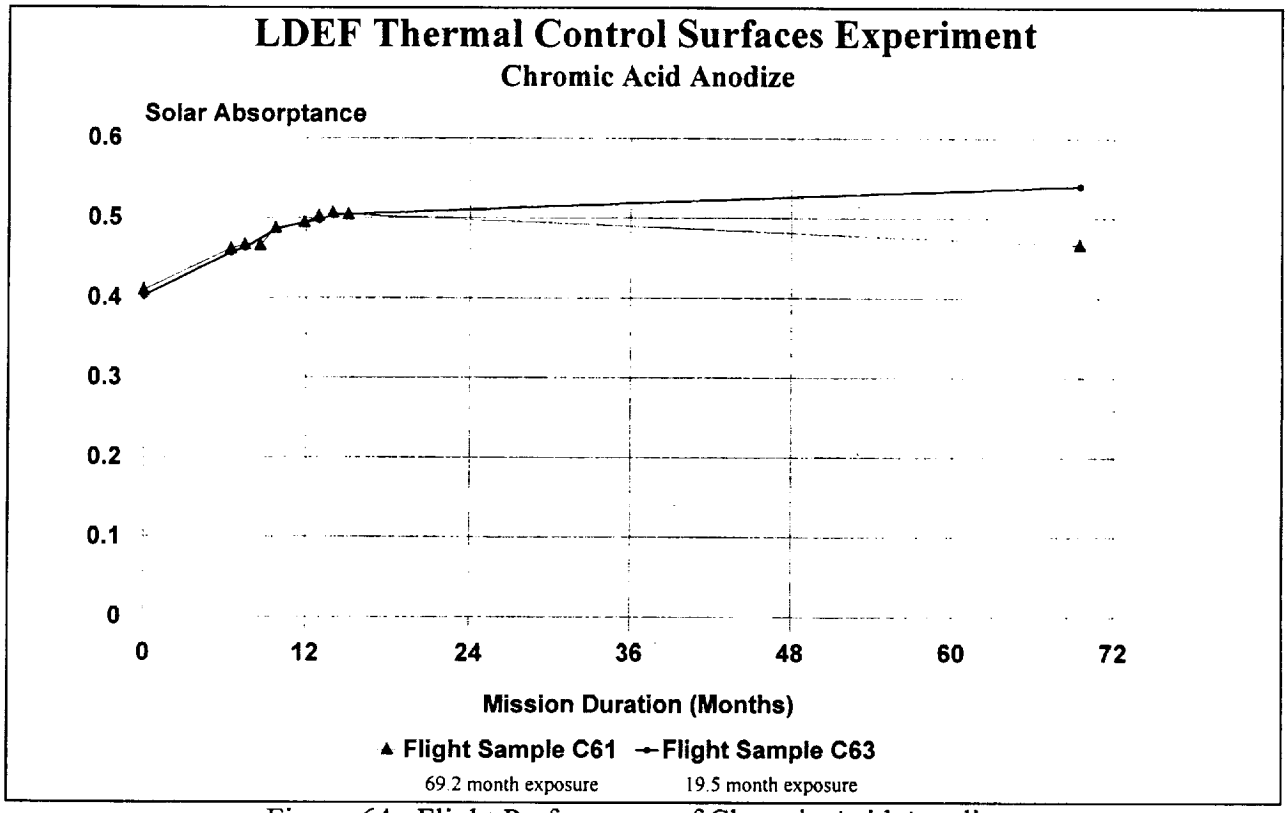

Figure 64. Flight Performance of Chromic Acid Anodize.

The silver Teflon surfaces on the TCSE underwent significant appearance changes. The most striking change observed on all the silver Teflon exposed in the LDEF RAM direction was that the surface color was changed to a diffuse, whitish appearance. AO erosion of the exposed silver Teflon surface is typical of that observed on previous flight experiments. Erosion of the exposed Teflon surface creates a non-uniform etching pattern as shown in the Scanning Electron Microscope (SEM) photograph in Figure 69. This results in a roughened surface with peaks ~1.5 microns apart which scatters incident light in a manner similar to a sand-blasted piece of glass.

Figure 70 shows a schematic cross section of the silver Teflon as applied to the aluminum surface. The silver Teflon is composed of an outer Teflon layer, a silver layer deposited on the Teflon, an inconel protective layer deposited on the silver, and Y966 acrylic pressure sensitive adhesive. The silver layer provides the high reflectance (low absorptance) and the Teflon provides the high emittance for thermal control. As seen in the schematic for undamaged Teflon, the incident light (solar flux) transmits through the smooth clear Teflon and specularly reflects off the silver layer. AO damage to the Teflon creates a roughened surface which causes scattering of the incident light.

While the AO roughened silver Teflon surfaces underwent striking appearance changes, the reflectance and solar absorptance did not degrade significantly due to this effect. For the 5 mil coatings with P223 adhesive, only small changes in reflectance (see Figure 71) and solar absorptance were measured. In addition there was very little change in emittance (see Tables 10-13 in Section 5.2).

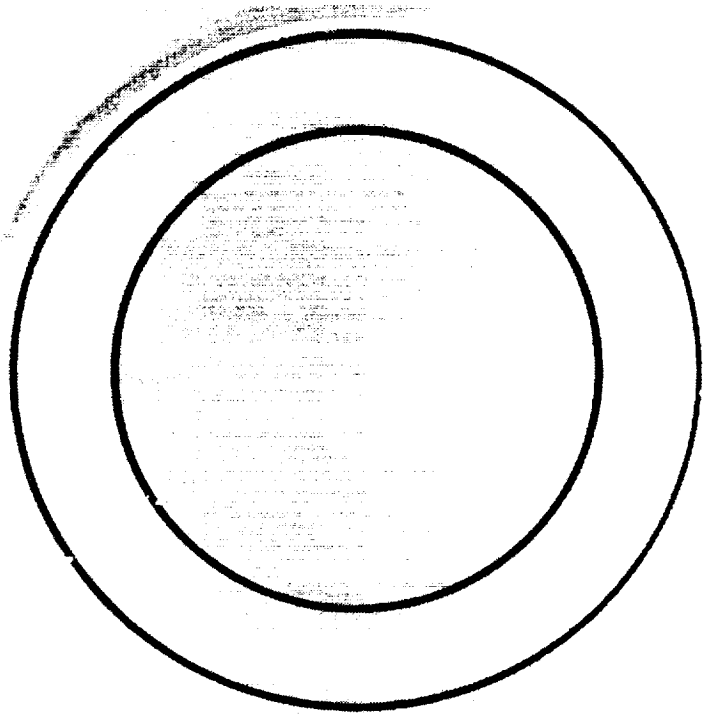

Figure 65. Anodize Sample with 19.5 Month Exposure.

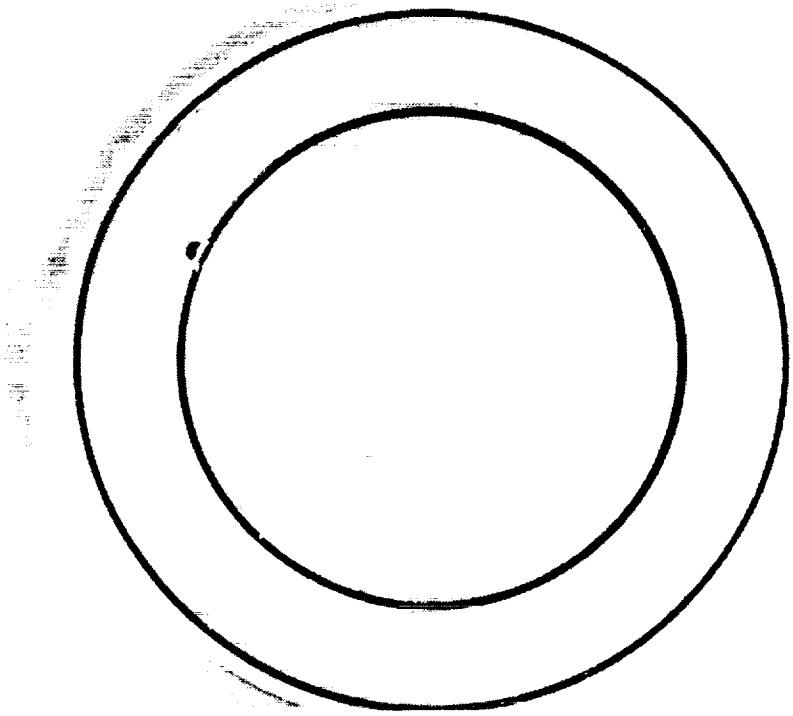

Figure 66. Anodize Sample with 69.2 Month Exposure.

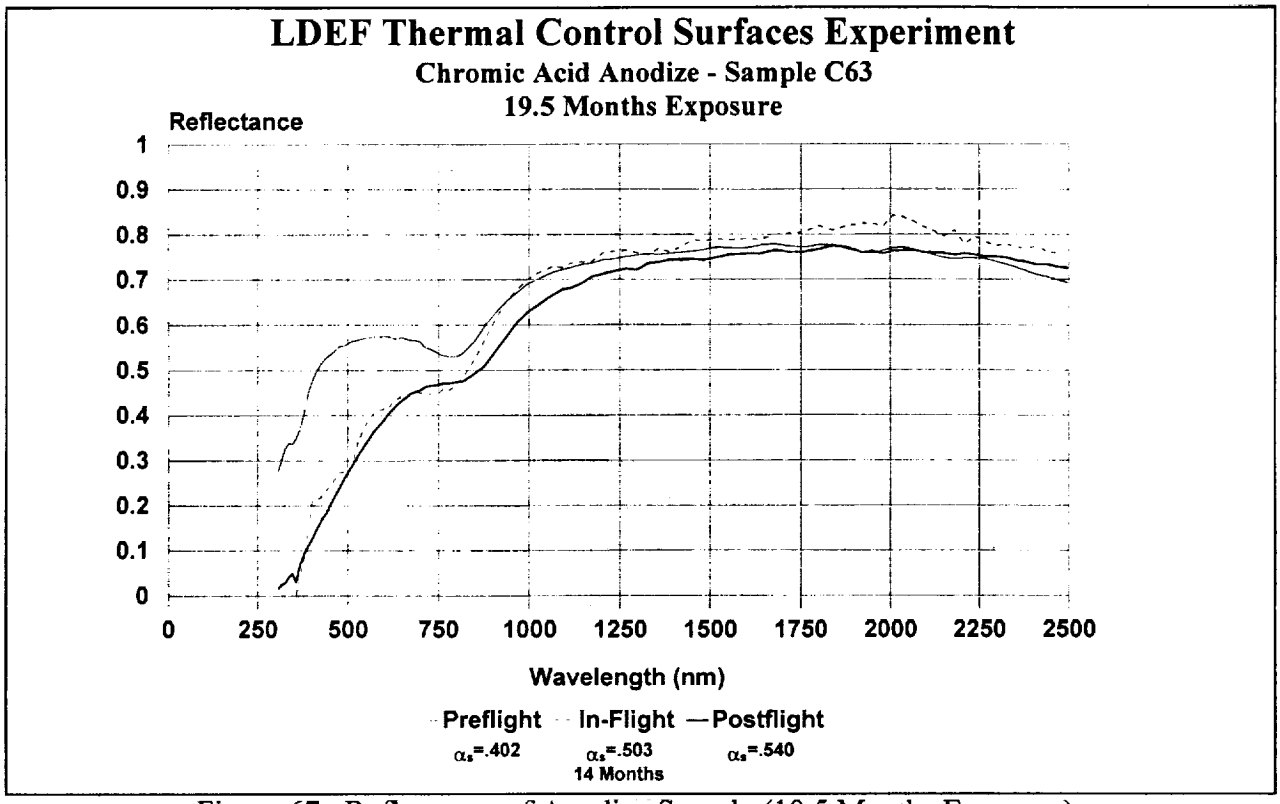

Figure 67. Reflectance of Anodize Sample (19.5 Months Exposure).

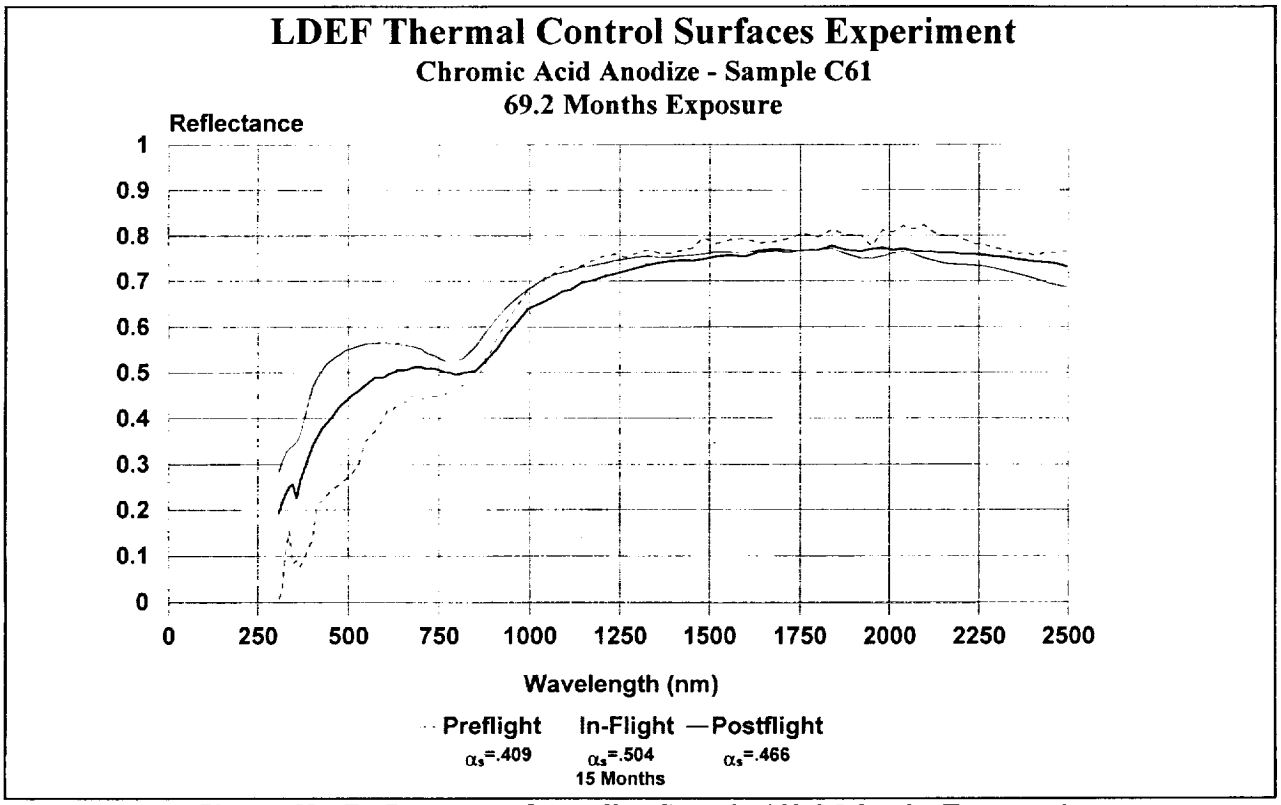

Figure 68. Reflectance of Anodize Sample (69.2 Months Exposure).

Figure 69. SEM of Exposed Teflon Surface Sample #S-1.

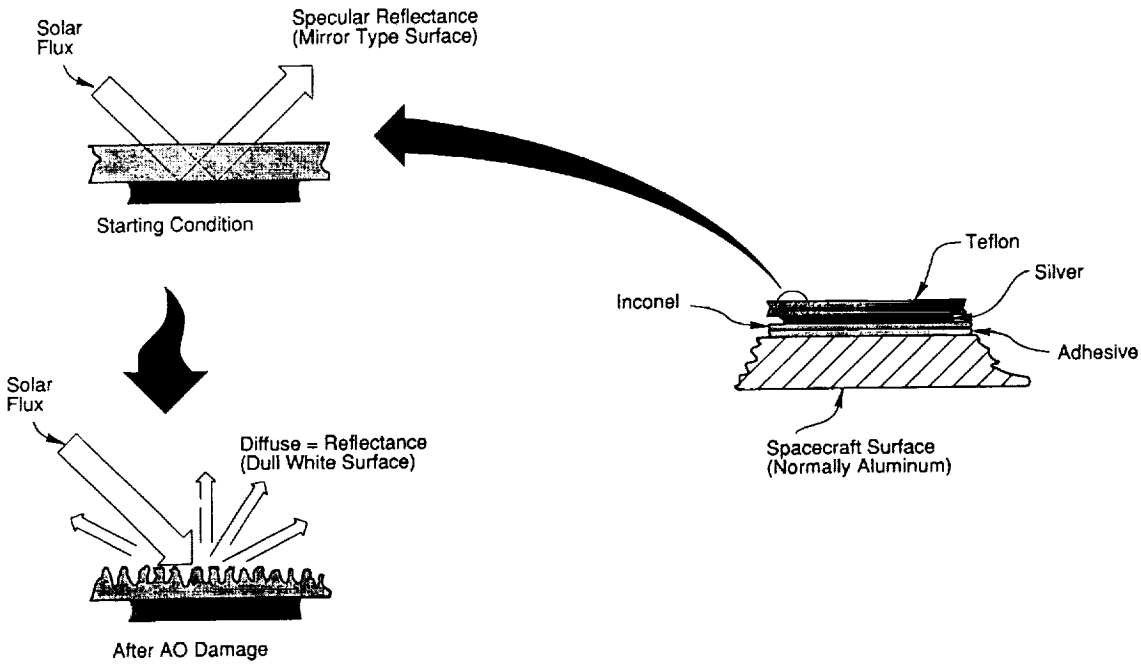

Figure 70. Silver Teflon Thermal Control Coating Atomic Oxygen Effect.

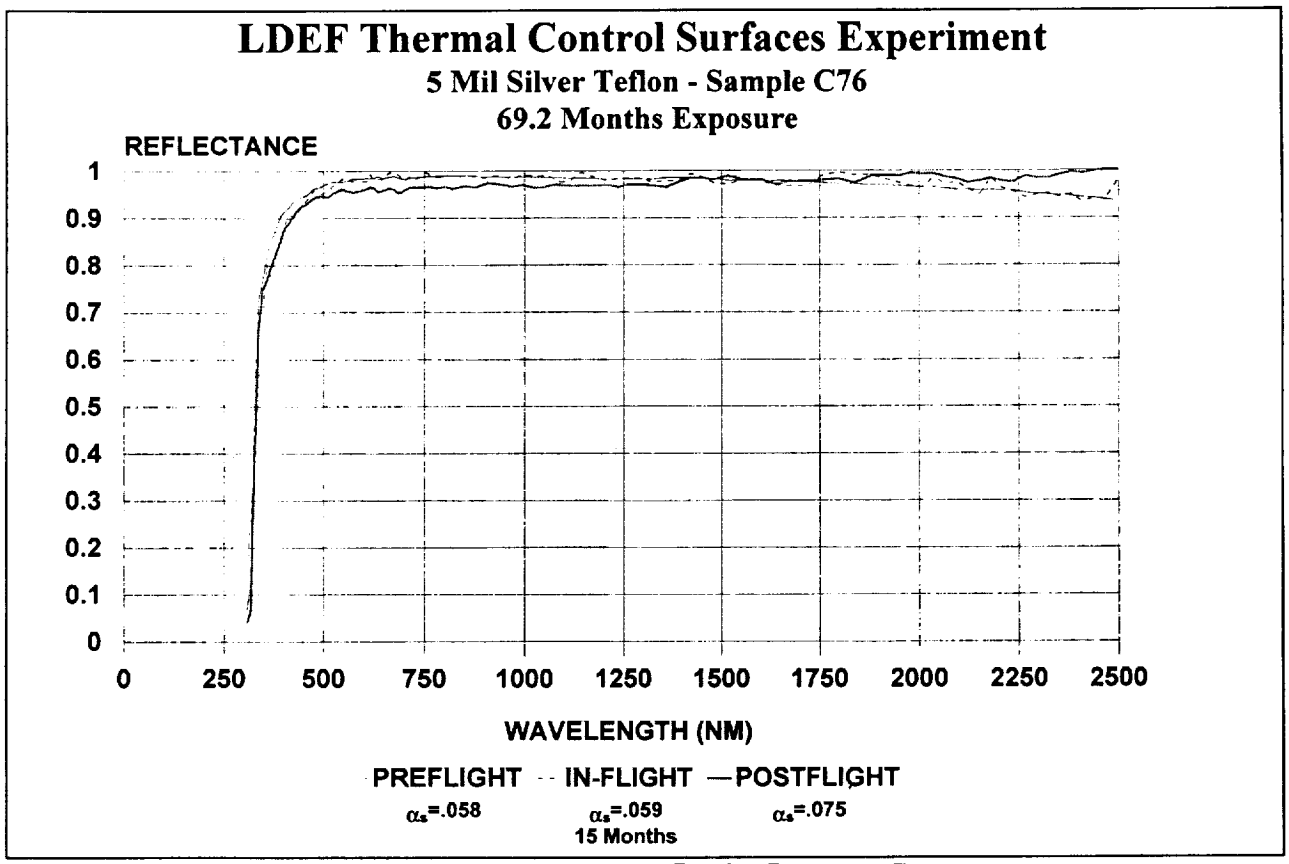

Figure 71. 5-Mil Silver Teflon Reflectance Curve.

The 0.05 mm (two mil) silver Teflon surfaces, however, did degrade significantly. The coatings had a brown discoloration. An overall view of the front thermal cover is shown in Figure 72 after removal from the TCSE main structure during post-flight disassembly. The front thermal cover has a Sheldahl 0.05 mm (2 mil) thick silver Teflon thermal control material applied with Y966 acrylic adhesive. Covered areas have no apparent damage and are still highly specular. Areas exposed to the space environment are clearly delineated and have a diffuse, whitish appearance with brown discoloration. This brownish discoloration varies from light brown to dark brown. Figure 73 is a photograph of a section of the TCSE front cover showing a demarcation line where part of the surface was exposed and part was protected by a small secondary cover. The protected area has the characteristic mirror-like finish while the exposed area (foreground) is whitish with brown streaking. The brown streaking is apparent only where it was exposed to the space environment. Changes in silver Teflon visual appearance are the result of two damage mechanisms: AO erosion and internal damage associated with cracking of the silver/inconel layer.

Samples were cut from the TCSE front cover for optical property measurements. Total hemispherical reflectance measurements were made on samples from different locations on the front cover having varying degrees of damage. Figure 74A is a plot of this data showing the magnitude of reflectance loss in the brownish discolored regions. For those regions having a low degree of the brownish discoloration, it can be seen that the total reflectance values are basically

unchanged with a solar absorptance (α_s) of 0.10 as compared to the ground reference sample (unexposed) with an α_s of ~0.08. The worse case brownish area had a solar absorptance as high as 0.49.

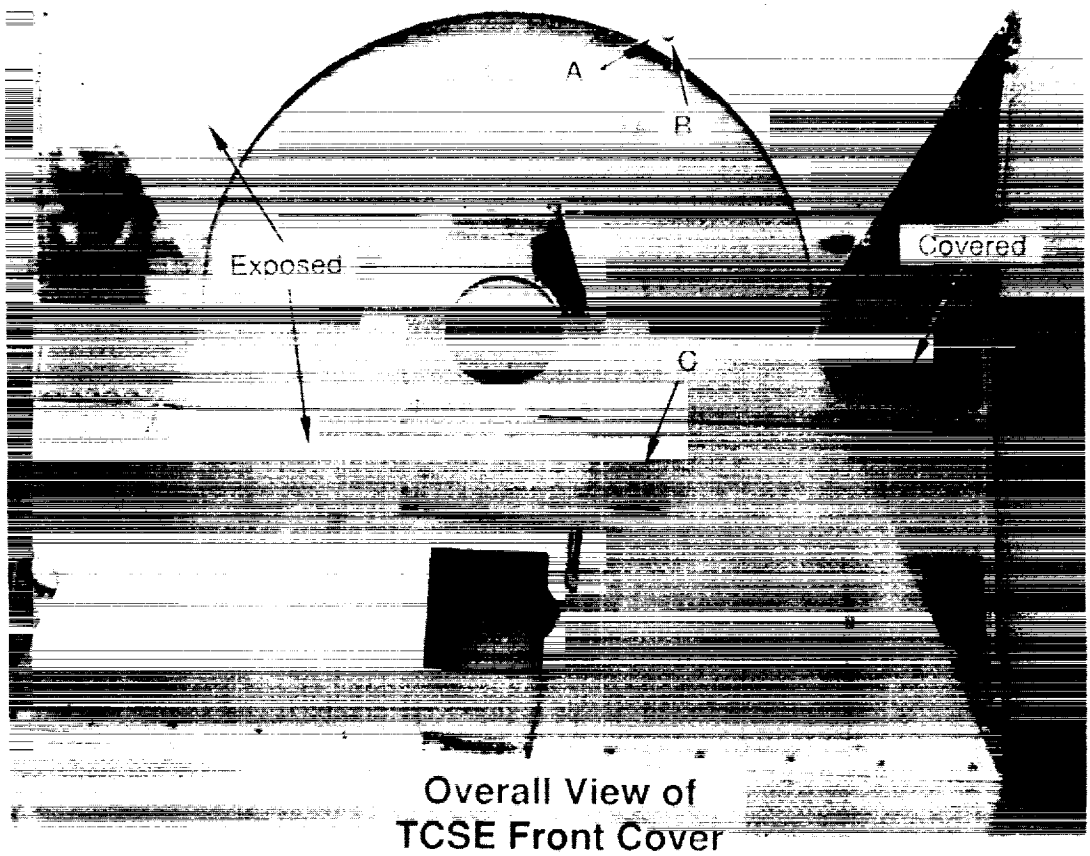

Figure 72. Overall View of TCSE Front Cover.

The emittance (ε_T) was also measured at several locations on the front panel and is plotted in Figure 74B. The protected areas were unchanged, but exposed regions degraded from an emittance of 0.68 to 0.48. Comparison with measurements of ground control samples shows that approximately 0.025 mm (0.001 inch) to .033 mm (0.0013 inch) of Teflon was removed by AO. Eddy current thickness measurements confirm these numbers.

Laboratory evaluation of these coatings with Nomarski microscopes revealed the discoloration was under the Teflon surface. Further investigation determined that the brown discoloration is associated with cracks in the silver-inconel metalized layer. Laboratory tests show that the application of the pre-adhesive type silver Teflon can crack the metalized layers. Removal of the paper backing on the adhesive and removal of air bubbles from beneath the silver Teflon can over-stress the metal layers causing significant cracking. It appears that a component of the adhesive migrated through the cracks into the interface with the Teflon over the long exposure to thermal vacuum. Subsequently, this internal contaminant was degraded by solar UV exposure causing the brown appearance. As a result, the reflectance decreased (see Figure 75) and more than doubled the solar absorptance.

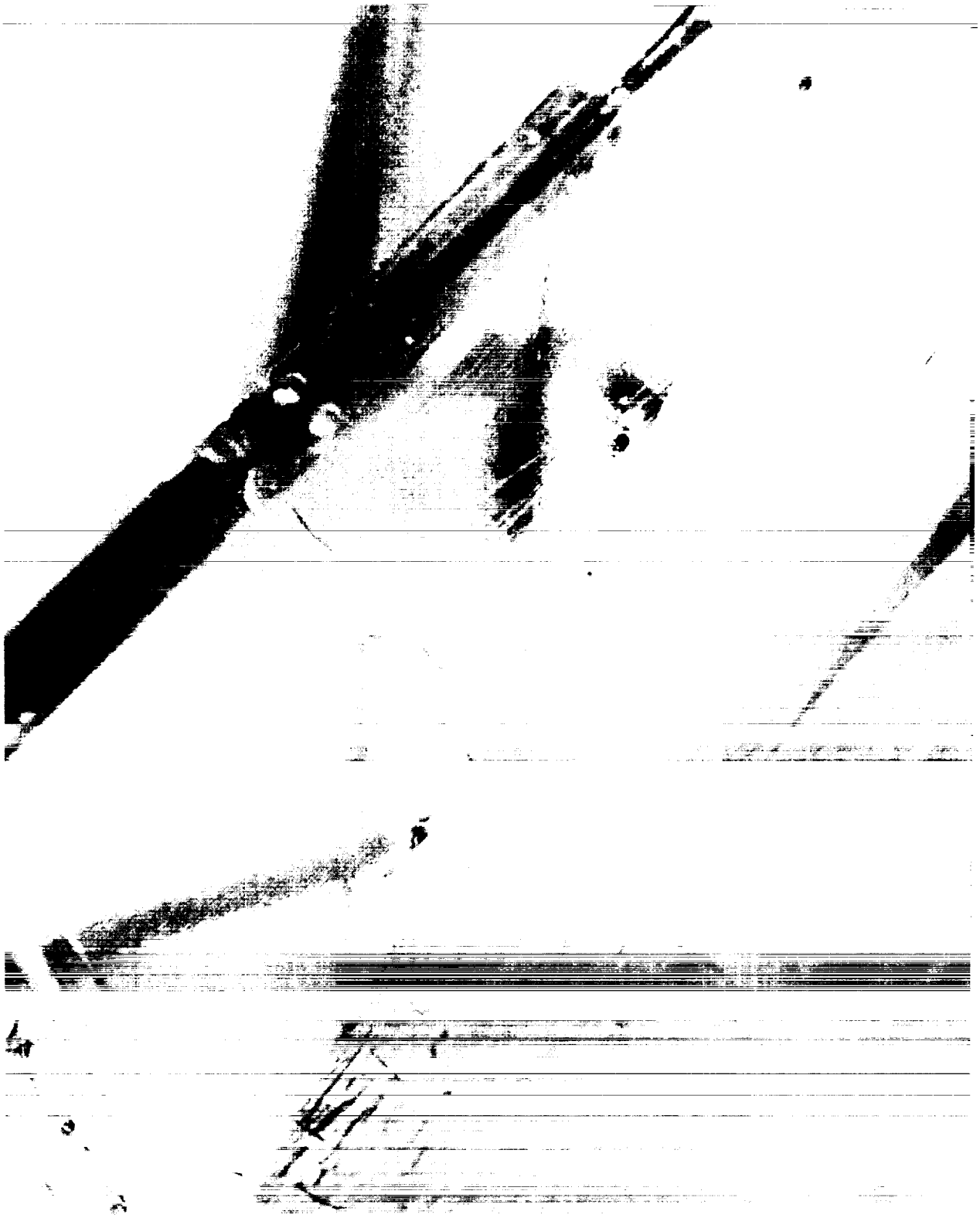

Figure 73. A Section of the TCSE Front Cover.

A. VARIATION IN REFLECTANCE PROPERTIES OF SILVER TEFLON

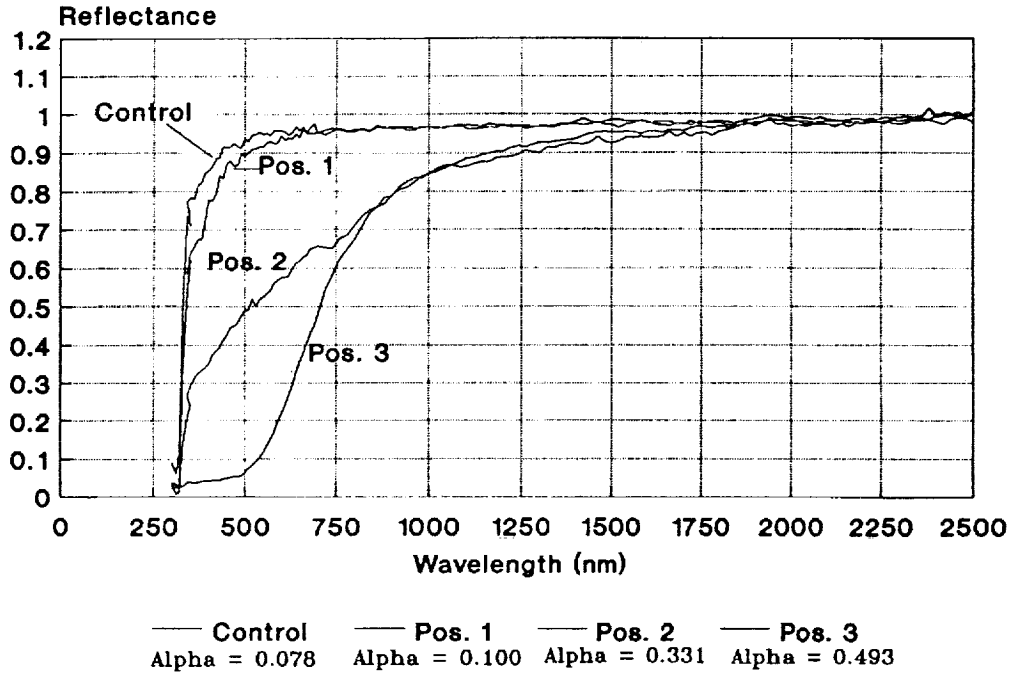

B. EMITTANCE OF SILVER TEFLON

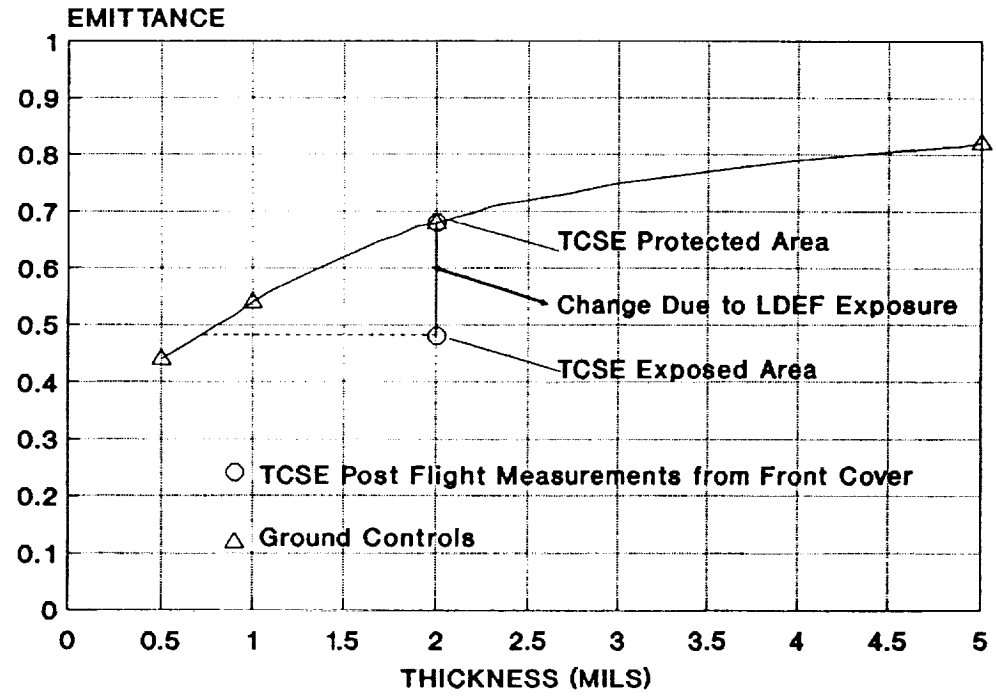

Figure 74. Optical Properties of TCSE Front Cover.

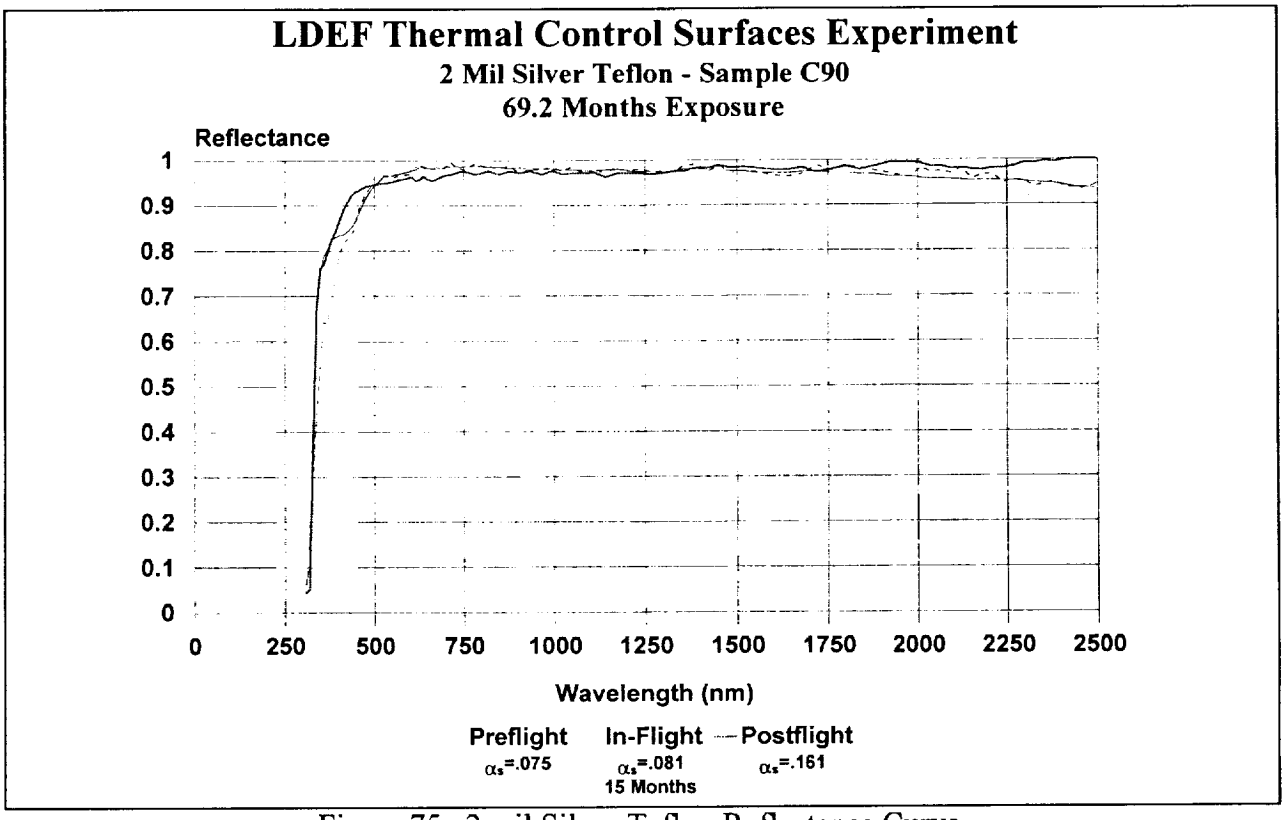

Figure 75. 2 mil Silver Teflon Reflectance Curve.

Optical measurements taken at position "1" in Figure 74A, show that AO roughening alone produces less than a 0.03 increase in solar absorptance. Larger increases in solar absorptance were measured at positions "2" and "3" where the brownish discoloration occurs. Details of the brownish discoloration will be described in the following sections.

5.1.6.1 Silver Inconel Layer Cracking

A close up of the silver Teflon covered area is shown in Figure 76, showing that the silver/inconel layer is cracked. Location "1" is typical of most of the covered region having a regular, straight cracking pattern. Location "2" is where the two silver Teflon layers meet and slightly overlap and is typical of areas that received excessive stress during application. When the silver Teflon material is stressed, the silver/inconel layer cracks, even to the point of shattering as it is bent around protrusions.

Figure 77 shows a cross section of silver Teflon during application. The silver/inconel layer undergoes severe stress during application as the Teflon layer is bent. The silver/inconel layer is on the outside of the bending radius and is stretched beyond its elastic limit and cracks. Ground tests were performed where new silver Teflon was applied to aluminum plates identical to the TCSE front thermal cover. Results show that when silver Teflon is applied to an aluminum substrate by the method shown in Figure 77, the silver/inconel layer cracks. Photomicrographs of silver Teflon before and after application to the aluminum plates are presented in Figure 78. The induced cracking pattern is in the silver/inconel layer. Note that

SEM inspection of new silver Teflon applied to aluminum failed to find any cracks in the Teflon surface. Results for silver Teflon with thicknesses from 0.25 mil to 5.0 mil show that cracking density decreases for increasing thicknesses of Teflon.

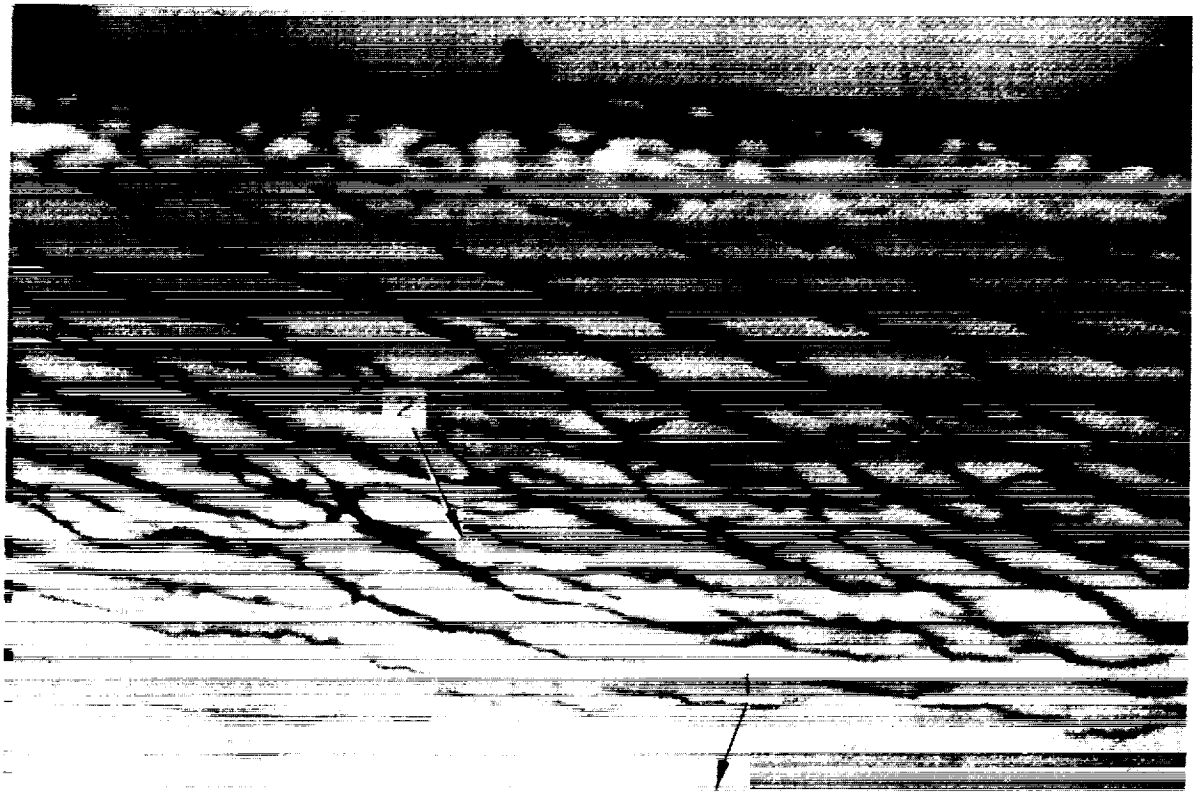

Figure 76. Cracking of Silver/Inconel Layer - Overlap Region.

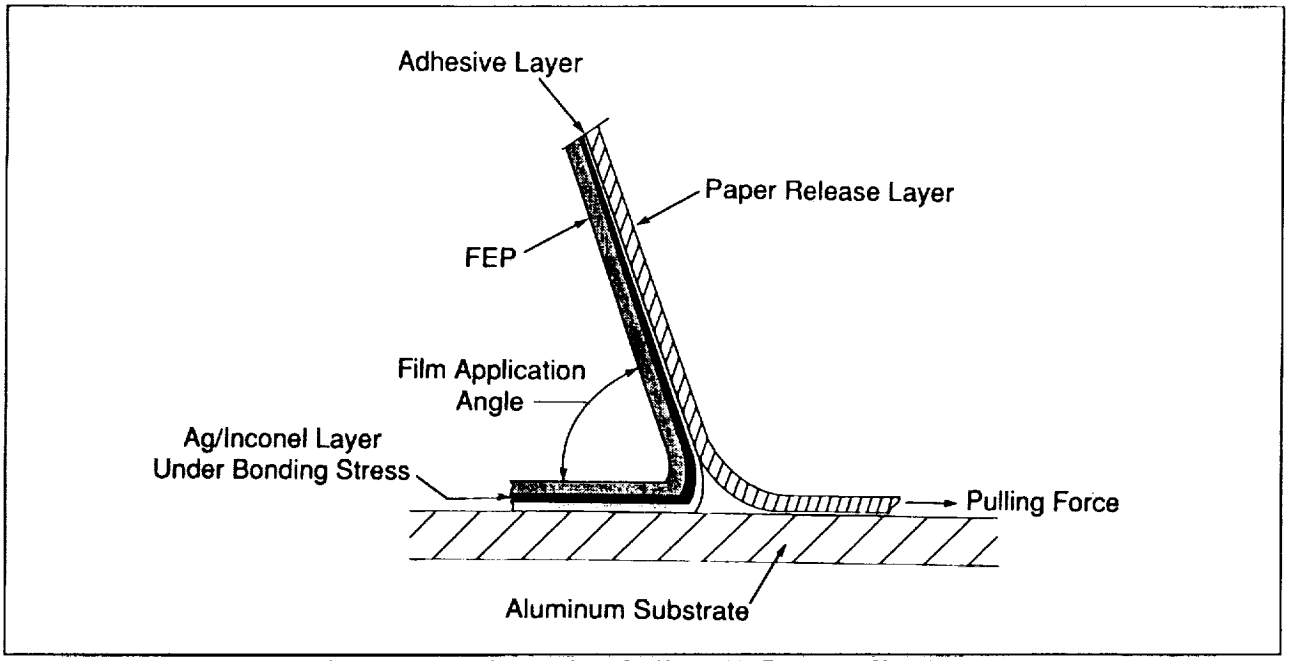

Figure 77. Schematic of Silver Teflon Application.

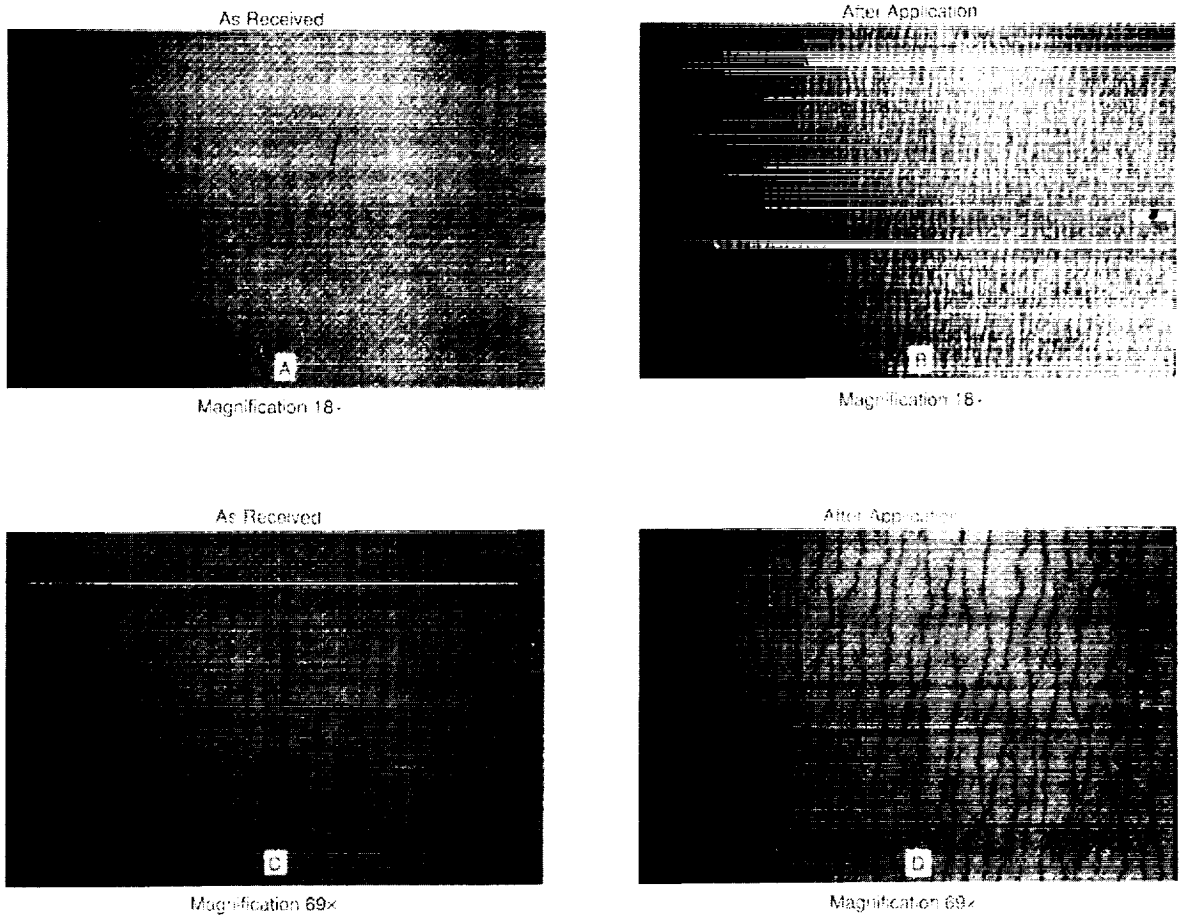

Figure 78. Silver Inconel Layer Cracking During Application of 2 mil Silver Teflon.

5.1.6.2 Silver Teflon Material Internal Damage

Silver Teflon on the TCSE that was exposed to AO and solar UV radiation has an overall whitish diffuse color. At specific locations (Figure 79C), a brownish streaking appearance is observed. Covered areas of silver Teflon had neither the whitish diffuse color nor the brownish discoloration.

Figure 79A provides a close-up view of a sample (S-1) cut from the TCSE front thermal cover showing the typical brownish discoloration. The SEM image of this sample (Figure 69) shows that the silver Teflon surface is not cracked nor is there any indication of a significant contaminant layer on the silver Teflon that could cause the brownish appearance. The TCSE silver Teflon was bonded to an aluminum substrate which prevented flexing of the material that might have caused cracks to show up in the top Teflon layer as has been observed on other experiments.

Visible microscopic examination also failed to find surface contamination in the brownish discolored areas. Internal damage to the silver Teflon material in the form of a brownish streaking effect was observed along the silver/inconel cracks. This brownish color

appears to have spread from silver/inconel cracks to the interface region between the Teflon and silver/inconel layer.

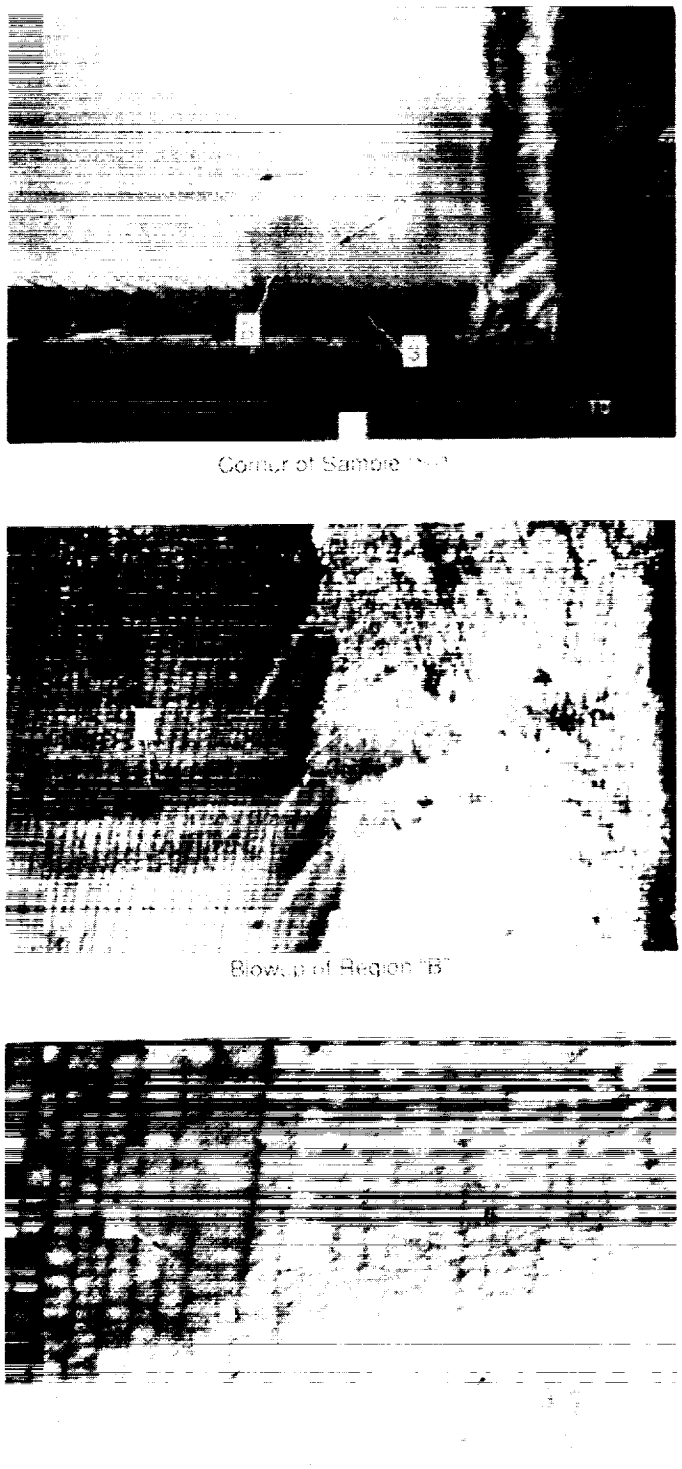

Figure 79. Silver Teflon "Brownish" Discoloration and Silver/Inconel Layer "Crack" Association.

Referring to the view of sample S-1 in Figure 79A, area "1" has the typical AO damage, but lacks the brownish discoloration, whereas area "2" has the typical brownish color. At area "3", in comparison, the surface diffuse layer of the Teflon was removed during the cutting operation returning the silver Teflon to its original specular appearance. In general, any contact, including touching or wiping of the Teflon surface which has the whitish diffuse color, returns it to its original specular appearance.

An enlargement of location "B" in Figure 79A is shown in Figure 79B. Note the brownish streaks/cracks going from area "1" to "2" were not disturbed by the removal of the surface diffuse layer on the Teflon.

Figure 79C is an enlargement of area "C" of Figure 79B. The intensity of the brownish darkening can be seen to be a function of the closeness and degree of silver/inconel layer cracking. Areas "1" and "2" of Figure 79C have the diffuse Teflon surface which blurs the image of the cracks. When the diffuse layer is removed, as in areas "3" and "4", a clearer image is seen of the silver/inconel cracks. These images demonstrate that the brownish streaking is not on the Teflon surface and, since the silver/inconel layer is opaque, the streaking must be located at the Teflon/silver interface. In addition, it appears that the discoloration, which is probably a component of the adhesive, spreads outward from the cracks between the Teflon/silver interface.

Based on the post-flight analysis, the brownish streaking was the result of a series of events starting with the initial cracking of the silver/inconel layer during application to the TCSE front thermal cover. Subsequent long-term exposure to thermal cycling and solar UV caused the brownish discoloration. The intensity of the brownish discoloration is a direct function of the crack density which appears to be caused by excessive handling or stretching.

The rate of change in reflectance in the silver Teflon active samples, and its resulting solar absorptance, did not change rapidly early in the TCSE mission. Figure 80 shows only a small increase in solar absorptance through the first 16 months of exposure. This indicates that this internal contamination and subsequent optical degradation occurs slowly over long space exposure.

5.1.7 White Tedlar Film

White Tedlar is another material that was expected to degrade over the 5.8 year LDEF mission due to solar UV exposure. Instead, the reflectance properties of this material improved slightly, as shown in Figures 81 and 82. The surface remained diffuse and white, similar to pre-flight observations. As with A276, Tedlar has been shown to be susceptible to AO erosion.[10] The erosion effect of AO is the apparent reason for the lack of surface degradation of these flight samples.

The TCSE in-flight data shows that only a small degradation in solar absorptance was seen early in the LDEF mission. This indicates that, as with the A276 samples, there was sufficient AO early in the mission to erode away damaged material or otherwise inhibit significant degradation. The subsequent high AO fluence then eroded away all the damaged

surface materials and even provided a slight improvement in solar absorptance. The Tedlar control samples show a small UV fluorescence which was not apparent in preliminary measurements of the flight samples.

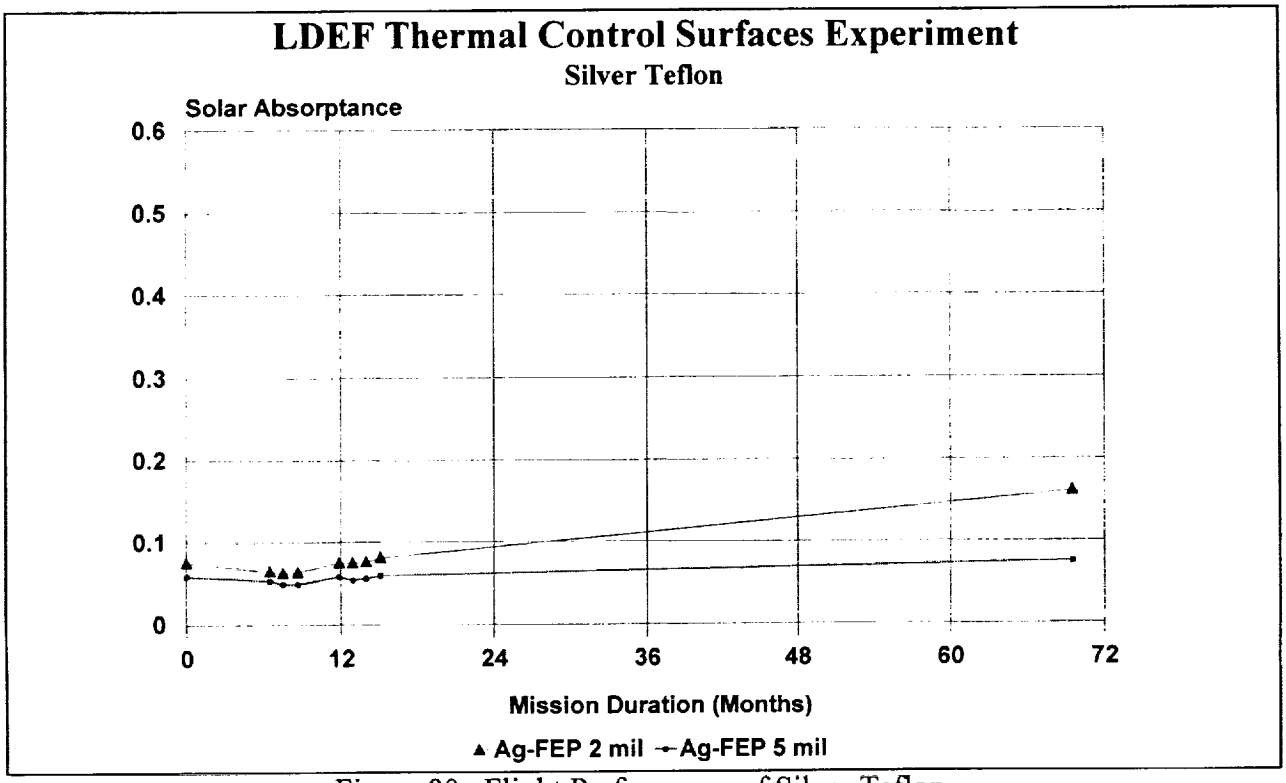

Figure 80. Flight Performance of Silver Teflon.

5.1.8 Black Paints

Two different black paints were flown on the TCSE - IITRI D111 and Chemglaze Z302. D111 is a diffuse black paint that performed very well with little change in either optical properties or appearance as a result of the TCSE mission. Figure 83 shows the reflectance of the D111 Black Paint and Figure 84 is a post-flight photograph of the sample. The D111 samples had some small imperfections in the coating that were seen in the pre-flight inspections. The IR reflectance shown in Figure 85 also demonstrates the stability of D111 for the LDEF exposure.

Z302 gloss black is the other black coating flown on the TCSE. Z302 has been shown to be susceptible to AO exposure.[4] In anticipation of these erosion effects, protective OI650 and RTV670 overcoatings were applied over some of the Z302 samples to evaluate their effectiveness. As expected, unprotected Z302 was heavily eroded by the AO exposure. Two of the TCSE Z302 coatings were exposed to the environment for the total 5.8 year LDEF mission. These unprotected Z302 sample surfaces eroded down to the primer coat. Two other samples were exposed for only 19.5 months and, while they did erode, still had good reflectance properties (see Figure 86).

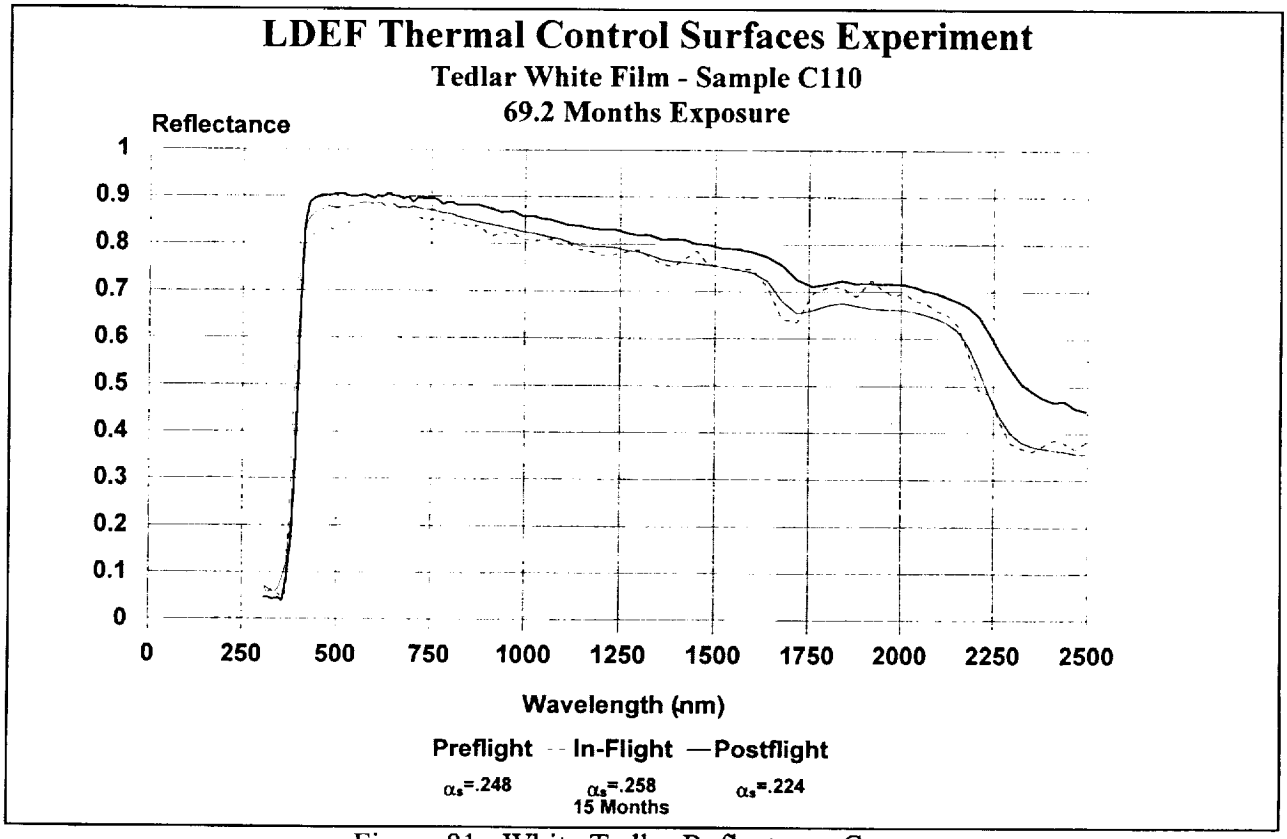

Figure 81. White Tedlar Reflectance Curve.

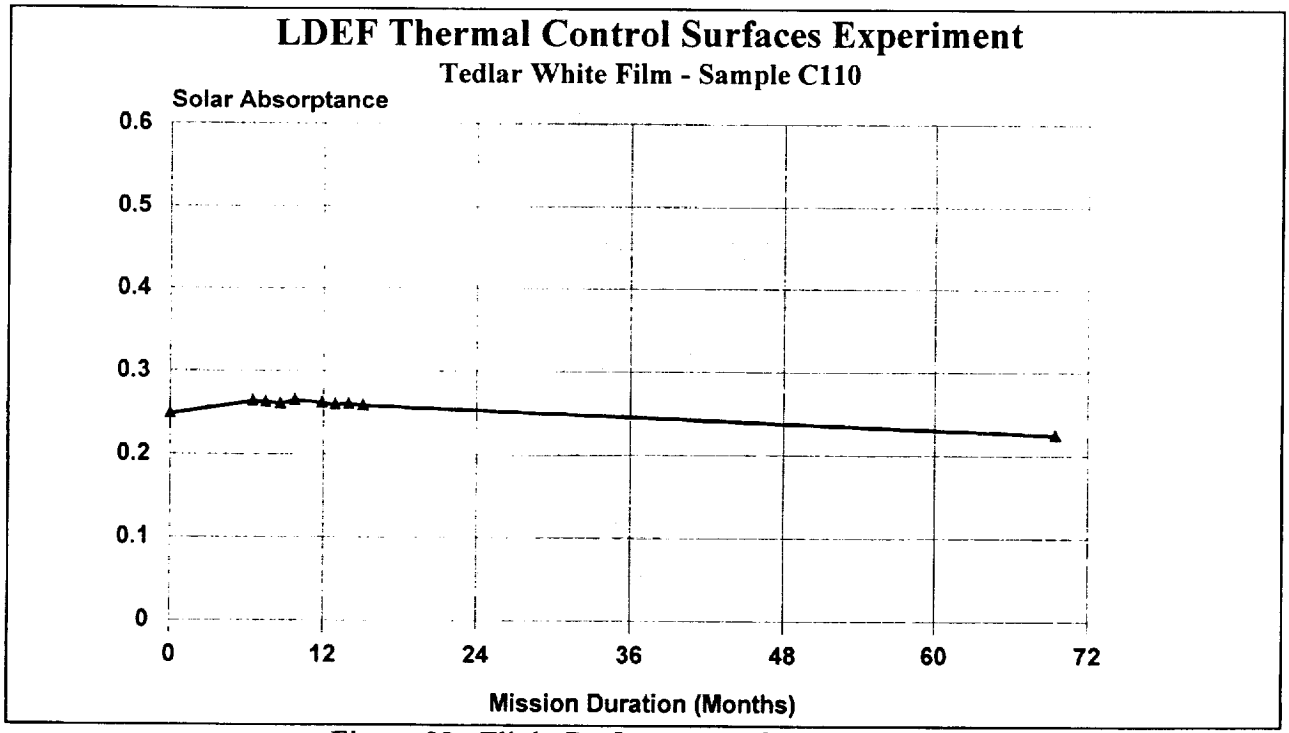

Figure 82. Flight Performance of White Tedlar.

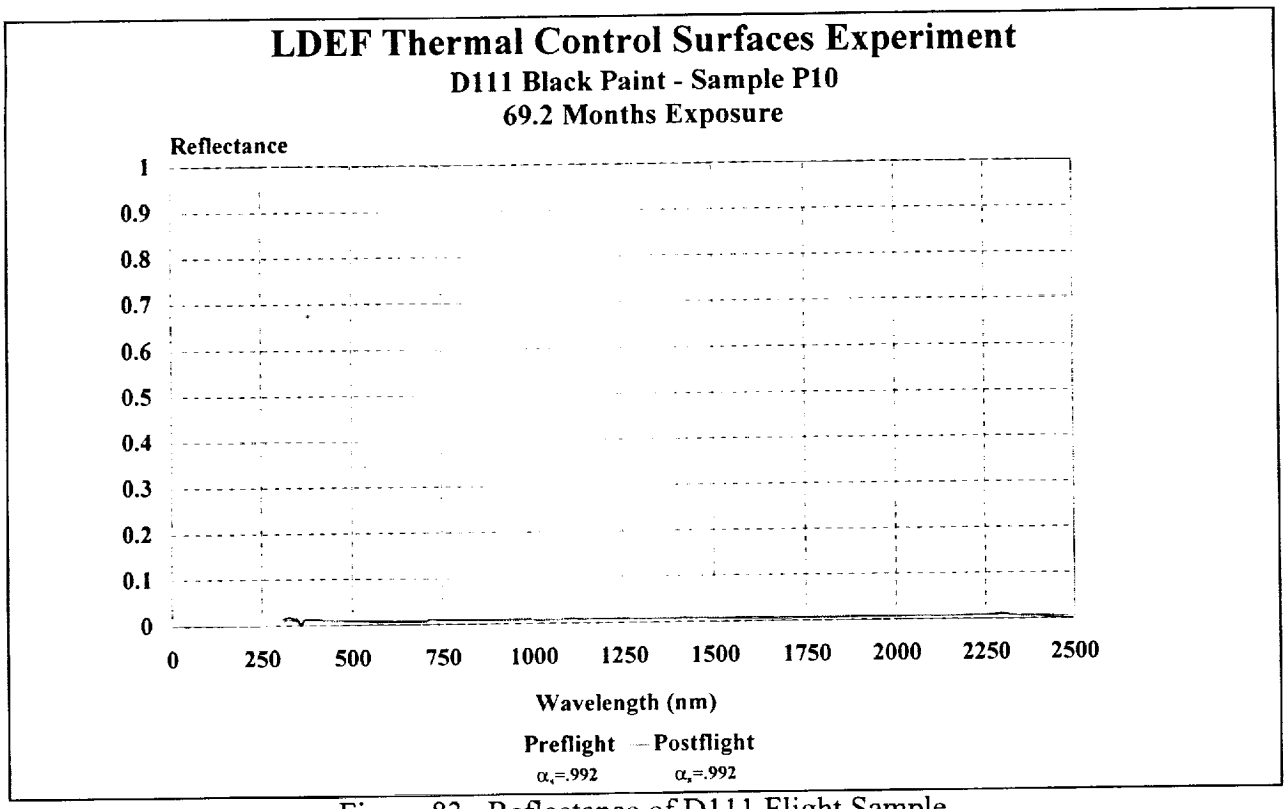

Figure 83. Reflectance of D111 Flight Sample.

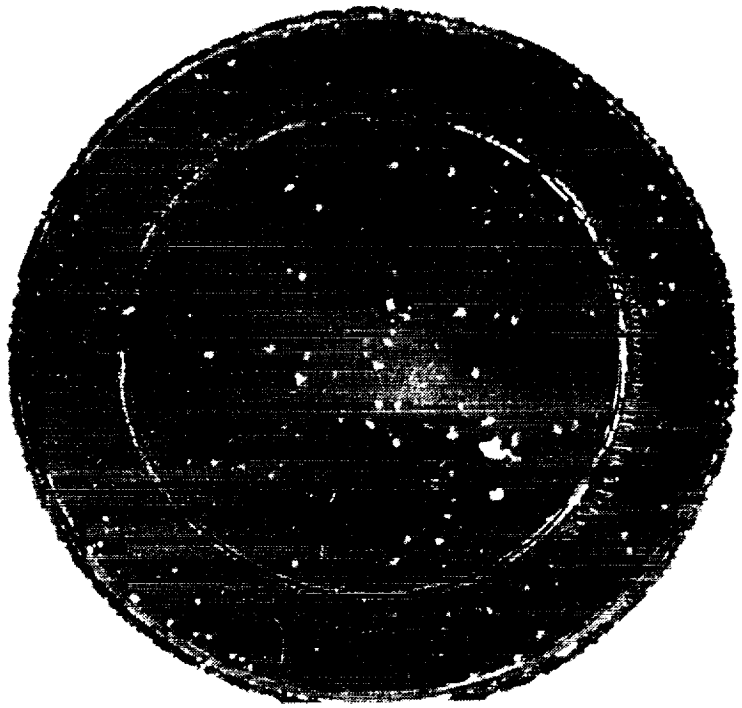

Figure 84. Post-flight Photograph of D111 Black Paint.

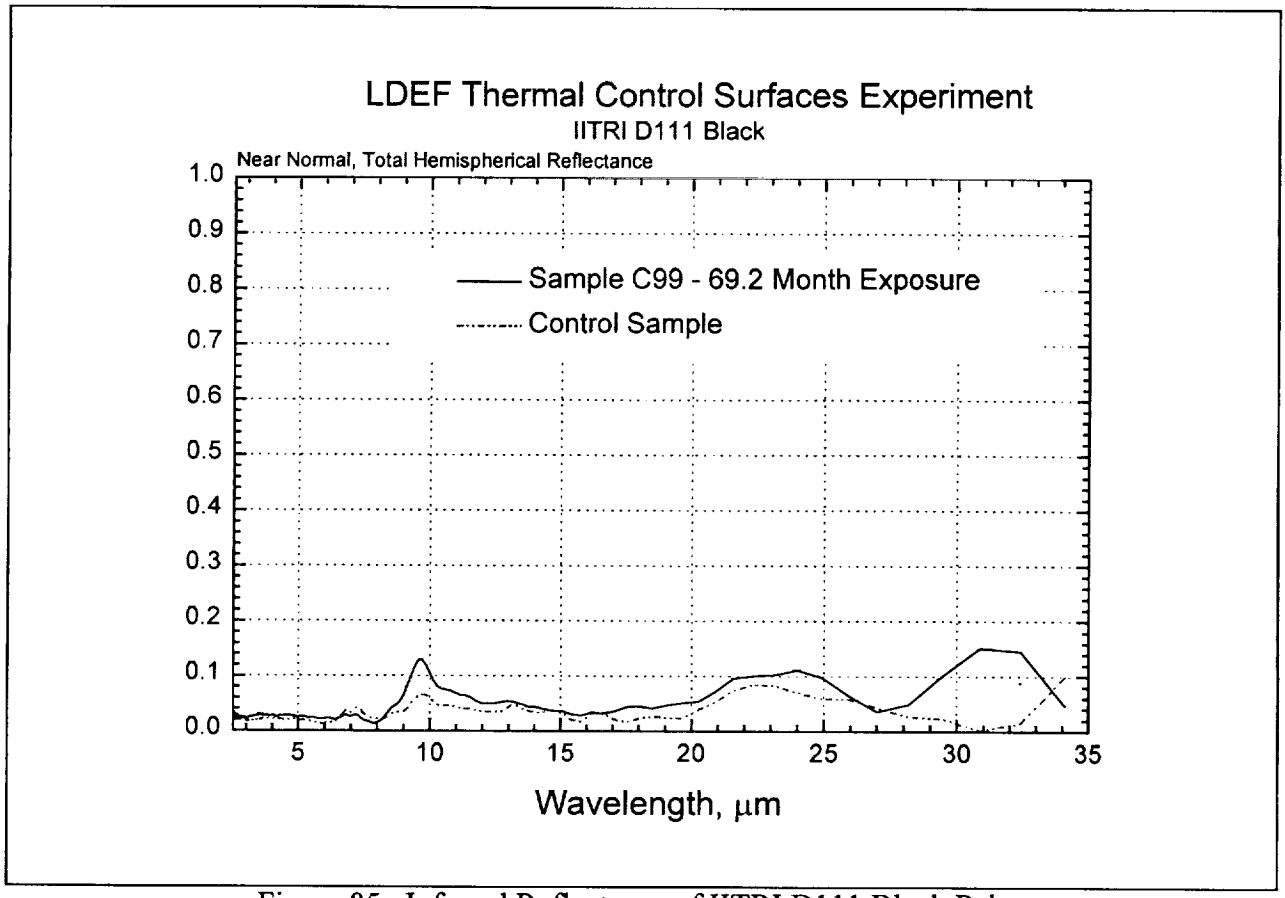

Figure 85. Infrared Reflectance of IITRI D111 Black Paint.

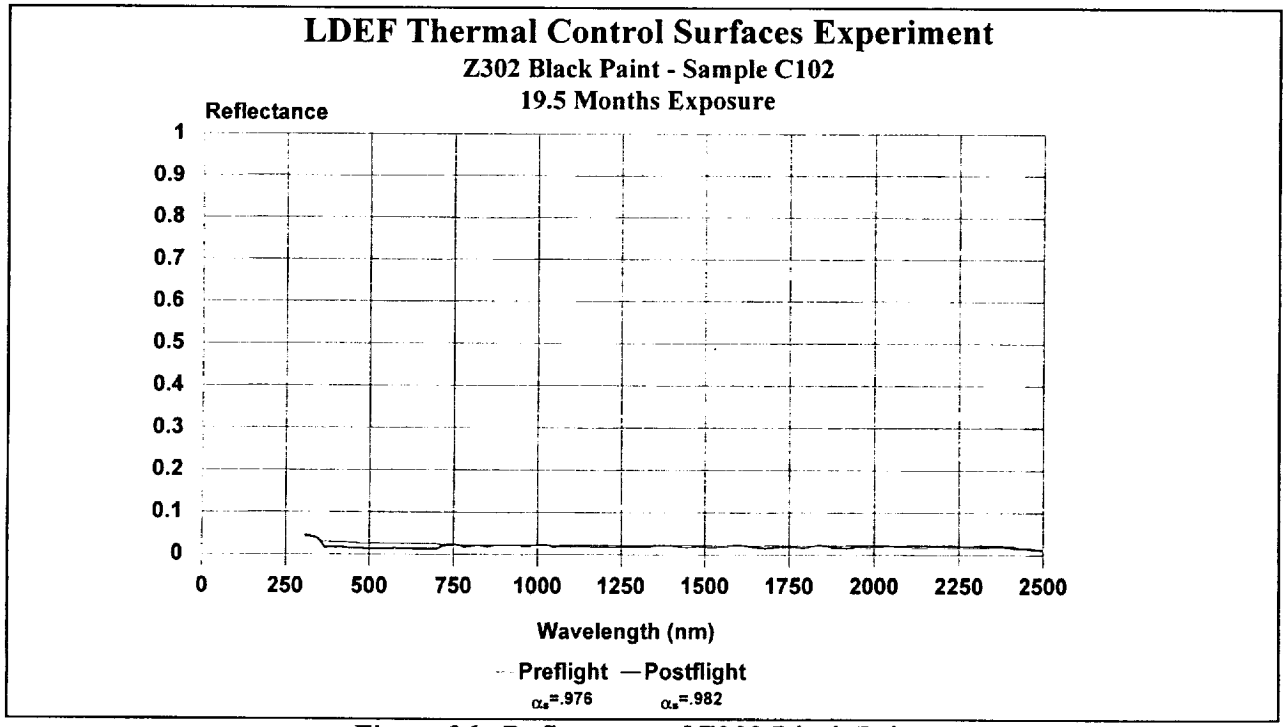

Figure 86. Reflectance of Z302 Black Paint.

The overcoatings for the Z302 behaved similarly to the overcoatings on the A276 samples (see Figures 87 and 88). The Z302 appears to have been protected by the overcoatings, but the overcoats cracked and crazed (see Figures 89 and 90). The coatings that were applied to the calorimeter sample holders are believed to have peeled away from the substrate because of the wider temperature excursions of these thermally isolated samples. The IR reflectance (Figures 91 and 92) of the overcoated samples shows llittle change for the exposed samples.

In addition, the fluorescence of the Z302 samples changed due to the LDEF exposure. Using a short wavelength UV black light, the unprotected Z302 exhibited a pale green fluorescence while the overcoated samples fluoresced bright yellow. Initial spectral analysis of the Z302 samples show that the control samples naturally fluoresce; however, the LDEF exposure caused a wavelength shift and an increase in the magnitude of the fluorescence. See Section 5.4 for results of fluorescence studies.

5.2 Optical Properties Trend Analysis

The increasing duration of space missions requires significant extrapolation of flight and ground simulation data to provide predictions of end-of-life properties for thermal control surfaces. This is particularly true for NASA programs such as the International Space Station, AXAF and the HST. The in-space optical measurements performed by the TCSE offer the unique opportunity to perform a trend analysis on the performance of materials in the space environment. Trend analysis of flight data provides the potential to develop an empirical prediction model for some of the thermal control surfaces. For material research, trend analysis of the TCSE flight data can provide insight into the damage mechanisms of space exposure.

The trend analysis for the TCSE samples has been limited to those materials that were not significantly eroded by the AO environment. The performance of several materials on the LDEF mission was dominated by AO effects. This is particularly true for unprotected A276 and Tedlar where the AO eroded away the surface layers faster than they were degraded by Solar UV. This resulted in a fresh surface with unchanged or slightly improved optical properties. Trend analyses have been performed on five materials:

- Z93 White Paint
- YB71 White Paint
- S13G/LO White Paint
- A276 White Paint and Protective Overcoats
- Silver Teflon

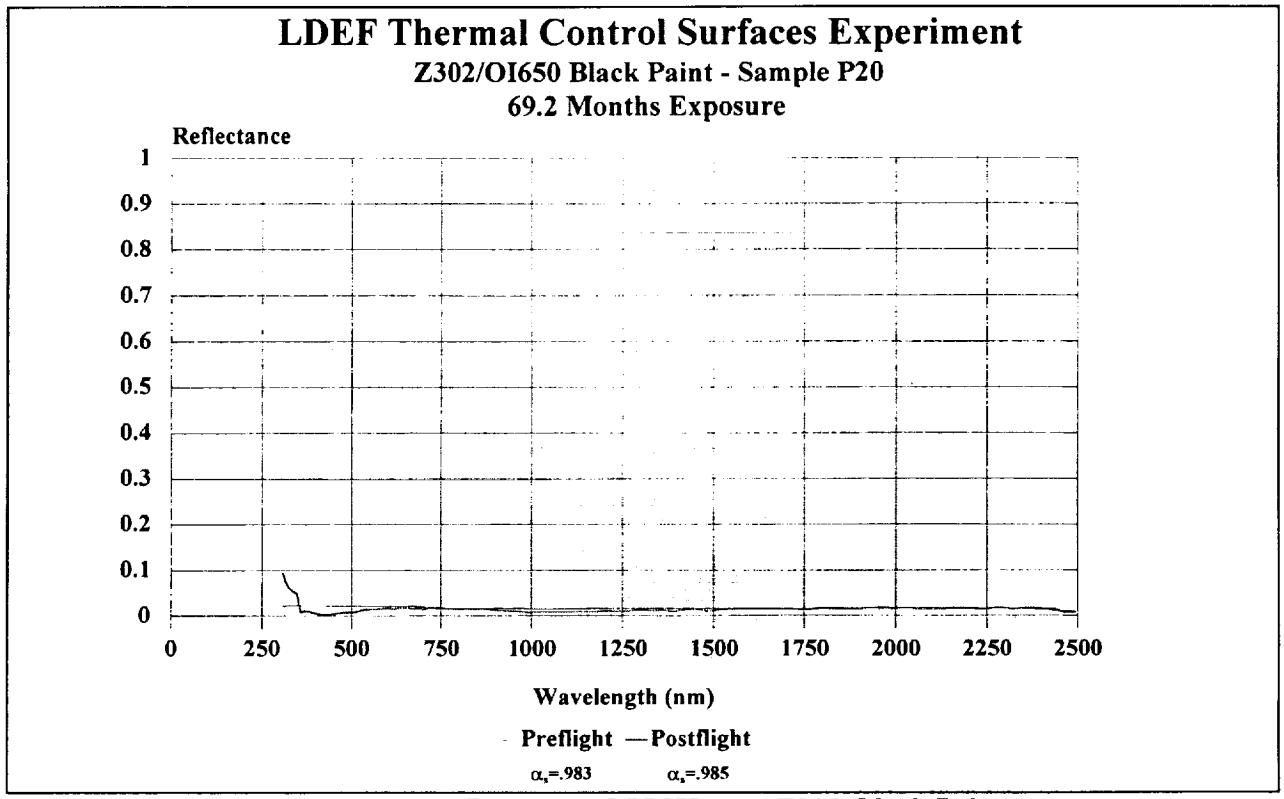

Figure 87. Reflectance of OI650 over Z302 Black Paint.

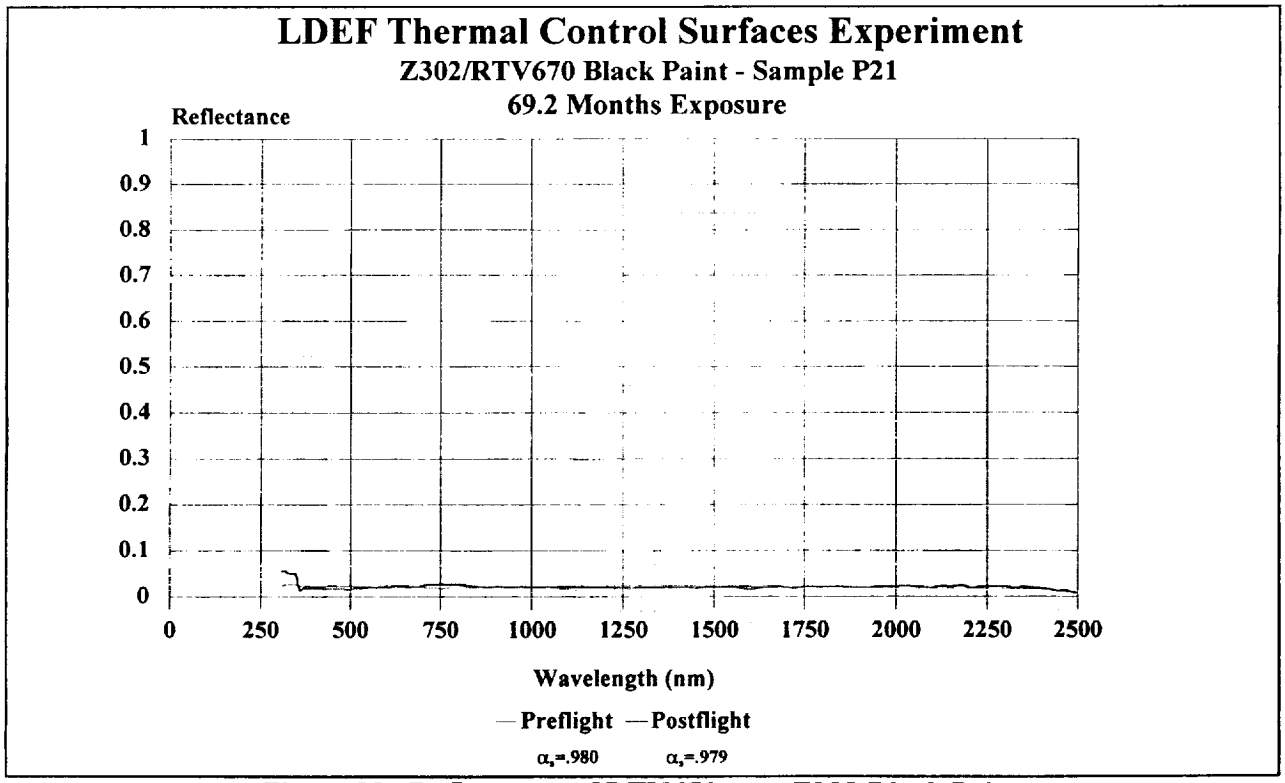

Figure 88. Reflectance of RTV670 over Z302 Black Paint.

Figure 89. Post-flight Photograph of OI650 Overcoated Z302.

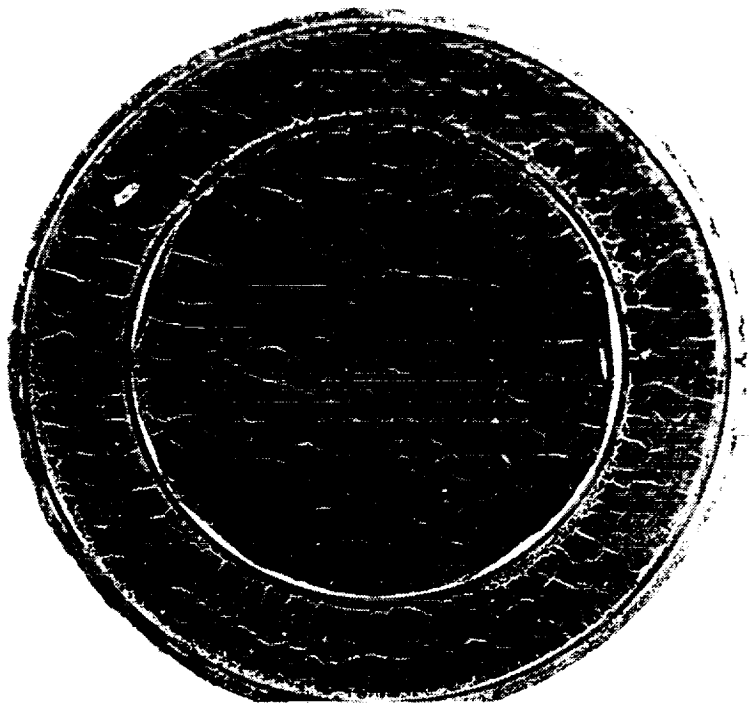

Figure 90. Post-flight Photograph of RTV670 Overcoated Z302.

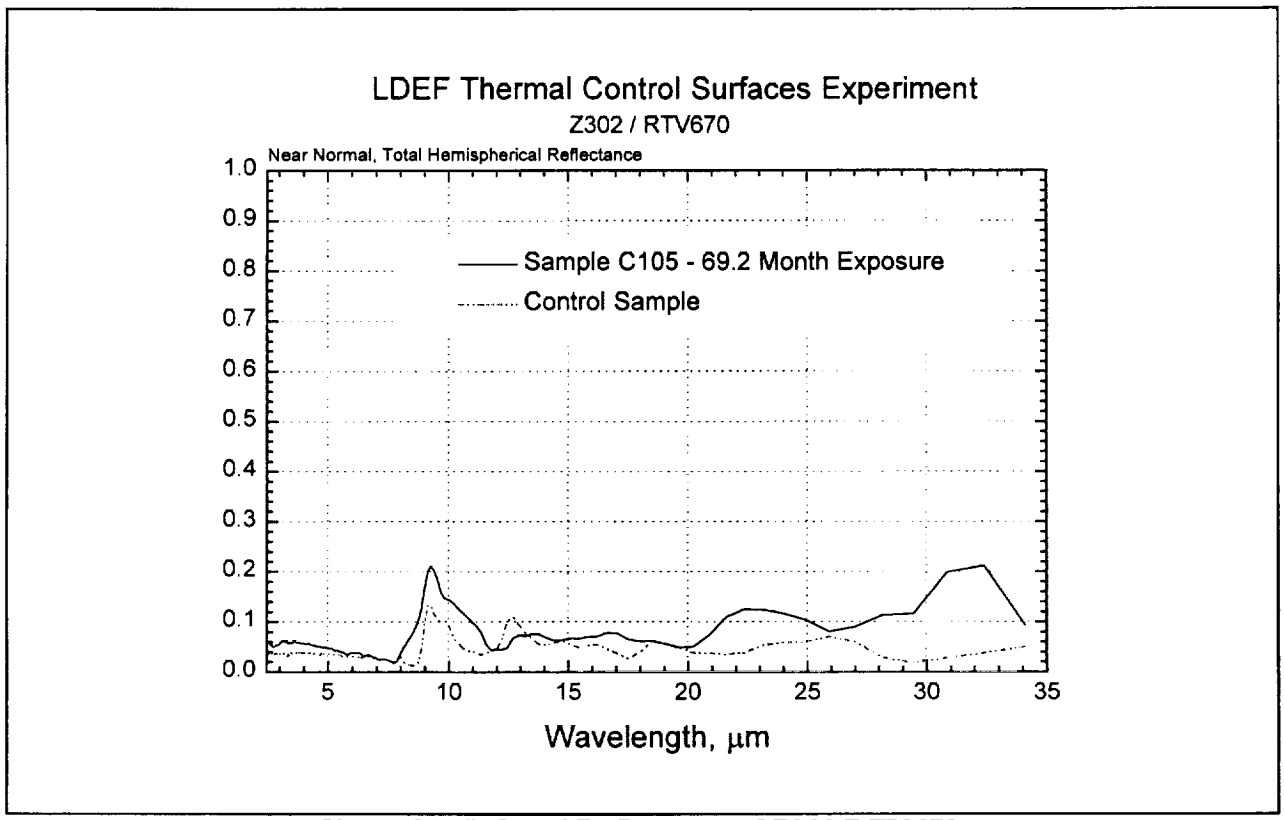

Figure 91. Infrared Reflectance of Z302/RTV670.

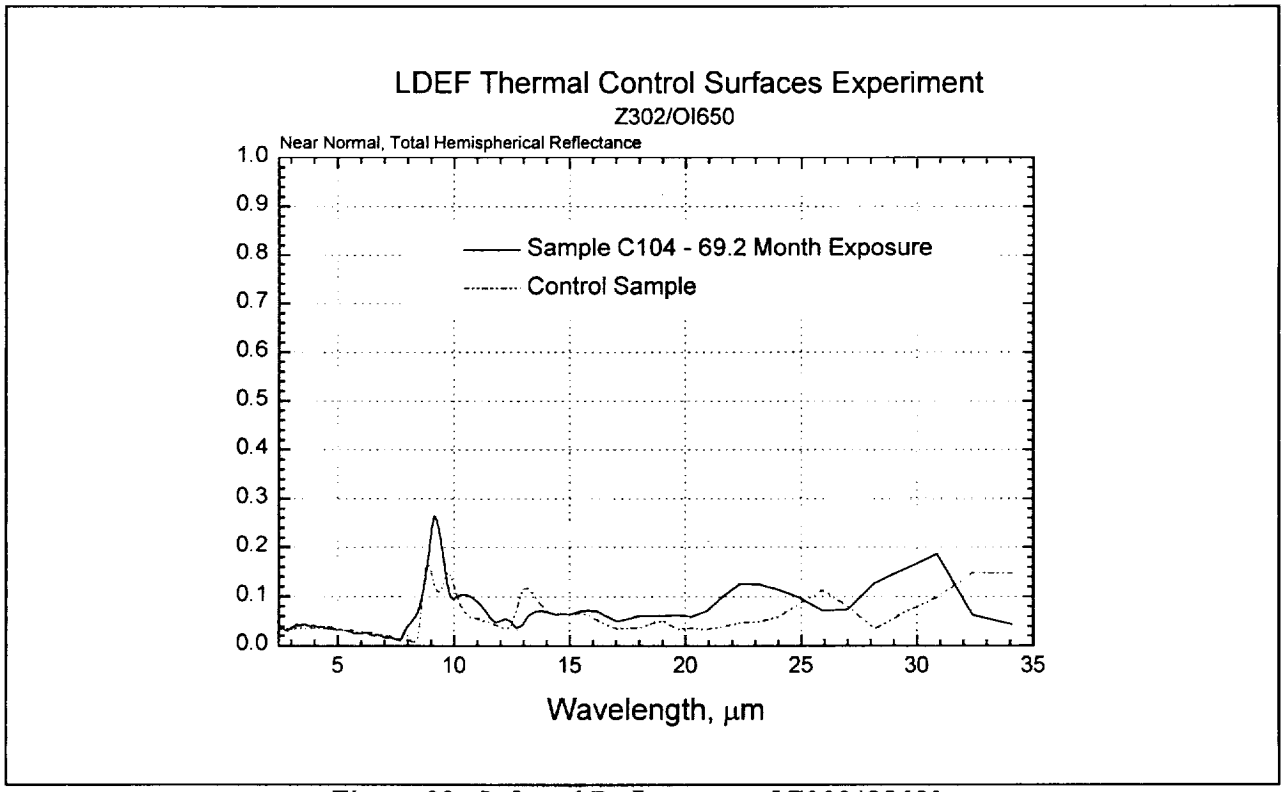

Figure 92. Infrared Reflectance of Z302/OI650.

These analyses were performed on both detailed spectral reflectance data and derived integrated solar absorptance (α_S). This data includes both in-space and ground based pre-flight and post-flight measurements. The solar absorptance data was analyzed using regression analysis to develop an empirical lifetime model for these materials. Empirical prediction models must be used with caution, however, because they can be misleading and have no scientific basis. The TCSE data provides the only in-situ optical data providing time history of the optical changes to materials exposed to the space environment. The analysis of this data provides the first insight into these time dependent material changes and enables the development of a prediction model. Other in-situ optical measurement experiments should be performed to verify this data and to provide data on new and improved materials. Several standard regression analyses were evaluated including polynomial, exponential, logarithmic and power. For integrated α_S the power regression analysis proved a better fit of the experimental data. The power regression line takes the form: $\alpha_S = e^{(a+b \bullet \ln(t))}$.

While the analysis of solar absorptance data is of great benefit to spacecraft designers, it is the analysis of the spectral data that provides the best insight into the different damage mechanisms of the space environment on materials. For most materials, there are more than one and potentially many competing mechanisms of damage due to the combined space environment. In many cases different damage mechanisms exhibit effects in different spectral ranges. The trend analysis of reflectance changes at different wavelengths will aid in separating different mechanistic effects.

In the following discussions, the results of the trend analyses are presented for the five selected materials. Data is shown for both integrated solar absorptance and spectral reflectance. The format of the data presentation is described in the first section for Z93 White Paint.

5.2.1 Z93 White Paint

Figure 93 shows the performance of Z93 for the LDEF mission. Solar absorptance is plotted versus exposure time. There appears to be at least two mechanisms that affected the Z93 solar absorptance during the LDEF mission. The first is a short term improvement (decrease) in α_S typical of silicate coatings in thermal vacuum. This improvement is normally associated with loss of water from the ceramic matrix. In ground simulation tests this process takes a much shorter time than the TCSE flight data suggests. This slower loss of water may be due to the cold temperature of the TCSE Z93 sample mounted on a thermally isolated calorimeter. The temperature of the Z93 sample ranged from approximately -55°C to +6°C but remained well below 0°C most of the time.

The short term improvement is dominant for the first year of exposure after which a long term degradation mechanism becomes dominant. The results of the power regression analysis for the short and long term effects are also shown on Figure 93. Figure 94 plots the long term regression model for Z93 on a log scale allowing extrapolation out to 30 years. The regression analysis projects a 30 year end-of-life value for Z93 of $\alpha_S = 0.185$. This predicted value is statistically a most likely value and not a worse case value.

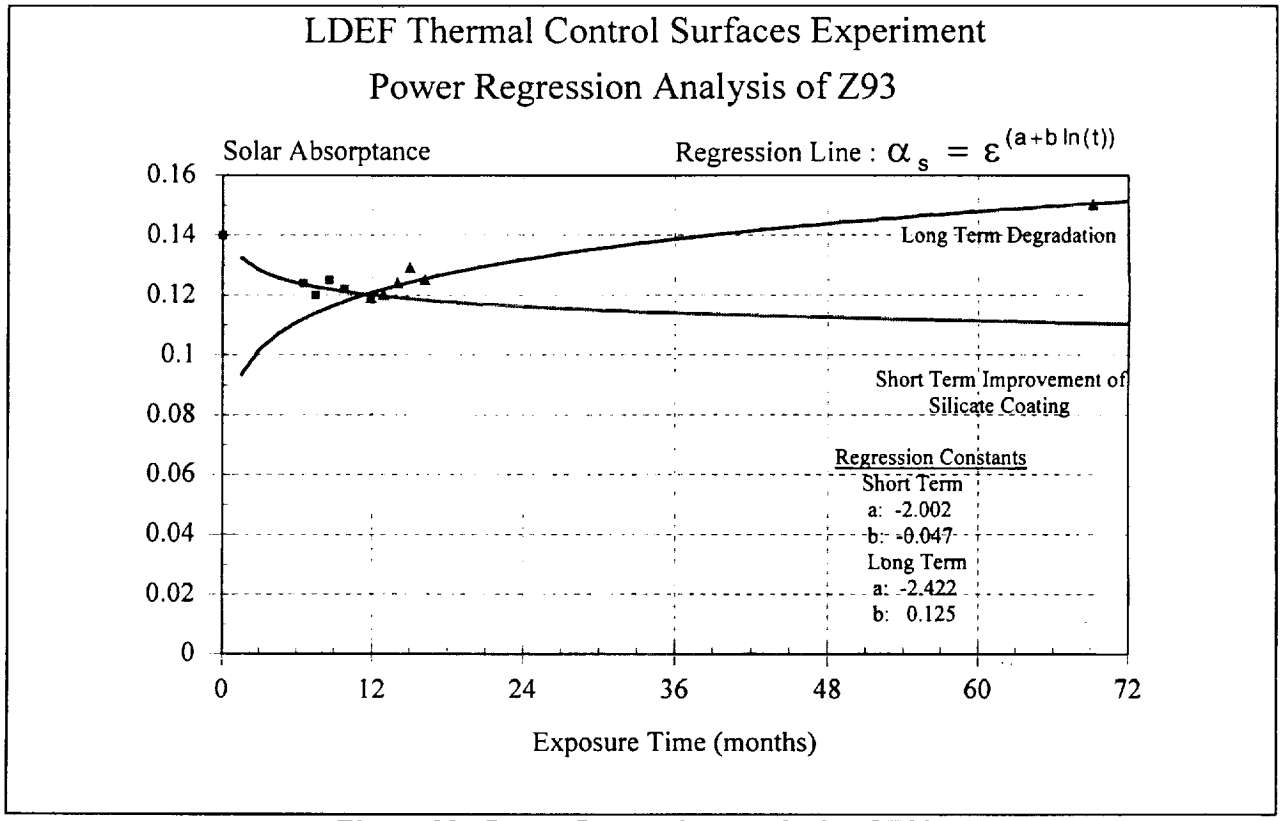

Figure 93. Power Regression Analysis of Z93.

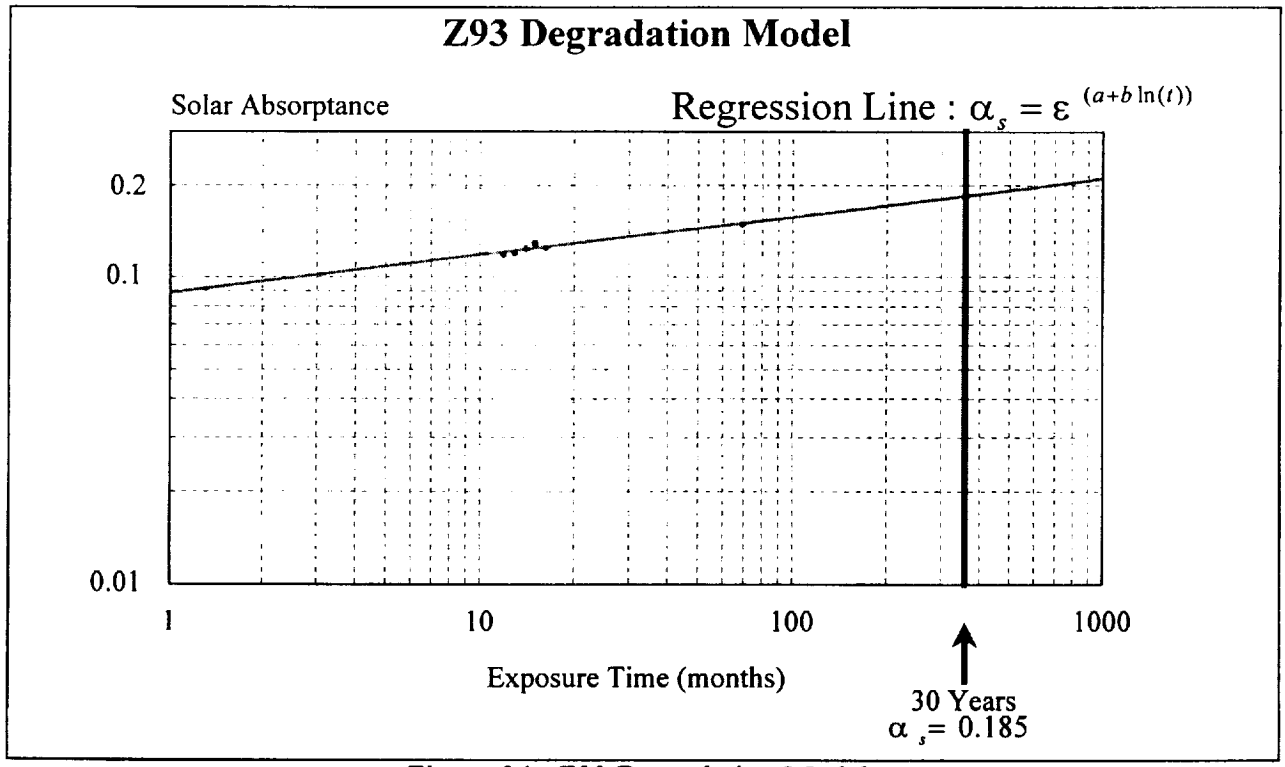

Figure 94. Z93 Degradation Model.

Figures 95 and 96 show the spectral reflectance data for Z-93. All spectral reflectance data presented in this paper are plotted as normalized change in reflectance.

$$\text{Delta } R/R = (\rho - \rho_o)/\rho_o$$

where: ρ_o = initial reflectance (time=0)

ρ = reflectance at time t

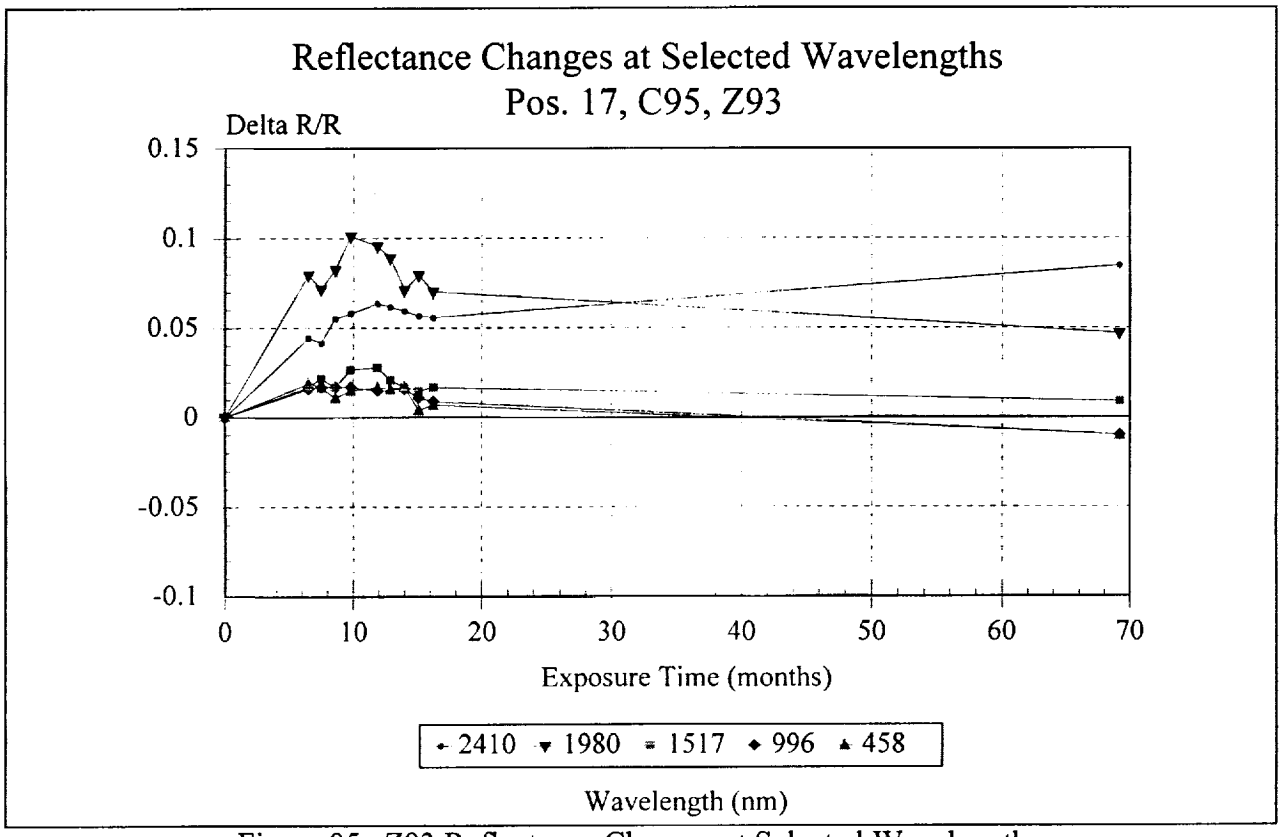

Figure 95. Z93 Reflectance Changes at Selected Wavelengths.

Figure 95 plots normalized reflectance change versus exposure time for five selected wavelengths while Figure 96 plots normalized reflectance change versus wavelength at four different exposure times. These data show that the short term improvement in reflectance of Z93 (attributed to loss of water) is broad banded with the major changes occurring in the IR as expected. It is somewhat surprising to also see this improvement at the shorter wavelengths. The longer term degradation mechanism occurs mainly below 1000 nm. Even though the changes are small, they are significant because the solar energy curve peaks in this spectral range.

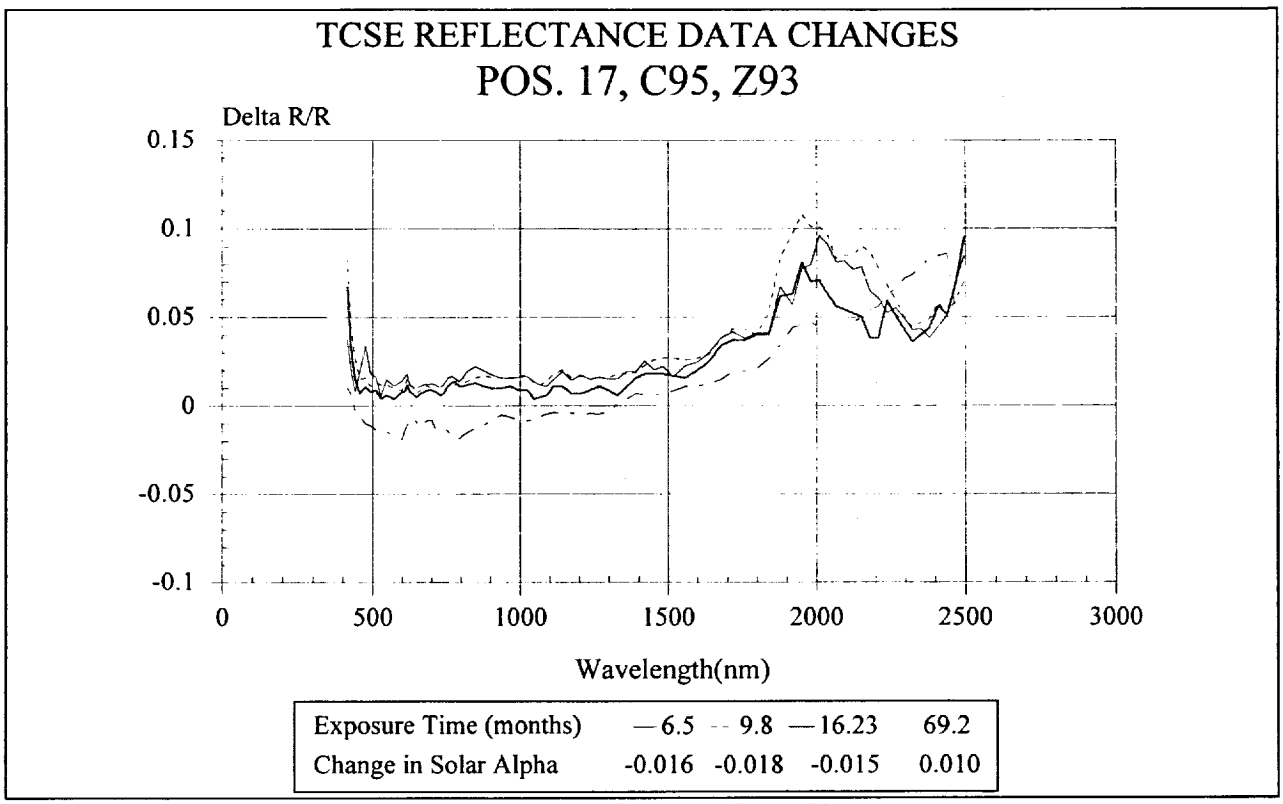

Figure 96. Z93 Reflectance Data Changes.

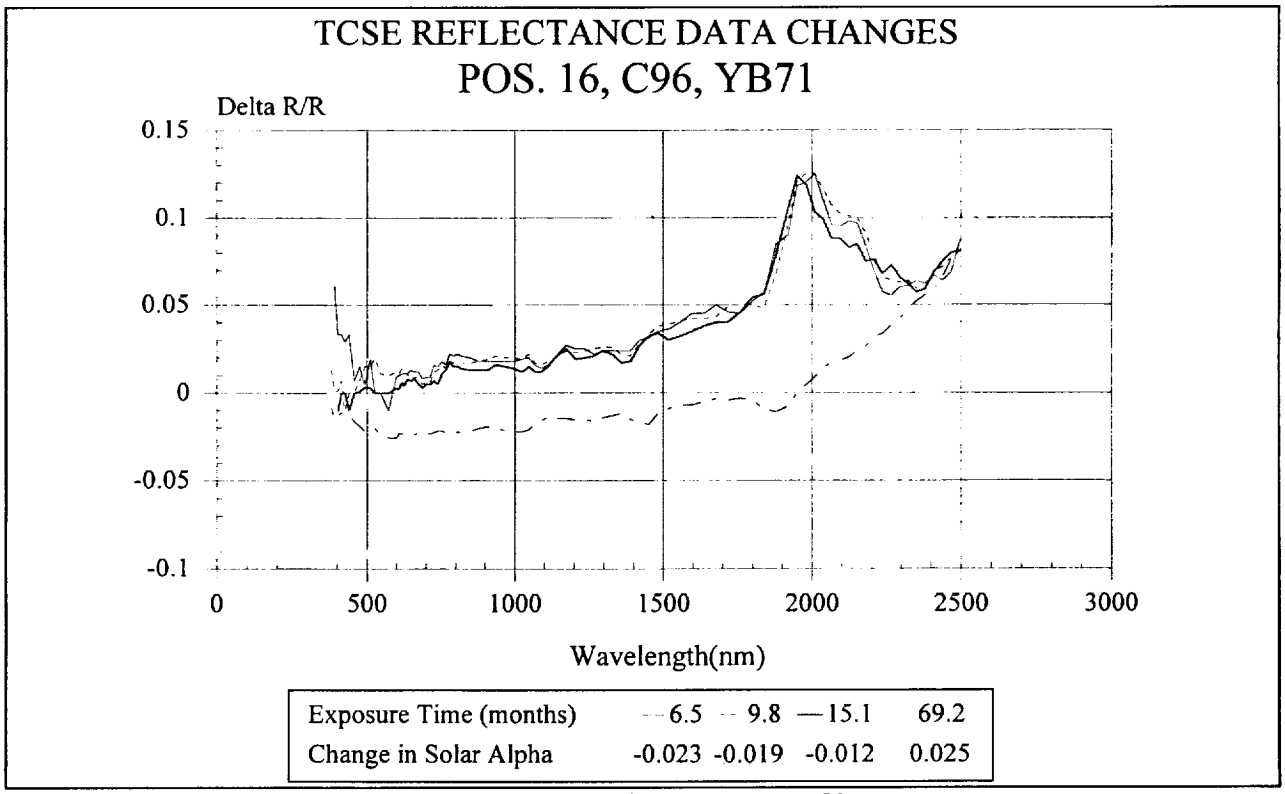

Figure 97. YB71 Reflectance Data Changes.

5.2.2 YB71 White Paint

YB71 exhibited very similar changes as Z93 during the LDEF mission as shown in Figure 97. The spectral reflectance changes for the first fifteen months are nearly identical for both materials (see Figures 96 and 97). This is not surprising as both white coatings use the same potassium silicate binder. What is surprising, however, is the greater degradation of spectral reflectance (and solar absorptance) of the YB71 over Z93 for the remaining 54 months. In ground simulation testing before the LDEF mission, YB71 was more stable than Z93.

5.2.3 S13G/LO White Paint

Figure 98 shows the solar absorptance changes for S13G/LO over the LDEF mission. As with most of the TCSE active samples, there is an initial period in which the rate of change is different than the subsequent changes. This indicates a different dominant damage mechanism than later in the mission. The regression analysis provides a good fit if the initial data point is ignored. The degradation model for S13G/LO is shown in Figure 99. Significant changes in S13G/LO were expected, but actual changes were somewhat larger than expected. Figures 100 and 101 show the spectral reflectance changes for S13G/LO. The only significant changes occurred below 1000 nm which resulted in the large changes in integrated solar absorptance.

5.2.4 A276 White Paint and Protective Overcoats

Chemglaze A276 is a widely used white coating that was known to erode in AO even before the LDEF mission. To evaluate their effectiveness, RTV670 and OI650 clear protective overcoats were applied to A276. Figures 102-104 show the performance of the three coating systems during the LDEF exposure. Figure 104 shows that without a protective overcoating, A276 had relatively small changes for the first sixteen months. Exposure to the very large AO fluence during the subsequent four years eroded the damaged surface layer exposing a surface with even better reflectance than the pre-flight surface. The A276 with the protective overcoatings degraded significantly. Figure 105 compares post-flight reflectance changes for the three A276 surfaces and an LDEF trailing edge A276 sample from Dr. Palmer Peters and Dr. John Gregory's AO114 experiment. The AO114 trailing edge sample saw only a small amount of AO and was significantly damaged by solar UV exposure. Some of the damage to the TCSE overcoated samples may be in the overcoat itself. However, as shown in Figure 105, the damage spectra of the UV degraded AO114 A276 samples is very similar to the TCSE overcoated samples in both magnitude and spectral range.

5.2.5 Silver Teflon

Samples of both 5 mil and 2 mil thick silver Teflon were flown on the TCSE active sample array. The 5 mil material was optically very stable for the LDEF mission. AO exposure resulted in the loss of approximately 1 mil of Teflon and a textured diffuse surface. Figure 106 shows the variation of solar absorptance versus exposure time for 5 mil silver Teflon. As with several other materials, an improvement (decrease) in solar absorptance was measured early in

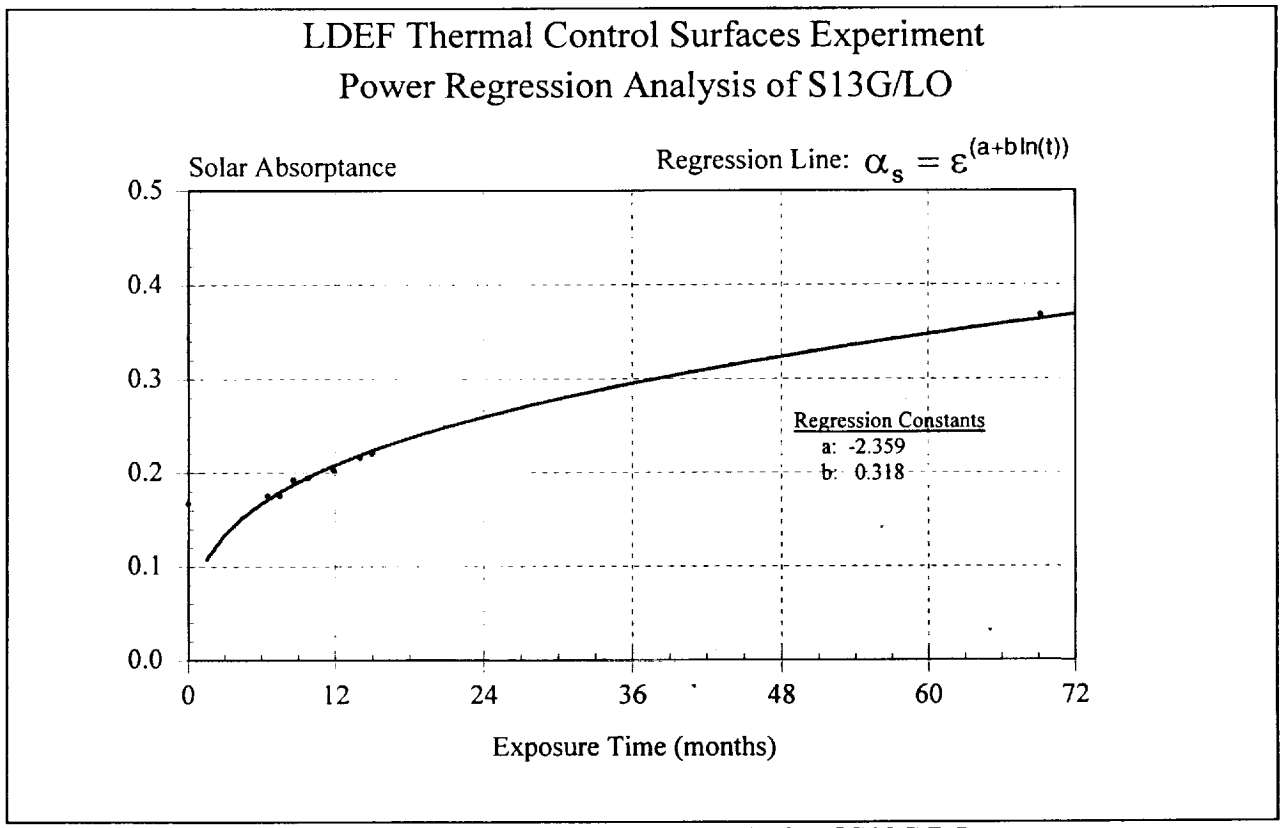

Figure 98. Power Regression Analysis of S13G/LO.

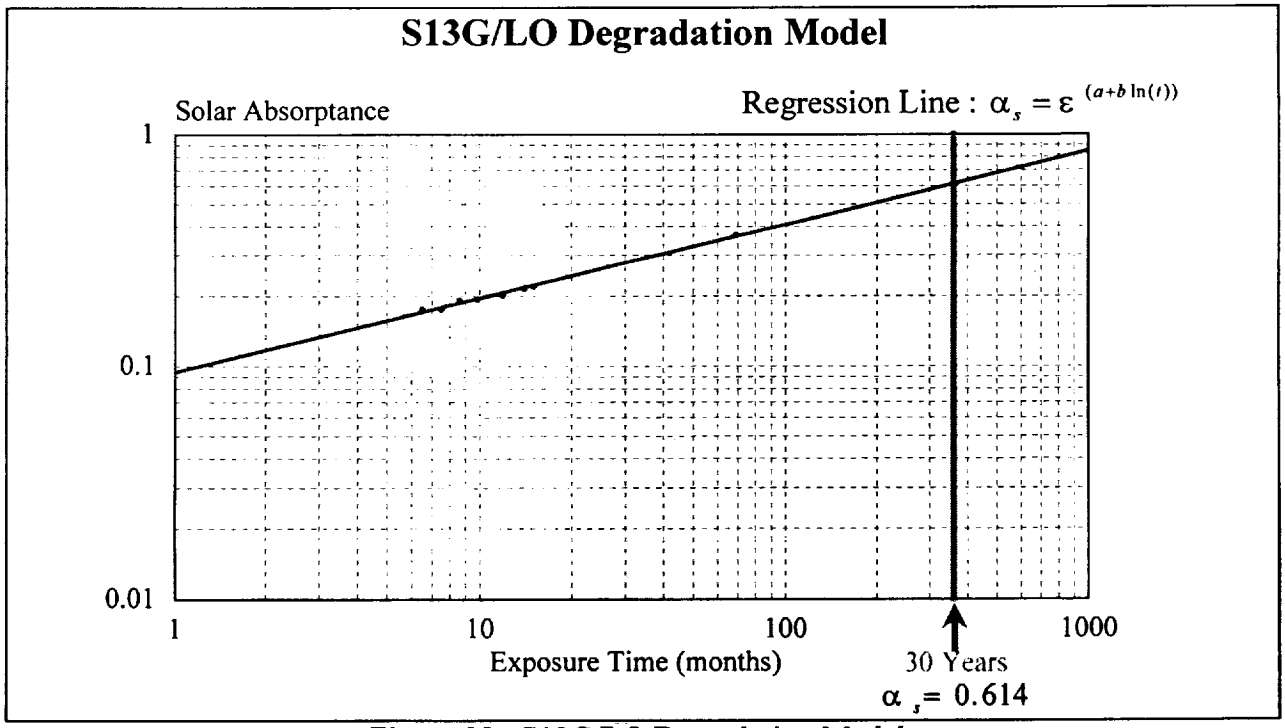

Figure 99. S13G/LO Degradation Model.

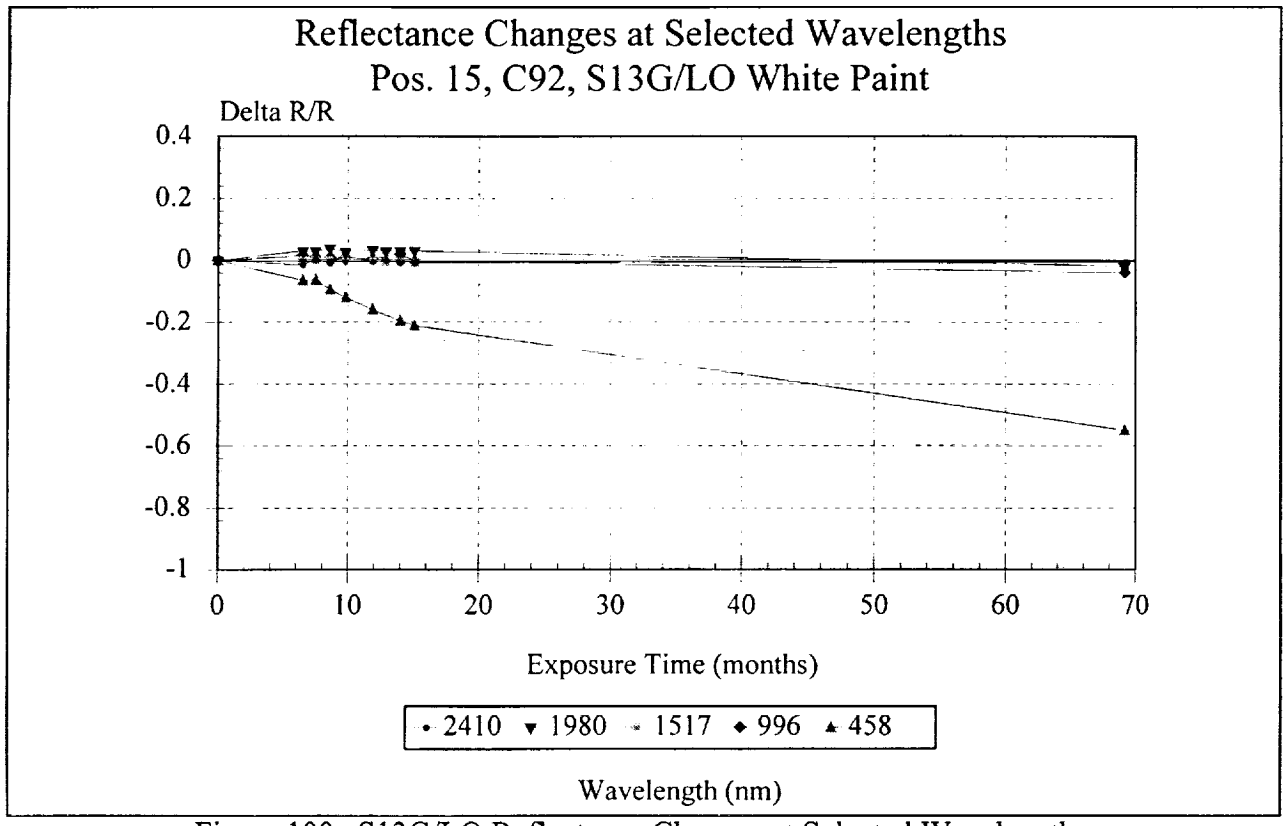

Figure 100. S13G/LO Reflectance Changes at Selected Wavelengths.

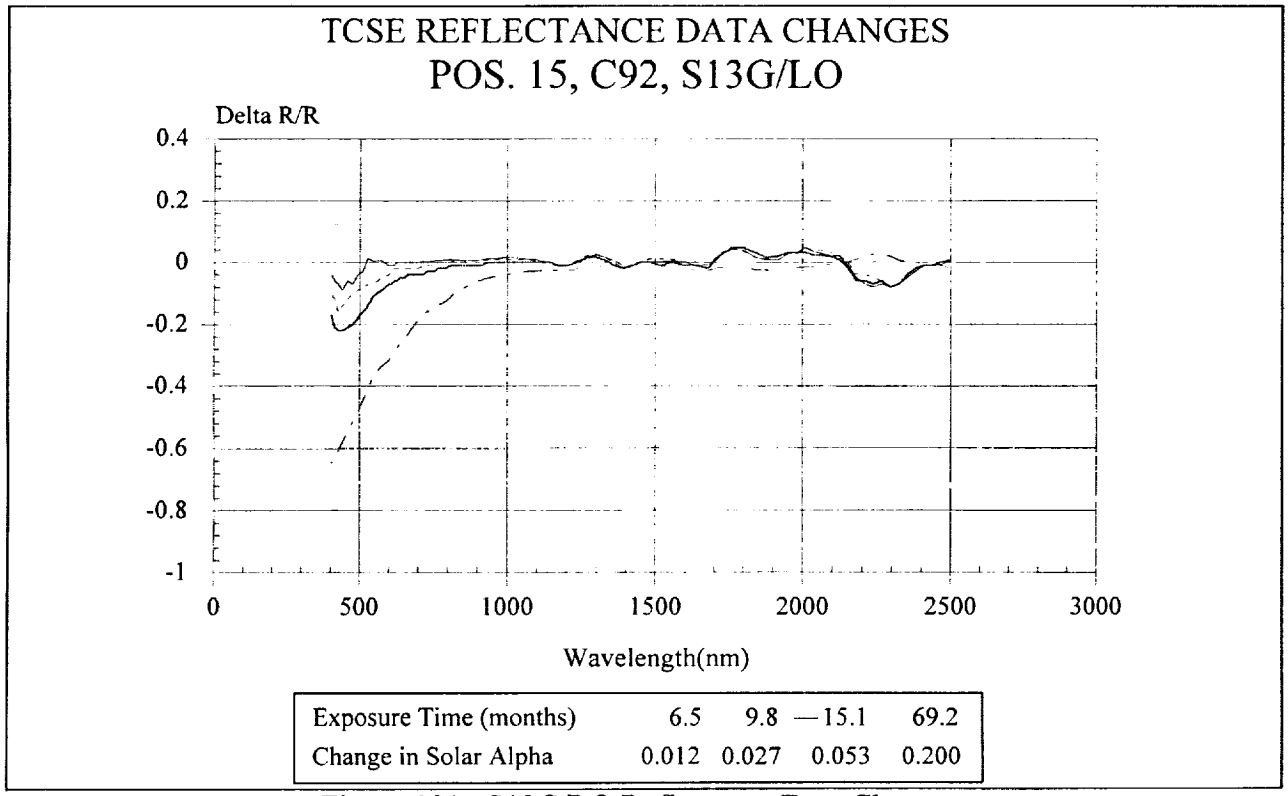

Figure 101. S13G/LO Reflectance Data Changes.

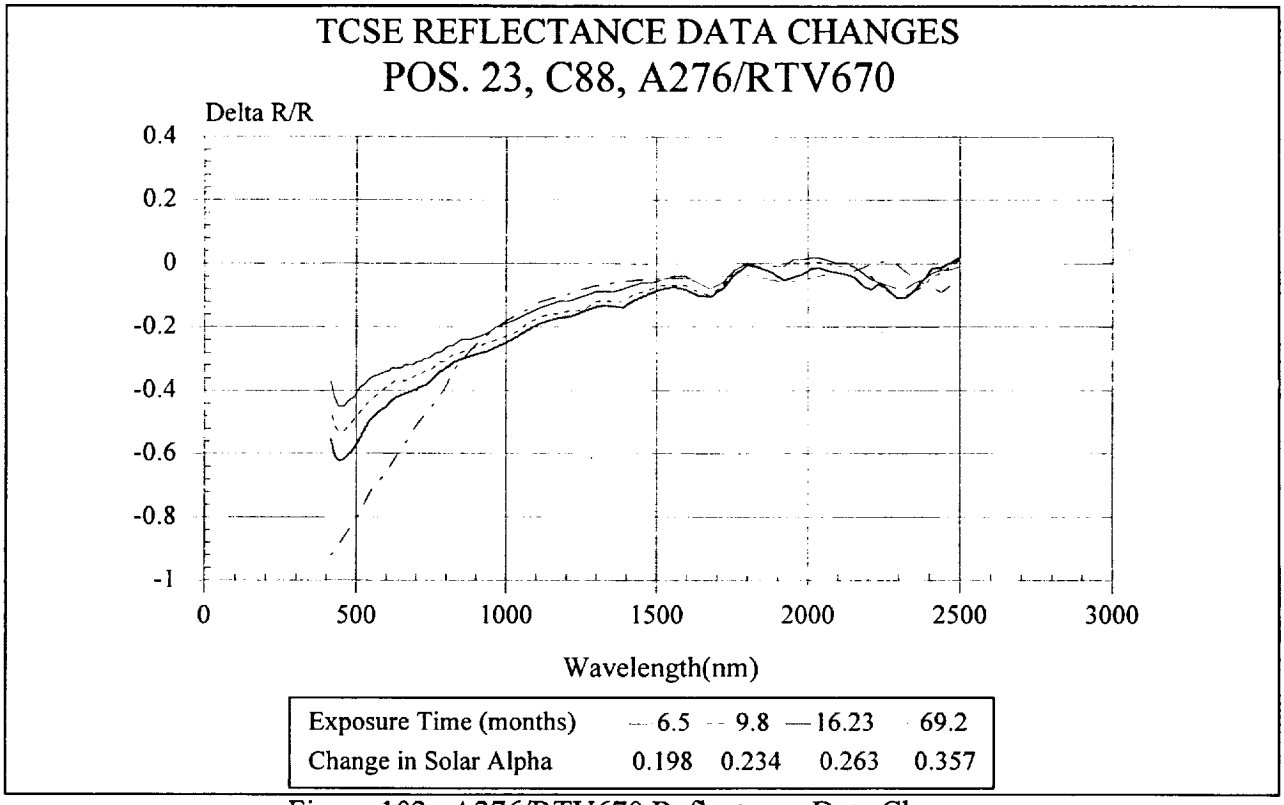

Figure 102. A276/RTV670 Reflectance Data Changes.

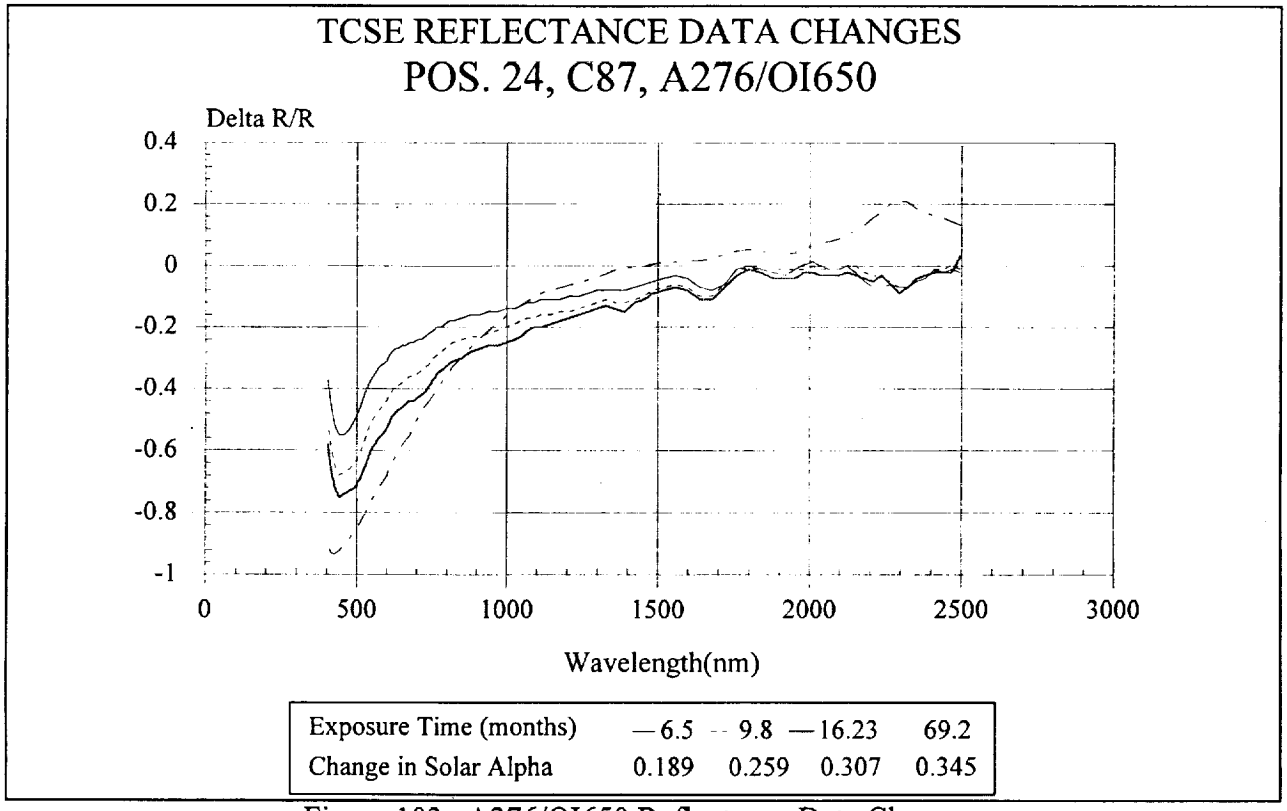

Figure 103. A276/OI650 Reflectance Data Changes.

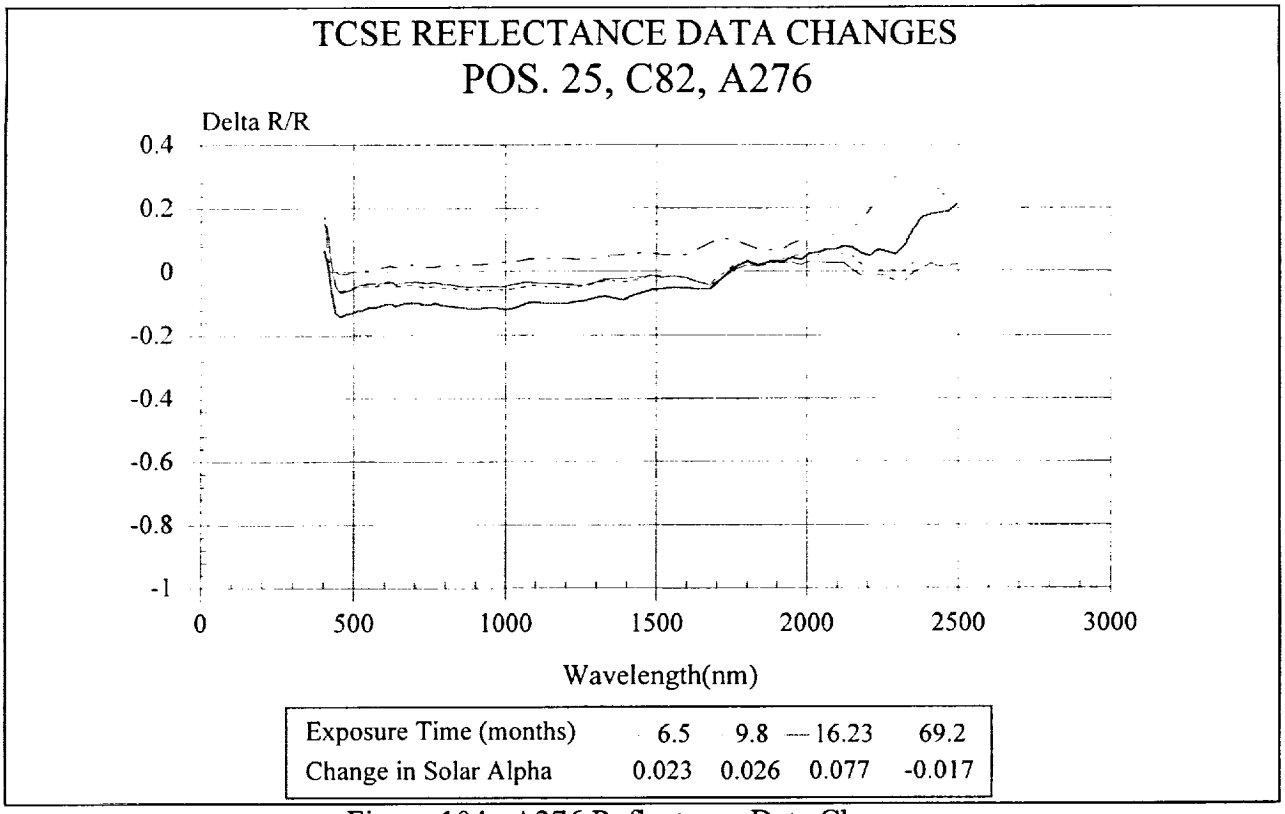

Figure 104. A276 Reflectance Data Changes.

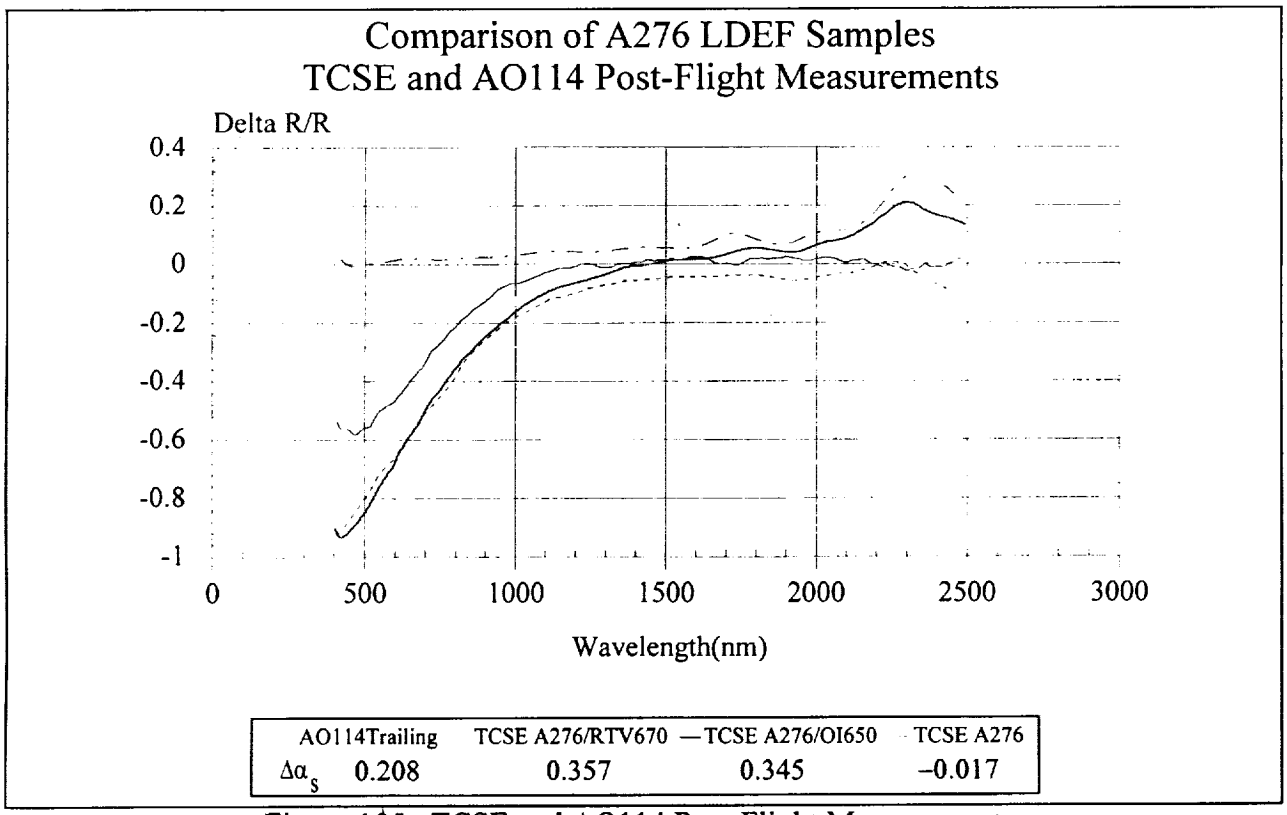

Figure 105. TCSE and AO114 Post-Flight Measurements.

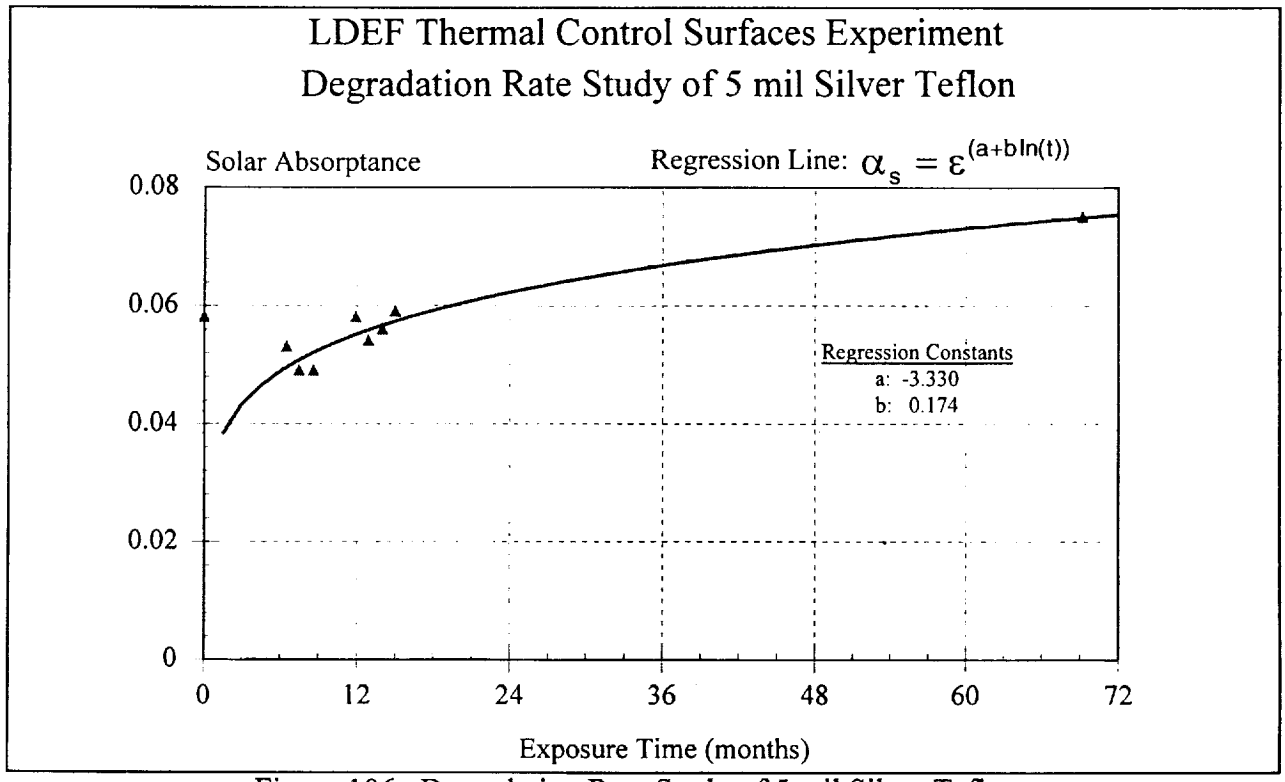

Figure 106. Degradation Rate Study of 5 mil Silver Teflon.

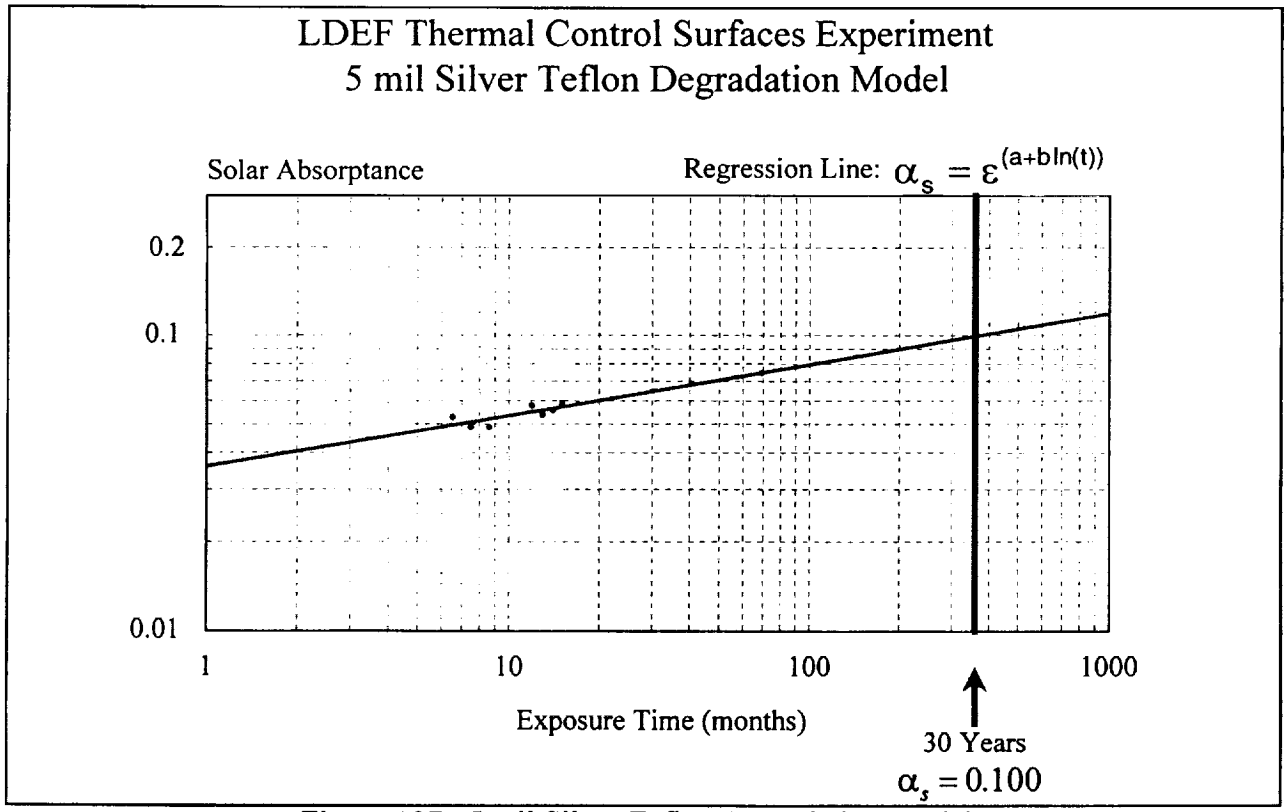

Figure 107. 5 mil Silver Teflon Degradation Model.

the mission. This was followed by a small degradation for the remainder of the mission. Power regression analysis provides a fair fit to this long term degradation. Figure 107 extends this degradation model and predicts an excellent 30 year solar absorptance of 0.1.

Figure 108 shows the spectral reflectance changes over the mission duration. A slight increase in the 1700 to 2500 nm IR range early in the mission is offset by the long term degradation below 1400 nm.

The 2 mil silver Teflon active sample was the same material that was applied to the TCSE front cover. This material suffered from an internal contamination and optical degradation that has been previously discussed in Section 5.2.6. Figure 109 shows the spectral reflectance changes of the 2 mil silver Teflon. The data up to 15 months is nearly identical to the 5 mil material. The degradation during the subsequent four years indicates that the internal contamination required several years to become significant.

5.2.6 Trend Analysis Summary

The TCSE in-space spectral reflectance measurements and analysis of this data demonstrate the benefit of active type materials space experiments. This time dependent data provides insight into how thermal control surfaces behave in the space environment and enables the development of lifetime prediction models.

The results of this effort are based on one space mission, a limited measurement data set, and, in most cases, only one sample of a material. While the quality of the data is excellent, the lifetime prediction models should be used with extreme caution. The extrapolated data is statistically a most likely value and not a worst case value.

The study of the trends in the TCSE spectral reflectance data provides a unique view of how materials degrade in the space environment. This data and the post-flight surface analysis demonstrate the very complex nature of the behavior of materials operating in this environment. Many issues remain in understanding the effects of the space environment on materials. Additional flight opportunities are needed for active optical experiments measuring these effects. To address this need, the In-Space Technical Experiments Program (IN-STEP) Optical Properties Monitor (OPM) has been developed and its initial mission is on the Russian Mir Space Station. The OPM is an in-space optical laboratory for the in-situ study of materials.[21]

5.3 In-Depth Material Analyses

An in-depth analysis of six of the TCSE test materials was performed. The coatings used for this study are Z93, S13G/LO, A276, A276/OI650, and A276/RTV560. The three basic materials (Z93, S13G/LO, and A276) were chosen because of their wide use in the spacecraft materials community with the exception of the silicone overcoated A276 samples. The two A276 with silicone overcoats were included in this effort because, at the time of their selection, they were the best candidates for studying the protective coating effects of silicone polymers on AO susceptible materials such as polyurethane (A276 binder).

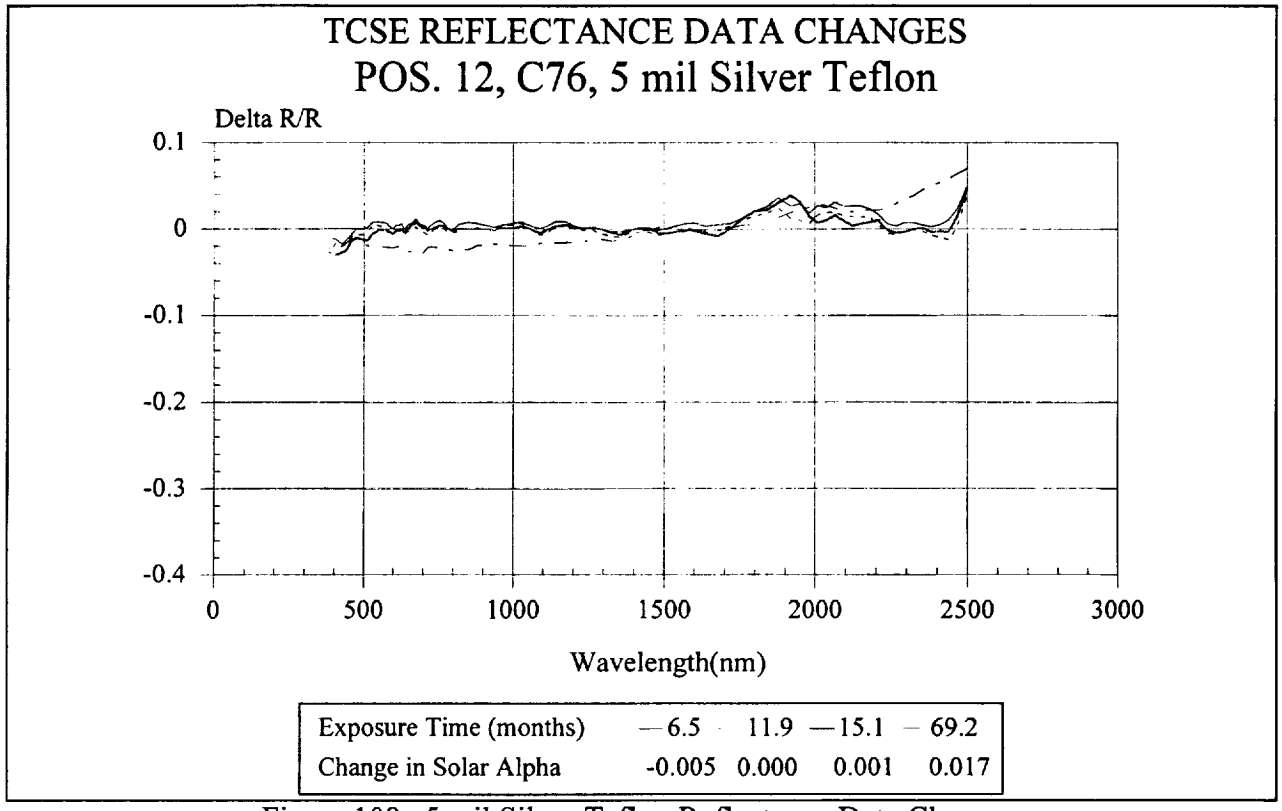

Figure 108. 5 mil Silver Teflon Reflectance Data Changes.

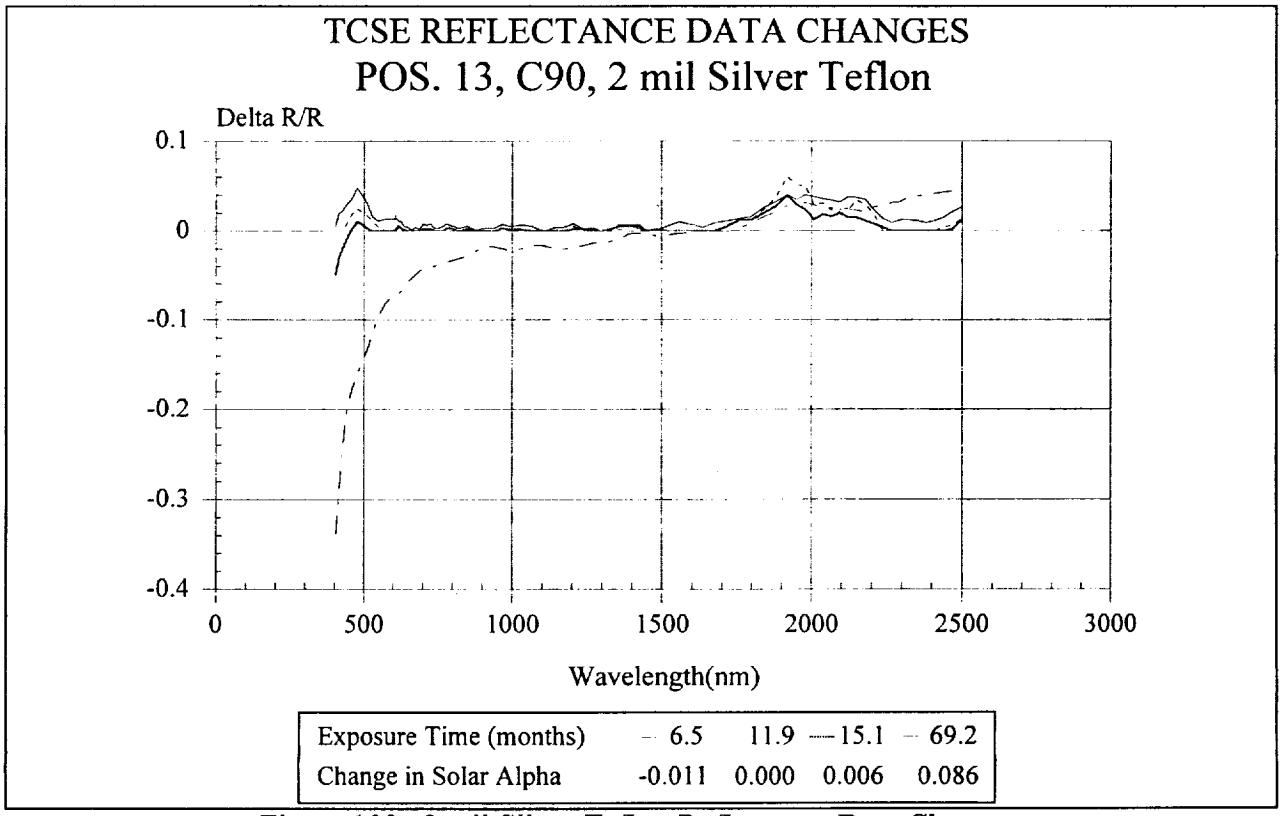

Figure 109. 2 mil Silver Teflon Reflectance Data Changes.

A variety of techniques were used to evaluate the effects of the LDEF LEO exposure on these samples including SEM, BDRF, XPS, DSC, and IR attenuated total reflectance (ATR) spectroscopy techniques. Utilization of these techniques are unique for thick film coatings and even more so for material samples that have spent almost six years in space exposed to the LEO environment.

5.3.1 Scanning Electron Microscopy (SEM)

SEM micrographs were taken of selected passive exposure samples and the control samples. Care was taken to minimize microscope energies to no more than two kilovolts. This was done to minimize any potential damage that the electron beam could cause to polymer based coatings.

5.3.1.1 Z93 White Paint

Evaluation of exposed and control samples of this coating demonstrate little change of the surface. The primary change, although minor, is the increased frequency of fractures throughout the surface (see Figures 110 [controlled sample] and 111 [exposed sample]) at magnification of 300X. Study of the photographs or the displayed images does not provide sufficient detail to determine if these cracks propagate to the substrate. However, this is not likely from the observations and experience with this coating. A far more subtle effect is a shrinkage or increased surface texture of the potassium silicate binder on individual particles and agglomerates as shown in Figures 112 and 113 at magnification of 6000X. One must study the photographs closely to detect this difference.

5.3.1.2 S13G/LO White Paint

The primary difference of this coating is the formation of numerous fractures on the exposed samples surface, none of which were found on the control sample (see Figures 114 and 115). This coating is an elastomer and will typically flex, bend, expand or contract as needed. It is thought that the surface layer of this coating has been converted into a glass resulting in shrinkage, induces stress and crack formation. Further evidence is presented in the XPS section which supports this hypothesis. Higher SEM magnification (3000X) of this coating showed no further significant changes (Figures 116 and 117).

5.3.1.3 A276 White Paint

This coating changed significantly from exposure to the LEO environment. The control sample has a very smooth flat appearance as shown in Figure 118. Figure 119 shows the LEO exposed surface has become very textured with individual particles or agglomerates detectable indicating removal of the polyurethane binder. This is in sharp contrast to the silicone overcoated A276 which remained generally smooth with some cracking.

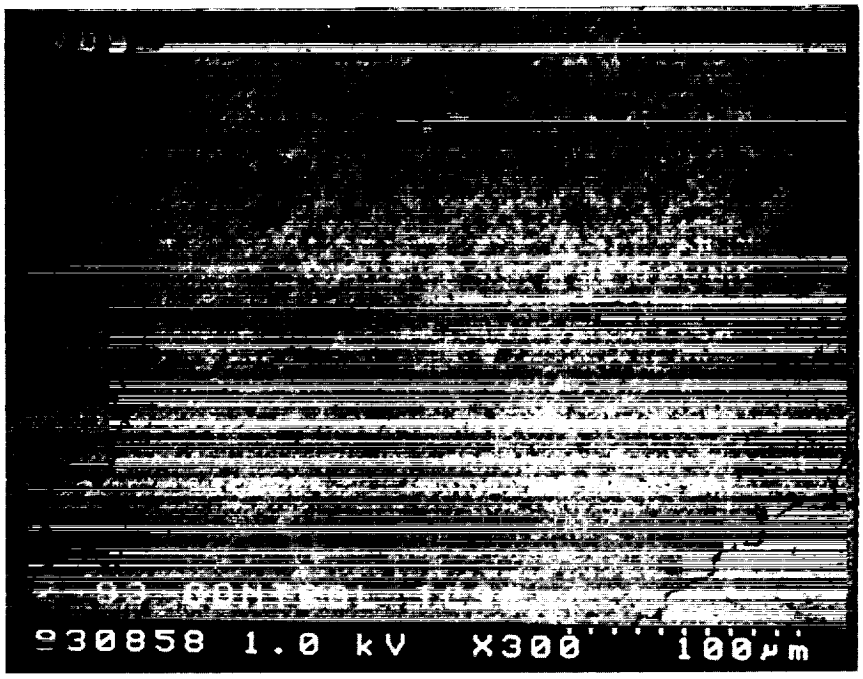

Figure 110. SEM Photograph (300X) of Z93 Control Sample.

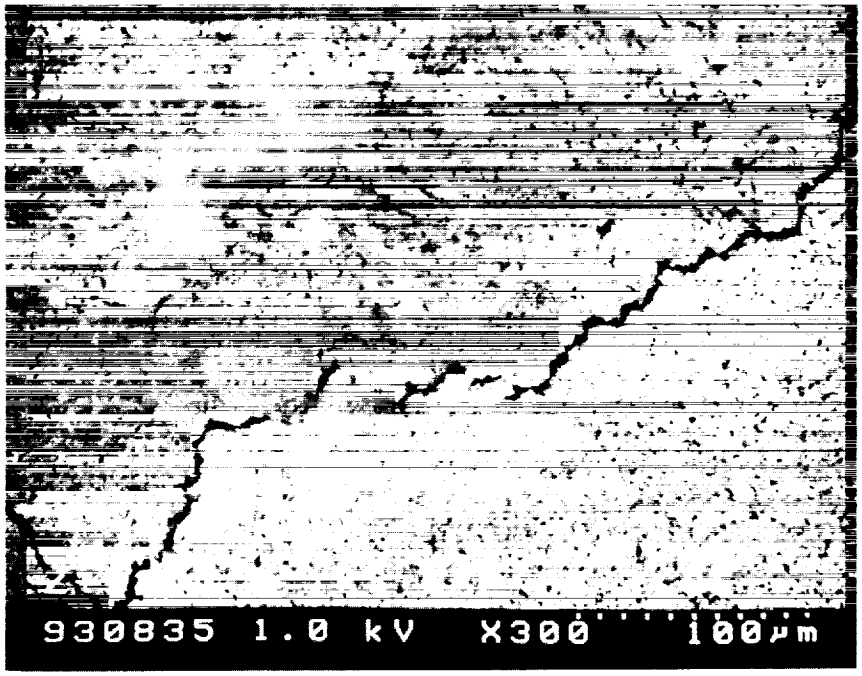

Figure 111. SEM Photograph (300X) of TCSE Z93 Sample Exposed for 5.8 Years.

Figure 112. SEM Photograph (6000X) of Z93 Control Sample.

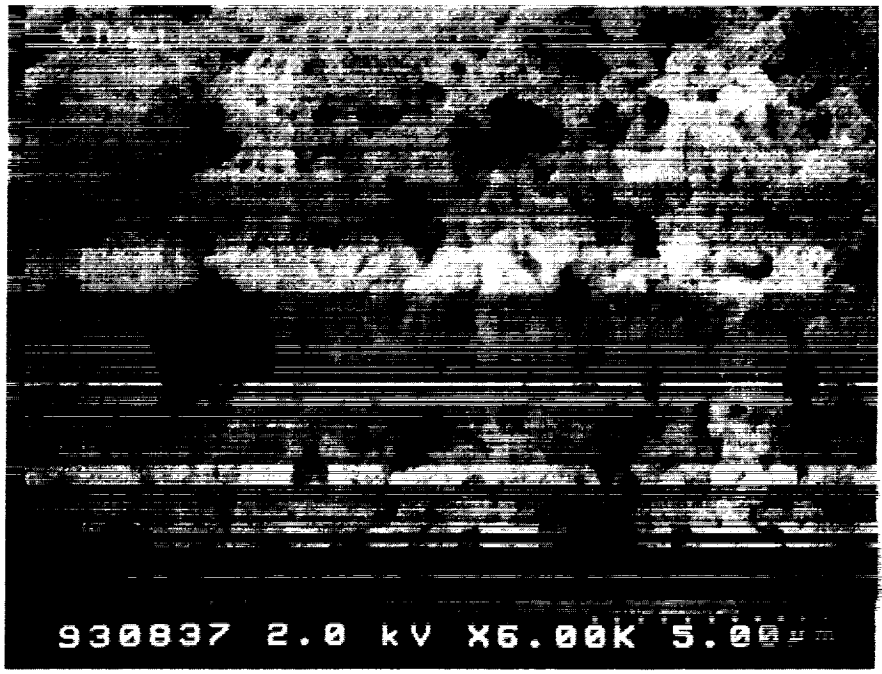

Figure 113. SEM Photograph (6000X) of the TCSE Z93 Sample Exposed for 5.8 Years.

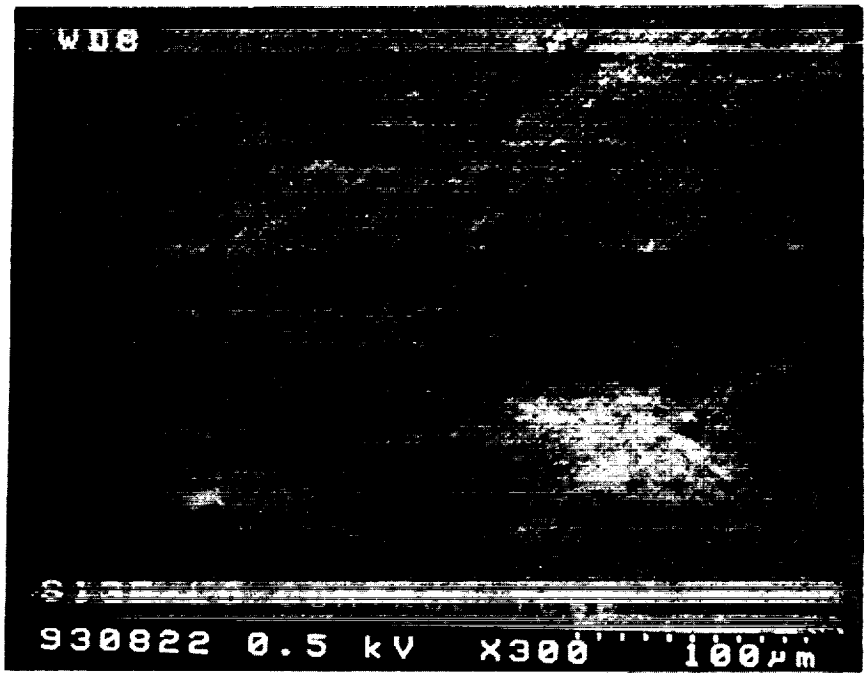

Figure 114. SEM Photograph (300X) of S13G/LO Control Sample.

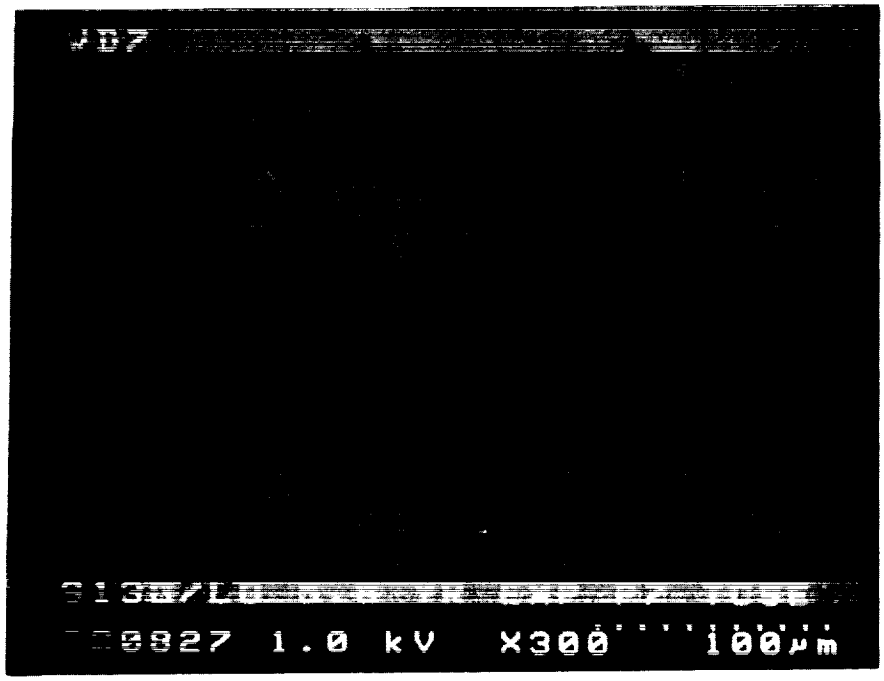

Figure 115. SEM Photograph (300X) of TCSE S13G/LO Sample Exposed for 5.8 Years.

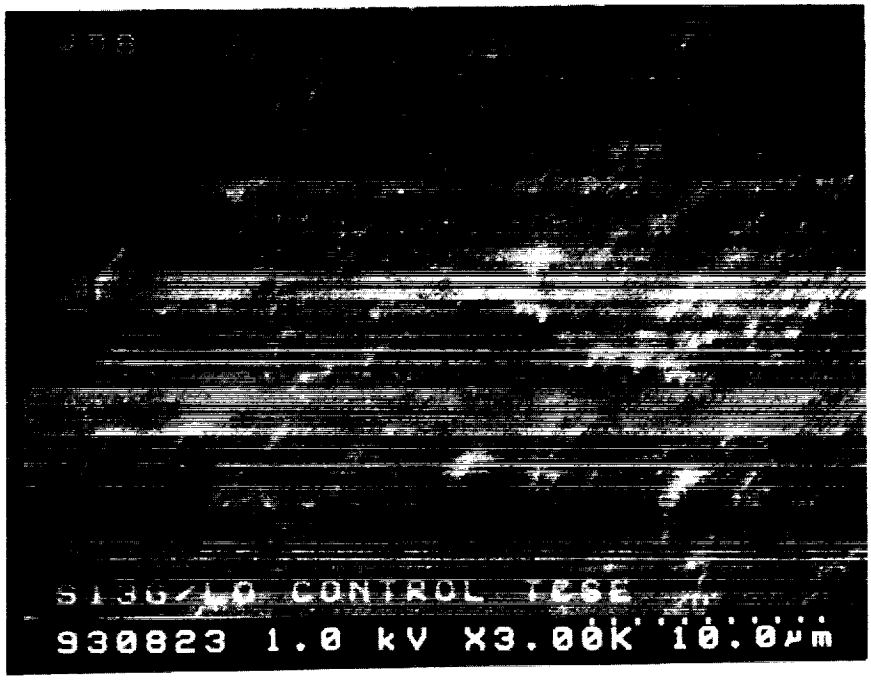

Figure 116. SEM Photograph (3000X) of S13G/LO Control Sample.

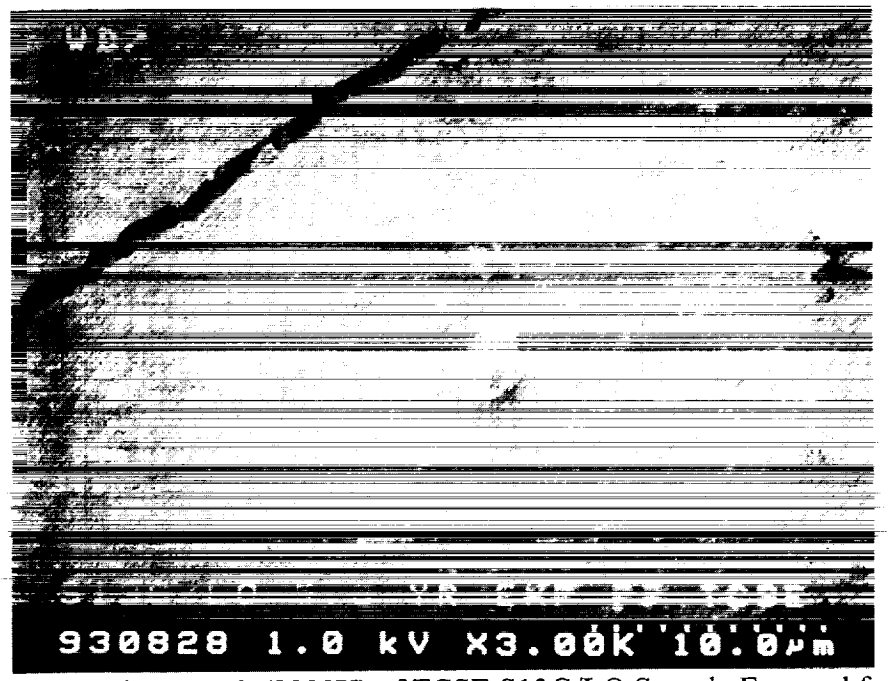

Figure 117. SEM Photograph (3000X) of TCSE S13G/LO Sample Exposed for 5.8 Years.

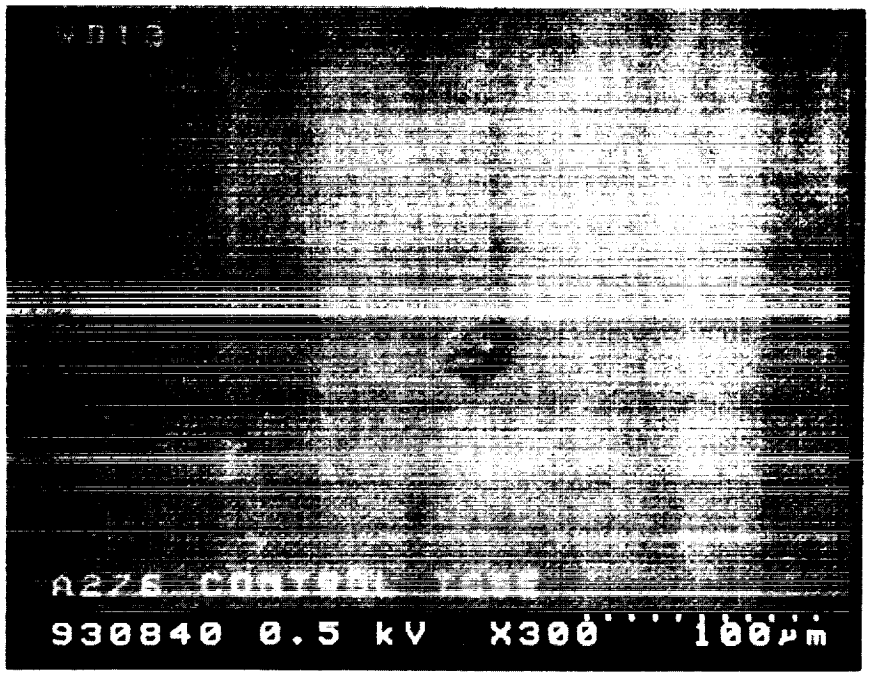

Figure 118. SEM Photograph (300X) of A276 Control Sample.

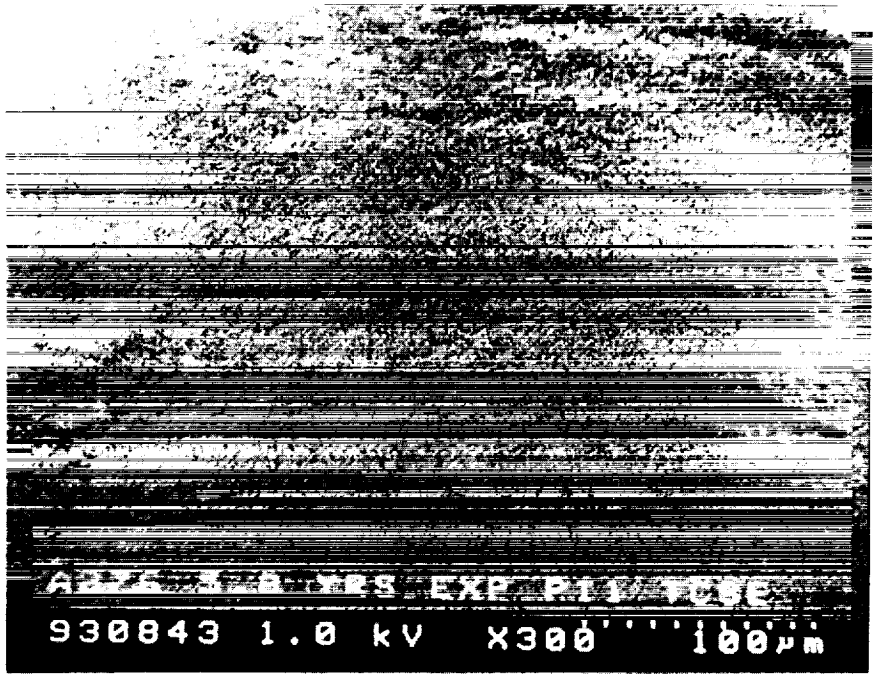

Figure 119. SEM Photograph (300X) of TCSE A276 Sample Exposed for 5.8 Years.

5.3.1.4 OI650/A276 Overcoated White Paint

Evaluation of this coating system by SEM for the control and exposed sample showed only minor surface changes as a result of exposure to the LEO environment. These minor changes are exhibited by increased frequency of surface cracking shown in Figures 120 (controlled sample) and 121 (exposed sample). However, surface color for this coating did change from white to brown as a result of LEO exposure.

5.3.2 IR Spectroscopy

IR reflectance (4000-600 cm-1) evaluation was done on Z93, S13G/LO, and A276 TSCE coatings. Measurements were done using a Nicolet 750 spectrometer with a IR microscope fitted with an attenuated total reflectance system. Z93 changed very little as shown in Figure 122. There are only minor changes in the magnitude of the various absorption bands and a slight shifting of these bands towards shorter wavelengths. S13G/LO and A276 (Figures 123 and 124, respectively) indicate a loss or conversion of organic binder material. This is indicated by the general reduction in absorption bands throughout the spectrum. A276 also shows a broadening and magnitude increase of the band located at about 3350 cm-1. This is likely water absorption from the increased surface morphology caused by AO interaction with A276 binder.

5.3.3 Bi-Directional Reflectance Function (BDRF)

Bi-directional reflectance evaluation was performed on Z93, S13G/LO, A276, and A276/OI650 white thermal control coatings. Measurements were done using a TMA scatterometer with five detectors set at the following angles: 5, 30, 60, 75, and 90 degrees. Z93 changed a small amount as shown in Figure 125. There is a slight decrease in surface roughness shown in Figure 125 by the greater slope of the curve for the exposed sample compared to the control sample. This interpretation is supported by SEM images. Of the four tested coatings, S13G/LO was affected the least from LEO exposure according to BDRF measurements shown in Figure 126. Again, this is corroborated through SEM photographs showing only very minor changes of the surface of S13G/LO. A276 BDRF data (Figure 127) indicate a substantial change in surface morphology. This is likely from AO erosion of organic binder material leaving a layer of pigment particles behind. This is demonstrated by the severe change in BDRF slope from high to near zero indicating conversion from a fairly specular surface to diffuse. OI650/A276 also shows a significant change in slope similar to A276 (Figure 128). However, SEM photographs do not show the highly diffuse surface of A276, but only the formation of numerous cracks in the silicone overcoat that have resulted in the detected BDRF changes.

5.3.4 X-Ray Photoelectron Spectroscopy (XPS)

Samples being analyzed with XPS were exposed to the instrument's vacuum chamber for a period of 48 hours prior to actual measurements for conditioning purposes. Table 14 summarizes the results of the XPS measurements. Of interest is the detection of fluorine on the exposed samples of Z93, A276, and OI650/A276 white thermal control coatings. Fluorine is thought to be from the metallized Teflon used as TCSE's thermal control and radiator surface.

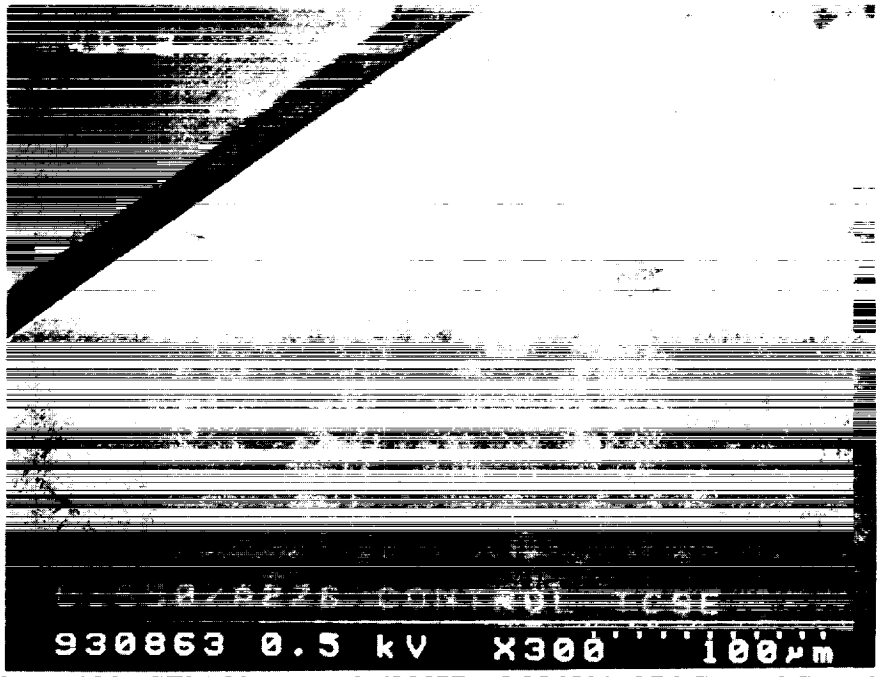

Figure 120. SEM Photograph (300X) of OI650/A276 Control Sample.

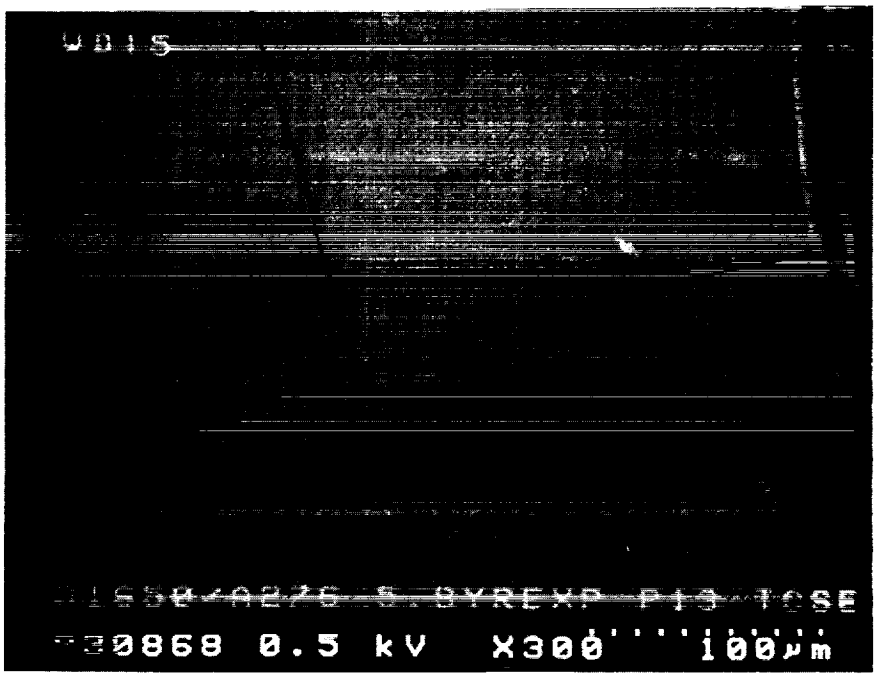

Figure 121. SEM Photograph (300X) of TCSE OI650/A276 Sample Exposed for 5.8 Years.

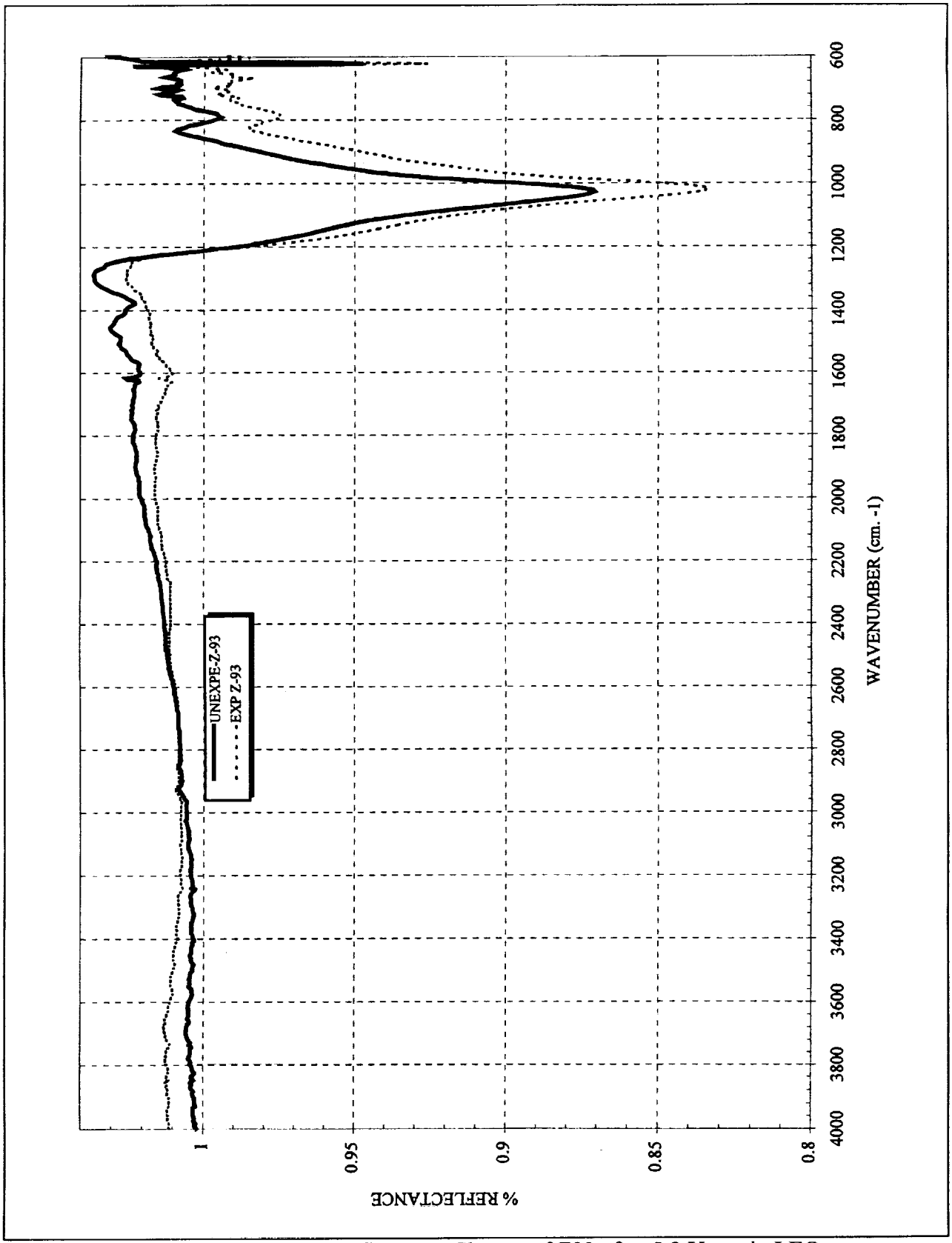

Figure 122. ATR IR Reflectance Change of Z93 after 5.8 Years in LEO.

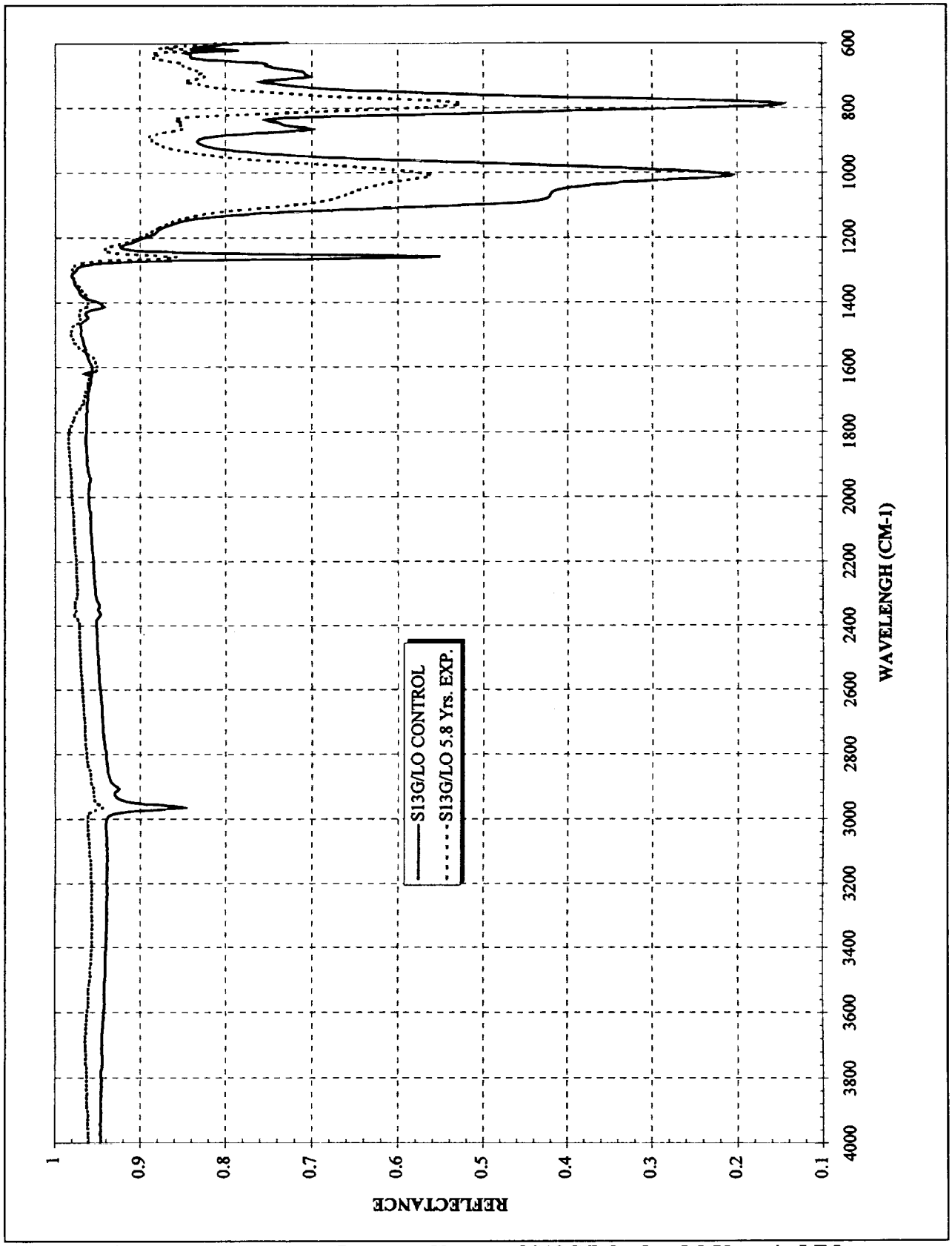

Figure 123. ATR IR Reflectance Change of S13G/LO after 5.8 Years in LEO.

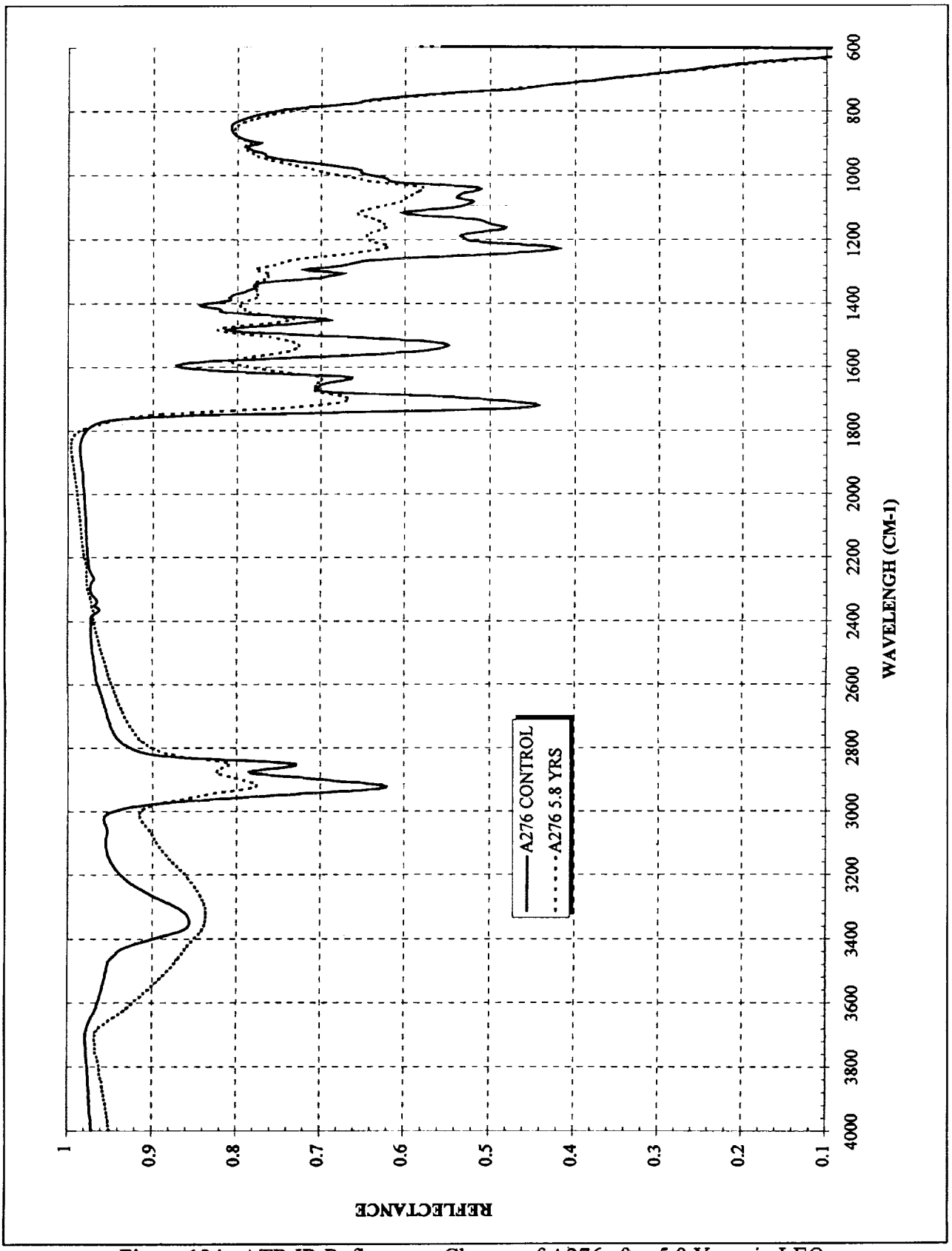

Figure 124. ATR IR Reflectance Change of A276 after 5.8 Years in LEO.

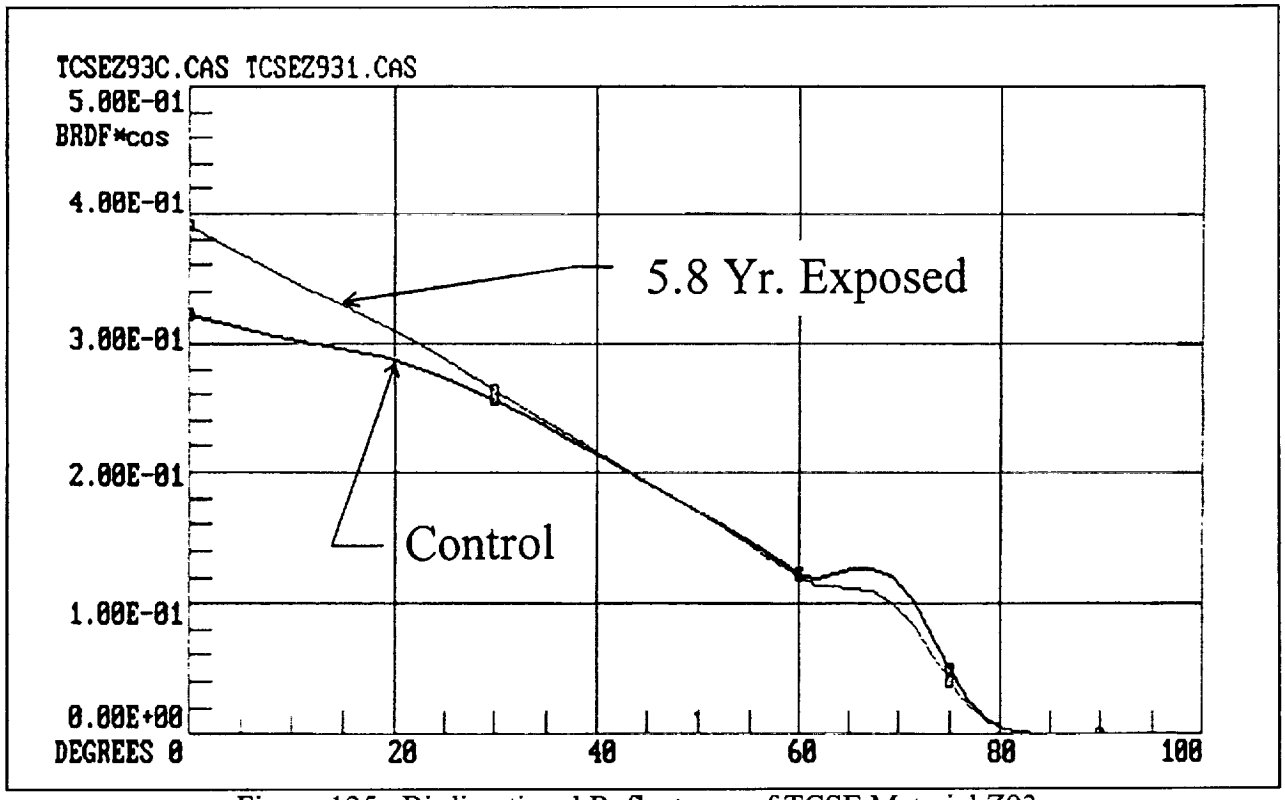

Figure 125. Bi-directional Reflectance of TCSE Material Z93.

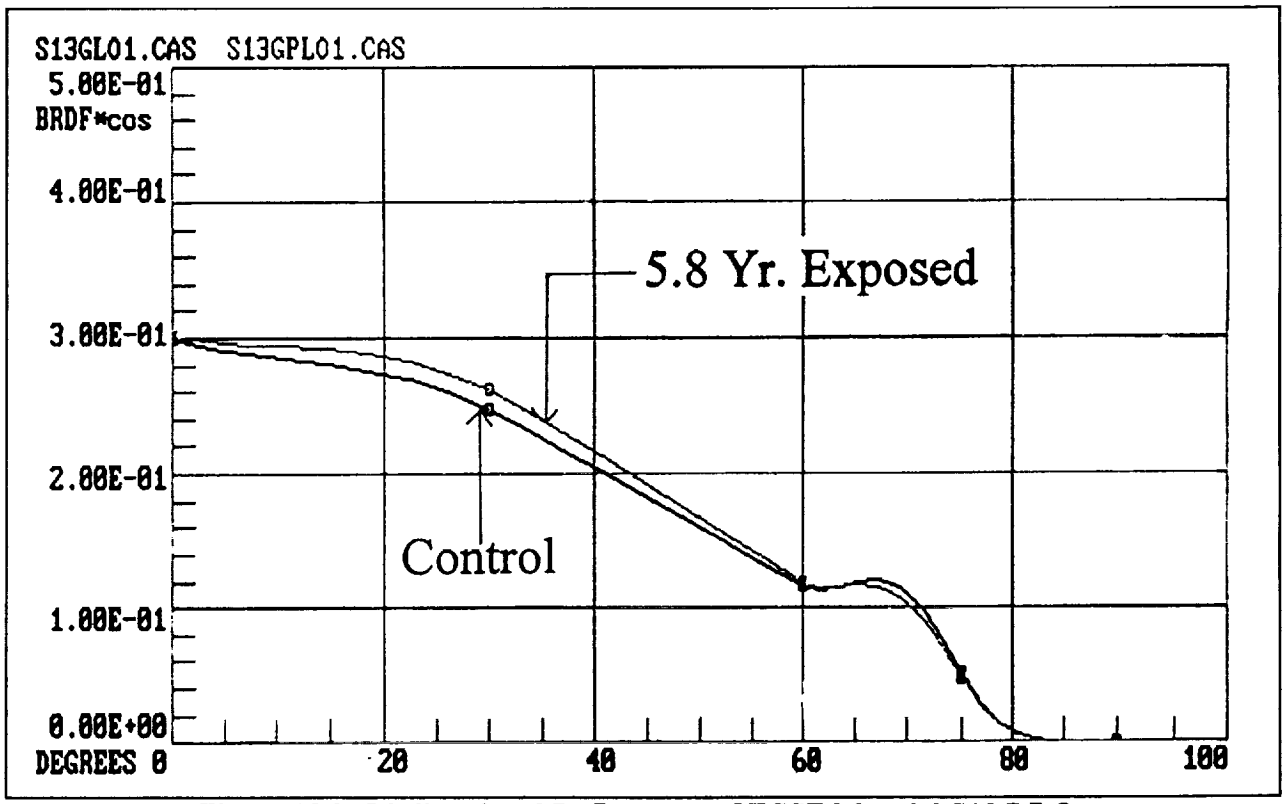

Figure 126. Bi-directional Reflectance of TCSE Material S13G/LO.

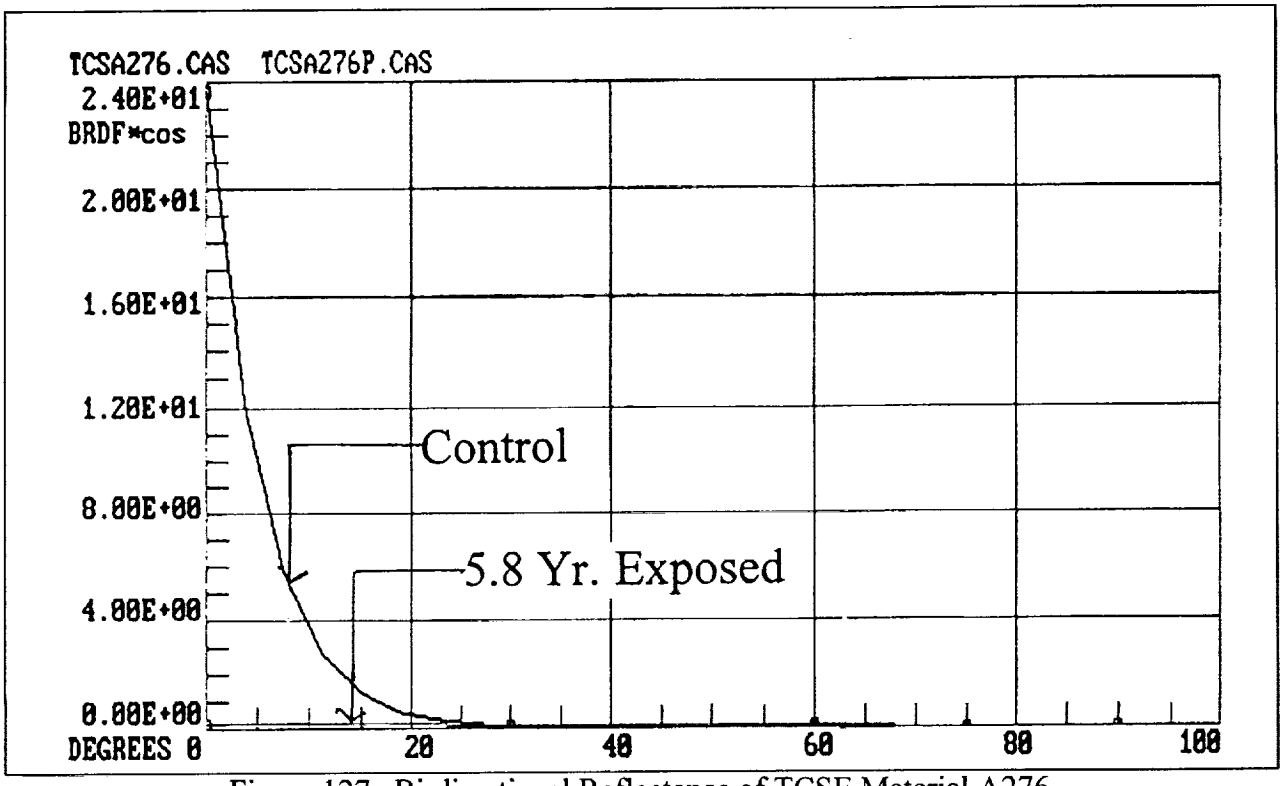

Figure 127. Bi-directional Reflectance of TCSE Material A276.

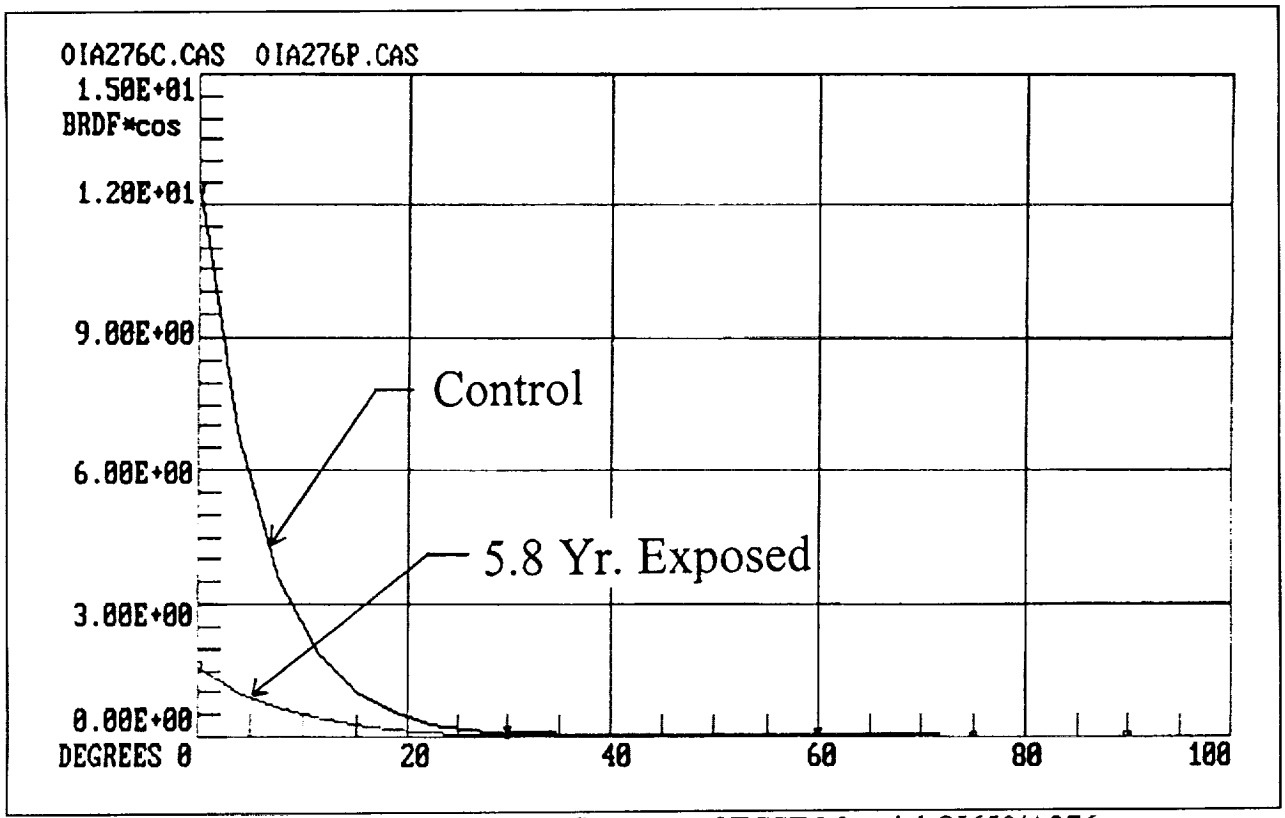

Figure 128. Bi-directional Reflectance of TCSE Material OI650/A276.

Table 14. XPS Elemental Atom Concentration of TCSE Samples.

MATERIAL	ELEMENT												
	C	O	Si	K	Zn	Ti	Al	Sn	N	P	Na	Cl	F
	ATOMIC CONCENTRATION												
S13G/LO Control	50.57	28.30	19.98	0.53					1.14	0.06			
S13G/LO Exposed	27.92	44.90	26.20	0.53						0.06	0.27	0.13	
Z93 Control	33.96	39.55	12.65	8.15	3.22				2.48				
Z93 Exposed	30.02	37.78	4.89	15.63	1.76						0.45		9.46
OI650/A276 Control	38.48	40.48	21.04										
OI650/A276 Exposed	23.69	52.12	20.85	0.54		0.54			1.17	0.67			0.43
A276 Control	77.41	17.91	0.71				0.02	0.26	3.67		0.02		
A276 Exposed	30.01	46.31	10.88			1.13	5.49	0.84	1.32		2.27		1.76

The general high abundance of carbon for all samples is expected for surfaces exposed to normal room air. Using Z93 as an inorganic reference material, it can be determined from studying this table that an atom concentration of about 30 is nominal for surfaces exposed to room air. Hence, the atomic concentration of 27.92, 23.69, and 30.01 for S13G/LO, OI650/A276, and A276, respectively, indicates the lack of carbon containing polymers remaining in the surface layers of these coatings. Values for Z93 may be slightly high because of this coating's propensity to react with air to form potassium carbonate as depicted in the following reaction.

$$K_2O{:}SiO_2 + CO_2 \rightarrow K_2CO_3 + SiO_2$$

This reaction explains the slightly higher atomic concentration of carbon for Z93 than the exposed S13G/LO and OI650 coatings which produce a glass surface layer upon exposure to AO. Polymers based on or containing carbon readily react with AO resulting in consumption of most, if not all, available carbon depending on duration of exposure.

All of the coatings, except Z93, had measurable increases in oxygen atomic concentration. For S13G/LO and OI650/A276 this is caused by the LEO environment, primarily AO, reacting with carbon containing groups attached to the $[O\text{-}Si\text{-}O\ Si\text{-}O]_n$ polymer backbone. In both cases, this oxidation reaction causes the increased detection of oxygen. On the exposed sample of A276, oxidation of the polyurethane binder also takes place resulting in the increased detection of oxygen. From SEM work, it is known that the exposed A276 surface is littered with TiO2 pigment particles. In addition, it is likely that SiO2 is also present on the surface since this material is widely used by the paint industry as an extender for a primary pigment or is used for viscosity control of the fluid paint. If this is an accurate assertion, it helps to explain the increased concentration of detected silicon and oxygen for the exposed sample of this coating. S13G/LO, whose surfaces were originally composed of a dimethyl silicone polymer, changed to a glass through removal of the dimethyl groups. Removal of these groups caused the detected higher atomic concentration for silicon. Exposed OI650/A276 differed from the S13G/LO even

though it also has a silicone surface (OI650). This is caused by the glass-like OI650 resin. OI650 has fewer methyl groups available for reaction with AO and, therefore, little change in silicon atomic concentration is measured.

Of all the samples, Z93 is the most intriguing from the standpoint of changes in concentration of silicon and oxygen. Of all the coatings flown on TCSE, Z93 was one of the most stable optically. However, through XPS, a noteworthy change in silicon and oxygen atom concentration has taken place. Study of higher magnification SEM images does provide some possible insight into this change. These images show a very subtle change in the coating that appears as shrinkage or loss of material. From XPS changes in silicon, oxygen, potassium, and SEM data, Z93 seems to be losing silicon and oxygen atoms. The mechanism for this occurrence is not understood. Other changes in atomic concentration for these coatings is likely due to handling or contamination of some form.

5.3.5 Differential Scanning Calorimeter (DSC) Measurements

Calorimetric measurements were performed on the TCSE control and passive flight samples using a dual sample DSC. These measurements were conducted to detect changes in the thermal behavior of selected TCSE flight exposed and ground control samples. Calorimetric samples were prepared via removal of a thin layer (≈ 1 mil) of each flight and control sample surface. Figure 129 illustrates the fashion in which this process was conducted. Samples were removed from the edge of the flight and control specimens to leave the center portion untouched for further analysis. Masses were recorded before and after the sample was sealed in the DSC test pan. Each sample run was then conducted using the dual sample capability of the instrument. Figure 130 shows the layout of the three sample compartments and the placement of the test samples. The top compartment contained an empty reference pan. This provided the reference for the differential measurements. The lower left compartment housed the flight sample while the lower right housed the laboratory control (unexposed) sample. All test runs were conducted using the same method. The equilibration temperature of -150°C was selected due to the low T_g (glass transition temperature) of most of the samples. This was achieved using a cooling column with LN_2 as the cooling medium.

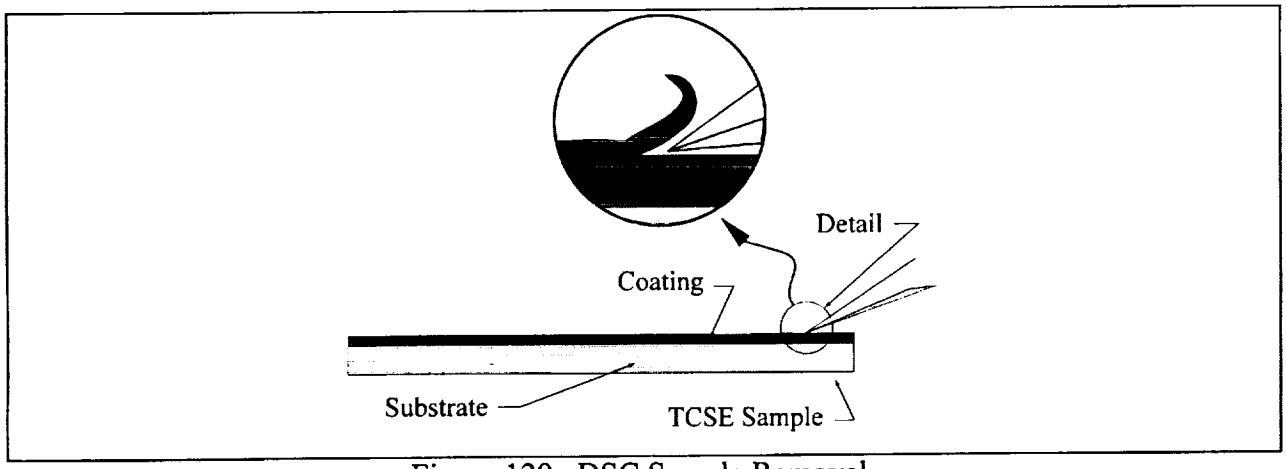

Figure 129. DSC Sample Removal.

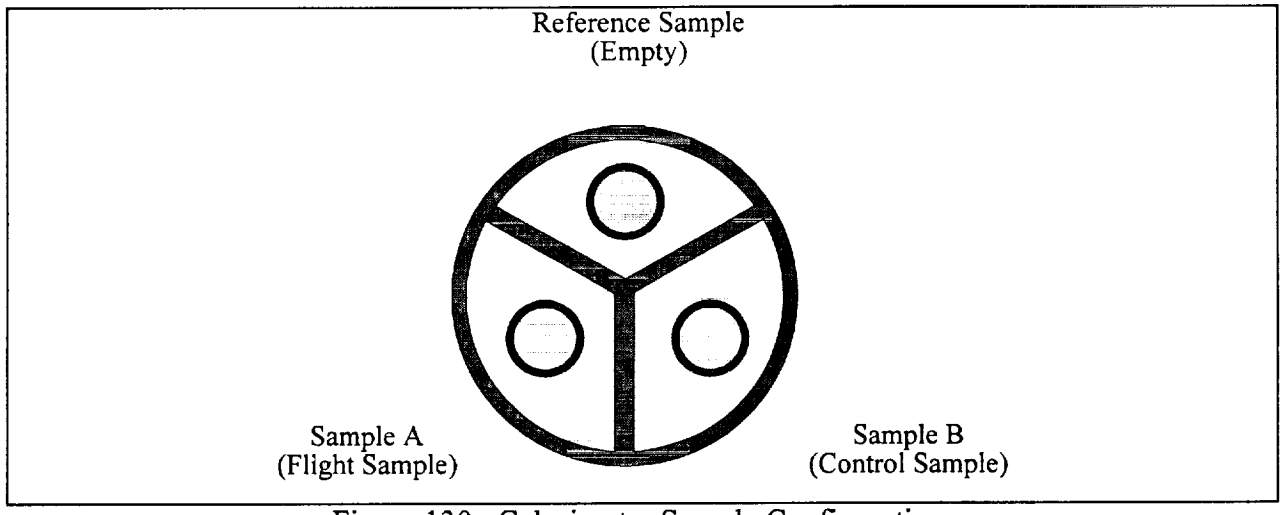

Figure 130. Calorimeter Sample Configuration.

Results from the investigations shown in Figures 131-134 indicate that changes in the sample were detectable with the DSC system and could be quantitatively recorded. This was performed by utilizing the data analysis software supplied with the instrument. Individual peaks are located by their onset and maximum values and then integrated with respect to a baseline curve. This is done to arrive at the total energy content of a particular transition or thermodynamic change. The actual changes in the materials are still not fully understood and, therefore, cannot be directly correlated to the changes observed with the DSC system. Further research and analysis into these phenomenon is necessary to determine these relationships. This investigation did, however, accomplish its goal to determine if these changes could be detected with a DSC system. Also proven is that this method of evaluating changes induced by space environmental exposure can be a valuable tool towards investigating these effects on thick film thermal control coatings.

5.4 Fluorescence Measurements

When the TCSE experiment was inspected upon its return to the laboratory, one technique employed was the use of an UV source ("black light") to look for fluorescing contaminants such as cloth fibers and oils or greases. It was obvious, when compared with similar unexposed materials and with sample controls, that changes had occurred in the visible fluorescent brightness of the thermal control samples and of the TCSE experiment hardware itself (Figure 135). The fluorescence was so striking in some cases, such as the black urethane based coating Z302, that it was decided to try to obtain quantitative measurements of the changes. The goals were to try to characterize the various types of coatings in terms of their fluorescent properties and to possibly learn if the observed changes could further elucidate effects of exposure to the space environment.

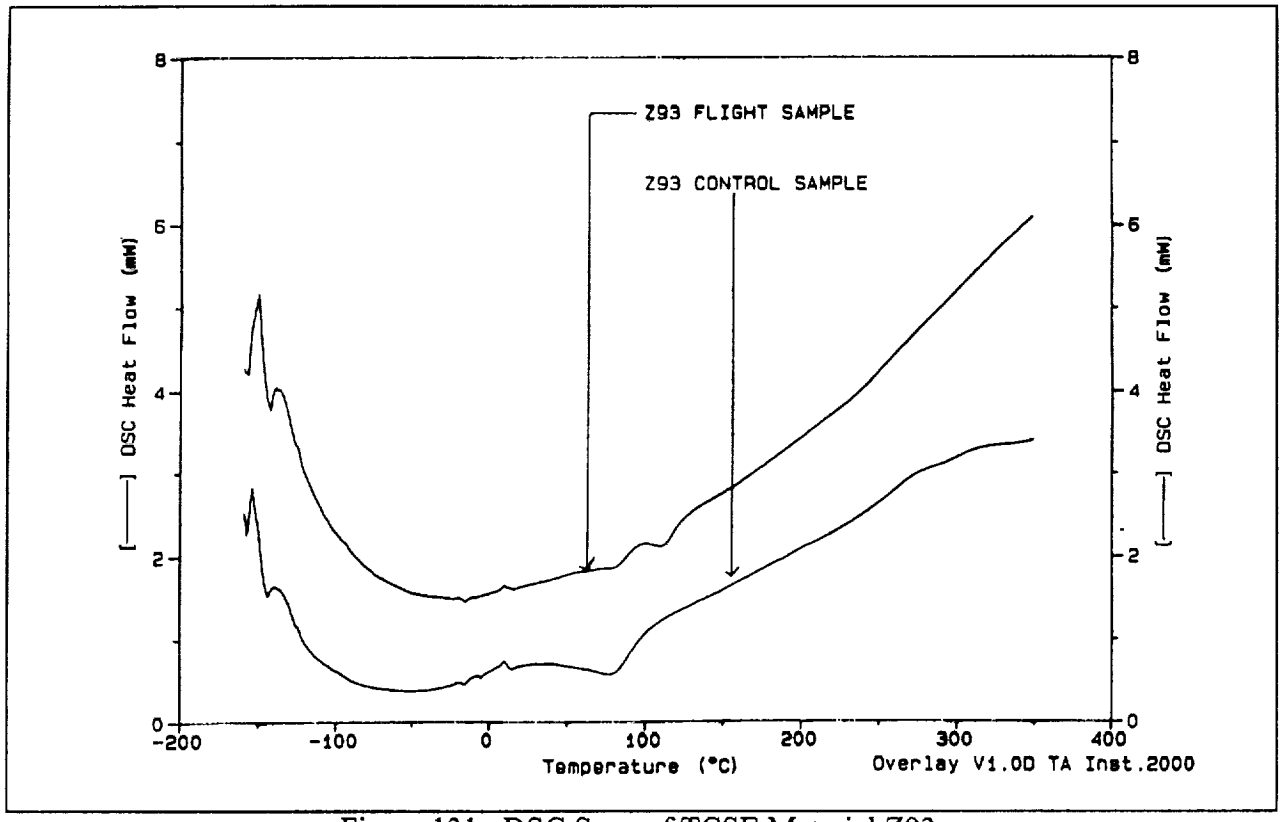

Figure 131. DSC Scan of TCSE Material Z93.

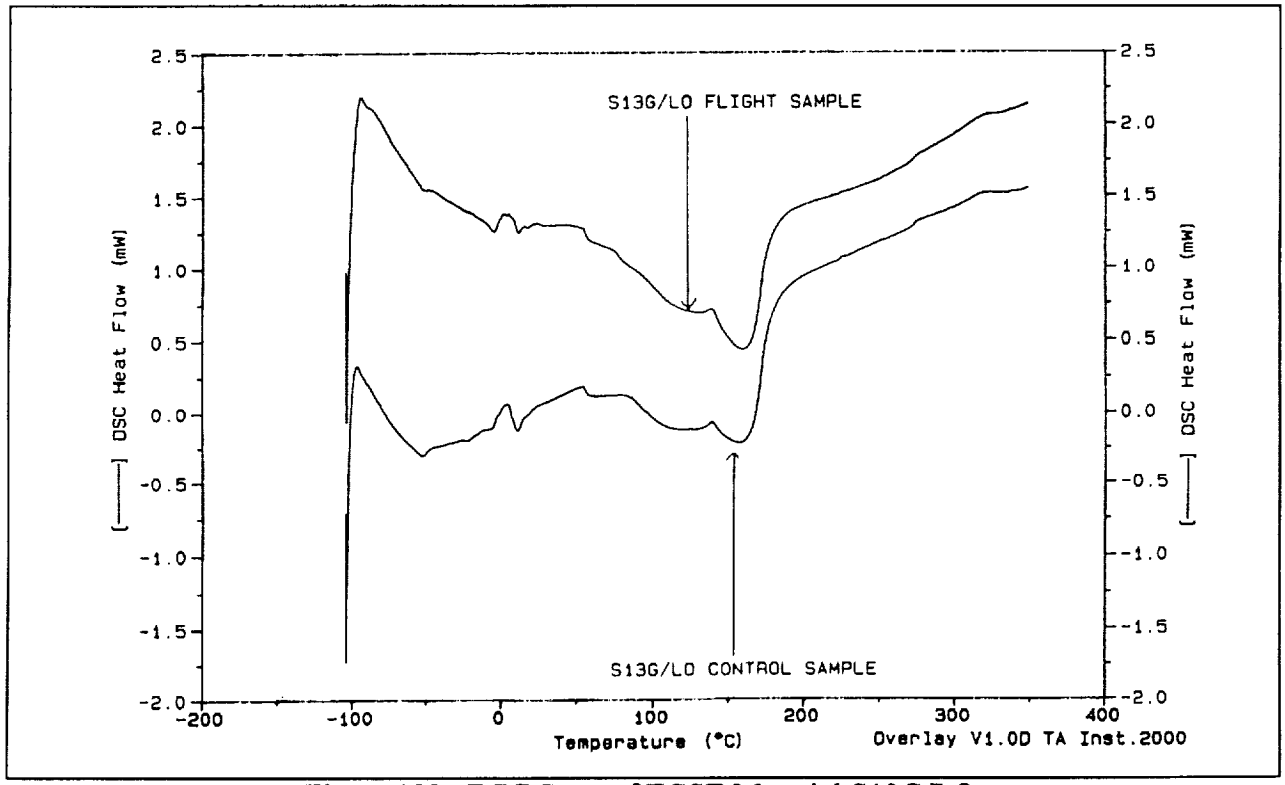

Figure 132. DSC Scan of TCSE Material S13G/LO.

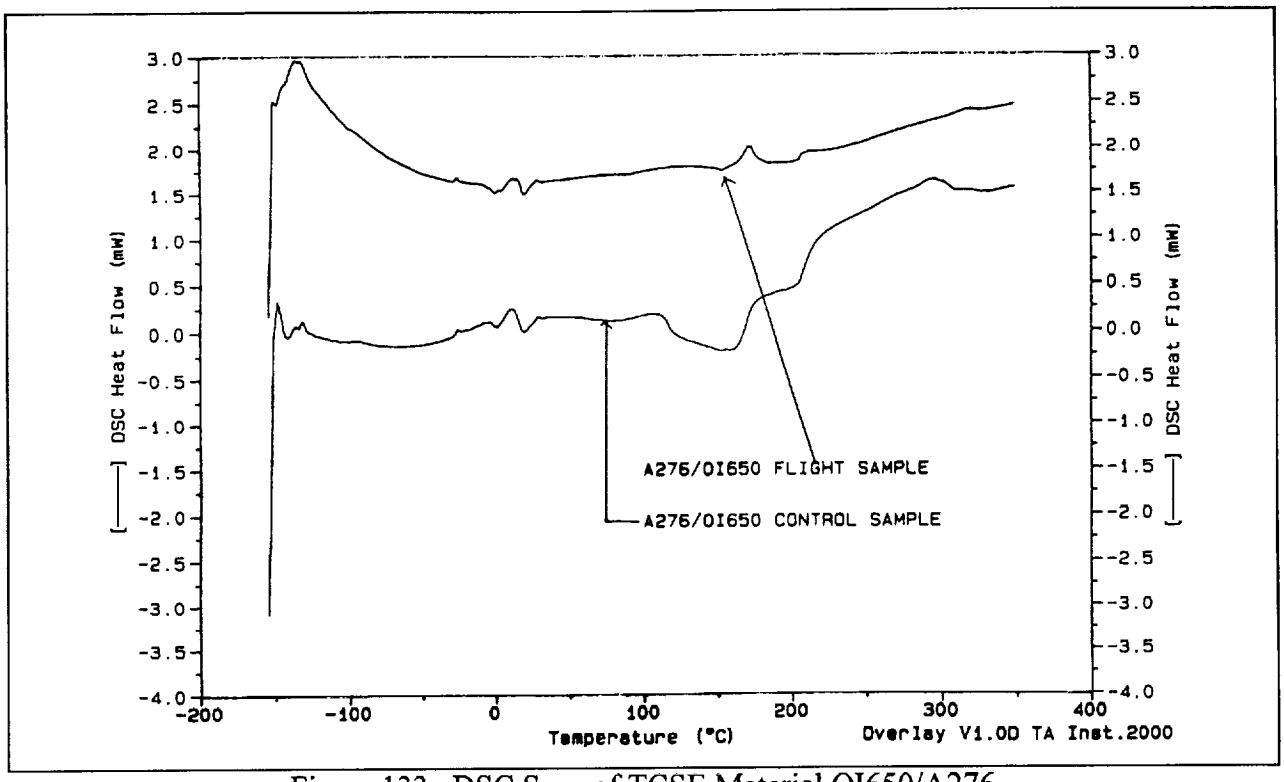

Figure 133. DSC Scan of TCSE Material OI650/A276.

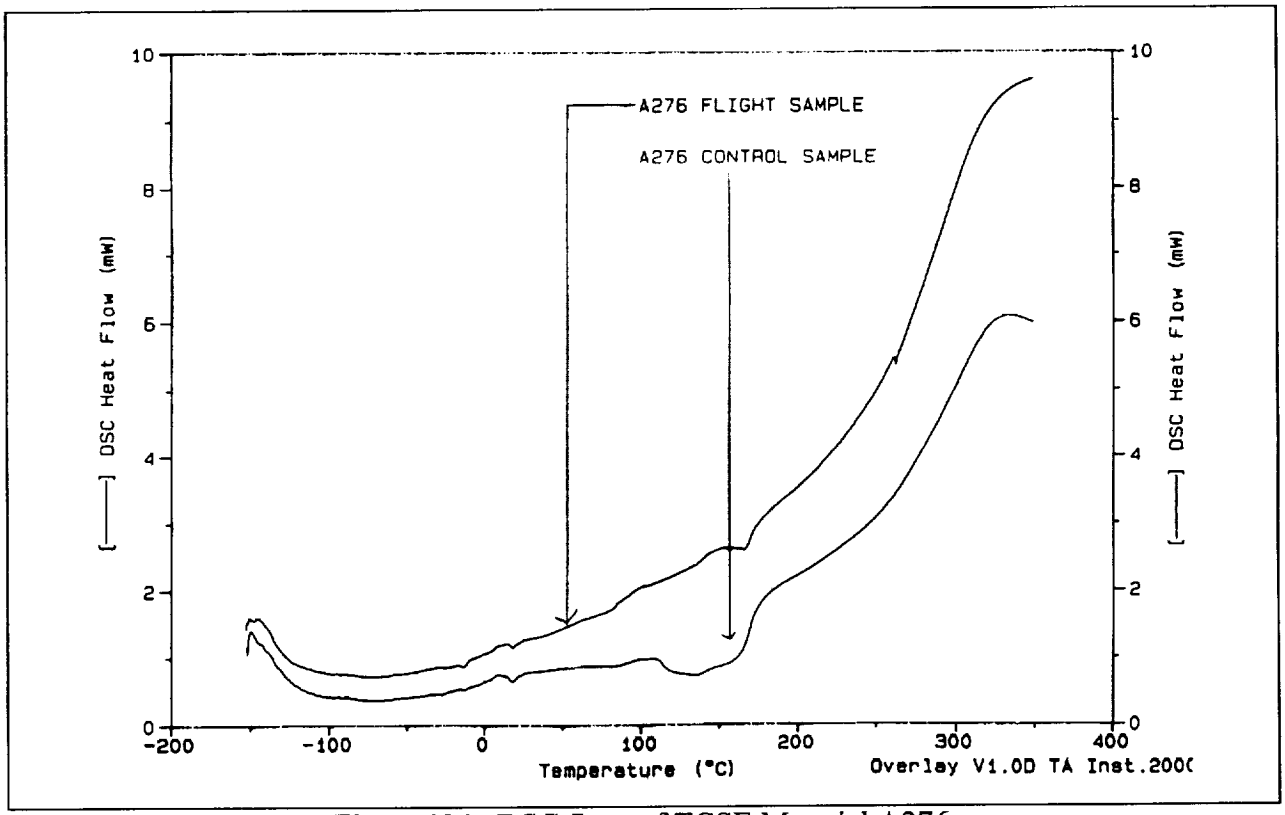

Figure 134. DSC Scan of TCSE Material A276.

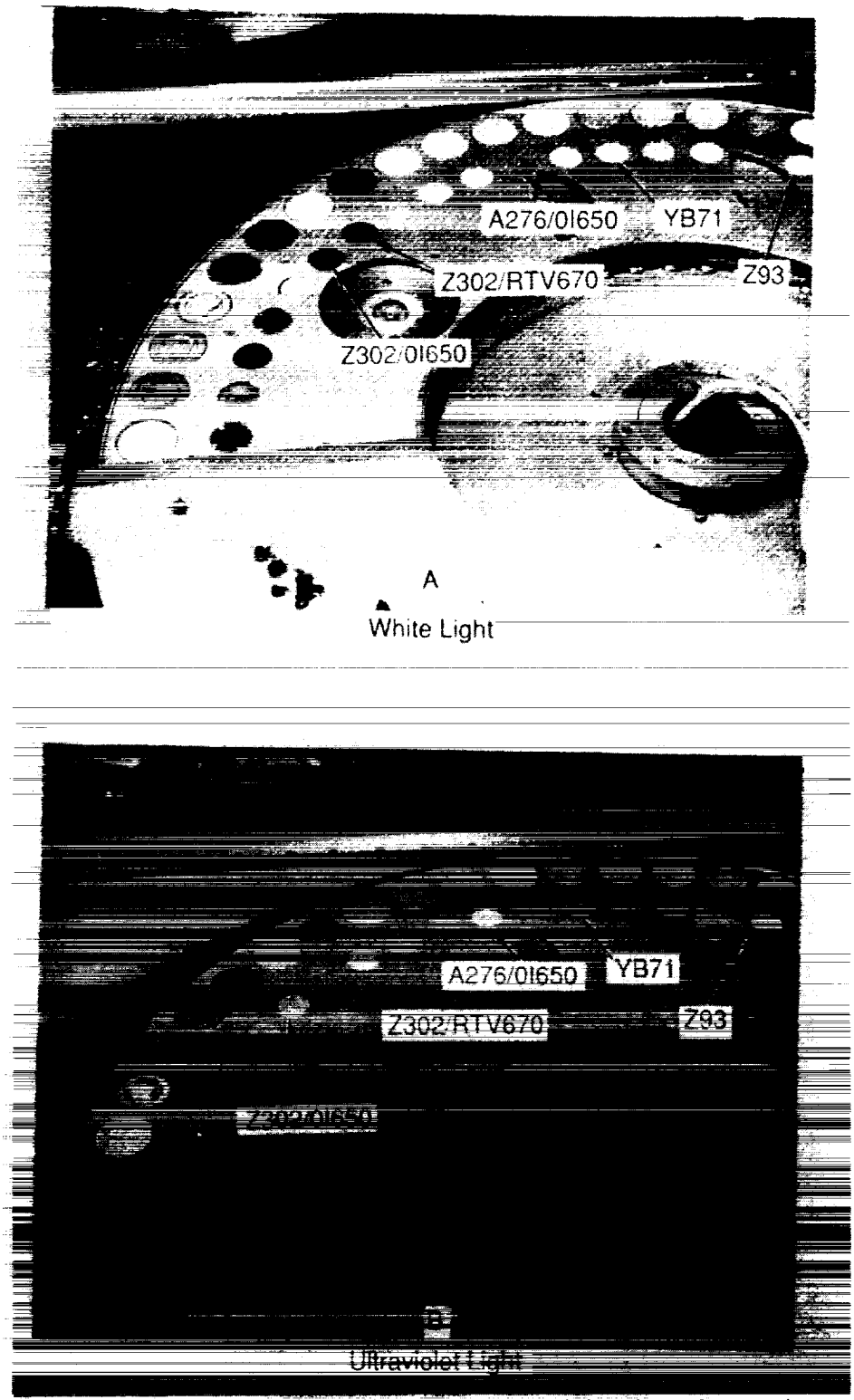

Figure 135. Post-Flight Fluorescence of Thermal Control Coatings Comparison of Samples Under White and Ultraviolet Light.

5.4.1 Fluorescence Measurement Description

Absolute fluorescence measurements were made using the following experiment set up and calibration procedure. A Beckman DK-2 Spectrophotometer using its 1P28 photomultiplier tube mounted in the spectroradiometric position was used to detect any fluorescent behavior from the samples. Fluorescence was induced by irradiating the sample, mounted at 45° to the optical beam, in line with the sample entrance port of the spectrophotometer (Figure 136). For these measurements, a one kw mercury-xenon lamp with a Schoeffel monochromator was used. It was found that use of the strong peak of 280 nm was convenient. Overall, the illuminating band was from 265 to 290 nm with the monochromator slits set at 1.5 mm. Measurements of output with this set up using a Molectron radiometer indicated an irradiance level of 0.5 mw/cm^2 at the sample (equivalent to about 1 sun in this band).

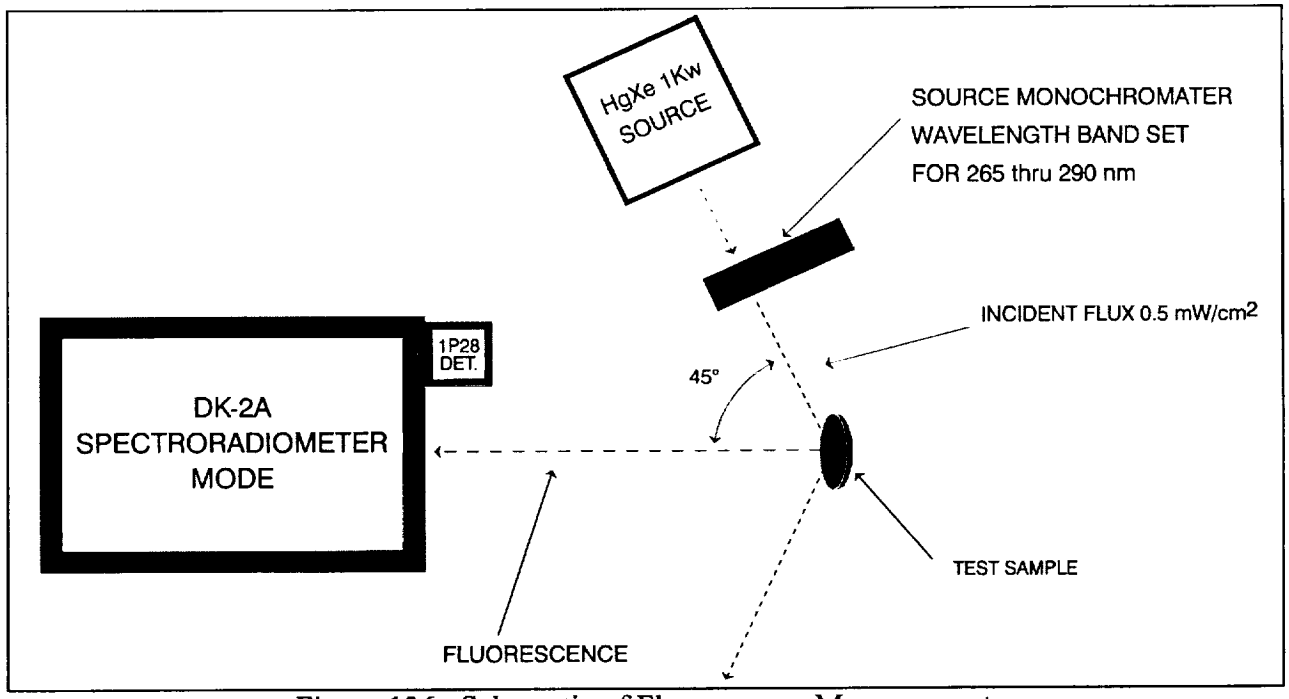

Figure 136. Schematic of Fluorescence Measurement.

To provide a calibration of the DK-2 spectrophotometer, a one kw quartz-halogen tungsten Standard of Total and Spectral Irradiance (Model 200H) supplied by Optronics Laboratories (traceable to NIST), was used in place of the Hg-Xe source (Figure 137). A 99% diffuse reflectance standard (from Labsphere, Inc. SRS-99-010-6561A) was placed at the sample location. Since this non-fluorescing standard provided essentially Lambertian reflectance of a known irradiance level, a calibration of the DK-2 as a system was made over its sensitive wavelengths (~300-650 nm). For ZnO pigmented coatings, it was also determined that the fluorescent energy is proportional to irradiance, over a factor of 5.5, and that there was no detectable change in fluorescent wavelength peaks for irradiance bands of 265-290 nm, 295-320 nm, and 310-340 nm.

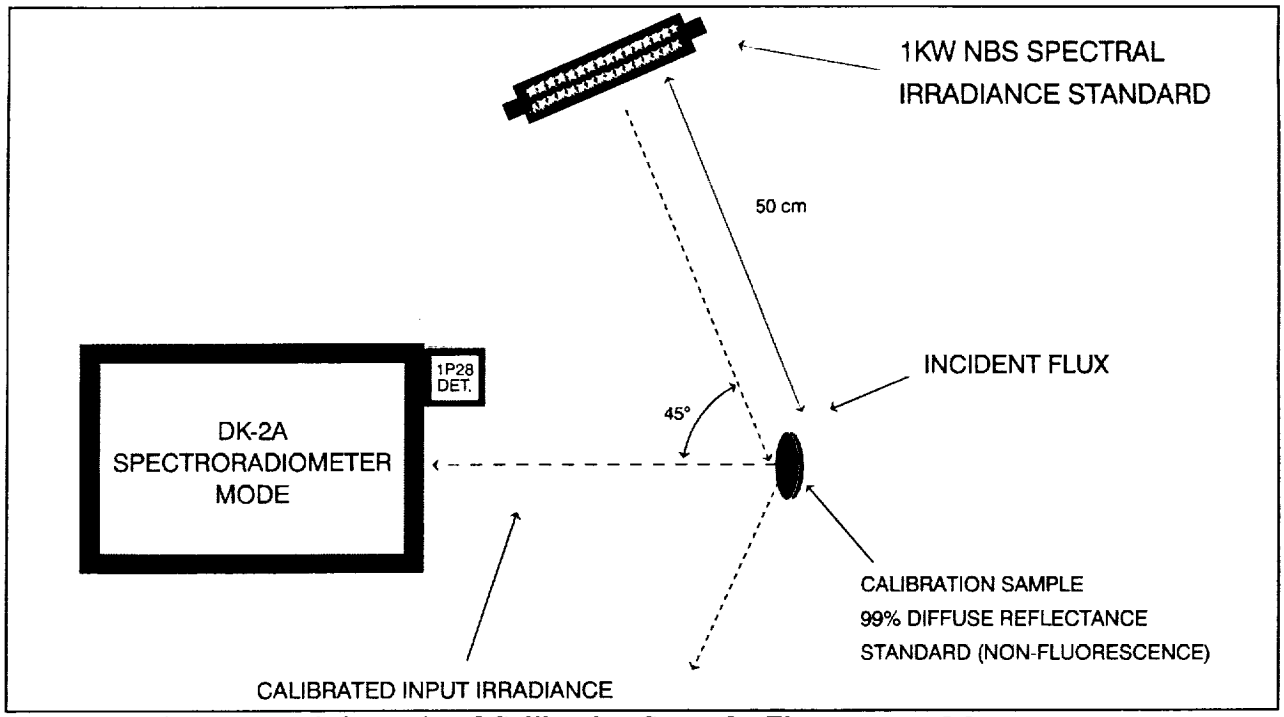

Figure 137. Schematic of Calibration Setup for Fluorescence Measurements.

5.4.2 Fluorescence Analysis

Three types of thermal control coating samples were found to exhibit rather strong fluorescence. These were: 1) coatings that used ZnO as a pigment, 2) coatings that used urethane as a binder, and 3) coatings that used urethane as a binder and had a thin silicone overcoat.

Other TCSE thermal control coatings samples that were measured and found not to have significant fluorescence were Z306 (a urethane based black paint), YB71 (silicate), and D111 (silicate). A white Tedlar flight sample did not fluoresce, while a laboratory specimen exhibited very weak fluorescence peaks at about 420-440 nm. Also measured were silver Teflon samples cut from the front cover of TCSE. Similar materials that were not exposed to the space environment were used for comparison.

Figures 138 and 139 allows comparison of the flight and control fluorescent spectra of Z302 and A276 urethane based coatings, respectively. The similarity in the control spectra from 400-575 nm is likely attributable to the fluorescence characteristics of the polyurethane binder. However, the spectra for the flight Z302 sample exposed for 19.2 months is somewhat unique in that the magnitude and band width of the fluorescence is less than most of the other polyurethane samples. This may be due to the erosion of the sample by AO and/or as a natural frequency shift of the material caused by exposure to the LEO environment. Fluorescence data is not available for Z302 exposed in the RAM direction for 5.8 years since it was completely eroded.

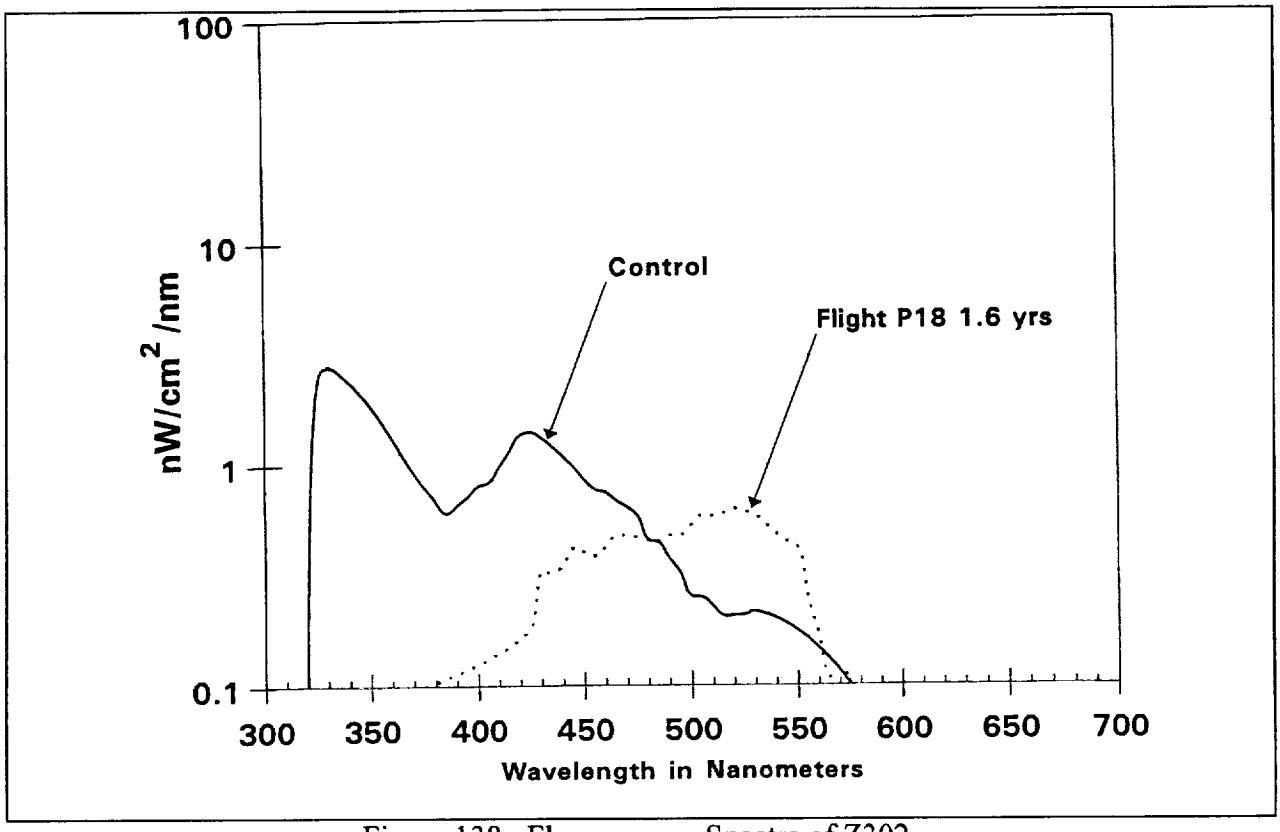

Figure 138. Fluorescence Spectra of Z302.

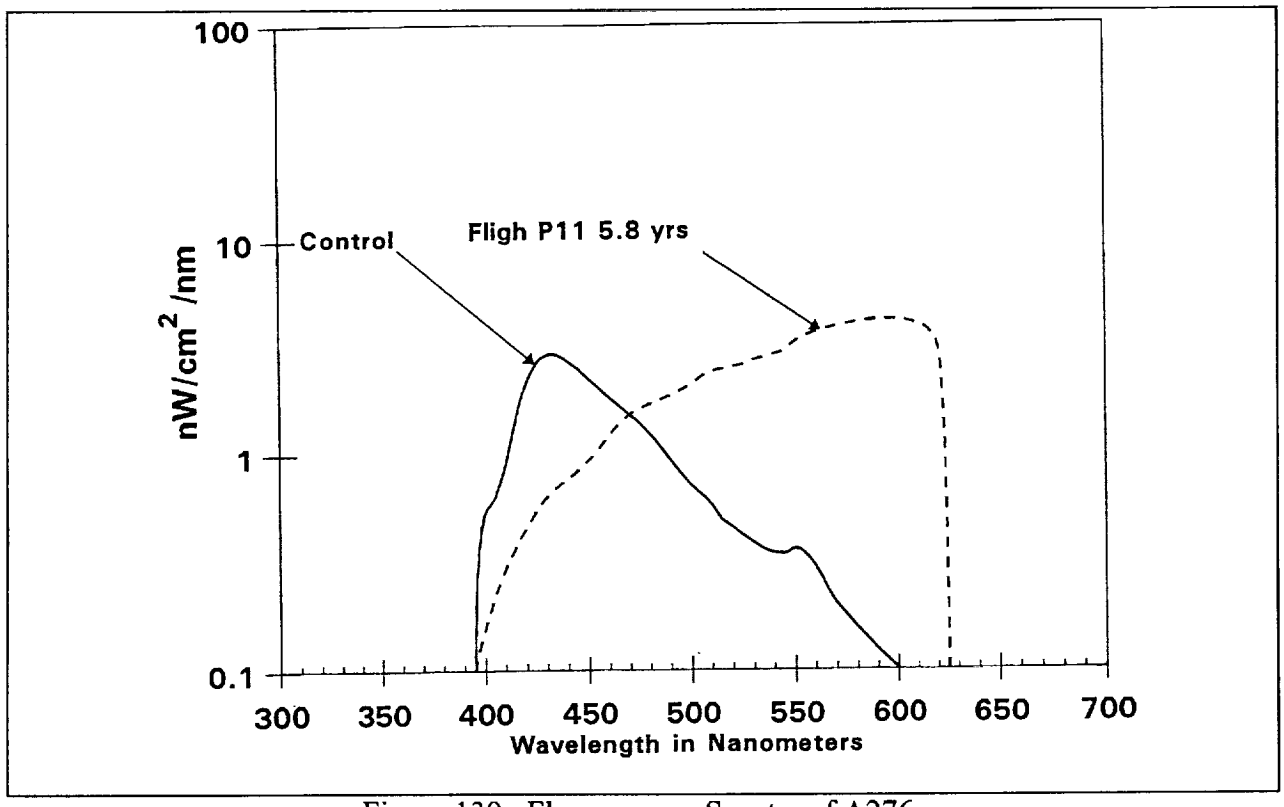

Figure 139. Fluorescence Spectra of A276.

The similarities shown in the spectra of Z302 and A276 with a OI650 silicone overcoat is even more striking (Figures 140 and 141). These figures tend to illustrate that the polyurethane samples, both Z302 and A276, overcoated with OI650 and then exposed to the flight environment fluoresce very similar to one another. In addition, the similarities between the overcoated and neat A276 polyurethane coatings fluorescence spectra are shown in Figures 139 and 141. The OI650 overcoated control samples have enhanced UV fluorescence attributable to the overcoat itself. This effect is not present in the flight exposed samples and, in fact, there is no fluorescence evidence that the overcoat is still present. The similarity in exposed A276 (neat and overcoated) spectra may be due to extensive crosslinking of the silane polymer on the surface. The crosslinking of the polymer modified the electronic and molecular structure and may have more effectively bonded the available electrons. The result is the electrons could no longer be excited to a higher, unstable energy level when exposed to UV irradiation and therefore the overcoat no longer fluoresced, but the fluorescence of the A276 was transmitted through the overcoat. Further evidence that crosslinking of the silane overcoat is a likely explanation for this phenomenon is that visual inspection of the surface of the overcoated samples shows significant cracking. This can be the result of the hardening and embrittlement of the polymer from increasing crosslinking based on optical properties measurements.[22] The overcoat has served its purpose to protect the Z302 from eroding.

The ZnO pigmented Z93 and S13G/LO coatings show remarkably similar fluorescence spectra for the control samples as well as those that were protected by an aluminum cover during flight (Figures 142-147). The spectra from the exposed samples generally appear similar, with unexplained weaker fluorescence on the TCSE P7, 5.8 years exposure S13G/LO sample (Figure 143) and on AO114 Wake mounted S13GLO sample (Figure 147). Especially, the Wake mounted sample shows a weak fluorescence and the absence of the 380 mm peak.

From Figure 142, Z93 spectra for 1.6 and 5.8 years exposure are shown, providing evidence that the change occurring is not linear with time and that the 380 and 520 nm fluorescence change rates may be different.

The slight fluorescent glow noticed on the TCSE front cover was measured and is shown in Figure 148. Measurements on non-flight Teflon failed to produce any detectable fluorescence. However, measurements of the 3M 966 high temperature acrylic adhesive used to apply the silver Teflon produced fluorescence that, like the silicone overcoat, extended into the UV (Figure 149). Upon exposure to strong UV for various periods of time, the spectra shifted toward the visible region during the first short exposure and did not continue to shift significantly, but fluorescence intensity continued to grow in this band.

5.4.3 Fluorescence Summary

It is clear that the fluorescence of the urethane based paints is produced by the urethane binder itself and not the various pigments. Hill[23] has correlated laser-induced fluorescence (LIF) with tensile strength of several polyurethane based materials. He also found LIF changes in LDEF Tray Clamps samples of A276 and Z306 supplied to him by Boeing.[24] It is not apparent if the specific LIF changes detected in the thermal control coatings is the same as

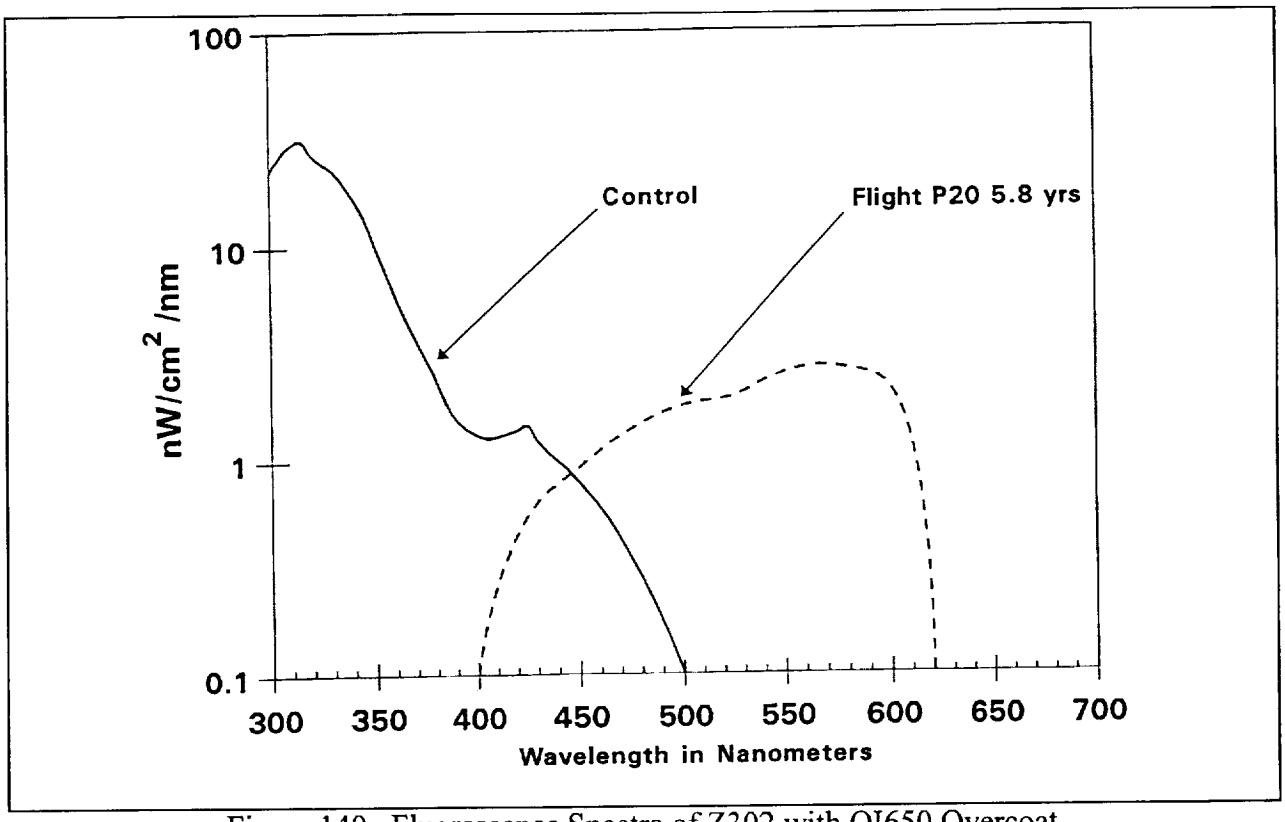

Figure 140. Fluorescence Spectra of Z302 with OI650 Overcoat.

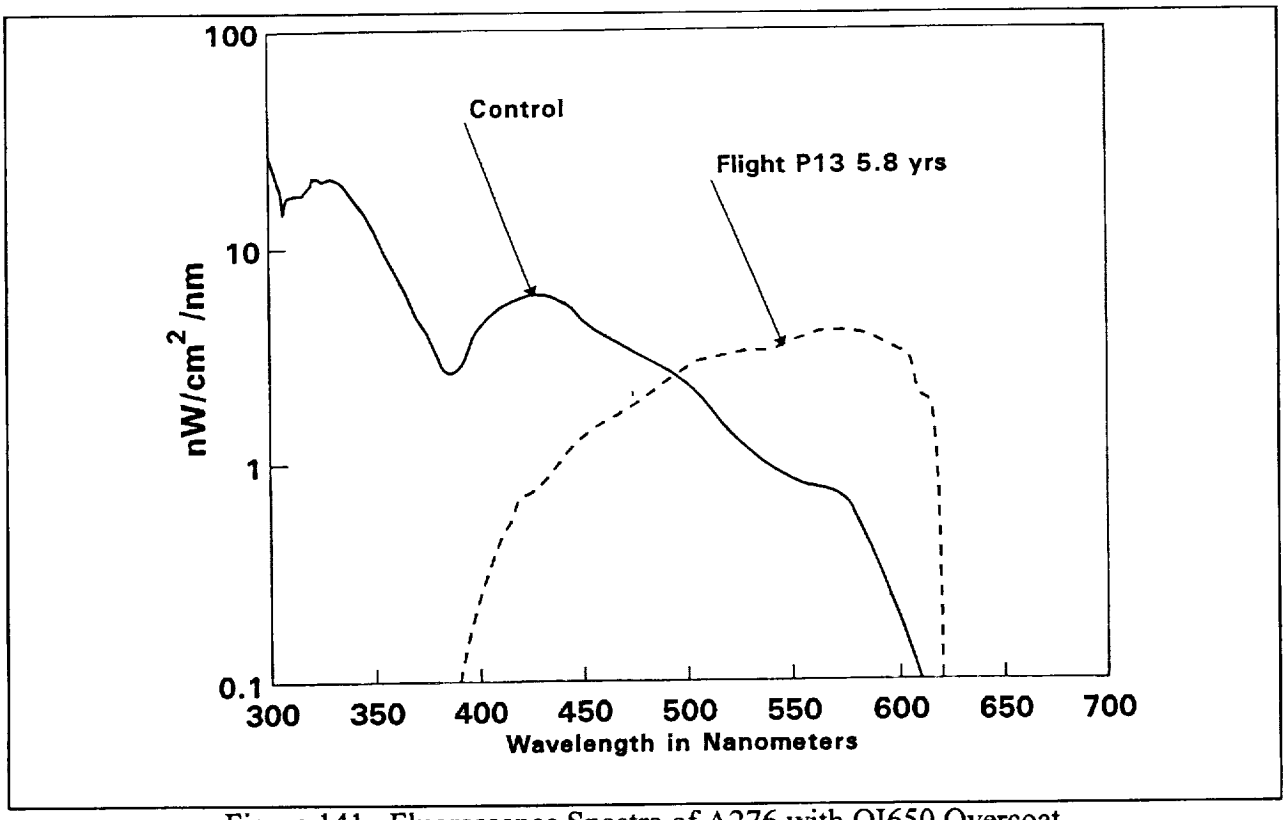

Figure 141. Fluorescence Spectra of A276 with OI650 Overcoat.

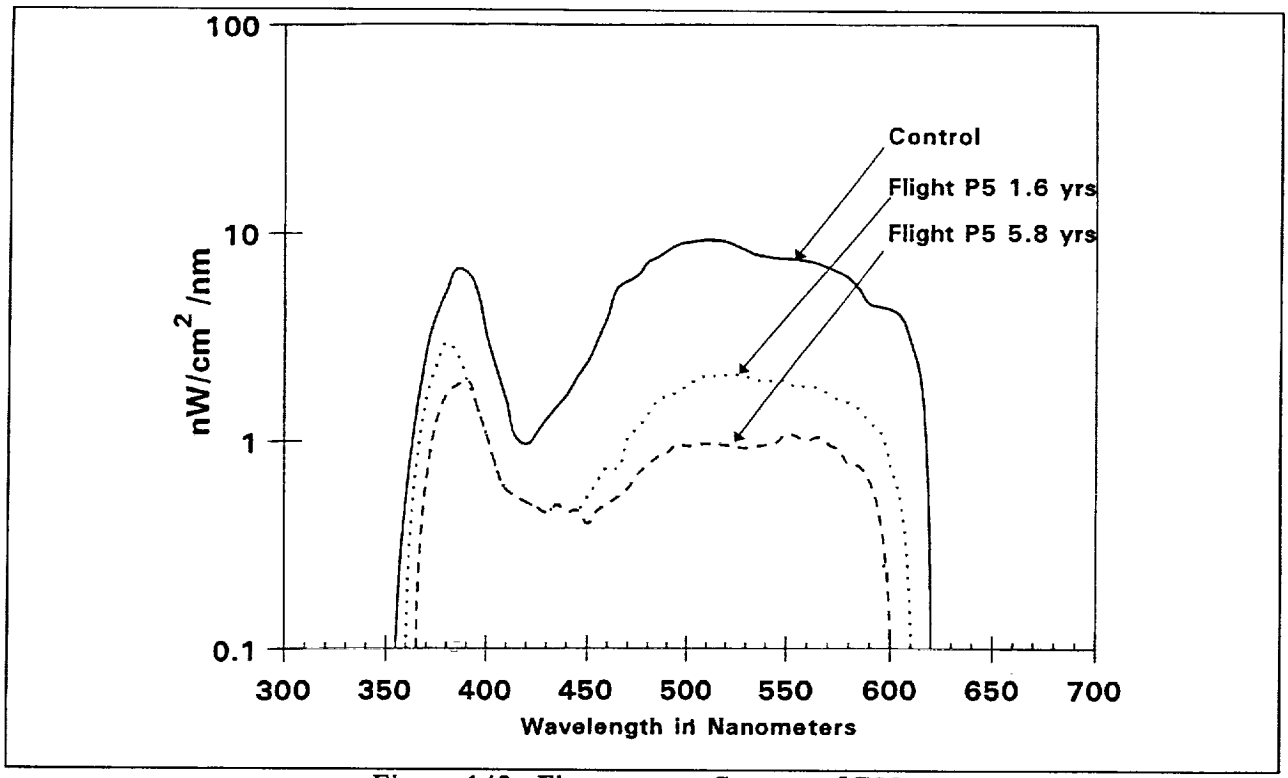

Figure 142. Fluorescence Spectra of Z93.

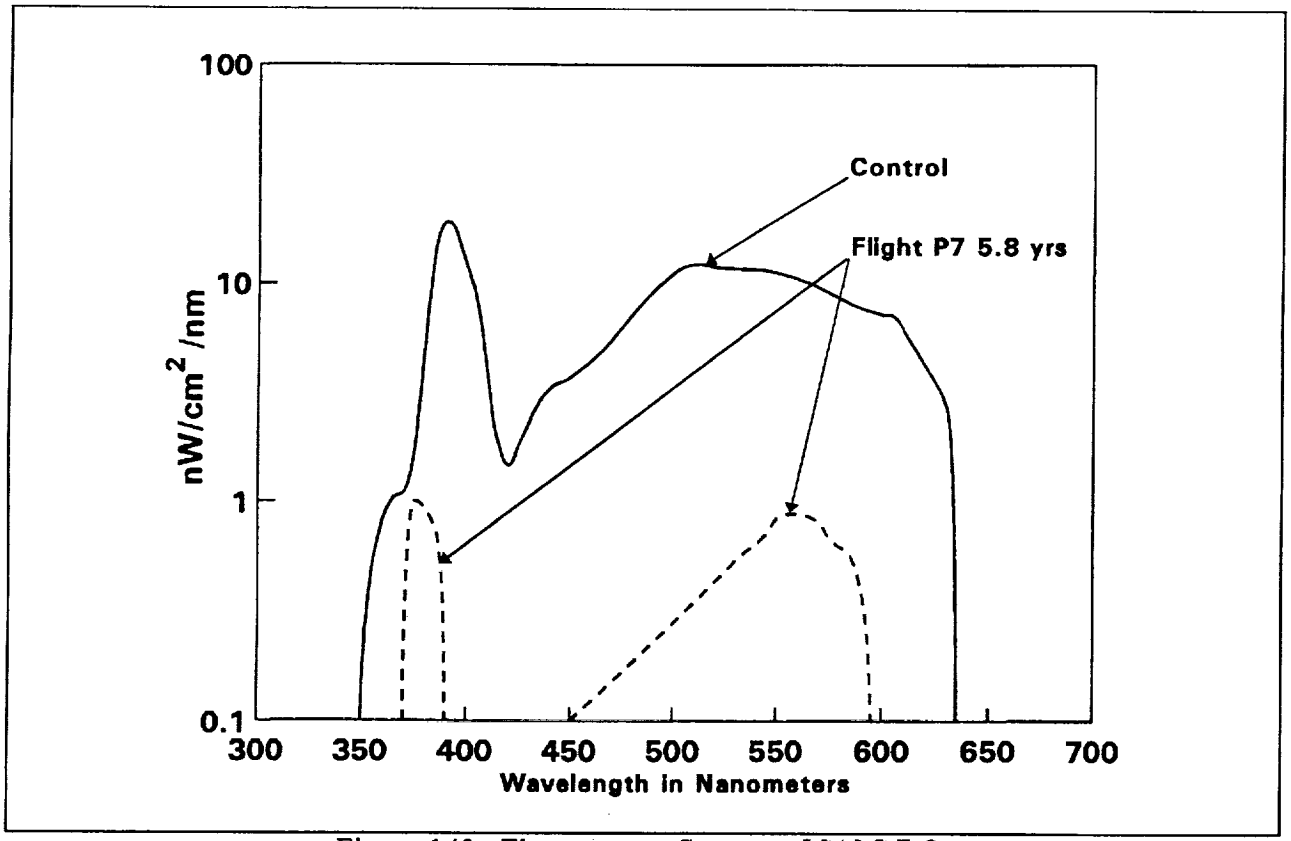

Figure 143. Fluorescence Spectra of S13G/LO.

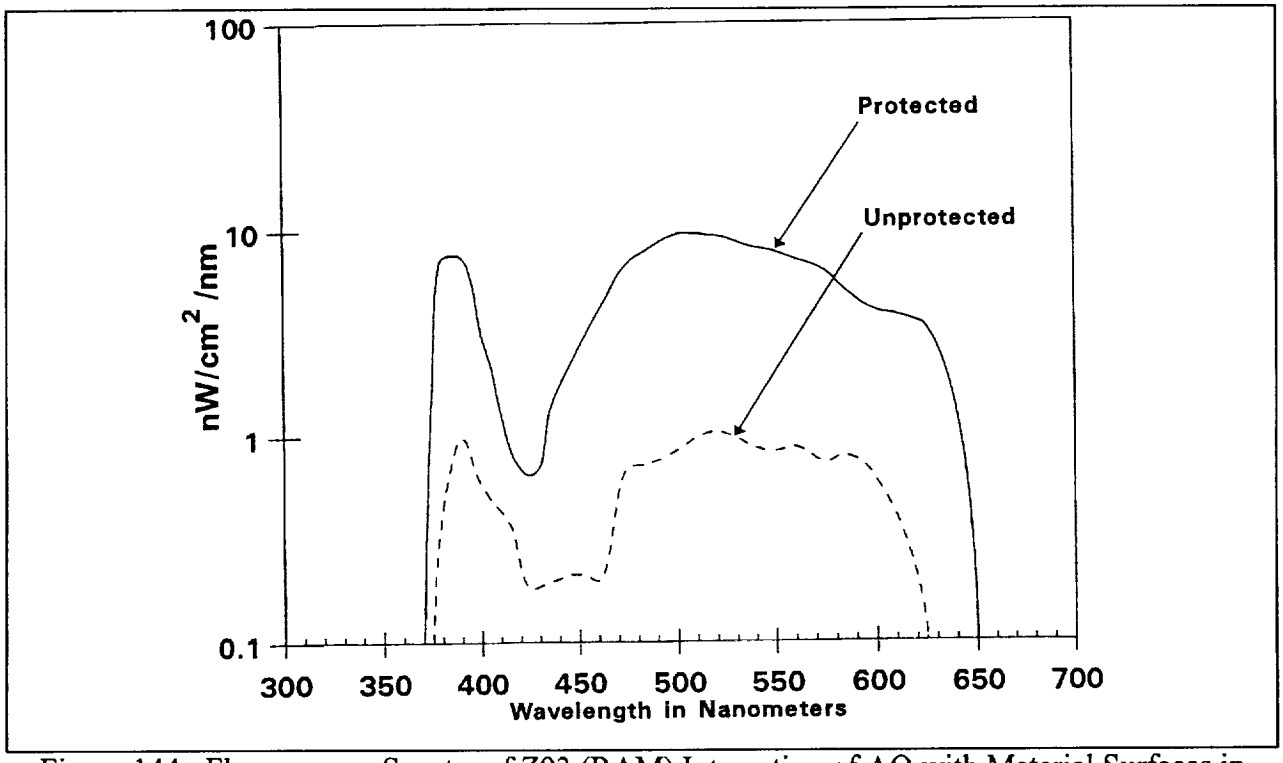

Figure 144. Fluorescence Spectra of Z93 (RAM) Interaction of AO with Material Surfaces in LEO AO114.

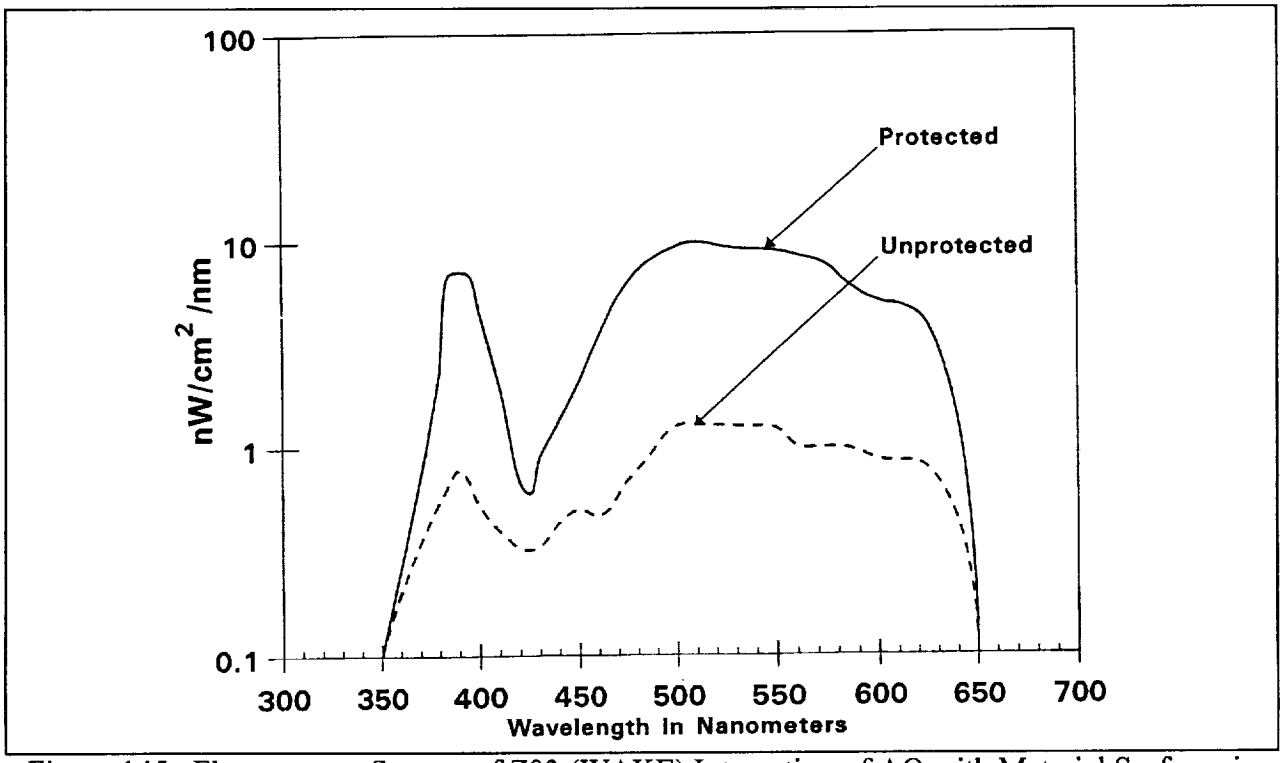

Figure 145. Fluorescence Spectra of Z93 (WAKE) Interaction of AO with Material Surfaces in LEO AO114.

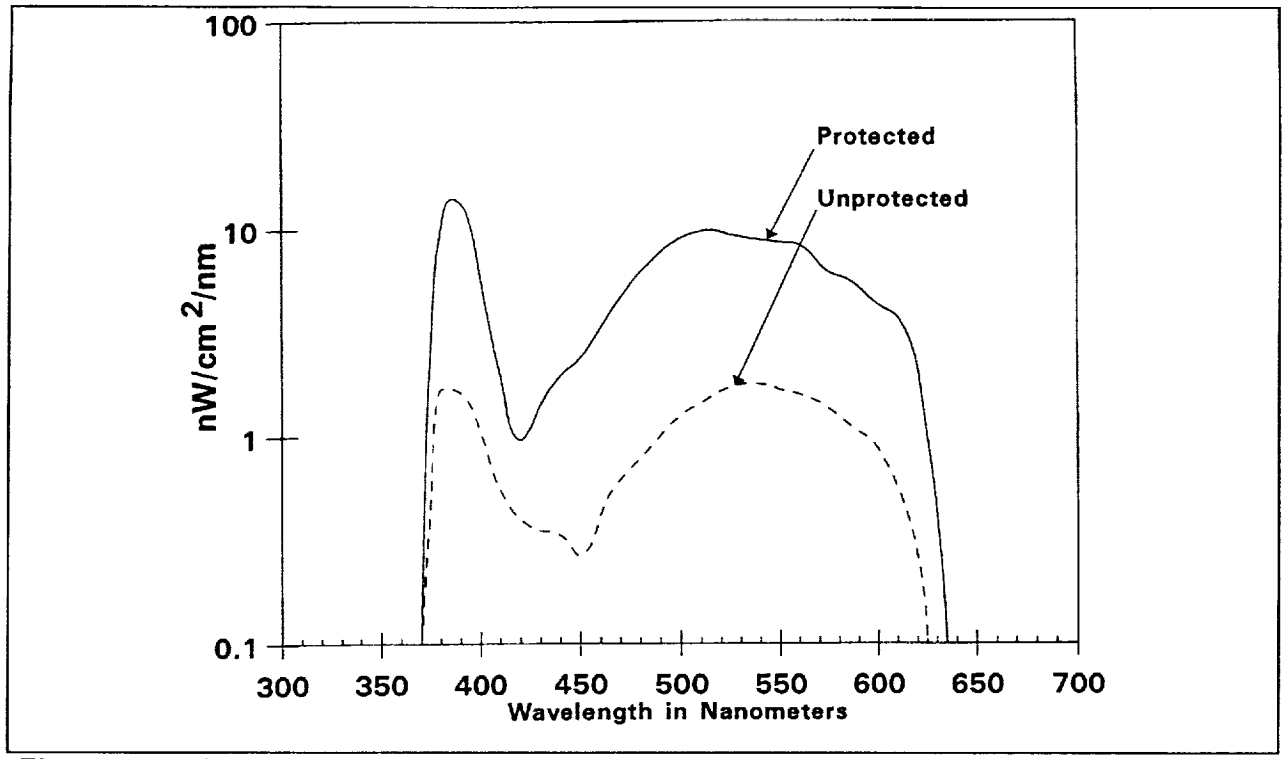

Figure 146. Fluorescence Spectra of S13G/LO (RAM) Interaction of AO with Material Surfaces in LEO AO114.

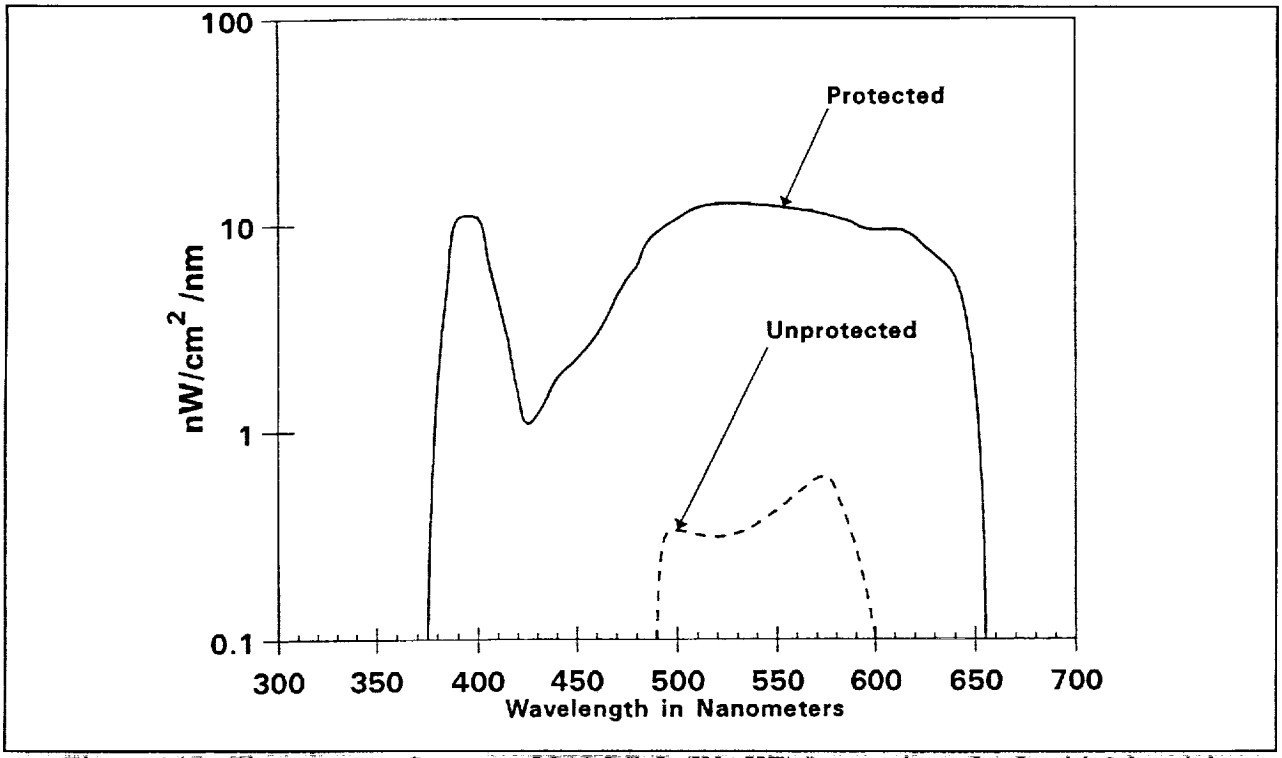

Figure 147. Fluorescence Spectra of S13G/LO (WAKE) Interaction of AO with Material Surfaces in LEO AO114.

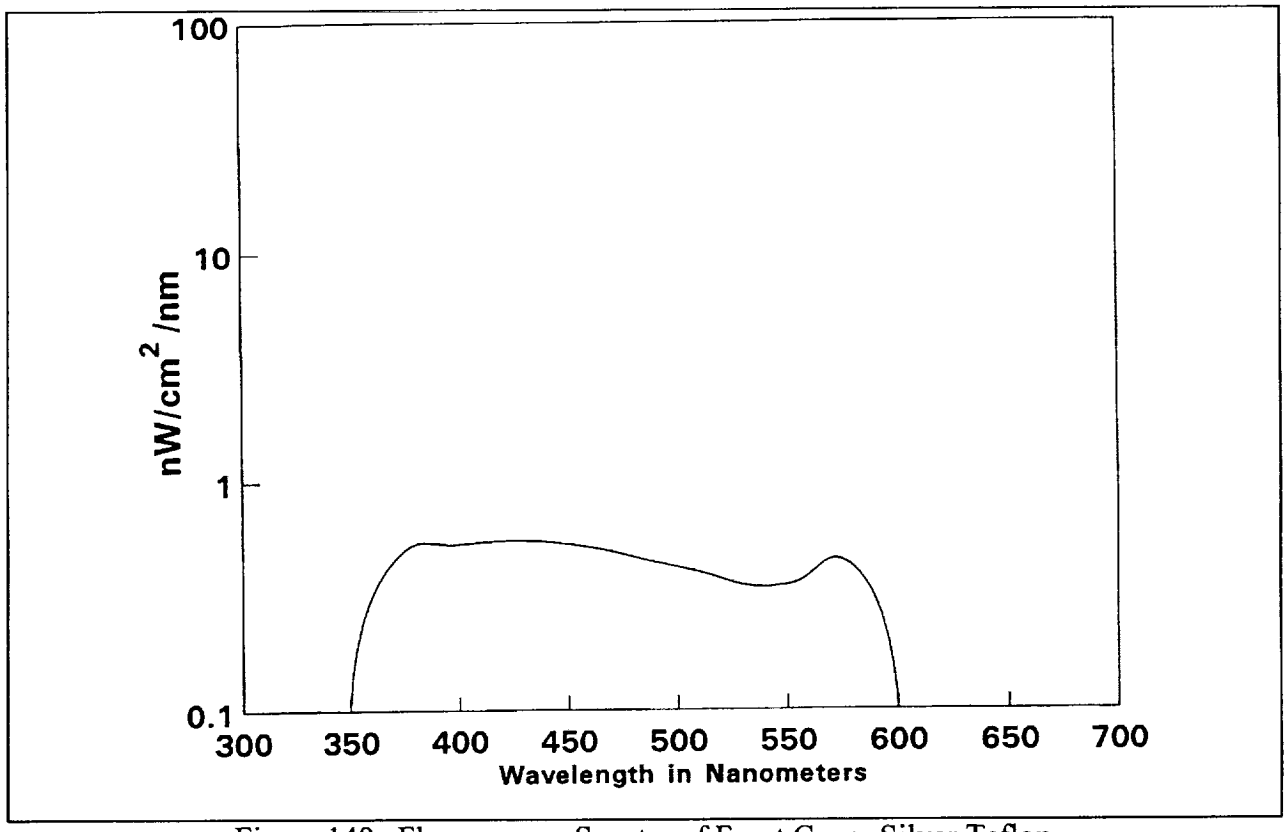

Figure 148. Fluorescence Spectra of Front Cover Silver Teflon.

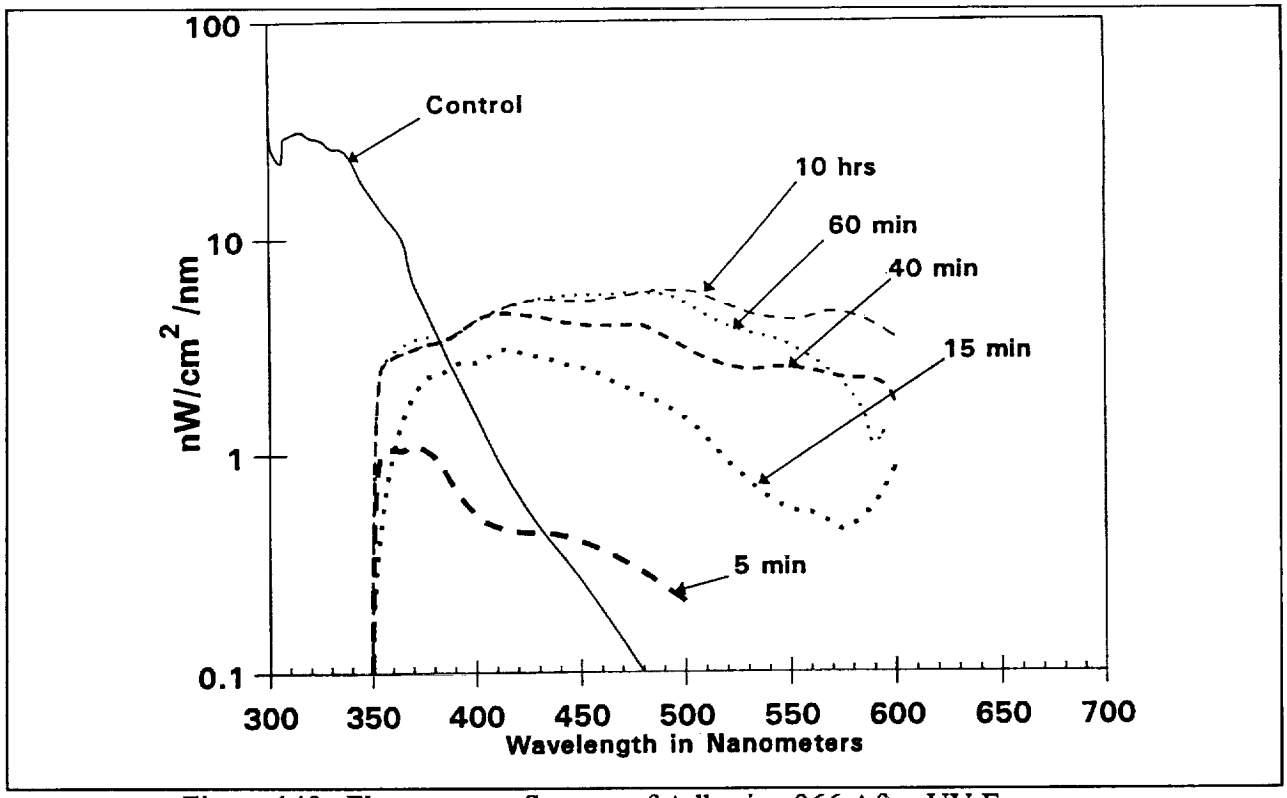

Figure 149. Fluorescence Spectra of Adhesive 966 After UV Exposure.

polyurethane/tensile strength LIF changes. Hill attributes the latter to "complex molecular and intermolecular relationships (such as cross-linking, scission, oxidation) that are altered during degradation".[23] Silicone overcoated urethane paints, although severely cracked and sometimes peeling seem to provide protection from AO erosion. From the measurements, not only does the initial enhanced UV fluorescence disappear after space exposure, but the resulting spectra closely matches that of the urethane paints without the silicone. If polyurethanes are to continue to be used in the space environment, it is necessary to better understand the degradation mechanisms involved. Fluorescence may prove to be a useful tool in this understanding as well as in the evaluation of the condition of polyurethane based materials.

The coatings containing ZnO (S13G/LO and Z93) exhibited fluorescent spectra apparently dominated by ZnO. Nicoll[25] showed that the UV (~380 nm) band wavelength peak shifts with wavelength toward the visible at about 0.12 nm/°C (Figure 150). This shift seems to correlate with the fundamental absorption edge shift. There is no shift in the visible band, but its intensity decreases with temperature. Kroeger[26] attributes this visible fluorescence (~520 nm) in ZnO to the presence of oxygen vacancies, that is, a non-stoichiometric zinc rich condition. It is tempting to attribute the reduction seen in this band for the LDEF S13G/LO and Z93 to the reaction of ZnO with AO. Streed[27] shows, in ground chamber tests, that fluorescence reduction in this band may be caused by UV and/or proton irradiation. Perhaps, in space, the reaction is indeed proceeding toward a stoichiometric mixture aided by the presence of zinc and oxygen in the lattice reacting as a result of exposure to the various high-energy environments.

Fluorescence of silver Teflon (TCSE front cover) is attributed to the micro-cracking that occurred during installation. The matching spectra of the UV irradiated adhesive used to apply the silver Teflon leaves little doubt of the source of the flight material fluorescence and also is an example of fluorescence as an additional analytical tool available to materials researchers and technologists.

5.5 Whisker/Cone Growth

During SEM investigations of the front thermal control cover, an interesting "growth" was discovered on its exposed Teflon surface. A field emission SEM was being used to investigate the AO damage to the silver Teflon coating as a function of AO incident angle. This "growth" has lead to a great deal of interest within the LDEF material investigator community and by various news media sources[28,29,30,31] of which some publications were of a rather dubious accuracy and intent.[32,33,34]

Figures 151 and 152 show the location on the front thermal control cover where the whisker/cone growth was found. The arrow in Figure 151 points at a gap between two of the front thermal control covers. Within this gap, a dark contamination deposit is apparent on the Teflon surface in Figure 152 on which the growth was located. This dark deposit, in contrast to the brownish streaks, was found to be a surface contamination deposit.

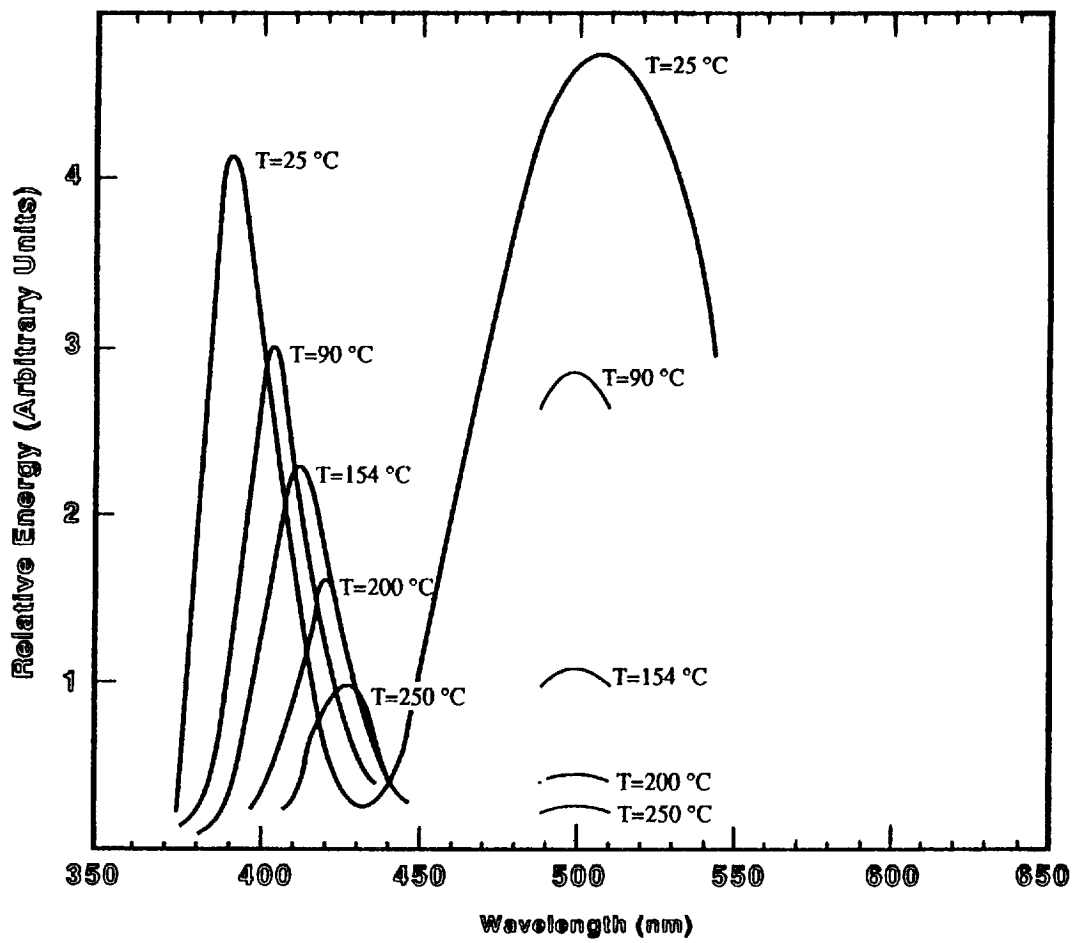

Relative energy emitted by hex, ZnO: [Zn] phosphor as a function of wavelength for different temperatures. Emission produced by a high current density electron beam, 100 MA focused and scanning a 3-in × 4-in television pattern at 20 kV.

Refer: Nicoll, F.H.; J. Amer.Opl. Soc. 38, 817 (1948)

Figure 150. Fluorescence ZnO.

All regions on the front cover having overlaps had a very narrow contamination deposit within their gaps. This deposit was ~3 mm in width by ~50 mm in length. Other growth areas may have existed on the front panel, but this was the only one found. In fact, a front cover sample section immediately below the growth region was provided to Dr. Stuckey/The Aerospace Corp. for analysis, but no growth was found on the contamination deposit on this sample.

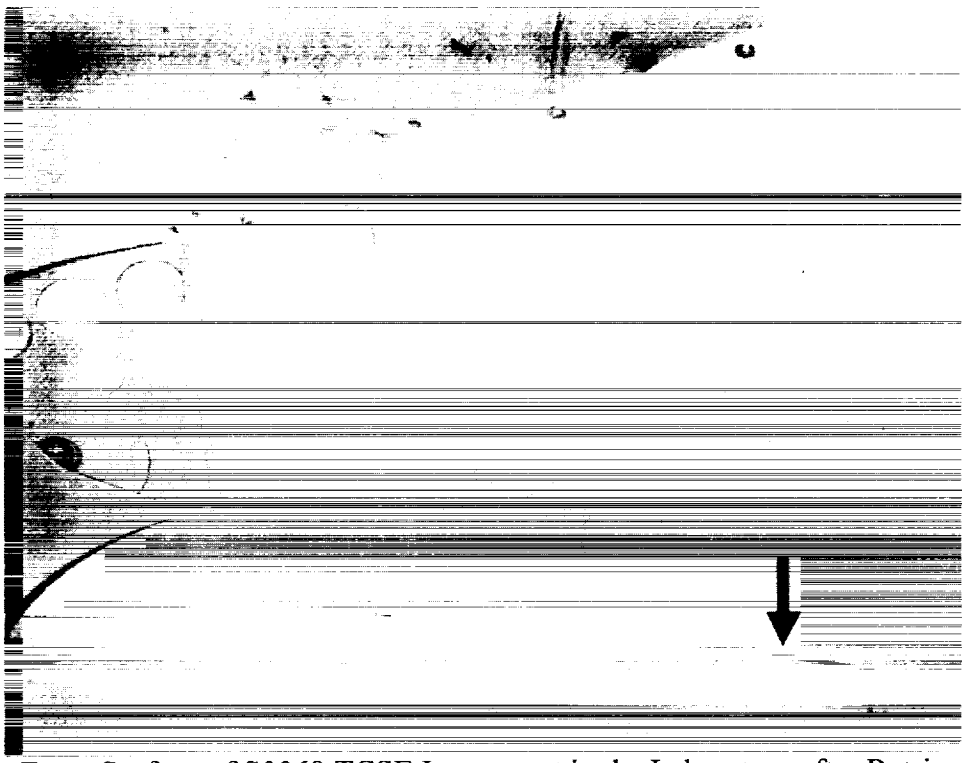

Figure 151. Front Surface of S0069 TCSE Instrument in the Laboratory after Retrieval Showing the Brown Streaks and the Gap (Vent) Between the Front Covers.

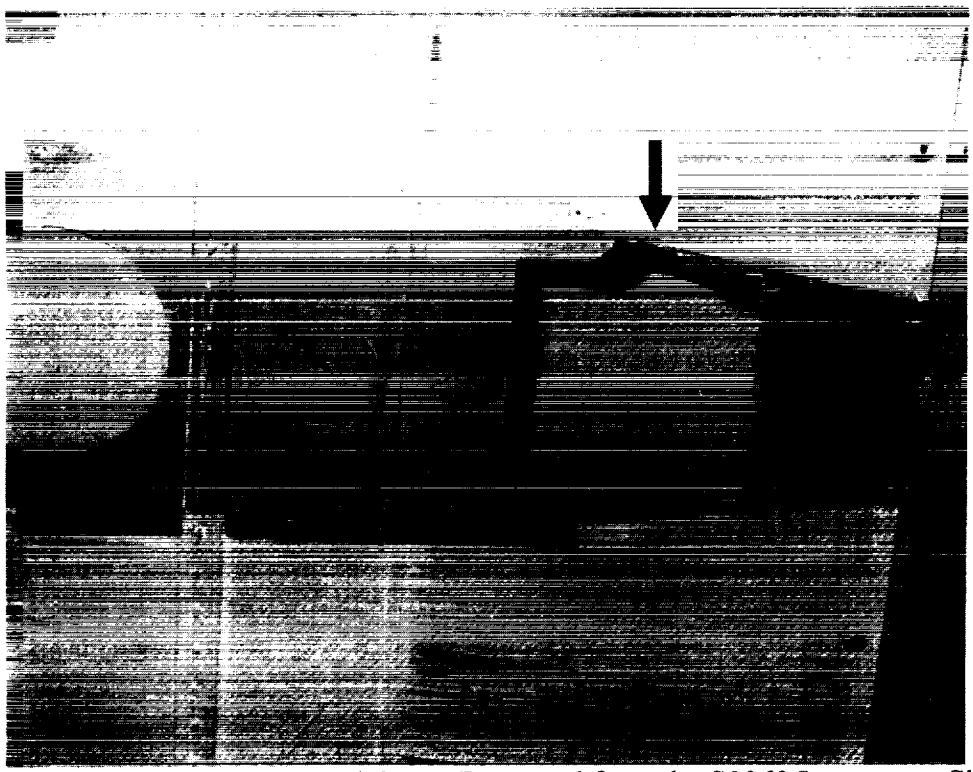

Figure 152. Front Thermal Control Cover Removed from the S0069 Instrument Showing Covered Regions, Exposed Regions, and location of Whisker/Cone "Growth".

The growth region is oriented parallel to the front thermal panel gap shown in Figure 151. SEM images in Figure 153 show that the growth is well ordered, oriented, directional, localized and varies in whisker concentration across the growth region. The growth surface shows no indication of surface facets. There are several stages of growth apparent in the SEM pictures. The base of the growth is a thin brittle dark layer on the Teflon which can be easily removed. In places, the base layer has separated from the Teflon substrate. Individual whisker/cones are translucent when viewed with a visible wavelength optical microscope.

There are two major growth orientations. One is normal to the surface aligned with the LDEF major axis; the other is parallel to the surface facing inward on one side and outward on the other side. The overall growth pattern appears to have some of the characteristics of a dendritic type growth with nucleation occurring along defect sites. The growth dimensions are on the order of 7 microns height and a fraction of a micron in diameter. A few growth units are larger, many are smaller. Individual growth units have a hollow tube down their center and have an inverted cone morphology. The growth surface does not appear eroded by the space environment, including AO exposure.

5.5.1 Biological Viability Testing Results

Analysis performed to date has indicated that the growth is not a standard fungus or mold type growth or contamination that could have occurred on the ground after flight.

Biological testing results were negative in that the unknown growth material did not respond to culturing on a nutrient agar. In addition, the acridine orange direct count epi fluorescence tests, which stain DNA to determine if the growth material is biological, were also negative. These tests were repeated for two different samples, one of which had not been exposed to the SEM vacuum and electron beam irradiation. Results were negative in both cases.

5.5.2 Electron Microprobe Elemental Analysis

Elemental analysis was performed on three areas of sample T-51 using Electron Dispersive X-ray Analysis (EDAX). The "interior area" was shielded from the exterior LDEF environment. The "growth area" was located in a gap between the front panel covers (Figure 151) which formed a vent path from the experiment interior and was partly shielded from AO and solar UV. The so called "no growth" area was exposed to the full space environment during the LDEF mission. Results of these analyses are shown in Figures 154, 155, and 156.

EDAX data for the interior location defined as the "unexposed/covered no growth region" on Figure 154a shows the presence of carbon (C), oxygen (O), fluorine (F), and silicon (Si). Although sulfur (S) is identified on the scan, it is very weak and may be questionable.

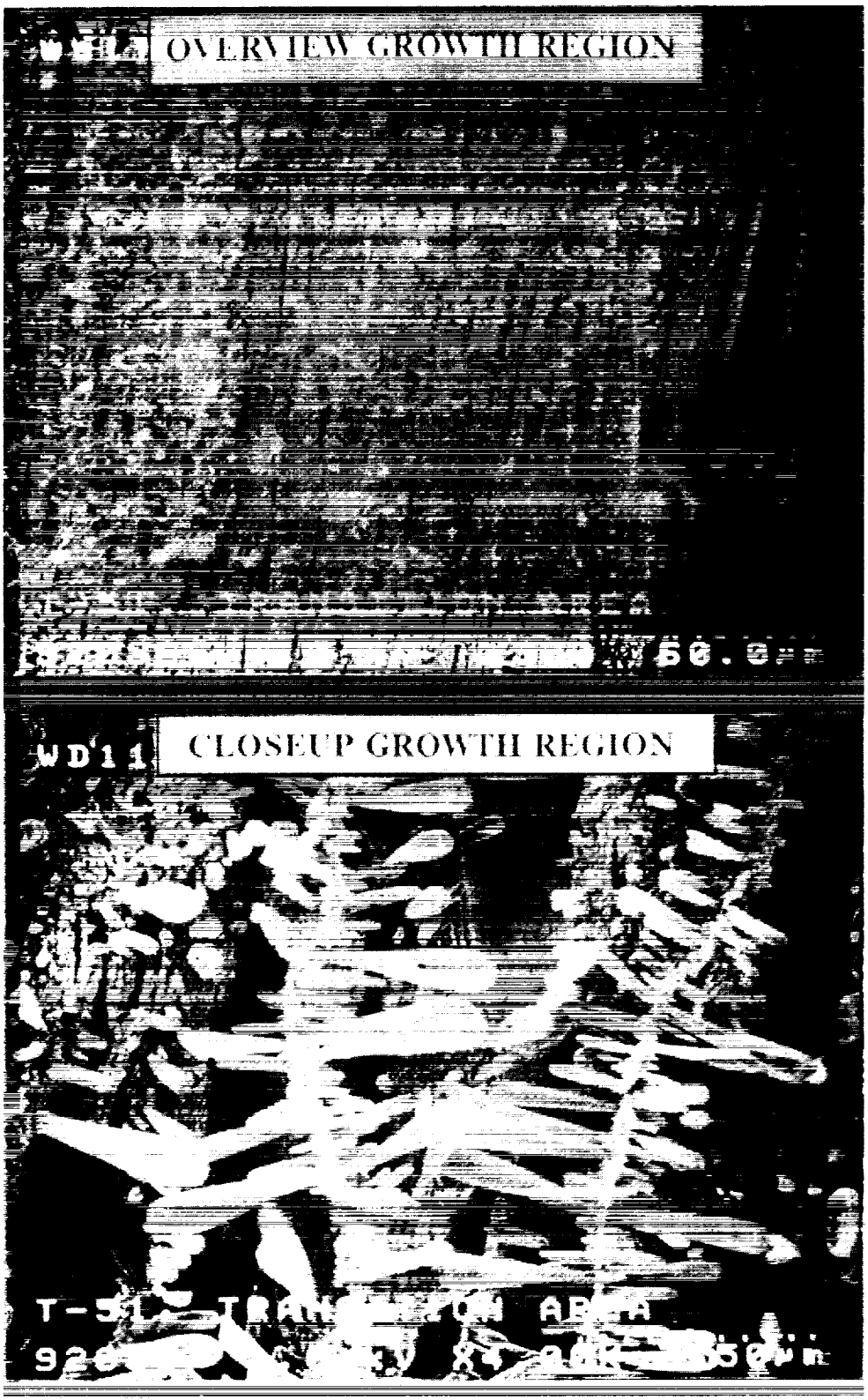

Figure 153. SEM Images of the Whisker/Cone Growth.

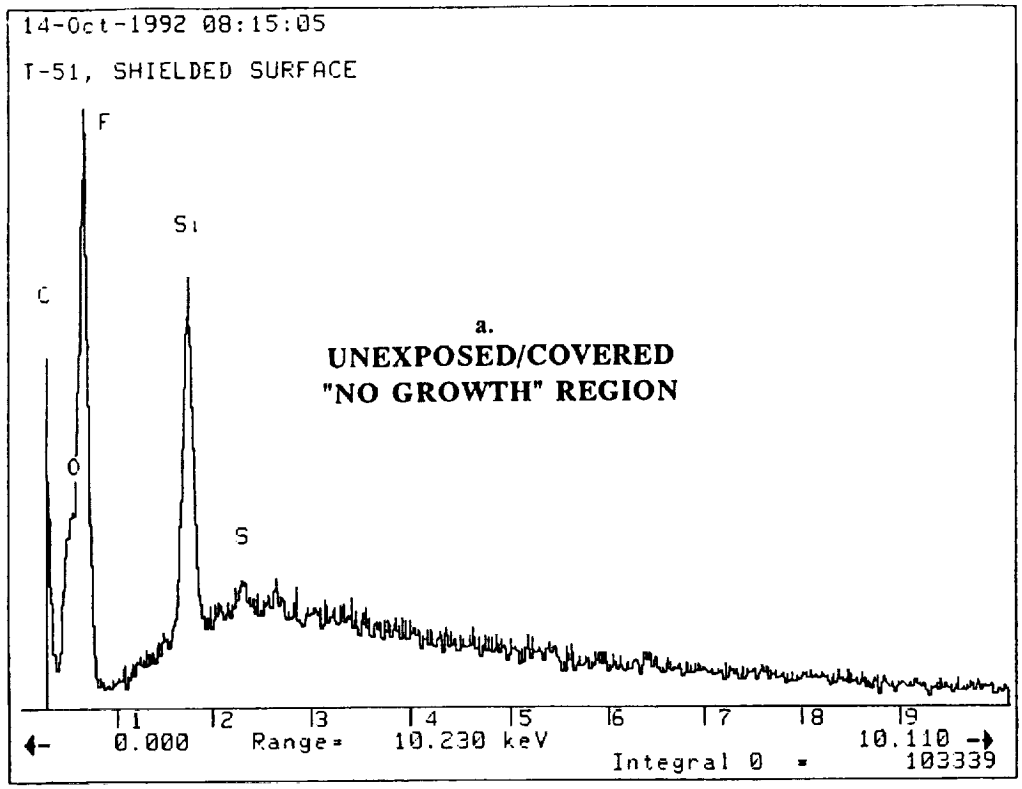

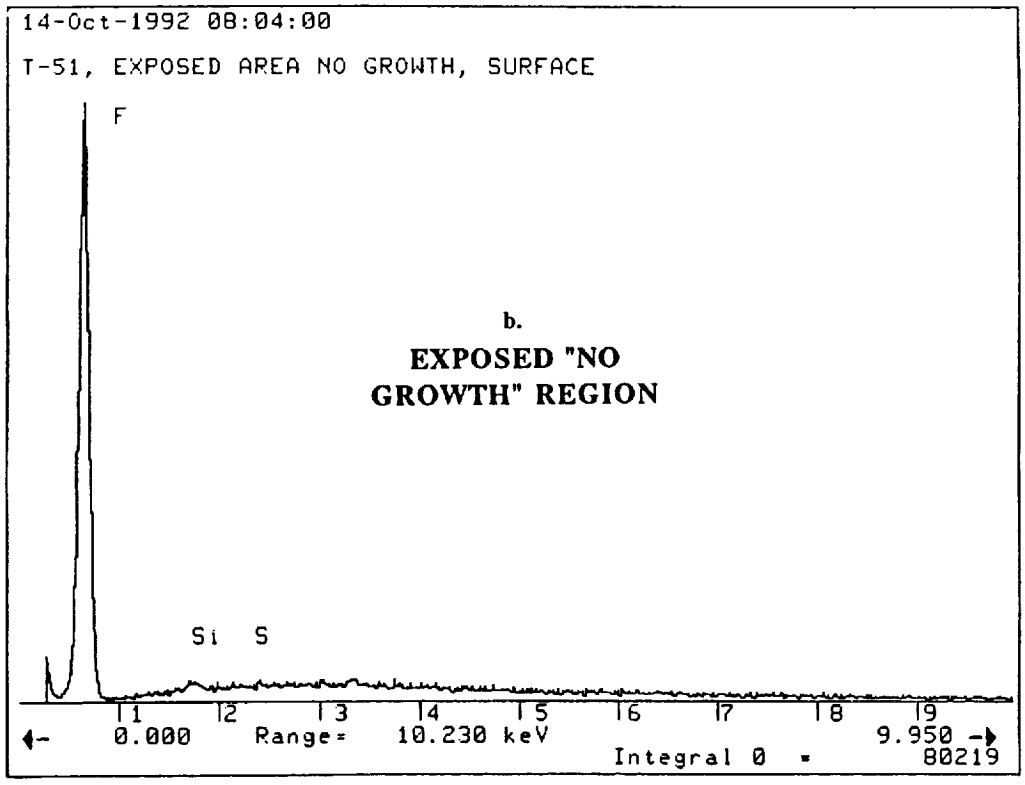

Figure 154. EDAX Data for the Silver Teflon Surface of Sample T51.

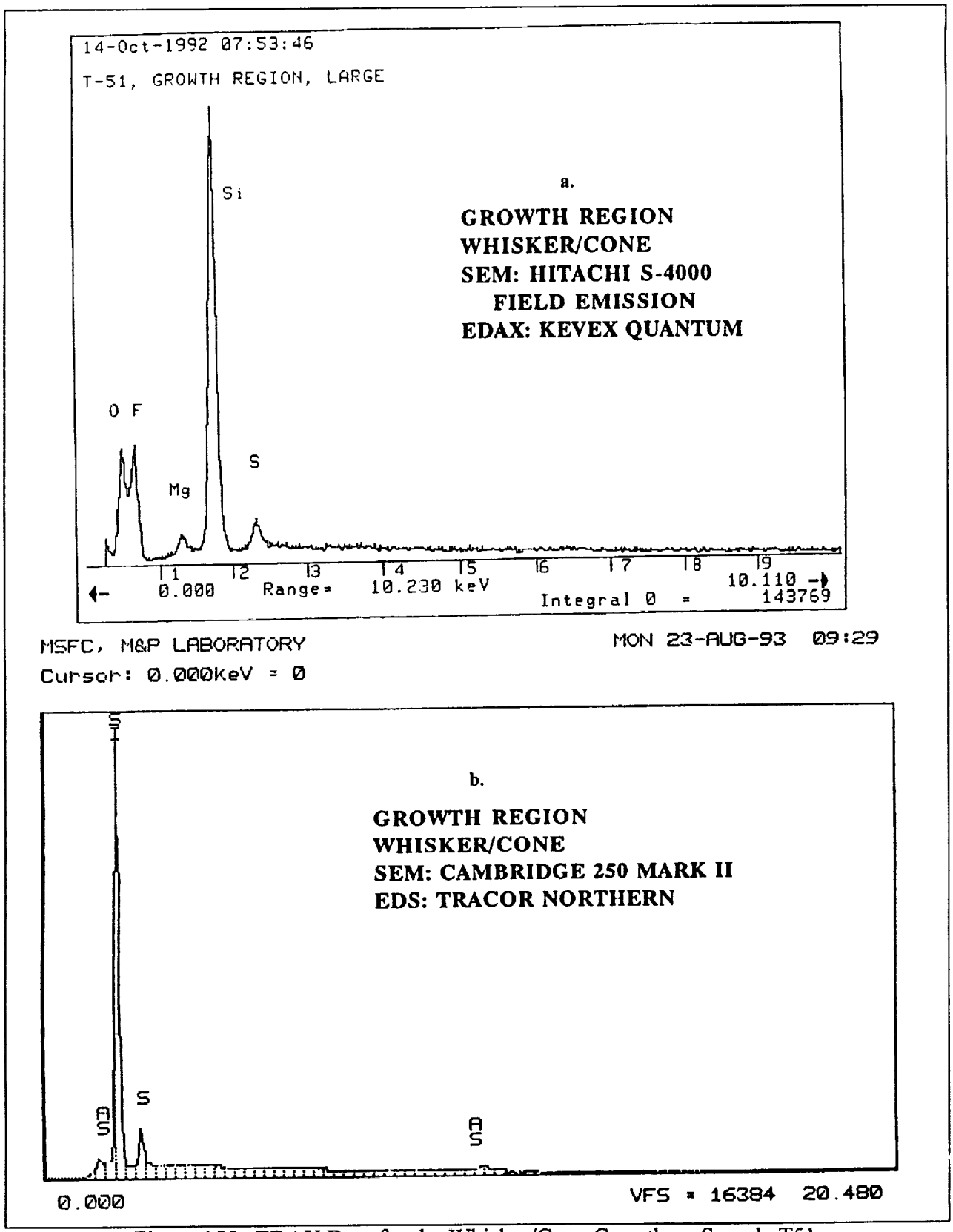

Figure 155. EDAX Data for the Whisker/Cone Growth on Sample T51.

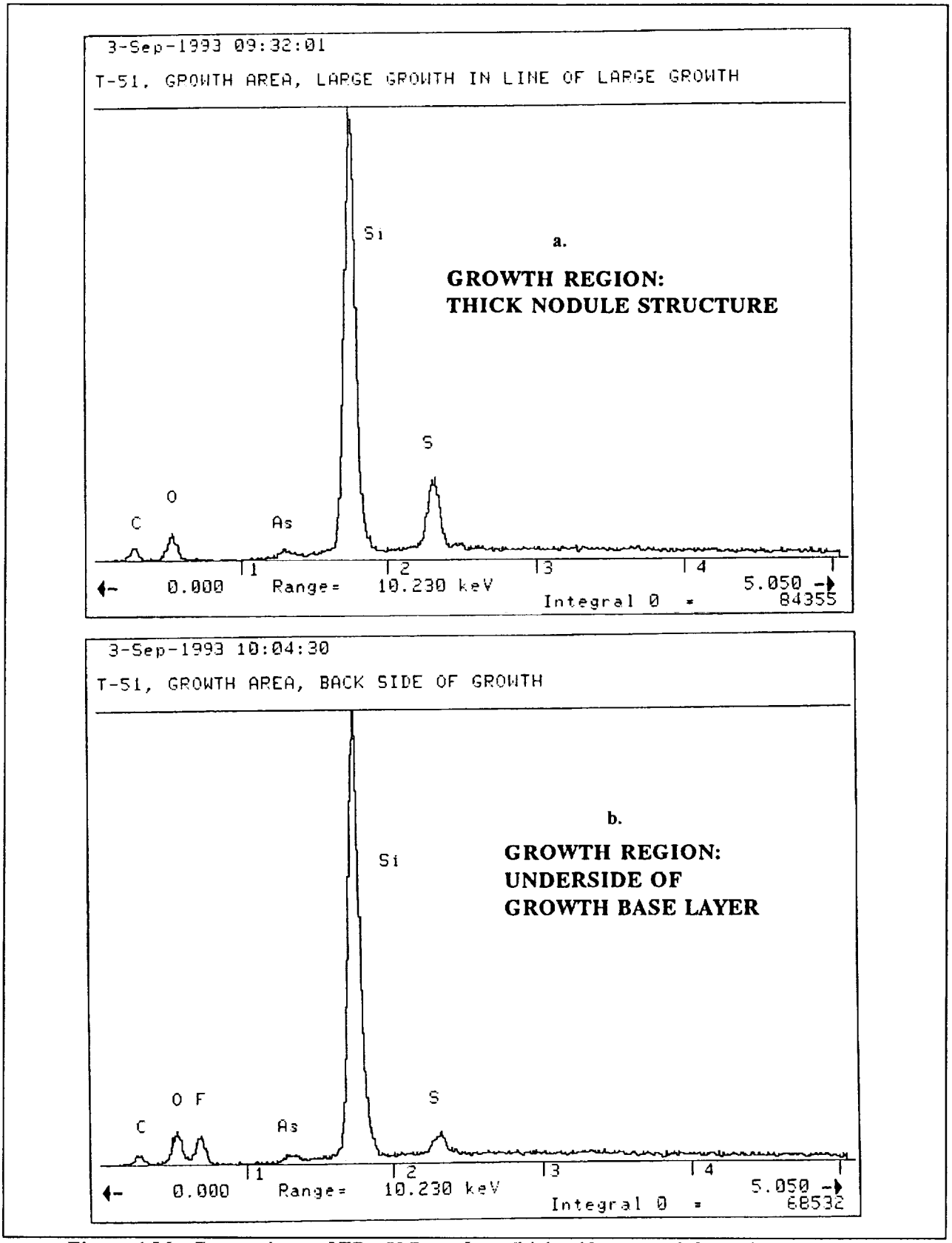

Figure 156. Comparison of EDAX Data for Whisker/Cones and Growth Base Layer.

In comparison, the EDAX data for the "no growth" exposed region on Figure 154b shows strong peaks for fluorine (F) and very weak peaks for silicon (Si) and no sulfur (S). A small hint of carbon (C) can be seen on scan, although it is not labeled. The small silicon peak may be from residual growth or contamination not obvious during the initial viewing of the SEM images. This data is consistent with a Teflon surface eroded by AO.

EDAX data for the growth region was based on focusing the SEM beam on a grouping of the inverted cone whiskers. EDAX scans for this region are shown in Figures 155a and 155b from two different instruments. A very strong silicon (Si) peak is detected, along with sulfur (S), oxygen (O), fluorine (F), and magnesium (Mg), when using the Hitachi S-4000. Notice that the fluorine (F) is greatly reduced from the "no growth" regions and is probably background from the Teflon substrate. This same sample was run in the Cambridge 250 Mark II, having a higher energy analysis capability, in order to confirm the magnesium and sulfur peaks. Surprisingly, the magnesium peak turned out to be arsenic (As). Both peaks for arsenic are present as shown in Figure 120b. Therefore, the peak in Figure 155a identified as Mg is most likely As.

In order to determine if the fluorine peak in Figure 155a was from the growth or was background scatter from the Teflon substrate, another series of EDAX scans were made, carefully focusing on the thickest growth area. Results of these scans are shown in Figure 156a. The fluorine (F) peak is now totally eliminated, proving that fluorine is not a typical component of the growth and the previous fluorine peak was from background scatter. Silicon (Si) is still the main peak and assumed to be the main component. Sulfur (S) shows as a clean peak, indicating its presence. Oxygen (O) still shows, but is weak. Interestingly, carbon (C) now shows up, but is also very weak. The arsenic (As) peak is also present, but is very weak.

Another set of scans were taken of the underside of the base material layer on which the growth is located. This layer is the darker material located at the base of the inverted cones as can be seen in Figure 153. On sample T51, some of the growth was disturbed while taking samples for the biological tests, thereby exposing the underside of some of the base material. Figure 156b is the result of a series of EDAX scans of this material. Most of the previously identified elements remain at the same ratio, except that the sulfur (S) peak is greatly reduced and the fluorine (F) peak now returns. This data indicates that some fluorine (F) is incorporated in the base material, but is not incorporated in the whisker/cones. Also, it appears that sulfur was principally incorporated into the whisker/cone growth during the growth process and not from the base material.

5.5.3 FTIR; Total Attenuated Microprobe Analysis

IR analysis of this phenomenon has been very complicated because of the complex chemistry across the sample surface and the very small size of the dendritic growth. The problem of size has been alleviated through the use of an IR microprobe system, but the complex chemistry across the sample still remains. For the purposes of this analysis, the scope will be limited to the Teflon substrate and the whisker/cone growth material.

Molecular microanalysis utilizing a scanning IR microprobe microscope was performed by Nicolet Instrument Corporation in Stamford, Connecticut. Figure 157 shows the IR spectra for Teflon flight control, Teflon flight sample exposed with no growth, and the whisker/cone growth (labeled dendritic growth). Teflon's characteristic absorption bands can be seen for both flight and control samples. The IR spectra for the whisker/cone growth show almost no structure. The large absorption band at 1057 cm-1 indicates a strong presence of Si-O-Si. The small absorption bands at 3601, 3628, 3705, and 3732 cm-1 indicate a weak presence of Si-OH. This data indicates that the whisker/cone growth is primarily a SiO_X glass type material.

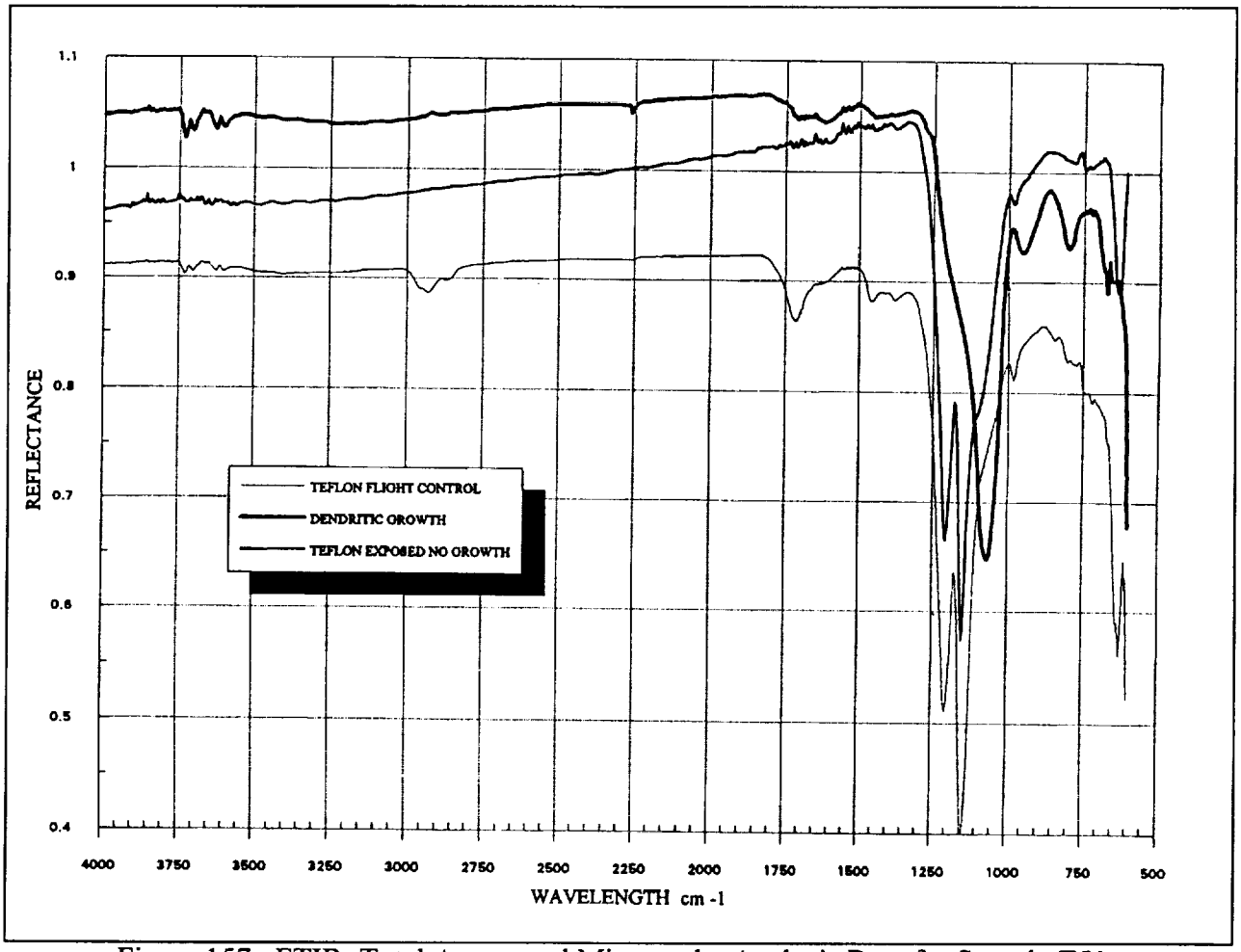

Figure 157. FTIR, Total Attenuated Microprobe Analysis Data for Sample T51.

In addition to the IR spectra, contact with the probe crystal during surface probing indicates that the whisker/cones are hard and brittle in comparison to the surrounding fluoro-carbon polymer. Again, this is consistent with a glassy or silicate type material.

5.5.4 Contamination Source: Sulfur

During post-flight investigation when the S0069 cover was removed, very odiferous fumes were detected. Gas samples were taken using organic (activate charcoal) vapor monitors

located inside the S0069 TCSE instrument with the shipping cover in place. Three monitors were located inside the instrument and one control was placed outside. Analysis identified the gas as dimethyldisulfide. Batteries were then removed and double bagged. Gas samples were taken from the bag using a vacuum bottle technique and analyzed at MSFC. As before, the gas was identified as dimethyldisulfide.

Figure 158 is a mosaic of photographs showing the returned flight batteries in the S0069 experiment tray (four batteries were used; one is hidden under the carousel). One of the batteries is shown with and without its lid in place. Individual cells are potted in the battery case, as can be seen in Figure 158. For these batteries it was found through investigations at MSFC** that after approximately three years (even in cold storage) the individual nickel cell safety pressure release would rupture. Figure 158 shows an individual cell with the pressure release ruptured. Dimethyldisulfide gas is vented by these cells when they rupture. In conjunction with the cell rupture, the battery case seal leaked when the o-rings (ethylene propylene) failed from compression set. Figure 158 clearly shows the magnitude of the compression set. A cross section of the flight o-ring compared to an unused o-ring shows that the flight o-ring has taken the shape of its groove indicating 100% compression set. The dimethyldisulfide gas vented from the batteries is the most likely source of the sulfur detected in the growth.

5.5.5 Contamination Source: Silicon/Silicone/Silicate

Silicone contamination has been identified at several locations on the LDEF.[35,36,37] Although no principal source of silicone has been identified internal to the S0069 instrument, it does appear from the data that a silicone source existed. Silicone under exposure to AO converts to a silicate.[38]

The possibility that the silicone source was external to the S0069 experiment has to be considered. Sources have been identified both internal to the LDEF and from the Shuttle.[39] The S0069 experiment did not have a direct line-of-sight to these sources and at orbital pressures the mean free path for molecular collisions is several kilometers, which would make it unlikely that the localized thick (several microns) silicone deposits found could have formed from returned flux. In addition, there appears to have been a flow of contamination from the interior of the S0069 experiment to the exterior. If the internal contamination deposits were from external sources, then the molecules would have to enter through vents and gaps in the front thermal panels normal to the RAM direction.

Rantanen[40] has performed calculations using the Integrated Spacecraft Environments Model (ISEM) which indicates potentially significant backscatter of outgassing contamination from the LDEF, back onto its RAM facing side. Further analysis is required to resolve this issue, but it may be that the silicone contamination layers originated from sources both internal and external to the S0069 experiment.

** Private communication with M. Martin/EB11 and M. Mendrek/EH24 MSFC.

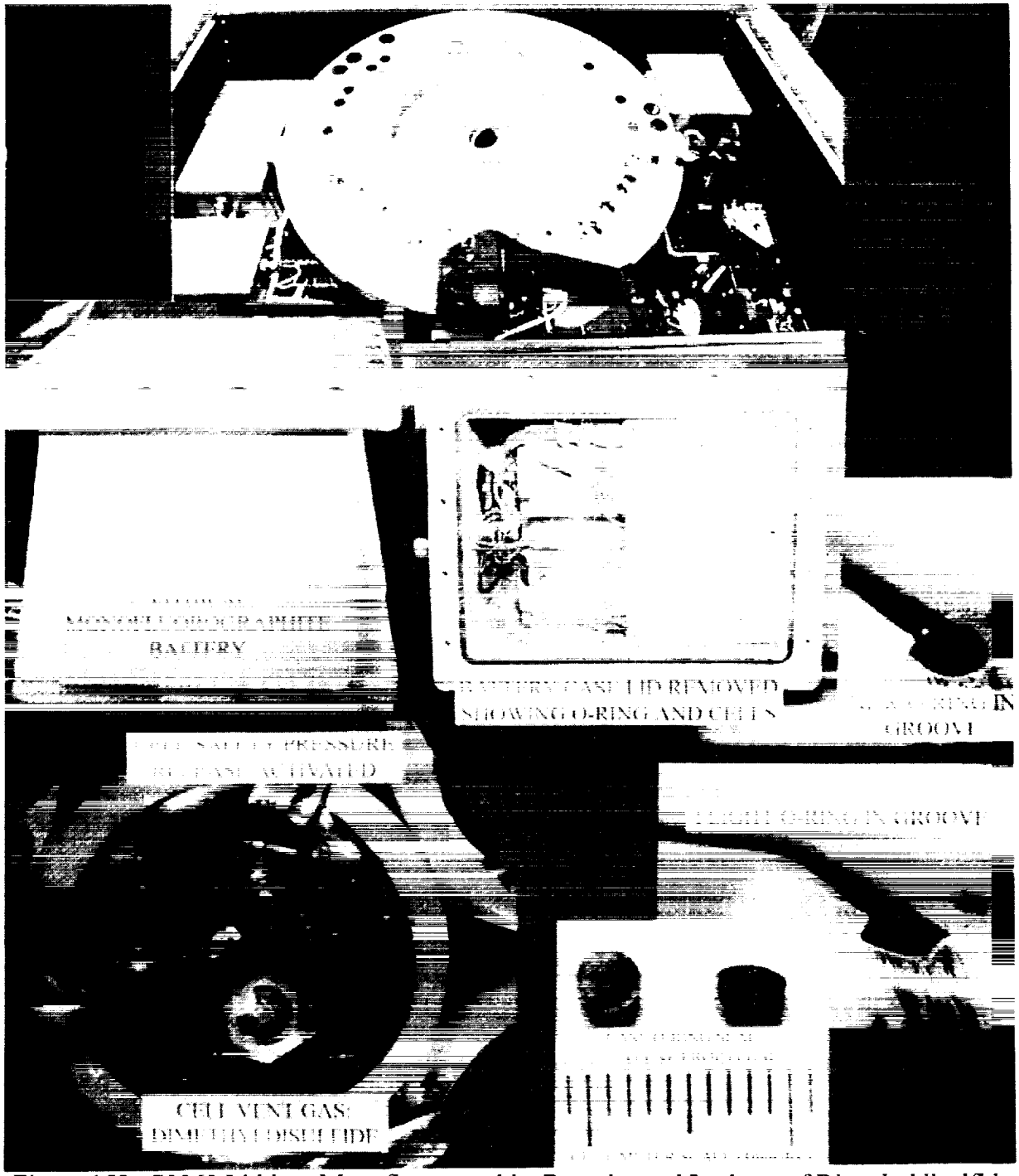

Figure 158. S0069 Lithium Monofluorographite Batteries and Leakage of Dimethyldisulfide Gas.

5.5.6 Contamination Source: Oxygen/Carbon/Fluorine/Arsenic

The principal source of oxygen is presumed to be from orbital AO. Fluorine identified in the growth base material could originate from the Teflon eroded by AO. Carbon is reasonably plentiful, located both in the Teflon and from practically all non-metallic materials used in the

TCSE instrument. Thermal vacuum bakeout of the S0069 instrument prior to flight should have reduced hydrocarbon sources to very low levels, consistent with ASTM E595.[41] The potential source of Arsenic has not been identified.

5.5.7 Discussion

Dr. R. Warner,[##] University of Minnesota, suggested that the growth may be similar to that reported by his colleague, Dr. G.K. Wehner. In Wehner's 1985 survey paper,[42] he discusses the conditions for cone formation during whisker growth by ion bombardment of metal surfaces. One of the earliest reported observations of cone formations is by Fuenterschulze and Tollmien[43] in their 1942 paper where they reported formation of cone forests on cathodes.

There are several growth characteristics reported by Wehner that are necessary for whisker and cone formations to occur. Most of the experiments reported were performed in a low energy ion sputtering high vacuum environment. Ion energies less than 500 ev were capable of achieving whisker growth with dissimilar metals. When the ion energies neared the sputtering threshold, whisker growth was observed. Whisker growth occurs when dissimilar metals are physically close (seed and substrate). Redeposition of sputtered materials results in unique formations of long thin and short thick cones. Inverted cones can also be formed. Whisker/cone orientation is not related to ion impact direction at low ion energies.

For the LDEF growth, the sputtering source was the orbital AO which, being neutral, is capable of "sputtering" or erosion of materials at much less energy than the sputtering threshold, although the rates are very slow.[44,45] AO impacts the RAM face of the LDEF (Figure 15) at ~8 Km/sec or with a kinetic energy of ~5 ev. Wehner found that for metals, whisker growth occurred at low energies only when surface temperatures were elevated. Surface temperatures on the front cover were measured to be below ambient during the first 18 months and thermal model predictions indicated low temperatures throughout the mission.

The major difference between these ground experiments and the flight growth is that metals were used in the studies reported by Wehner, while the growth found on the TCSE experiment is non-metallic and initially polymeric which tends to undergo conversion at low temperatures. As a consequence, cones reported by Wehner were mostly faceted as one would expect, while the TCSE cones were not faceted. Interestingly, both hollow and inverted cone formations were reported, but no inverted hollow cones were reported by Wehner.

Taking into account all the growth conditions between flight and ground experiments makes the growth mechanism less likely to be the true "ion sputtering" related phenomena as reported by Wehner, but a very similar low energy neutral AO related erosion phenomena.

[##] Private communication with Dr. R. Warner in October 1992.

5.5.8 Conclusions: Proposed Growth Scenario

After LDEF orbital insertion, exposure to AO initiates surface erosion of the Teflon surface on the front thermal control cover. Since the LDEF was inserted in a high orbit and the solar cycle was in a low period, the AO flux was also low. Therefore, the erosion rate was low. At the vent/gap interface where growth occurred, the Teflon surface erosion was in the form of roughly parallel ridges versus the normal peak and valley hill type surface texture found in the exposed areas. In time, outgassed molecules of silicone and other contaminants reached this narrow gap between the front thermal covers, which provided a vent, resulting in deposition of thin layers of contamination. Solar UV photons incident on the Teflon interacted with the thin silicone contamination layer to form longer chain, lower vapor pressure, silicone materials. This photodeposition process continued, resulting in a thick, brown varnish type layer. Away from the gap, the silicone contamination flux was dispersed to such low levels that the AO erosion of Teflon dominated and no silicone buildup could be sustained.

As the AO level increased, resulting from the LDEF orbital decay and solar cycle heading towards a high period, the silicone was transformed to a silicate.[36,38] At about 3 years into the mission, the battery cells ruptured, venting a continuous source of dimethyldisulfide gas. At this period in time, all growth elements existed. Figure 159 is a schematic of the growth environmental conditions and associated hardware orientation.

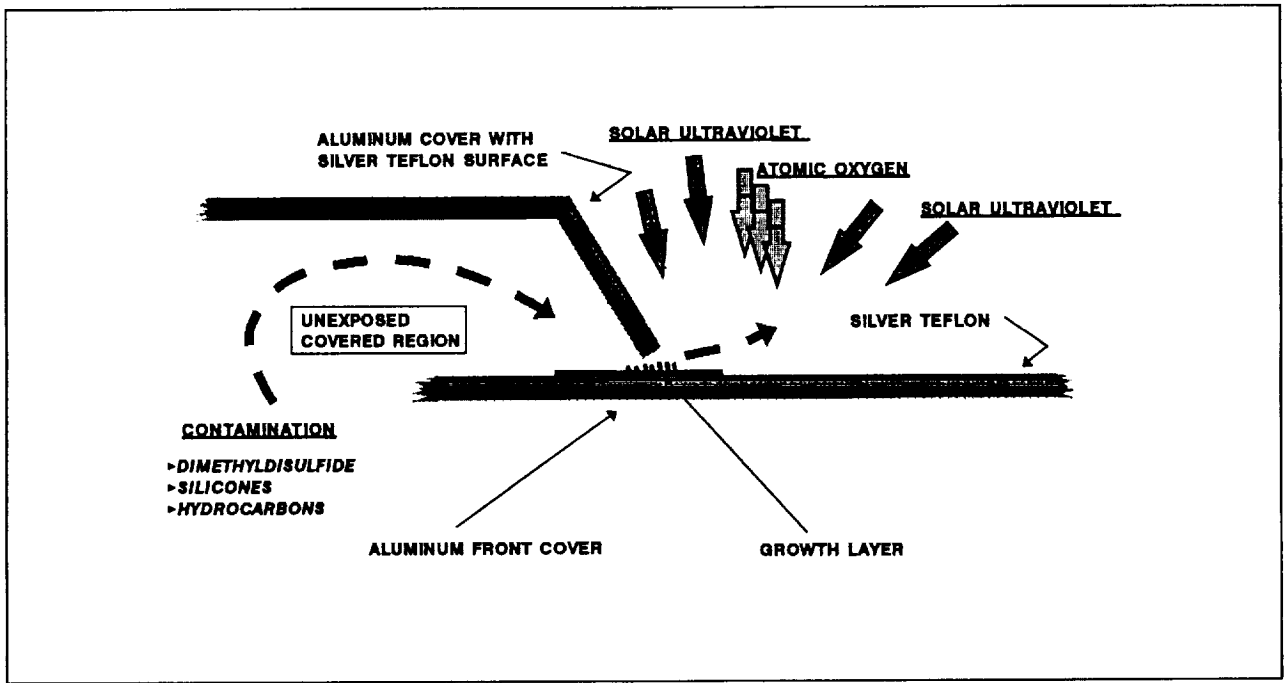

Figure 159. Schematic of Space Environmental Growth Conditions for the Whisker/Cone Growth.

Initially, hollow whiskers are formed which slowly form inverted cones as growth progresses. Growth is driven by redeposition of silicate contamination by AO erosion or "sputtering". Simultaneously, dimethyldisulfide outgassing molecules react with AO freeing

sulfur, possibly in the form of a sulfate (SO_3) which is then incorporated into the whisker/cone growth. Sulfate has a solubility in silica of <0.6%;[46] therefore, the sulfur concentration should be low, as was found from the EDAX data.

The proposed scenario fits the existing data and knowledge of events. As other observations of similar growth are reported and analyzed,[47] a better understanding of the growth process can be developed. With a better understanding of this intriguing whisker/cone growth phenomena, intentional growth can be performed, thereby providing a means to process material on a microscale with unique surface morphologies and physical characteristics.

6.0 DATA AND FLIGHT HARDWARE ARCHIVAL

To preserve the TCSE data and flight hardware, archival and storage procedures have been carried out. This is in addition to the many papers that were published and presented (see Appendix A, TCSE Bibliography) to distribute the TCSE data to the aerospace community.

All TCSE flight hardware, except for the batteries, flight samples, and the front cover, were wrapped in protective film and placed in the TCSE flight tray. Selected documentation was also placed into the tray. The ground tray cover was fastened to the tray to secure the items in the tray.

The following hardware and documentation were reinstalled or wrapped in protective film and place in the tray:

- Flight data recorder
- Loose calorimeter hardware
- Flight data on 5.25" floppy disks
- Front cover #1
- Front cover #2
- Middle cover
- Lexan thermal standoff
- Originals of the notebooks and logs
- Flight battery seals
- Carousel cover
- 5 bags of sample brackets
- 6 bags of assorted fasteners and hardware
- 2 display boxes with flight recorder o-rings
- Flight data pack drawings
- Various loose thermocouples, sensors, etc.

The sealed-up TCSE tray and the GSE racks were placed in bonded storage at MSFC. The flight batteries were disposed of since they present a chemical hazard. The remaining items will be retained by the PI and the Co-I, Mr. James M. Zwiener.

Three sets of TCSE documentation were prepared for archival. One set is being sent to the LDEF archives at LaRC. The second set is being delivered to the Co-I, Mr. James M. Zwiener, at MSFC. The third set is retained by the PI at AZ Technology. Each set of documentation includes a complete set of available TCSE hardware drawings and a complete set of TCSE and related photographs.

7.0 SUMMARY

The TCSE was the most comprehensive materials exposure experiment flown at that time. The TCSE is also the most complex system, other than the LDEF with experiments, recovered from space after extended exposure. The serendipitous extended exposure of the prolonged LDEF mission only added to the significance of the data gathered by the TCSE.

The performance of the materials tested on the TCSE ranges from very small changes to very large changes in optical and mechanical properties. The stability of some of the materials such as Z93, YB71, and silver Teflon (with P223 adhesive) shows there are some stabile thermal control surfaces that are candidates for long term space missions. The materials that significantly degraded provided the opportunity to study the space environment/material interactions.

The TCSE has provided excellent data on the behavior of materials and systems in the space environment. Many expected effects did happen, but in some cases the magnitude of these effects were more or less than expected or were offset by competing processes. A number of unexpected changes were also observed, such as the changes in the UV fluorescence of many materials. However, the TCSE did incur a few system anomalies that made some of the post-flight analyses more difficult. For instance, the loss of the first six months of flight data due to the recorder malfunction is probably the most significant. These few anomalies did not prevent the TCSE from meeting its design and experimental goals. In all, the TCSE was an unqualified success.

REFERENCES

1. Wilkes, D.R., Hummer, L.L.; ""Thermal Control Surfaces Experiment Initial Flight Data Analysis." Final Contract Report NAS8-38689, AZ Technology Report No. 90-1-100-2, June 1991.
2. Wilkes, D.R. and Hummer, L.L.; "LDEF Thermal Control Surfaces Experiment, Post-Flight System Functional Check-Out Final Report", AZ Technology Report No. 90-2-103-1, Boeing Aerospace and Electronics Contract HJ-3234, October 10, 1990.
3. Brown, M.J., Hummer, L.L., and Wilkes, D.R.; "Measurement and Analysis of LDEF/TCSE Flight Samples Final Report," AZ Technology Report No. 90-2-107-1, Boeing Aerospace and Electronics Contract HK-7879, February 22, 1991.
4. Whitaker, A.F., Little, S.A., Harwell, R.J., Griner, D.B., DeHaye, R.F.; "Orbital Oxygen Effects on Thermal Control and Optical Materials, STS-8 Results." AIAA-85-0416, January 14, 1985.
5. Zerlaut, G.A., Gilligan, J.E., and Ashford, N.A.; "Investigation of Environmental Effects on Coatings for Thermal Control Large Space Vehicles." IIT Research Institute Report U6002-97, 1971.
6. Reichard, Penelope J. and Triolo, J.J.; "Pre-flight Testing of the ATS-1 Thermal Coating Experiment." Proc. of the AIAA Thermophysics Specialist Conference, AIAA Paper 67-333, April 17-20, 1967.
7. Wilmhurst, T.H.; "Signal Recovery from Noise in Electronic Instrumentation.' Adam Hilger Ltd, 1981.

8. Banks, B.A.; "LDEF Yaw Estimated at Eight Degrees", LDEF Spaceflight Environmental Effects Newsletter, Vol. II, Number 1, March 15, 1991.
9. Bourassa, R.J. and Gillis, J.R.; "Atomic Oxygen Flux and Fluence Calculation for Long Duration Exposure Facility (LDEF)", LDEF Supporting Data, Contract NAS1-18224, January 1991.
10. Berrios, W.M.; "Long Duration Exposure Facility Post-Flight Thermal Analysis, Orbital/Thermal Environment Data Package," NASA LaRC, Hampton, VA, October 3, 1990.
11. Benton, E.V. and Heinrich, W.; "Ionizing Radiation Exposure of LDEF," University of San Francisco Report USF-TR-77, August 1990.
12. "Meteoroid and Debris Impact Features Documented on the LDEF, A Preliminary Report", April 1990, JSC #24608.
13. "A Comparison of Procedures to Determine the Status of the TCSE Flight Recorder," LEC Project Number D3-1571-2000.
14. "Long Duration Exposure Facility (LDEF) Experimenter Users Handbook", LDEF Project Office, Langley Research Center, Hampton, VA, Report No. 840-2, January 15, 1978 (Draft Version).
15. Wilkes, D.R.; "A Numerical Integration Scheme to Determine Hemispheric Emittance, Solar Absorptance, and Earth Infrared Absorptance from Spectral Reflectance Data", NASA TMX-53918, September, 1969.
16. Park, J.J.; "EOIM GSFC Materials", Atomic Oxygen Working Group Meeting, Washington, D.C., January 23, 1984.
17. Pippin, G.; "Materials SIG Summary Document Released", LDEF Spaceflight Environmental Effects Newsletter, Vol. I, Number 8, January 23, 1991.
18. Zerlaut, G.A., Gilligan, J.E.; "Study of In-situ Degradation of Thermal Control Surfaces", NASA Contract NAS8-21074 Final Report. IITRI Report U6061-29, February 20, 1970.
19. Gilligan, J.E. and Harada, Y.; "Development of Space Stable Thermal Control Coatings for Use on Large Space Vehicles", NASA Contract NAS8-26791, IITRI Report C6233-57, March, 1976.
20. Zerlaut, G.A. and Harada, Y.; "Stable White Coatings," IITRI Report IITRI-C207-27, NASA Contract NAS7-100, January, 1964.
21. Wilkes, D.R.; "Next Generation Optical Instruments and Space Experiment Based on the LDEF Thermal Control Surfaces Experiment (S0069)", Second LDEF Post-Retrieval Symposium, San Diego, CA, NASA CP-3194, June 1992.
22. Wilkes, D.R., et. al.; "Thermal Control Surfaces on the MSFC & LDEF Experiments", LDEF Materials Workshop, Hampton, VA, November, 1991.
23. Hill, R.H. Jr. and Feuer, H.O. Jr.; "Laser-Induced Fluorescence Inspection of Polyurethane", Proceedings of the 17th Symposium on Nondestructive Evaluation, April 17-20, 1989, San Antonio, TX.
24. Hill, R.H. Jr.; "Laser-Induced Fluorescence of Space-Exposed Polyurethane", Southwest Research Institute Report 15-9682, April 6, 1992.
25. Nicoll, F.H.; "Temperature Dependence of Emission Bands of ZnO Phosphors", Journal of the Optical Society of America, Vol. 39, 1948.
26. Kroeger, Vink, et. al.; "The Origin of Fluorescence in Self-Activated ZnS, CdS, and ZnO", Journal of Chemical Physics.

27. Streed, E.R.; "Experimental Study of the Combined Space Environment Effects on ZnO/Potassium Silicate", Themophysics of Spacecraft and Planetary Bodies, ed. by G. Heller, 1967.
28. Zwiener, J.M.; "Unusual "Growth" Found on LDEF Surface", LDEF Newsletter, Vol. III, No. 4, August 15, 1992, pp. 4-7.
29. Burkey, M.; "LDEF Reveals 'Unusual Growth'", The Huntsville Times, Monday, October 19, 1992.
30. Burkey, M.; "Space Growth", Final Frontier, February 1993, p. 6.
31. Baker, S.; "Mystery Stuff from Outer Space", OMNI, December 1993, p. 87.
32. Strauss, S.; "It's not of this Earth, Mystery growth formed in space baffles NASA scientists", Houston Chronicle, Wednesday, Sept. 9, 1992, p. 9A.
33. "Stowaway from Space; Mysterious growth rides in on shuttle - terrifies experts", National Examiner, January 12, 1993.
34. Rothstein, A.; presented highly edited NASA video on Sightings, TOX TV #54, May 12, 1993.
35. Hemminger, C.S.; "Surface Contamination on LDEF Exposed Materials", LDEF Materials Workshop, NASA Conference Publication 3162, Part 1, November 19-22, 1991, pp. 159-174.
36. Harvey, G.A.; "Silazane to Silica", LDEF - 69 Months in Space Second Post-Retrieval Symposium, NASA Conference Publication 3194, Part III, June 1992, pp. 797-810.
37. Pippin, G. and Crutcher, R.; "Contamination on LDEF: Sources, Distribution, and History", LDEF - 69 Months in Space Second Post-Retrieval Symposium, NASA Conference Publication 3194, Part III, June 1992, pp. 1023-1032.
38. Banks, B.A., Gebauer, L., and Hill, C.M.; "Atomic Oxygen Interactions with FEP Teflon and Silicones on LDEF", LDEF - 69 Months in Space First Post-Retrieval Symposium, NASA Conference Publication 3134, Part II, June 1991, pp. 801-806.
39. Harvey, G.; "Sources and Transport of Silicone NVR", LDEF Materials Workshop, NASA Conference Publication 3162, Part 1, November 19-22, 1991, pp. 174-184.
40. Rantanen, R. and Carruth, M.R.; "Modeling of LDEF Contamination Environment", LDEF Materials Results for Spacecraft Applications Conference, NASA Conference Proceedings (scheduled for publication by mid 1994).
41. American Society for Testing and Materials Standard Test Method; "Total Mass Loss (TML) and Collected Volatile Condensable Materials (CVCM) from Outgassing in a Vacuum Environment", ASTM E 595-77.
42. Wehner, G.K.; "Cone Formation as a Result of Whisker Growth on Ion Bombarded Metal Surfaces", J. Vac. Sci. Technol. A 3(4), Jul/Aug 1987, p. 1821-1835.
43. Guenterschulze, A. and Tollmien, W.V.; Z. Phys, Vol. 119, 1942, p. 685.
44. Hansen, R.H., et. al.; "Effects of Atomic Oxygen on Polymers", Journal of Polymer Sciences: Part A, Vol. 3, 1965, pp. 2205-2211.
45. Whitaker, A.F., et. al.; "Atomic Oxygen Effects on LDEF Experiment A0171", LDEF - 69 Months in Space Second Post-Retrieval Symposium, NASA Conference Publication 3194, Part III, June 1992, pp. 1125-1135.
46. Holland, L., "The Properties of Glass Surfaces", Chapman and Hall, Ltd., London 1964, pp. 207-208.

47. Edelman, J.; "LDEF is not Unique Surface Growths on Other Missions", LDEF Newsletter, Volume IV, No. 1, March 30, 1993 (information provided by Dr. R.L. Kruse, Monsanto, Springfield, MA and Dr. D. Schwam, Case Western Reserve University, for the LDCE 1, 2, & 3 flown on STS-46, July 1992).

APPENDIX A
TCSE Bibliography

1. Wilkes, Zwiener, "LDEF Thermal Control Surfaces Experiment", AIAA Space Programs and Technology, Huntsville, AL, September 1990.
2. Wilkes, Hummer, "LDEF TCSE (S0069) Post-Flight System Functional Check-Out", Final Test Report, Contract HJ-3234, AZ Technology Report No. 90-2-103-1, February 1991.
3. Wilkes, Hummer, Brown, "Measurement and Analysis of LDEF/TCSE Flight Samples", Contract HK-7879, AZ Technology Report No. 90-2-107-1, February 1991.
4. Wilkes, Hummer, "Thermal Control Surfaces Experiment Initial Flight Data Analysis", Final Contract Report NAS8-38689, AZ Technology Report No. 90-1-100-2, June 1991.
5. Wilkes, Zwiener, "Initial Materials Evaluation of the Thermal Control Surfaces Experiment (S0069)", First LDEF Post-Retrieval Symposium, Orlando, FL, NASA CP-3134, June 1991.
6. Zwiener, Wilkes, et al., "Unusual Material Effects Observed on the Thermal Control Surfaces Experiment (S0069)", First LDEF Post-Retrieval Symposium, Orlando, FL, NASA CP-3134, June 1991.
7. Wilkes, Zwiener, et al., "Thermal Control Surfaces on the MSFC LDEF Experiments", LDEF Materials Workshop, Hampton, VA, November 1991.
8. Zwiener, Wilkes, et al., "Fluorescence of Thermal Control Coatings on Experiment S0069 and AO114", LDEF Materials Workshop, Hampton, VA, November 1991.
9. Wilkes, Zwiener, "The Thermal Control Surfaces Experiment (TCSE) on LDEF", AIAA 92-2166, AIAA Coatings Technologies for Aerospace Systems Specialist Conference, Dallas, TX, April 1992.
10. Wilkes, "Next Generation Optical Instruments and Space Experiment Based on the LDEF Thermal Control Surfaces Experiment (S0069)", Second LDEF Post-Retrieval Symposium, San Diego, CA, NASA CP-3194, June 1992.
11. Wilkes, Zwiener, et. al., "The Continuing Materials Analysis of the Thermal Control Surfaces Experiment (S0069)", Second LDEF Post-Retrieval Symposium, San Diego, CA, NASA CP-3194, June 1992.
12. Zwiener, Wilkes, et. al., "Fluorescence Measurements of the Thermal Control Coatings on LDEF Experiments S0069 and AO114", Second LDEF Post-Retrieval Symposium, San Diego, CA, NASA CP-3194, June 1992.
13. Wilkes, Zwiener, et. al., "Trend Analysis of In-Situ Spectral Reflectance Data from the Thermal Control Surfaces Experiment (TCSE)", Third LDEF Post-Retrieval Symposium, Williamsburg, VA, NASA CP-3275, November 1993.
14. Zwiener, Wilkes, et. al., "Whisker/Cone Growth on the Thermal Control Surfaces Experiment #S0069", Third LDEF Post-Retrieval Symposium, Williamsburg, VA, NASA CP-3275, November 1993.
15. Wilkes, "Thermal Control Surfaces Experiment", Final Report, Contract NAS8-38939, AZ Technology Report No. 90-1-108-054, August 1997.

REPORT DOCUMENTATION PAGE

Form Approved
OMB No. 0704-0188

1. AGENCY USE ONLY *(Leave Blank)*	2. REPORT DATE	3. REPORT TYPE AND DATES COVERED
	January 1999	Contractor Report (Final)

4. TITLE AND SUBTITLE
Thermal Control Surfaces Experiment

5. FUNDING NUMBERS
NAS8–38939

6. AUTHORS
D.R. Wilkes

7. PERFORMING ORGANIZATION NAMES(S) AND ADDRESS(ES)
AZ Technology, Inc.
4901 Corporate Drive, Suite 101
Huntsville, AL 35805

8. PERFORMING ORGANIZATION REPORT NUMBER
M–905

9. SPONSORING/MONITORING AGENCY NAME(S) AND ADDRESS(ES)
George C. Marshall Space Flight Center
Marshall Space Flight Center, AL 35812

10. SPONSORING/MONITORING AGENCY REPORT NUMBER
NASA/CR—1999–209008

11. SUPPLEMENTARY NOTES
Prepared for Materials and Processes Laboratory, Science and Engineering Directorate
Technical Monitor: Jim Zwiener

12a. DISTRIBUTION/AVAILABILITY STATEMENT
Unclassified–Unlimited
Subject Category 18
Standard Distribution

12b. DISTRIBUTION CODE

13. ABSTRACT *(Maximum 200 words)*

This report is the final experiment report for the TCSE and summarizes many years of hardware development and analyses. This final report serves as the contract final report for NASA Contract NAS8–38939, but encompasses work also performed under other contracts including NAS8–36289 and Boeing HV–3234 and HR–7879. Also included are analyses presented in a number of TCSE papers that were prepared and given at scientific conferences including three LDEF Post-Retrieval Symposiums.

14. SUBJECT TERMS
Thermal Control Surfaces Experiment

15. NUMBER OF PAGES
163

16. PRICE CODE
A08

17. SECURITY CLASSIFICATION OF REPORT	18. SECURITY CLASSIFICATION OF THIS PAGE	19. SECURITY CLASSIFICATION OF ABSTRACT	20. LIMITATION OF ABSTRACT
Unclassified	Unclassified	Unclassified	Unlimited